



Document title/ titre du document

SOLAR ORBITER: CONSOLIDATED REPORT ON MISSION ANALYSIS

prepared by/*préparé par* J. M. Sánchez Pérez
G. I. Varga

reference/*référence* SOL-ESC-RP-05500

issue/*édition* 4

revision/*révision* 0

date of issue/*date d'édition* 2016-10-28

status/*état* Approved/Applicable

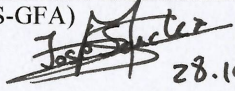
Document type/*type de document* RP

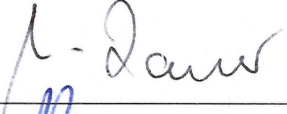

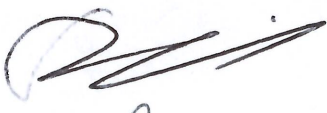
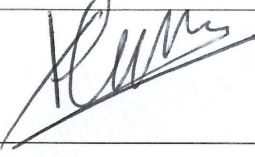
Distribution/*distribution* See list inside



A P P R O V A L

Title	Solar Orbiter: Consolidated Report on Mission Analysis	issue 4	revision 0
Titre		issue	revision

author	J. M. Sánchez Pérez, G. I. Varga (OPS-GFA)	date	2016-10-28
auteur	 28.10.16	date	

approved by	M. Lauer (OPS-GFS) SOLO Flight Dynamics Manager	date	
approuvé par		date	31/10/2016
	A. Accomazzo (OPS-OP) SOLO Ground Segment Manager		
			31/10/2016
	S. Strandmoe (SRE-PSS) SOLO Systems Manager		
	P. Olivier (SRE-PSQ) SOLO PA Manager		
			1 Nov 16
	P. Kletzke (SER-PS) SOLO Project Manager		
			01-Nov-2016



A P P R O V A L

Title	Solar Orbiter: Consolidated Report on Mission Analysis	issue 4	revision 0
Titre		issue	revision

author	J. M. Sánchez Pérez, G. I. Varga (OPS-GFA)	date	2016-10-28
auteur		date	

approved by	M. Lauer (OPS-GFS) SOLO Flight Dynamics Manager	date	
approuvé par		date	
	A. Accomazzo (OPS-OP) SOLO Ground Segment Manager		
	S. Strandmoe (SRE-PSS) SOLO Systems Manager	Digitally signed by Stein E. Strandmoe DN: cn=Stein E. Strandmoe, o=ESA/ ESTEC, ou=SRE-PSS, email=stein.strandmoe@esa.int, c=NL Date: 2016.10.28 21:01:27 +02'00'	
	P. Olivier (SRE-PSQ) SOLO PA Manager		
	P. Kletzkine (SER-PS) SOLO Project Manager		



C H A N G E L O G

<i>reason for change /raison du changement</i>	<i>issue/issue</i>	<i>revision/revision</i>	<i>date/date</i>
New Creation	1	0	May, 12, 2010
Including more information on solar conjunctions, launch targets tables & corrections	1	1	June, 10, 2010
Update of launch scenarios: Dec. 2016 discarded, Sep. 2018 modified. Including navigation analysis	2	0	Sep., 09, 2011
Including modifications as per review by project	2	1	Oct., 06, 2011
Include 2017 July and 2018 October trajectories & Ariane 5 ECA backup launch scenario	3	0	Sep., 12, 2012
Added project signature. Including analysis to reduce duration of eclipse for 2017 July trajectory. Update launcher injection correction and Delta-V budget. Include analysis of flight programs for Ariane 5 ECA launch. Include discussion on requirements for industry.	3	1	Oct., 08, 2012
Major modification. Document describes launch options on late 2018 and 2019/2020 backups with Atlas V launch.	4	0	Oct., 28, 2016

C H A N G E R E C O R D

Issue: 4 Revision: 0

<i>reason for change/raison du changement</i>	<i>page(s)/page(s)</i>	<i>paragraph(s)/paragraph(s)</i>
---	------------------------	----------------------------------



TABLE OF CONTENTS

TABLE OF CONTENTS	4
LIST OF FIGURES	6
LIST OF TABLES	10
ACRONYMS AND ABBREVIATIONS	12
1 INTRODUCTION	13
1.1 Purpose and Scope	13
1.2 Structure of the Document	13
1.3 Reference Documents	14
2 MISSION DESIGN OVERVIEW	16
2.1 Design Driver Requirements	16
2.2 Mission Baseline	17
2.3 Considerations for the end of mission	18
2.4 Optimization of data return	19
2.4.1 Downlink Index	21
3 TRAJECTORY ANALYSIS	22
3.1 2018 Launch Option E	23
3.1.1 Description	23
3.1.2 Science Properties	35
3.1.3 Ground Station Visibility	40
3.1.4 GAMs Details	44
3.1.5 LEOP	49
3.2 2018 Launch Option D	54
3.2.1 Description	54
3.2.2 Science Properties	63
3.2.3 Ground Station Visibility	68
3.2.4 GAMs Details	71
3.2.5 LEOP	73
3.3 2018 October Launch	77
3.3.1 Description	77
3.3.2 Science Properties	84
3.3.3 Ground Station Visibility	89
3.3.4 GAMs Details	92
3.3.5 LEOP	94
3.4 2019 & 2020 February Launch	97
3.4.1 Description	97
3.4.2 Science Properties	107
3.4.3 Ground Station Visibility	112
3.4.4 GAMs Details	116
3.4.5 LEOP	119



3.5	Summary	125
4	LAUNCH WINDOWS ANALYSIS	128
4.1	Atlas V 411 Launch from KSC	128
4.2	2018 Option E Launch Window	130
4.2.1	Launch Targets	135
4.3	2018 Option D Launch Window	136
4.3.1	Launch Targets	139
4.4	2018 October Launch Window.....	140
4.4.1	Launch Targets	143
4.5	2019 February Launch Window	145
4.5.1	Launch Targets	149
4.6	2020 February Launch Window	150
4.6.1	Launch Targets	153
4.7	Summary	154
5	NAVIGATION ANALYSIS	156
5.1	Assumptions	156
5.2	Launcher Injection Correction and Initial OD.....	160
5.3	Trajectory Navigation of all GAMs.....	161
5.3.1	Impact of Increased Dynamic Noise	173
5.3.2	Dispersion of the science orbits.....	175
5.3.3	Operational Approach to Reduce Measurements	176
5.3.4	Contingency Case – Thruster Failure	177
5.4	Summary	179
6	DELTA-V BUDGET	180
7	CONCLUSIONS	181
7.1	Requirements applicable to industry	182
8	TRAJECTORY FILES	186
9	DISTRIBUTION LIST	187
10	APPENDIX A – DETAILED DATA OF REMOTE SENSING WINDOWS	188
10.1	2018 Option E Launch	188
10.2	2018 Option D Launch.....	192
10.3	2019/2020 February Launch.....	196



LIST OF FIGURES

Figure 2-1 Illustration of “bad” downlink case for 4:3 orbit – 2018 October	20
Figure 2-2 Illustration of “good” downlink case for 4:3 orbit – 2017 January	20
Figure 3-1 Graphical representation of the angles used in the V-infinity diagram	26
Figure 3-2 2018 Launch Option E: V-infinity diagram for the sequence of resonances.....	27
Figure 3-3 2018 Launch Option E: X-Y Trajectory projection from launch until GAM-V4.....	28
Figure 3-4 2018 Launch Option E: X-Y Trajectory projections from Launch to End of Mission.....	29
Figure 3-5 2018 Launch Option E: X-Z and Y-Z Trajectory projections	29
Figure 3-6 2018 Launch Option E: Science orbits projection on the Sun-Earth rotating frame	30
Figure 3-7 2018 Launch Option E: Spacecraft distance to Sun, Venus and Earth.....	31
Figure 3-8 2018 Launch Option E: SSE and SES angles.....	31
Figure 3-9 2018 Launch Option E: SSE and SES angles – Detail of conjunctions.....	32
Figure 3-10 2018 Launch Option E: Variation of Earth-Spacecraft range-rate	33
Figure 3-11 2018 Launch Option E: Variation of Earth-Spacecraft Doppler	34
Figure 3-12 2018 Launch Option E: Variation of Earth-Spacecraft Doppler-rate	34
Figure 3-13 2018 Launch Option E: Spacecraft solar latitude + Spacecraft distance to the Sun.....	36
Figure 3-14 2018 Launch Option E: projection of science orbits wrt Sun Equator and North Pole	36
Figure 3-15 2018 Launch Option E: Evolution of apsides and points of extreme solar latitude.....	37
Figure 3-16 2018 Launch Option E: Evolution of Earth distance and potential downlink	37
Figure 3-17 2018 Launch Option E: Evolution of time spent below different Sun ranges	39
Figure 3-18 2018 Launch Option E: Spacecraft rotation velocity about the Sun.....	40
Figure 3-19 2018 Launch Option E: Spacecraft equatorial declination.	41
Figure 3-20 2018 Launch Option E: Daily period of visibility from ESA DS stations.....	42
Figure 3-21 2018 Launch Option E: Daily duration of visibility from ESA Deep Space stations.....	43
Figure 3-22 2018 Launch Option E: Daily period of visibility from ESA Deep Space stations.....	43
Figure 3-23 2018 Launch Option E: Projection of hyperbolas for Venus GAMs.....	45
Figure 3-24 2018 Launch Option E: Projection of hyperbolas for Earth GAM.....	46
Figure 3-25 2018 Launch Option E: Doppler rate around GAM pericentres.....	46
Figure 3-26 2018 Launch Option E: Communication angles in the proximity to GAMs	48
Figure 3-27 2018 Launch Option E: ground track for first LEOP day.....	49
Figure 3-28 2018 Launch Option E: elevation from ground stations.....	50
Figure 3-29 2018 Launch Option E: slant-range, Doppler and Doppler-rate at first acquisition	51
Figure 3-30 2018 Launch Option E: Earth, Sun & S/C relative geometry at early LEOP.....	51
Figure 3-31 2018 Launch Option E: communication angles in the first 24 hours of LEOP	52
Figure 3-32 Solar Orbiter Star Tracker Configuration (extracted from [30])	52
Figure 3-33 2018 Launch Option E: distances applicable to METIS cap ejection	53
Figure 3-34 2018 Launch Option D: V-infinity diagram	56
Figure 3-35 2018 Launch Option D: X-Y Trajectory projection from launch until GAM-V2	57
Figure 3-36 2018 Launch Option D: X-Y Trajectory projections from Launch to End of Mission	58
Figure 3-37 2018 Launch Option D: X-Z and Y-Z Trajectory projections.....	58
Figure 3-38 2018 Launch Option D: Science orbits projection in the Sun-Earth rotating frame.....	59
Figure 3-39 2018 Launch Option D: Spacecraft distance to Sun, Venus and Earth	59
Figure 3-40 2018 Launch Option D: SSE and SES angles.....	60
Figure 3-41 2018 Launch Option D: SSE and SES angles – Detail of conjunctions	60
Figure 3-42 2018 Launch Option D: Variation of Earth-Spacecraft range-rate.....	61
Figure 3-43 2018 Launch Option D: Variation of Earth-Spacecraft Doppler.....	62
Figure 3-44 2018 Launch Option D: Variation of Earth-Spacecraft Doppler-rate.....	62



Figure 3-45 2018 Launch Option D: Spacecraft solar latitude + Spacecraft distance to the Sun	64
Figure 3-46 2018 Launch Option D: projection of science orbits wrt Sun Equator and North Pole.....	64
Figure 3-47 2018 Launch Option D: Evolution of apses and points of extreme solar latitude	65
Figure 3-48 2018 Launch Option D: Evolution of time spent below different Sun ranges.....	66
Figure 3-49 2018 Launch Option D: Spacecraft rotation velocity about the Sun	67
Figure 3-50 2018 Launch Option D: Evolution of Earth distance and potential downlink.....	67
Figure 3-51 2018 Launch Option D: Spacecraft equatorial declination.....	68
Figure 3-52 2018 Launch Option D: Daily period of visibility from ESA DS stations.	69
Figure 3-53 2018 Launch Option D: Daily duration of visibility from ESA Deep Space stations	70
Figure 3-54 2018 Launch Option D: Daily period of visibility from ESA Deep Space stations.	70
Figure 3-55 2018 Launch Option D: Projection of hyperbolas for Venus GAMs	72
Figure 3-56 2018 Launch Option D: Projection of hyperbolas for Earth GAMs.....	72
Figure 3-57 2018 Launch Option D: Doppler rate around GAM pericentres	73
Figure 3-58 2018 Launch Option D: ground track for first LEOP day	74
Figure 3-59 2018 Launch Option D: elevation from ground stations	75
Figure 3-60 2018 Launch Option D: Earth, Sun & S/C relative geometry at early LEOP	75
Figure 3-61 2018 Launch Option D: distances applicable to METIS cap ejection	76
Figure 3-62 2018 October Launch: V-infinity diagram for the sequence of resonances	79
Figure 3-63 2018 October Launch: X-Y Trajectory projections from Launch to End of Mission.....	80
Figure 3-64 2018 October Launch: X-Z and Y-Z Trajectory projections	80
Figure 3-65 2018 October Launch: Spacecraft distance to Sun, Venus and Earth.....	81
Figure 3-66 2018 October Launch: SSE and SES angles.....	81
Figure 3-67 2018 October Launch: SSE and SES angles – Detail of conjunctions	82
Figure 3-68 2018 October Launch: Variation of Earth-Spacecraft range-rate	83
Figure 3-69 2018 October Launch: Variation of Earth-Spacecraft Doppler	83
Figure 3-70 2018 October Launch: Variation of Earth-Spacecraft Doppler-rate.....	84
Figure 3-71 2018 October Launch: Spacecraft solar latitude + Spacecraft distance to the Sun	85
Figure 3-72 2018 October Launch: projection of science orbits wrt Sun Equator and North Pole.....	85
Figure 3-73 2018 October Launch: Evolution of apses and points of extreme solar latitude	86
Figure 3-74 2018 October Launch: Evolution of time spent below different Sun ranges.....	87
Figure 3-75 2018 October Launch: Spacecraft rotation velocity about the Sun	88
Figure 3-76 2018 October Launch: Evolution of Earth distance and potential downlink.....	88
Figure 3-77 2018 October Launch: Spacecraft equatorial declination.....	89
Figure 3-78 2018 October Launch: Daily period of visibility from Malargüe.....	90
Figure 3-79 2018 October Launch: Daily period of visibility from Cebrosos.....	90
Figure 3-80 2018 October Launch: Daily period of visibility from New Norcia.....	90
Figure 3-81 2018 October Launch: Daily duration of visibility from ESA Deep Space stations	91
Figure 3-82 2018 October Launch: Daily period of visibility from ESA Deep Space stations.	91
Figure 3-83 2018 October Launch: Projection of hyperbolas for Venus GAMs	93
Figure 3-84 2018 October Launch: Projection of hyperbolas for Earth GAMs.....	93
Figure 3-85 2018 October Launch: Doppler rate around GAM pericentres	94
Figure 3-86 2018 October Launch: ground track for first LEOP day	95
Figure 3-87 2018 October Launch: elevation from ground stations	95
Figure 3-88 2018 October Launch: Earth, Sun & S/C relative geometry at early LEOP.....	96
Figure 3-89 2018 October Launch: distances applicable to METIS cap ejection	96
Figure 3-90 2019 & 2020 February Launch: V-infinity diagram.....	100
Figure 3-91 2019 & 2020 February Launch: X-Y Trajectory projection from launch until GAM-V2	101
Figure 3-92 2019 & 2020 February Launch: X-Y Trajectory projections	102
Figure 3-93 2019 & 2020 February Launch: X-Z and Y-Z Trajectory projections	102



Figure 3-94 2019 & 2020 February Launch: Science orbits projection in the Sun-Earth rotating frame	103
Figure 3-95 2019 & 2020 February Launch: Spacecraft distance to Sun, Venus and Earth	103
Figure 3-96 2019 & 2020 February Launch: SSE and SES angles	104
Figure 3-97 2019 & 2020 February Launch: SSE and SES angles – Detail of conjunctions.....	104
Figure 3-98 2019 & 2020 February Launch: Variation of Earth-Spacecraft range-rate	105
Figure 3-99 2019 & 2020 February Launch: Variation of Earth-Spacecraft Doppler	106
Figure 3-100 2019 & 2020 February Launch: Variation of Earth-Spacecraft Doppler-rate	106
Figure 3-101 2019 & 2020 February Launch: Spacecraft solar latitude + distance to Sun.....	108
Figure 3-102 2019 & 2020 February Launch: projection of science orbits wrt Sun Equator and North Pole.....	108
Figure 3-103 2019 & 2020 February Launch: Evolution of apses and points of extreme solar latitude	109
Figure 3-104 2019 & 2020 February Launch: Evolution of time spent below different Sun ranges ...	110
Figure 3-105 2019 & 2020 February Launch: Spacecraft rotation velocity about the Sun.....	111
Figure 3-106 2019 & 2020 February Launch: Earth distance and potential daily downlink	111
Figure 3-107 2019 & 2020 February Launch: Spacecraft equatorial declination.	112
Figure 3-108 2019 & 2020 February Launch: Daily period of visibility from ESA DS stations.....	113
Figure 3-109 2019 & 2020 February Launch: Daily duration of visibility from ESA DS stations.	114
Figure 3-110 2019 & 2020 February Launch: Daily period of visibility from ESA DS stations.....	114
Figure 3-111 2019 February Launch: Daily period of visibility during 1-year parking orbit.	115
Figure 3-112 2019 February Launch: Daily duration of visibility during 1-year parking orbit.	116
Figure 3-113 2019 February Launch: Daily period of visibility during 1-year parking orbit.	116
Figure 3-114 2019 & 2020 February Launch: Projection of hyperbolas for Venus GAMs.....	118
Figure 3-115 2019 & 2020 February Launch: Projection of hyperbolas for Earth GAMs	118
Figure 3-116 2019 & 2020 February Launch: Doppler rate around GAM pericentres.....	119
Figure 3-117 2020 February Launch: ground track for first LEOP day.....	120
Figure 3-118 2020 February launch: elevation from ground stations	120
Figure 3-119 2020 February launch: Earth, Sun & S/C relative geometry at early LEOP.	121
Figure 3-120 2019 February Launch: ground track for first LEOP day.....	122
Figure 3-121 2019 February launch: elevation from ground stations	122
Figure 3-122 2019 February launch: Earth, Sun & S/C relative geometry at early LEOP.	123
Figure 3-123 2020 February Launch: distances applicable to METIS cap ejection.....	124
Figure 3-124 Evolution of perihelion radius	126
Figure 3-125 Evolution of solar inclination	126
Figure 3-126 Evolution of potential science data return	127
Figure 3-127 Evolution of integrated $(1/R_{\text{sun}})^2$	127
Figure 4-1 2018 Option E launch window: variation of launch infinite velocity and DLA.....	130
Figure 4-2 2018 Option E launch window: variation of Venus infinite velocity and final solar inclination.....	131
Figure 4-3 2018 Option E launch window: variation of minimum and maximum Sun distances.	131
Figure 4-4 2018 Option E launch window: variation of perihelion radius of science orbits.....	131
Figure 4-5 2018 Option E launch window: variation of eclipses duration and longest eclipse	132
Figure 4-6 2018 Option E launch window: variation of longest safe-mod blackout and solar conjunction periods.....	132
Figure 4-7 2018 Option E launch window: variation of minimum altitude at all GAMs	133
Figure 4-8 2018 Option E launch window: evolution of angles from Star Tracker bore sight to Earth and Moon limbs in the nominal attitude.....	134
Figure 4-9 2018 Option E launch window: evolution of angles from Star Tracker bore sight to Earth and Moon limbs in the alternative attitude	134



Figure 4-10 2018 Option D launch window: Launch targets and solar inclination.....	137
Figure 4-11 2018 Option D launch window: Perihelion of science orbits and maximum Sun distance	137
Figure 4-12 2018 Option D launch window: GAM eclipse duration and minimum altitude.....	137
Figure 4-13 2018 Option D launch window: evolution of angles from Star Tracker bore sight to Earth and Moon limbs in the nominal attitude	138
Figure 4-14 2018 Option D launch window: evolution of angles from Star Tracker bore sight to Earth and Moon limbs in the alternative attitude	138
Figure 4-15 2018 October launch window: variation of launch infinite velocity	141
Figure 4-16 2018 October launch window: variation of maximum Sun distance.....	141
Figure 4-17 2018 October launch window: variation of perihelion radius and GAM fly-by altitude.....	141
Figure 4-18 2018 October launch window: variation of GAM eclipses and occultations	141
Figure 4-19 2018 October launch window: evolution of angles from Star Tracker bore sight to Earth and Moon limbs in the nominal attitude	142
Figure 4-20 2018 October launch window: evolution of angles from Star Tracker bore sight to Earth and Moon limbs in the alternative attitude	142
Figure 4-21 2019 February launch window: launch targets and solar inclination	145
Figure 4-22 2019 February launch window: Altitude and eclipse duration at GAM-E1	146
Figure 4-23 2019 February launch window: perihelion and aphelion radius of 1-year heliocentric parking orbit	146
Figure 4-24 2019 February launch window - Outwards: evolution of angles from Star Tracker bore sight to Earth and Moon limbs in the nominal attitude.....	147
Figure 4-25 2019 February launch window - Outwards: evolution of angles from Star Tracker bore sight to Earth and Moon limbs in the alternative attitude.....	147
Figure 4-26 2019 February launch window - inwards: evolution of angles from Star Tracker bore sight to Earth and Moon limbs in the nominal attitude	148
Figure 4-27 2019 February launch window - inwards: evolution of angles from Star Tracker bore sight to Earth and Moon limbs in the alternative attitude	148
Figure 4-28 2020 February launch window: launch targets and solar inclination	150
Figure 4-29 2019/2020 February launch window: Perihelion of science orbits.....	151
Figure 4-30 2019/2020 February launch window: GAM eclipse duration and minimum altitude	151
Figure 4-31 2019/2020 February launch window: longest safe mode blackout.....	151
Figure 4-32 2020 February launch window: evolution of angles from Star Tracker bore sight to Earth and Moon limbs in the nominal attitude.....	152
Figure 4-33 2020 February launch window: evolution of angles from Star Tracker bore sight to Earth and Moon limbs in the alternative attitude	152
Figure 5-1 Evolution of knowledge and dispersion errors after launch (2018 Option E)	160
Figure 5-2 B-plane 3- σ delivery ellipses for GAM-V1 to GAM-E1	168
Figure 5-3 B-plane 3- σ delivery ellipses for GAM-V4 to GAM-V7	169
Figure 5-4 B-plane 3- σ delivery ellipses for GAM-V8.....	170
Figure 5-5 Delta-V Sun aspect angle distributions for post-GAM clean-up TCMs.....	172
Figure 5-6 Comparison of Delta-V required for the regarded DDOR scenarios.....	177



LIST OF TABLES

Table 2-1 Evolution of Earth phasing for various Venus resonant orbits	21
Table 3-1 2018 Launch Option E: Deterministic Delta-V Manoeuvres.....	24
Table 3-2 2018 Launch Option E: trajectory Summary	25
Table 3-3 2018 Launch Option E: Mission Parameters	25
Table 3-4 2018 Launch Option E: Solar Conjunction Periods.....	32
Table 3-5 2018 Launch Option E: Longest periods of communications blackout if S/C enters safe mode (longer than 7 days only)	32
Table 3-6 2018 Launch Option E: Characteristics of perihelion and extreme points of solar latitude ..	38
Table 3-7 2018 Launch Option E: Number and duration of passes close to the Sun	39
Table 3-8 Location of ESA Deep Space Ground Stations.....	40
Table 3-9 2018 Launch Option E: Characteristics of GAMs and eclipse/occultation durations.....	44
Table 3-10 2018 Launch Option E: infinite velocity vectors and B-plane target of GAMs	45
Table 3-11 2018 Launch Option D: Trajectory Summary	55
Table 3-12 2018 Launch Option D: Mission Parameters	55
Table 3-13 2018 Launch Option D: Solar Conjunctions.....	61
Table 3-14 2018 Launch Option D: Characteristics of perihelion and extreme points of solar latitude	65
Table 3-15 2018 Launch Option D: Number and duration of passes close to the Sun.....	66
Table 3-16 2018 Launch Option D: GAM Properties	71
Table 3-17 2018 Launch Option D: infinite velocity vectors and B-plane target of GAMs	71
Table 3-18 2018 October Launch: Mission Summary	78
Table 3-19 2018 October Launch: Mission Parameters	78
Table 3-20 2018 October Launch: Solar Conjunction Periods.....	82
Table 3-21 2018 October Launch: periods of MGA safe mode blackout	82
Table 3-22 2018 October Launch: Characteristics of perihelion and extreme points of solar latitude ..	86
Table 3-23 2018 October Launch: Number and duration of passes close to the Sun.....	87
Table 3-24 2018 October Launch: Characteristics of GAMs and eclipse/occultation durations	92
Table 3-25 2018 October Launch: infinite velocity vectors and B-plane target of GAMs	92
Table 3-26 2019 & 2020 February Launch: Trajectory Summary	99
Table 3-27 2019 & 2020 February Launch: Mission Parameters	99
Table 3-28 2019 & 2020 February Launch: Solar Conjunctions	105
Table 3-29 2019 & 2020 February Launch: Characteristics of perihelion and extreme points of solar latitude	109
Table 3-30 2019 & 2020 February Launch: Number and duration of passes close to the Sun	110
Table 3-31 2019 & 2020 February Launch: GAM Properties.....	117
Table 3-32 2019 & 2020 February Launch: infinite velocity vectors and B-plane target of GAMs ...	117
Table 4-1 2018 Option E launch window: Star tracker blinding events during LEOP	135
Table 4-2 2018 Option E launch window: Launch Targets.....	136
Table 4-3 2018 Option D launch window: Star tracker blinding events during LEOP.....	139
Table 4-4 2018 Option D launch window: Launch targets	140
Table 4-5 2018 October launch window: Star tracker blinding events during LEOP.....	143
Table 4-6 2018 October launch window: Launch targets	144
Table 4-7 2019 February launch window: Star tracker blinding events during LEOP	149
Table 4-8 2019 February launch window: Launch targets	149
Table 4-9 2020 February launch window: Star tracker blinding events during LEOP	153
Table 4-10 2020 February launch window: Launch targets	153



Table 4-11 Summary of launch windows parameters	155
Table 5-1 Timeline for GAM operations – inbound Venus GAM or Earth GAM.....	158
Table 5-2 Timeline for GAM operations – outbound Venus GAM.....	158
Table 5-3 Assumptions for the orbit determination and navigation models	159
Table 5-4 Requirements on launch vehicle injection errors from LIRD [18]	160
Table 5-5 Navigation analysis: times and geometry properties of TCMs	162
Table 5-6 Navigation analysis: TCM Delta-V statistics (DDOR Cebreros-Malargüe only).....	164
Table 5-7 Navigation analysis: B-plane delivery errors (DDOR Cebreros-Malargüe only).....	166
Table 5-8 Navigation analysis: accumulated Delta-V statistics	170
Table 5-9 Navigation analysis: B-plane delivery errors.....	171
Table 5-10 Navigation analysis: accumulated Delta-V statistics for increased NGA of $2 \cdot 10^{-11} \text{ km/s}^2$	173
Table 5-11 Navigation analysis: B-plane delivery errors for increased NGA of $2 \cdot 10^{-11} \text{ km/s}^2$	174
Table 5-12 Navigation analysis: orbital errors achieved after each GAM	175
Table 5-13 Navigation analysis: accumulated Delta-V statistics for “Mixed” 1-DDOR-baseline strategy.	176
Table 5-14 Parasitic Delta-V for thruster failure.....	177
Table 5-15 Navigation results in case of thruster failure at GAM-E1 and at GAM-V5	178
Table 6-1 Delta-V Budget	180
Table 8-1 Description of OEM files accompanying this document	186
Table 10-1 2018 Launch Option E: remote sensing windows from GAM-E1 to GAM-V4	188
Table 10-2 2018 Launch Option E: remote sensing windows from GAM-V4 to GAM-V5.....	189
Table 10-3 2018 Launch Option E: remote sensing windows from GAM-V5 to GAM-V7.....	190
Table 10-4 2018 Launch Option E: remote sensing windows from GAM-V7 to GAM-V8.....	191
Table 10-5 2018 Launch Option E: remote sensing windows from GAM-V8 to end of mission.....	192
Table 10-6 2018 Launch Option D: remote sensing windows from GAM-E1 to GAM-V2.....	192
Table 10-7 2018 Launch Option D: remote sensing windows from GAM-V2 to GAM-V3	193
Table 10-8 2018 Launch Option D: remote sensing windows from GAM-V3 to GAM-V4	194
Table 10-9 2018 Launch Option D: remote sensing windows from GAM-V4 to mission end.....	195
Table 10-10 2019/2020 February Launch: remote sensing windows from GAM-E1 (GAM-E2 in 2019) to GAM-V3	196
Table 10-11 2019/2020 February Launch: remote sensing windows from GAM-V3 to GAM-V4.....	197
Table 10-12 2019/2020 February Launch: remote sensing windows from GAM-V4 to GAM-V5.....	198
Table 10-13 2019/2020 February Launch: remote sensing windows from GAM-V5 to GAM-V7.....	199
Table 10-14 2019/2020 February Launch: remote sensing windows from GAM-V7 to mission end .	200



ACRONYMS AND ABBREVIATIONS

AOS	Acquisition of Signal	LOS	Loss of Signal
AU	Astronomical Unit (1 AU = 149597870.66 km)	LST	Local Solar Time
BECO	Booster Engine Cut-Off (Atlas V)	LV	Launch Vehicle
CCAM	Collision and Contamination Avoidance Maneuver (Atlas V)	MECO	Main Engine Cut-Off (Atlas V)
CPS	Chemical Propulsion System	EME2000	Earth's Mean Equator and Equinox of J2000.0 reference frame (also referred as J2000 reference frame)
CReMA	Consolidated Report on Mission Analysis	MES	Main Engine Start (Atlas V)
CSG	French Guiana Space Center	MGA	Medium Gain Antenna
ΔDOR	Double Differential One-way Range (or DDOR)	MJD2000	Modified Julian Date 2000 (Days from 2000-01-01 at 00:00)
DLA	Declination of Launch Asymptote	NASA	National Aeronautics and Space Administration
DLi	Downlink Index	NECP	Near Earth Commissioning Phase
DSM	Deep Space Manoeuvre	NGA	Non-Gravitational Accelerations
DSN	Deep Space Network	NMP	Nominal Mission Phase
EELV	Evolved Expendable Launch Vehicle	NNO	New Norcia
EAP	Etage d'Acceleration a Poudre = Solid Acceleration Boosters (Ariane 5)	OEM	Orbit Ephemeris Message
EEM	End of Extended Mission	PLF	Payload Fairing (Atlas V)
EMP	Extended Mission Phase	Ra	Radius at Aphelion
ENM	End of Nominal Mission	RCS	Reaction Control (Sub)system
EPC	Etage Principal Cryogenique = Main Cryogenic Stage (Ariane 5)	RLA	Right Ascension of Launch Asymptote
ESA	European Space Agency	Rp	Radius at Perihelion
ESC-A	Etage Supérieur Cryogenique – A = Upper Cryogenic Stage (Ariane 5)	S/C	Spacecraft
ESOC	European Space Operations Centre	SA	Solar Array
ESTEC	European Space Research and Technology Centre	SAA	Solar Aspect Angle
ESTRACK	ESA Tracking Station Network	Solo	Solar Orbiter
GAM	Gravity Assist Manoeuvre	SRB	Solid Rocket Boosters (Atlas V)
GTO	Geostationary Transfer Orbit	SSRD	Space Segment Requirements Document
HGA	High Gain Antenna	SWT	Science Working Team
HPBW	Half Power Beam Width	TBC	To Be Confirmed
ICRF	International Celestial Reference Frame	TBD	To Be Defined
i_{ecl}	Ecliptic Inclination	TCM	Trajectory Correction Manoeuvre
i_s	Solar Inclination, Inclination wrt Sun Equator	ULA	United Launch Alliance
KSC	Kennedy Space Centre	V_{∞}	Infinite Velocity or V-infinity
LEOP	Launch and Early Orbit Phase	WOL	Wheel-Offloading
LIRD	Launch Vehicle Interface Requirements Document	wrt	With respect to
		ω	Rotation velocity



1 INTRODUCTION

1.1 *Purpose and Scope*

The scope of this document is to present the mission analysis work performed by ESA OPS-GFA at ESOC for the Solar Orbiter mission studies.

This document presents full analysis of the trajectories currently considered for the Solar Orbiter (Solo) mission. Currently the only regarded launch vehicle is a NASA-provided Atlas V 411 to be launched from Kennedy Space Centre (KSC).

Thorough analysis was performed during 2015 and 2016 by the Solar Orbiter ESA team in coordination with the science instrument's principal investigators to find alternative trajectories for the 2018 launch opportunity and adequate backup options in 2019 and 2020.

This document contains the description of the following trajectories:

- 2018 October: this is the current contractual baseline for the spacecraft manufacture and for the launch contracts.
- 2018 Option D: a modification of the previous 2018 October launch option in order to produce a dramatic improvement of the overall science data return. In fact, this option offers the highest capability of data return of all known trajectories for Solar Orbiter.
- 2018 Option E: a trajectory based on a novel cruise phase making use of multiple Venus GAMs before a single Earth GAM that allows a very fast start of the science operations and offers as well a large improvement in terms of data return as compared to 2018 October. This is in fact the trajectory endorsed by the Solar Orbiter SWT and currently regarded as baseline. This document focuses more on the description of this trajectory.
- 2019 February: allowing launch 4 months later than the baseline, it actually uses the same trajectory as in 2020 February, but launching 1 year earlier into an heliocentric 1:1 Earth resonant "parking orbit".
- 2020 February launch: allowing launch 16 months later than the baseline, this trajectory requires a short cruise phase and provides very good performance in terms of science and data return.

1.2 *Structure of the Document*

Section 2 reviews the mission design driver requirements and describes the mission baseline.

Section 3 presents the analysis of a reference trajectory from launch to end of mission for each of the regarded launch opportunities.

Section 4 analyses the launch windows for each launch opportunity.

Section 5 presents the results of the navigation analysis for the mission.

Section 6 summarises the Delta-V budget.



1.3 Reference Documents

1. J. Martí-Canales, *Solar Orbiter Mission Requirements Document*, SOL-EST-RS-49, Issue 4, Rev 1, 12 Dec. 2007.
2. D. Müller, R.G. Marsden, *Solar Orbiter Science Requirements Document*, SOL-EST-RS-185, Oct 2010.
3. J. Rodríguez-Canabal, *Solar Orbiter. Mission Analysis for Launch 2017-2018. Mission Analysis Report*, SOL-ESC-RP-GFA-JRC-MAD, Draft, June 2009.
4. J. M. Sanchez Perez, *Solo Mission Design: Transfer Options with Launch in 2017-2018*, OPS/GFA WP 546, Issue 2, Rev. 0, May. 2011.
5. I. Tanco, *Solar Orbiter Preliminary Operational concept for Gravity Assist Manoeuvres*, SOL-ESC-ME-00001, 29 Nov. 2010.
6. CCSDS, *Orbit Data Messages. Blue Book*, CCSDS 502.0-B-2, Issue 2. November 2009 (<http://public.ccsds.org/publications/BlueBooks.aspx>)
7. COSPAR/IAU Workshop on Planetary Protection, *COSPAR PLANETARY PROTECTION POLICY*, 20 October 2002; As Amended to 24 March 2011.
8. United Launch Alliance, *Atlas V Launch Services User's Guide*, Revision 11, March 2010.
9. E. Haddox, J. Ollivierre, *Solar Orbiter Preliminary Launch Vehicle Performance & Trajectory Assessment*, NASA/KSC/VA-H1/EMH, Rev. 1, 2011-10-18 – ITAR restricted.
10. G.J. O'Neil, D. Piryk – Thermal Analysis Group, *Solar Orbiter PRE-ATP/PRE-ITA Trajectory Profiles*, Presentation, LSP-F-325.06, Rev. B, June 2012.
11. United Launch Alliance - E. Haddox, *Solar Orbiter – Preliminary Injection Accuracy Assessment*, Rev. 1, Dec. 2011 – ITAR restricted/ULA proprietary.
12. Arianespace, *Ariane 5 User's Manual*, Issue 5 Revision 1, July 2011.
13. Arianespace, *Feasibility mission analysis, Trajectory & performance study, ExoMars mission on A5-ECA*, A5-NT-1-H-018-AE, Issue 1 rev 0, 2007-01-18.
14. Arianespace, *Feasibility mission analysis – Trajectory & performance study Laplace mission on Ariane 5-ECA*, A5-NT-1-H-049-AE, Issue 1 rev 0, 2011-03-21.
15. Arianespace, *Preliminary Mission Analysis – Trajectory & Performance Study on Ariane 5-ECA BepiColombo Mission*, A5-DAMP-1/50760-H-02-AE, Issue 2, Rev. 0, 2011-10-19.
16. J.M. Sánchez Pérez, *Solar Orbiter: backup launch options with Ariane 5*, HSO-GFA WP574, Issue 1, Rev. 1, 2012-03-12.
17. J.M. Sánchez Pérez, *Memo - Solar Orbiter : LEOP analysis*, SOLO-HSO-GFA-MEM-2011-1, 2011-12-14.
18. Astrium, *Solar Orbiter Launch Vehicle Interface Requirements Document (LIRD)*.
19. S. Strandmoe, *Solar Orbiter Space Segment Requirements Document*, SOL-EST-RS-1717, Issue 3, Rev 5, October 2015.
20. E. Haddox, J. Ollivierre, *Solar Orbiter Preliminary Launch Vehicle Performance & Trajectory Assessment*, NASA/KSC/VA-H1/JCO, Rev. 1, 2013-02-26 – ITAR restricted.
21. J.M. Sánchez Pérez, *Solar Orbiter: analysis of LEOP for Atlas V 411 launches*, SOL-ESC-ME-50004, 2013-02-06.
22. J.M. Sánchez Pérez, *Solar Orbiter: On raising the altitude of Venus GAMs*, SOL-ESC-ME-50006, Issue 1.1, 2013-10-10.
23. J.M. Sánchez Pérez, *Solar Orbiter: Launch Windows*, SOL-ESC-TN-50005, Issue 1.0, 2014-10-14.
24. Arianespace, *Feasibility mission analysis – Trajectory & performance study Solar Orbiter mission on Ariane 5-ECA*, A5-NT-1/51660-H-03-AE, Issue 1 rev 1, 2014-12-19.
25. J.M. Sánchez Pérez, W. Martens, *Solar Orbiter: 2018-2020 Launch Options Favouring Data Return*, SOL-ESC-TN-50007, Issue 2.2, 2016-03-04.



26. R. Edwards, *Atlas V 401 / 411 Solar Orbiter Observatory Leading Edge Integration Trajectory*, ULA-TP-13-272, 2013-09-18 – ITAR restricted.
27. J.M. Sánchez Pérez, *Solar Orbiter: Navigation analysis of 2017 July trajectory*, SOL-ESC-ME-50005, 2013-05-29.
28. J.M. Sánchez Pérez, *Solar Orbiter: Analysis of Delta-DOR Measurements for the Navigation of Earth Gravity Assist Manoeuvres*, SOL-ESC-ME-50003, 2013-01-14.
29. AIRBUS DEFENCE&SPACE, *Solar Orbiter Propellant & Delta-V Report*, SOL.S.ASTR.RP.00040, Issue 4, 2015-12-04.
30. AIRBUS DEFENCE&SPACE, *Solar Orbiter AOCS Assumptions*, SOL.S.ASTR.TN.00090, Issue 8.0, 2016 July.
31. E. Haddox, *Solar Orbiter Results of ULA Trajectory Study for “Option E” Launch Opportunity*, NASA Launch Services Program – Flight Dynamics Branch, 2016-04-19 – ITAR restricted.
32. J.M. Sánchez Pérez, *Solar Orbiter: METIS cap post-release trajectory analysis*, SOL-ESC-TN-50008, MAS WP-611, 2016-02-05.



2 MISSION DESIGN OVERVIEW

2.1 *Design Driver Requirements*

The Solar Orbiter mission is devoted to the exploration of the Sun and the heliosphere and will have to make observations of the Sun from close-up distances and at high solar latitudes with a 35° goal. It has undergone several mission studies in the last 10 years and has presently a consolidated design.

To address the scientific objectives [1, 2], the mission profile must allow:

- to explore the innermost regions of the solar system using both in situ and remote-sensing instruments.
- to study the Sun from close distance
- to fly by the Sun tuned as much as possible to its rotation allowing for observation of the solar surface and the space above from a near co-rotating point, and
- to provide observations of the Sun's polar regions from out of the ecliptic.
- to provide an adequate downlink capability of the data generated by the scientific payload (this point is addressed more in detail in Section 2.4)

The spacecraft itself imposes also other constraints to the mission design:

- The solar array development in order to reach close distances to the Sun is critical for the success of the mission. A low-risk approach fully based on Bepi Colombo heritage has been decided at project level. This translates into the trajectory requirement that the spacecraft shall not get closer to the Sun than 0.28 AU.
- The maximum distance to the Sun is also limited by the capabilities of the spacecraft thermal and power generation systems. The current limitation of 1.48 AU from the Sun was established by the trajectory for launch on 2018 October in the latest version of this document.
- In order to minimize the propellant on-board the spacecraft the trajectory shall be ballistic, that is, there are no sizeable deterministic deep space manoeuvres. However, typically small deterministic manoeuvres in the order of 1-3 m/s are necessary to adjust the heliocentric trajectory between 2 swing-bies of the same planet.

Furthermore, operational requirements have been also regarded for the definition of the Solar Orbiter trajectories. In particular solar superior conjunctions preventing the communication with and the command of the spacecraft in the proximity of Gravity Assist Manoeuvres (GAM) have been avoided.

In order to implement safe GAMs a minimum altitude of 350 km at the closest approach to the planet is considered as a constraint in the mission design. This value adds some margin on top of the 300 km minimum altitude for which the spacecraft is designed for. The margin is needed to account for dispersions during the actual navigation of the GAMs.

Some of the design requirements and goals are in contradiction. Thus the minimum Sun distance of 0.28 AU imposes a limitation for the closer approach and the level of co-rotation that can be achieved during the mission. The maximum angular rate that can be achieved with the minimum perihelion constraint is about 8.3 deg/day, which has to be compared to the 14 deg/day of the Sun internal rotation rate.



2.2 *Mission Baseline*

The mission is currently based on launch with a NASA-provided expendable evolved launch vehicle (EELV), Atlas V 411 version, to be launched from Kennedy Space Centre (KSC), USA.

To satisfy the mission scientific requirements, during the science phase the spacecraft shall have several orbits with a perihelion close to the 0.28 AU constraint and the inclination with respect to the solar equator (solar inclination, i_s) should reach a value above 33° . The design goal for the overall mission duration, from launch to last Venus encounter, is assumed around 10 years.

Direct injection into Solar Orbiter's operational orbit is beyond the launch vehicle performance and the capabilities of the spacecraft. The following considerations lead to a feasible trajectory solution:

1. Repeated Gravity Assist Manoeuvres (GAM) with Venus can raise the solar inclination to the required value if the arrival relative velocity with respect to Venus is larger than 18 km/s.
2. Direct injection into an Earth-Venus trajectory with that relative velocity at Venus arrival will require a hyperbolic excess velocity, V_∞ , at Earth greater than 10 km/s, which is beyond the capabilities of the LV.
3. Using a sequence of GAMs with Venus and Earth it is possible to leave Earth within the capabilities of the LV and arrive with the required high relative velocity at Venus. Of all the planets, Earth and Venus are selected because:
 - They provide solutions within a reasonable duration of the cruise phase.
 - They provide transfers compliant with the maximum distance to the Sun of 1.5 AU.
 - The gravitational attraction of Mercury is too weak to justify the added complexity of including Mercury GAM.

It has been found that the optimal interplanetary transfer trajectory is based on a launch towards Venus where the swing-by conditions are selected to follow a trajectory that returns to Earth. This Earth swing-by is already performed at a high relative velocity. By deflecting again the heliocentric trajectory and targeting Venus again, the required very high relative velocity is achieved that allows initiating the operational phase.

A strategy typically leading to good performance in terms of cruise duration and high relative velocity considers the sequence Launch-Venus-Earth-Earth-Venus. Solar inclinations of at least 33° require cruise durations over 3.2 years [4]. Fast cruise opportunities also exist with the sequence Launch-Venus-Venus-Earth-Venus allowing similar solar inclinations with cruise durations of around 2 years, but the occurrence of such trajectories is scarcer.

The initial solar inclination of the operational orbit will not have the required value, and it will be increased by selecting the orbital period of the operational orbit to be in resonance with the orbital period of Venus, and designing a sequence of GAM with Venus that will gradually increase the solar inclination. The design of the sequence of resonances with Venus is a complex trajectory problem in which the maximization of the science return and several constraints such as the minimum distance to the Sun and the avoidance of superior conjunctions near the GAMs have to be regarded. The design process for each trajectory is described in Section 3.

In general, the resonances with Venus that are mostly used for the operational orbit are the 4:3 (4 spacecraft revolutions by 3 Venus revolutions) and the 3:2. The 4:3 resonance, with a spacecraft orbit period of roughly 168 days, is typically used in the initial phase of the science mission in order to maintain the perihelion above the 0.28 AU constraint. The 3:2 resonance, with a spacecraft orbit period of 150 days, is used afterwards as it provides a faster increase of the solar inclination while the perihelion is kept closer to the Sun. However, also other Venus resonances like 1:1, 5:4 and 5:3 are of interest for some of the trajectories described in this document.



2.3 *Considerations for the end of mission*

The end of the mission requires special attention. All trajectories described in this document assume that during the science phase the spacecraft will be always injected into an orbit in resonance with Venus. However, this may not be required for the orbit achieved after the last Venus GAM. A simple alternative is to target a heliocentric orbit that is not in a “short” resonance with Venus (the targeting will try to break the resonance, but an eventual close flyby of Venus many years later is not to be discarded). This heliocentric orbit will remain stable for a long time and the spacecraft will be able to continue performing science observations until eventually propellant depletion (as wheel-offloading manoeuvres would still be required) or a critical subsystem failure lead to the mission end.

In this document it has been considered more interesting to have a final orbit that is in resonance with Venus. The mission has been analysed assuming that it will end just before the spacecraft encounters Venus again in this final orbit. Therefore, the Delta-V allocated for the mission allows navigating through all Earth and Venus GAMs until reaching this final operational orbit.

However, in the real operations the mission does not necessarily need to end before encountering Venus. In fact even after about 10 years mission the spacecraft health and remaining on-board propellant could still allow continuing the operations by performing an additional Venus GAM. The target orbit after this additional Venus GAM will have to be decided based on its science interest and the spacecraft health. Among a number of possibilities it could be decided: to increase as much as possible the solar inclination; to raise the perihelion thus trying to preserve the old spacecraft fit for a longer time; maybe even to reduce the perihelion below the 0.28 AU constraint trying to get a last set of observations from an unprecedented Sun distance even if this can cost the spacecraft. In addition the target orbit could be again in resonance with Venus and if so this would leave the possibility open for a future Venus GAM with a further mission extension, if possible.

From the trajectory point of view the last orbit in resonance with Venus gives then flexibility to continue changing the heliocentric orbit by implementing Venus GAMs, although this is subject to the condition of still having enough propellant to perform an adequate navigation. On the contrary once the spacecraft is injected into an orbit that is not in Venus resonance there will be no possibility to modify this heliocentric orbit.

A final consideration about collision with Venus: if the spacecraft loses controllability during one of the science orbits in resonance with Venus there is a certain probability that it will impact the planet. This probability will be very small assuming that the post swing-by TCM after the last Venus GAM could be performed and larger otherwise. However, the COSPAR Planetary Protection Policy [7] classify Venus as Category II body that has no specific planetary protection requirement and no mitigation measures have to be taken to prevent a collision. The Planetary Protection Policy requires only documentation work to the mission such as the preparation of a planetary protection plan, pre- and post-launch analyses detailing impact strategies and an End-of-Mission report.



2.4 Optimization of data return

Further analysis of the October 2018 trajectory opportunity (Section 3.3) revealed an inferior data downlink capability than the previous trajectories considered for 2017 launch. This affects particularly one of the core science periods spent in a 4:3 resonant orbit (S/C:Venus revolutions) covering 1.8 years of the NMP. Improving the data downlink during this part of the mission is considered critical in order to maximize the science return and fulfil the science objectives.

The downlink capability scales approximately as $1/D^2$, where D is the distance spacecraft-Earth. With the current communications assumptions Solar Orbiter can achieve a downlink data rate of 202 kbps at a distance of 1 AU. Closer to Earth the data rate is assumed to grow up to a maximum of 998 kbps for distances below 0.45 AU.

All Solar Orbiter trajectories implement series of increasingly inclined orbits in resonance with Venus; with a 4:3 orbit (1.845 years between the two swing-bys) covering a significant period of the NMP. For instance, in the previous baseline trajectory for 2017 January, there were two successive 3:4 orbits in the NMP covering an interval of 3.69 years. This orbit has a period of 0.46 years, and a synodic period with Earth of 0.85 years, close to two full orbits (0.92 years). Therefore, relative to the Earth the orbits are seen in pairs in terms of downlink, with a “bad” orbit (5.5 months around the superior conjunction between the spacecraft and the Earth), then a “good” orbit (5.5 months around the inferior conjunction), which correspond to the closest distances and the highest downlink capability.

Thus the driver for the downlink capability of this 4:3 orbit is the true anomaly of the spacecraft at inferior conjunction: at perihelion (~ 0.3 AU from the Sun), the minimum Earth distance cannot be smaller than ~ 0.7 AU, while only at aphelion (typically 0.85 to 0.9 AU in the 4:3 orbit), the minimum distance can be below the 0.45 AU limit allowing the maximum data rate. Assuming 8 hours of daily visibility, this provides ~ 11 Gbits/day around perihelion to be compared against the maximum data return of 27.4 Gbits/day around aphelion. Even more importantly, the differential angular rotation is much larger at perihelion than at aphelion; hence the duration of the downlink peak at perihelion is much shorter, while at aphelion the maximum data rate can be sustained for a few months. Clearly trajectories aiming at downlink maximization have to use the configuration with the aphelion close to inferior conjunction.

The optimization of the data return is illustrated by the next 2 examples of 4:3 orbits of trajectories that have been considered in the Solar Orbiter mission design. A “bad” case is taken from the 2018 October trajectory scenario and a “good” case is taken from the old 2017 January baseline.

Figure 2-1 illustrates the “bad” downlink case of 2018 October trajectory. On the left, there is a projection of the 4:3 orbit (leg between 4th Venus GAM =V4 and 5th Venus GAM =V5) on the Sun-Earth rotating frame, in which the Sun and Earth are fixed and represented by yellow and blue symbols, respectively. The obvious advantage of this representation is that distances to the Sun and the Earth can be visualized simultaneously. The bad phasing with respect to the Earth becomes evident, with all 4 aphelia far away from Earth and the closest approaches occurring at every other perihelion pass. The plot to the right gives the evolution of Earth and Sun distances within the 4:3 orbits. In addition, the estimated daily data return assuming a standard 8-hour visibility pass is provided.

The important point is that the Earth distance remains above 1 AU for most of the whole “bad” orbit, peaking up to 1.7 AU at the last aphelion. The distance to Earth never gets closer than 0.7 AU, even during the perihelia close to inferior conjunction. Furthermore, the duration and extent of the dips in distance close to perihelion (which corresponds to a peak in downlink rate) during the “better” orbit is rather short. The end product is that the downlink capability of these 4:3 orbits is very low.

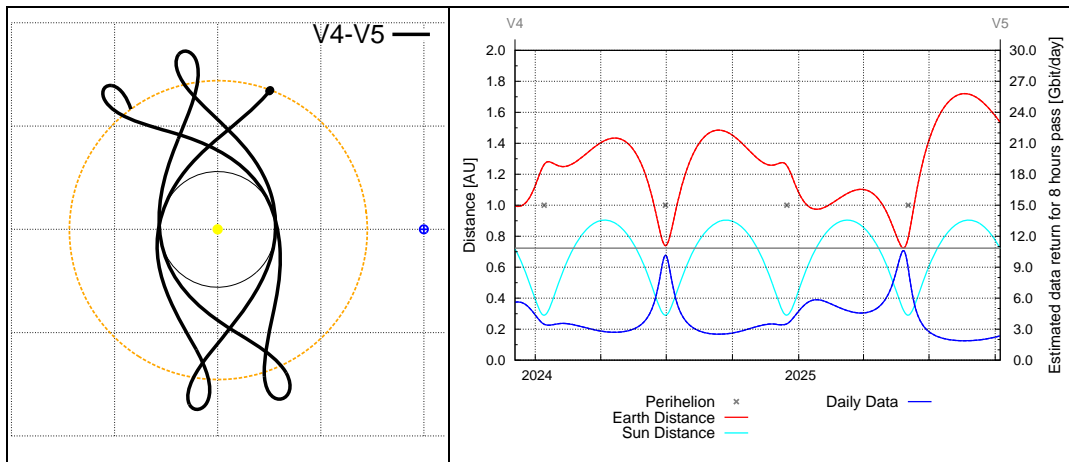


Figure 2-1 Illustration of “bad” downlink case for 4:3 orbit – 2018 October

Figure 2-2 illustrates the “good” downlink case of 2017 January. The situation is vastly improved when the inferior conjunction is close to aphelion. The first pair of orbits starts at an Earth-Sun-Venus angle (in the following ESV) of only -8° . There is a first aphelion close to superior conjunction with low downlink capability, but this is by far compensated by the next aphelion short after the inferior conjunction. Indeed the maximum data rate is maintained over a period of 2 months providing a huge downlink capability. Data acquired during the first orbit can be stored on board and transmitted during the second orbit, which has more than enough downlink capability for such extra load.

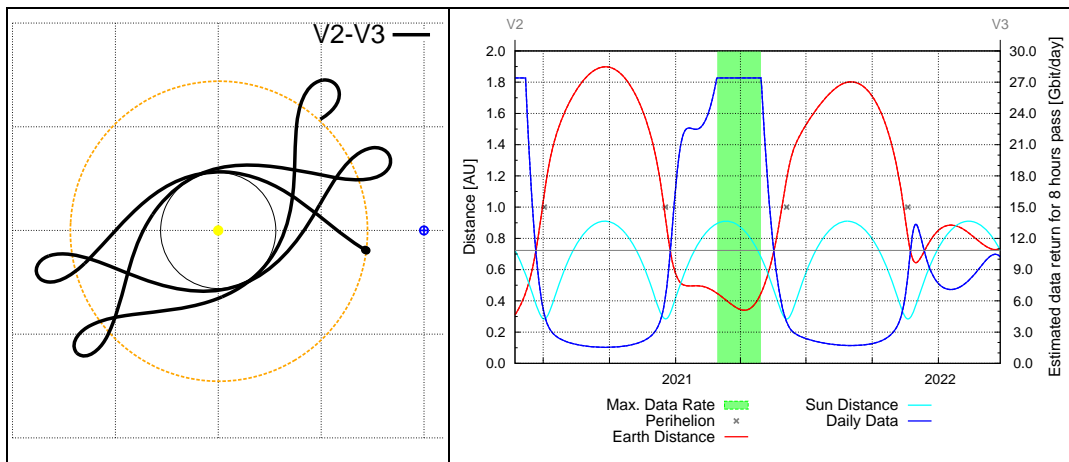


Figure 2-2 Illustration of “good” downlink case for 4:3 orbit – 2017 January

As given in the next table, the Earth-Sun-Probe angle drifted per orbit in the Venus resonant orbits regarded for Solar Orbiter is close to 180° . Particularly critical is the situation for the 4:3 resonance and even worse for the 5:4, for which the orbit period is almost in 2:1 resonance with the Earth and thus the geometry relative to Earth remains almost unchanged. A badly phased aphelion will remain so for the entire duration of the resonance. For the last resonances 3:2 and 5:3, typically used during EMP, the drift with respect to the Earth is faster so that the chances are higher that one aphelion or even two are providing a good phasing for downlink.



Venus resonance (SC:V)	Period (days)	Period (y)	Ratio with Earth	E-S-P drift per orbit (deg)	E-S-P drift per orbit vs. 180 deg (deg)	Total accumulated E-S-P drift (deg)
1:1	224.7	0.615	1.6255	138.5	-41.5	138.5
5:4	179.8	0.492	2.0319	182.8	2.8	-165.9
4:3	168.5	0.461	2.1673	193.9	13.9	55.6
3:2	149.8	0.410	2.4383	212.4	32.4	-82.9
5:3	134.8	0.369	2.7092	227.1	47.1	55.6

Table 2-1 Evolution of Earth phasing for various Venus resonant orbits

The conclusion is clear: in order to favour the science data return, the mission design shall avoid the configuration with the inferior conjunction at perihelion and aphelion far away from the Earth, especially at the 4:3 and 5:4 resonances during NMP.

An extensive trajectory search has been carried out at ESOC's Mission Analysis Section in 2015 in order to find adequate trajectories for Solar Orbiter with launch in the 2018-2020 timeframe with the focus on maximizing the overall data return capability [25]. A number of trajectories have been analysed in detail and further studied by the SWT to assess their convenience for the mission science. A down selection process lead to endorse 2 of the analysed trajectories: Options D & E, as alternative to the 2018 October trajectory described in the previous issues of the CReMA, as well as in this one.

2.4.1 DOWNLINK INDEX

It is recognized that a trajectory parameter is needed to assess the downlink capability of an orbit. A possibility is to define some assumptions in terms of bit rates and daily coverage durations and compute the total accumulated data downlinked. The problem with this approach is that the values provided will depend strongly on the communications assumptions making it complicated to perform comparisons of results computed by different teams or at different times.

Alternatively we propose to define a downlink index that is only based on geometric properties of the trajectory. This downlink index (in the following DLi) is defined as the time average of a capped $1/D^2$ function excluding the solar conjunction periods (SES angle $< 3^\circ$) as follows:

$$DL_{index} = \frac{1}{\Delta t} \int_{t_0}^{t_0+\Delta t} \frac{1}{D_*^2} dt \quad D_* = \begin{cases} D & \text{if } SES > 3 \text{ deg and } D > D_{min} \\ D_{min} & \text{if } SES > 3 \text{ deg and } D \leq D_{min} \\ \infty & \text{if } SES \leq 3 \text{ deg} \end{cases}$$

A minimum Earth distance (D_{min}) value of 0.45 AU has been used in agreement with the Earth distance limit at which the maximum data rate is assumed. In the practice the integral is computed by adding up the daily values during the computation period Δt .

The reason to average in time instead of reporting an absolute index is to allow better comparison of Venus resonant orbits with different overall durations. The DLi has units of AU^{-2} , but these units might be omitted in the following. A DLi of 1 indicates an average downlink capability corresponding to an Earth distance of 1 AU. Orbits with better downlink capability show larger values. As an example of the applicability of this index, take the “bad” and “good” 4:3 orbits of Figure 2-1 and Figure 2-2, they result in DLi of 0.88 and 1.68, respectively. So quantitatively the downlink capability of the “good” orbit is 1.91 times that of the “bad” orbit.

As an indication, assuming 8-hour daily coverage passes and a bit rate of 201.5 kbps (GMSK Turbo $\frac{1}{4}$), an orbit with a DLi of 1 will allow a data return of 2.1 Tbit per year.



3 TRAJECTORY ANALYSIS

The current mission design is considering 3 different trajectories with launch in the 2018 September-November timeframe. The launch periods of these trajectory options overlap considerably, so that they shall not be considered as possible primary and backup opportunities, but as different alternatives from which one will be finally implemented.

The 3 trajectory options currently regarded are the following, in the order of priority given by the Solar Orbiter Project Team and Solar Orbiter SWT (also the order of appearance in this chapter):

- 2018 Launch Option E: trajectory based on a fast cruise and with very good data return properties and science properties, currently regarded as baseline.
- 2018 Launch Option D: trajectory with excellent data return properties.
- 2018 October Launch: described already in previous versions of this document (CReMA 3.1) and currently the contractual baseline for the spacecraft manufacture and launch contracts.

In addition, as backup trajectories the following are regarded:

- 2020 February: trajectory with very fast cruise and excellent data return and science properties.
- 2019 February: same trajectory of 2020 February, but launched 1 year earlier and putting the spacecraft into a “parking orbit” in 1:1 resonance with Earth. Cruise is longer than in 2020 and the trajectory will have to be truncated at the end in order to comply with the lifetime requirement, but it still provides a good performance in terms of the science return.

This section provides a detailed description of a reference trajectory selected for each of the launch opportunities. The results are relevant for spacecraft design, mission science return and operations. The level of detail of the results and fidelity of the models used in the analysis can differ from one trajectory to another depending on the relevance and current status of analysis of the given option. In addition, for their commonality the 2019 and 2020 February trajectories are described in a single chapter.

A detailed analysis of the corresponding launch periods is covered by Section 4.



3.1 2018 Launch Option E

3.1.1 DESCRIPTION

This trajectory is based originally on a short EVVEV transfer that requires a rather large infinite velocity at launch. The arc from launch to Venus is direct taking about half a year and then the spacecraft needs to perform a 2:2 resonance with Venus (1.2 years) such as to provide an adequate phasing for the next Venus-Earth arc. In the real operations it is not possible to perform a 2:2 resonance with Venus unless a significant Delta-V is imparted such as to fly-by Venus at a very large distance after 1 revolution and then adjust the trajectory back to have a close fly-by at the second Venus encounter. Being Solar Orbiter trajectory ballistic and given the relatively small Delta-V capacity of the spacecraft, it has been decided to design the trajectory for 2 consecutive 1:1 Venus resonances and thus a total of 3 Venus GAMs during cruise. A disadvantage of this is the need for navigation Delta-V for the additional GAM. Designing the Venus GAMs at altitudes of several thousand km reduces the sensitivity to navigation errors thus relaxing the required Delta-V for trajectory corrections.

The maximum Sun distance in this trajectory is only 1.12 AU and is reached during the Venus-Earth arc. Therefore Solar Orbiter spacecraft should not need a hibernation phase. The perihelion sinks down to 0.346 AU after GAM-E1 allowing the start of NMP after a cruise phase of only 2.2 years. The Earth-Venus arc offers 2 perihelion passes at low solar inclination before encountering Venus in the outbound leg. This trajectory allows one of the fastest cruise phases that have been found in the analysed launch timeframe leading to a solar inclination above 33 deg in less than 10 years [25].

The sequence of resonances 4:3 3:2 3:2 5:3 3:2 has been selected to provide close perihelions below 0.3 AU for the rest of the NMP and a gradual increase of the solar inclination to 21 deg. The first 3:2 resonance of the EMP raises the perihelion to 0.326 AU with solar inclination over 28 deg and then the 5:3 resonance provides another 5 perihelion passes below 0.3 AU with an inclination over 31 deg. The final 3:2 resonance has been added after GAM-V8 to reach a final inclination close to 33 deg. The overall trajectory duration including the entire 3:2 resonance is 10.53 years.

The 4:3 science orbit is reached 3.15 years after launch with a very good phasing at an Earth-Sun-Venus angle of -27 deg that provides one of the aphelia in an almost inferior conjunction configuration. The downlink capability of this orbit is very large providing a downlink index (DLi, see Section 2.4.1) of 2.09 AU^{-2} . The following orbits provide a rather acceptable overall downlink capability.

The reference trajectory used to describe the mission in this chapter corresponds to launch on September 30th 2018. This reference transfer trajectory is described by:

1. Launch in from Earth with an escape velocity of 5.17 km/s and declination of the escape velocity of about -9°.
2. 6 months after launch, an outbound Venus GAM, with a pericentre height of more than 15000 km, injects the spacecraft into a heliocentric orbit in a 1:1 resonance with Venus.
3. 1 Venus revolution later (7.5 months) the spacecraft performs another outbound Venus GAM at an altitude of 11000 km and is inserted again in a 1:1 resonance with Venus.
4. 1 Venus revolution later (7.5 months) the spacecraft performs the third Venus GAM at an altitude of about 5800 km and is injected in an orbit towards the Earth.
5. About 6 months later and 2.25 years after launch an Earth GAM at low altitude, close to the 350 km constraint, will inject the spacecraft into the initial heliocentric operational orbit with perihelion of 0.345 AU.



6. After passing by the perihelion 2 times and describing almost 2 orbits, an outbound Venus GAM at the lowest permissible altitude (350 km) will inject the spacecraft into an heliocentric orbit in 4:3 resonance with Venus and a perihelion of 0.295 AU and solar inclination of 13 deg.
7. Outbound Venus GAMs are repeatedly used such as to have the sequence of Venus resonances 4:3 3:2 3:2 5:3 3:2 steadily increasing the solar inclination and providing good observation and data return conditions during the rest of the science mission, NMP and EMP.

The closest approach to the Sun occurs in the 3:2 resonance after GAM-V5 just grazing at the 0.28 AU constraint.

Table 3-2 and Table 3-3 present a summary of the main events/parameters of the mission.

The trajectory has been computed with high-fidelity models that include the orbit perturbations due to the planet's 3rd body effect and the solar radiation pressure. Small deterministic Delta-V manoeuvres, in the order of just a few m/s, are required to adjust the trajectory between pairs of resonant GAMs.

Table 3-1 shows the details of the deterministic manoeuvres required to adjust the trajectory. In the arcs V1-V2 and V2-V3 during the cruise, 2 small Delta-V manoeuvres are needed with a total of 2.64 m/s. During the sequence of resonances of the science phase, small Delta-V manoeuvres are always required between two Venus GAMs. Since the Venus encounters are outbound, the Delta-V manoeuvres have been placed in the last arc from aphelion to perihelion before the GAM about 20 days after the aphelion pass, which was found beneficial in terms of Delta-V. This location of the manoeuvres minimizes the interaction with science operations and increases the distance to the Sun. An exception is the Delta-V manoeuvre before GAM-V5, which has been advanced one aphelion to avoid a superior solar conjunction to occur too close to the Delta-V manoeuvre. Overall the entire trajectory requires 9.8 m/s. This value includes a last Delta-V manoeuvre of 3.6 m/s that will only be needed in case of a mission extension with the implementation of an extra GAM-V9. Deducting this last manoeuvre, the deterministic Delta-V required for the trajectory is roughly 6 m/s.

Arc	Date	Days to GAM	Rs [AU]	Delta-V [m/s]
V1-V2	2019-06-03	165	0.926	0.07
V2-V3	2020-01-17	162	0.914	2.57
E1-V4	2021-08-05	111	0.939	0.33
V4-V5	2023-01-07	265 ¹	0.819	1.92
V5-V6	2024-09-23	89	0.724	0.66
V6-V7	2025-12-09	97	0.689	0.11
V7-V8	2027-10-15	96	0.628	0.53
V8-V9	2028-12-13	120	0.642	3.57 ²

Table 3-1 2018 Launch Option E: Deterministic Delta-V Manoeuvres

¹ Located 2 aphelions before the next Venus GAM to avoid conflict with solar superior conjunction

² Only required if mission extended with an extra Venus GAM



Phase	Cruise				NMP			EMP		
Trajectory arc	L-V1	V1-V2	V2-V3	V3-E1	E1-V4	V4-V5	V5-V6	V6-V7	V7-V8	V8-End
Start	2018-09-30	2019-04-04	2019-11-14	2020-06-26	2021-01-01	2021-11-23	2023-09-28	2024-12-21	2026-03-15	2028-01-18
Flight time at start (years)	0.00	0.51	1.12	1.74	2.25	3.15	4.99	6.22	7.46	9.30
Duration (days)	185	225	225	189	327	674	449	449	674	450
Number of revolutions Venus Resonance	0	1 1:1	1 1:1	0	1	4 4:3	3 3:2	3 3:2	5 5:3	3 3:2
Period (days)	255.8	224.8	224.8	305.4	202.9	168.5	149.8	149.8	134.8	149.8
R at aphelion (AU)	1.012	0.929	0.916	1.124	1.007	0.899	0.824	0.779	0.734	0.724
R at max. latitude (AU)	0.990	0.905	0.585	0.649	0.428	0.357	0.348	0.398	0.403	0.515
R at min. latitude (AU)	0.573	0.526	0.791	1.122	0.643	0.588	0.522	0.540	0.441	0.482
R at perihelion (AU)	0.566	0.518	0.531	0.648	0.345	0.295	0.280	0.325	0.295	0.380
Perihelion latitude (deg)	-6.409	-3.297	1.955	6.338	2.084	6.270	8.489	9.979	3.135	-3.311
ω at perih. (deg/day)	2.639	2.995	2.861	2.143	5.924	7.450	7.733	5.744	6.299	4.061
Ecliptic inclination (deg)	1.92	3.74	8.92	12.21	2.51	7.73	15.93	22.72	25.78	27.50
Solar inclination (deg)	6.79	3.53	3.48	6.42	5.09	13.02	21.29	28.08	31.14	32.85
Heliolatitude > 25 deg (days/orbit)								13.1	19.5	30.7
Heliolatitude < -25 deg (days/orbit)								23.9	23.0	27.4
Downlink index (1/AU ²)	3.87	0.43	1.29	4.45	1.56	2.09	1.23	1.79	1.05	1.56

Table 3-2 2018 Launch Option E: trajectory Summary

Absolute Minimum Sun Distance (AU)	Absolute Maximum Sun Distance (AU)	Absolute Maximum Earth Distance (AU)	Maximum Solar Latitude (deg)	Maximum Angular Rate (deg/day)
0.280	1.124	2.006	-32.85	7.733
First achieved after GAM V5	Achieved after GAM V3	Achieved after GAM E1	First achieved after GAM V8	First achieved after GAM V5
2020-07-02	2020-10-25	2021-07-01	2028-03-12	2024-01-12

Table 3-3 2018 Launch Option E: Mission Parameters

Figure 3-2 shows a graphical representation that summarizes the sequence of resonances at Venus. Since the position of Venus on its orbit and the modulus of the hyperbolic velocity at GAM V2 are fixed by the second Earth-Venus arc, the only two parameters that are left to select the post-GAM heliocentric orbit are two angles defining the direction of the infinite velocity vector.

Level lines of the relevant trajectory parameters have been drawn in the V-infinity direction diagram. The two angles chosen for the representation are the right ascension and declination of the infinite velocity vector in a Sun-Venus intrinsic reference frame as shown in Figure 3-1. The right ascension α is measured in-plane from the direction of the Venus velocity vector and is positive towards the Sun. Thus, a right ascension of 0 deg means a direction along Venus velocity, -90 deg along the Sun-Venus radius (outwards), 90 deg anti-radial (inwards) and 180 deg against Venus velocity. The declination δ is the angle between the vector and Venus orbital plane.

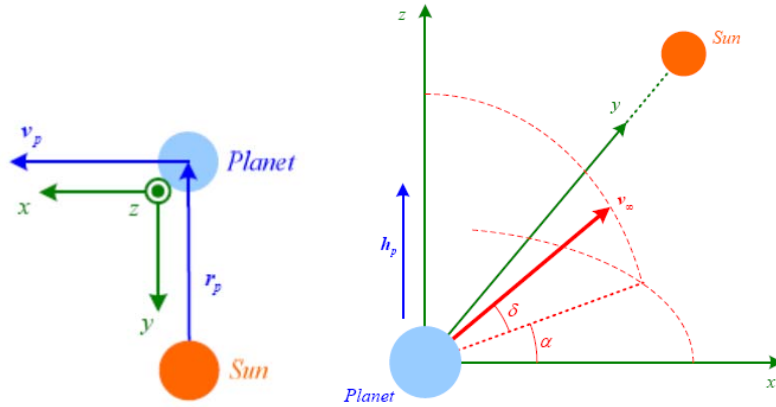


Figure 3-1 Graphical representation of the angles used in the V-infinity diagram

Five types of level lines have been plotted in Figure 3-2:

- Equal perihelion radius – red lines. The minimum perihelion constraint of 0.28 AU is represented with a thick red line.
- Equal solar inclination – green lines
- Equal rotational velocity about the Sun – magenta lines
- Equal solar latitude of the perihelion – cyan lines
- Resonance condition – blue lines: only the most relevant cases are presented 1:1, 5:4, 4:3, 3:2, 5:3 and 2:1.

One point of the diagram, represented with a cross, corresponds to the direction of the infinite velocity vector, either incoming or outgoing, and is related via the plot with the characteristics of the heliocentric orbit. A GAM produces a change of the infinite velocity vector and allows therefore moving on the diagram. GAMs are represented with an arrow from the direction of the arrival/incoming velocity pointing towards the direction of the departure/outgoing velocity vector. The displacement that a GAM can provide is limited by the maximum deflection achievable assuming a closest approach of 350 km to the Venus surface.

The sequence of resonances 4:3-3:2-3:2-5:3-3:2 used in this trajectory is presented in the figure. The circle on the top-right of the figure corresponds to the second Earth-Venus arc in which the perihelion is about 0.35 AU. The spacecraft arrives to Venus outwards (right ascension about -108 deg) with a hyperbolic velocity of 17.46 km/s. In order to maximize the increase of the solar inclination the trajectory moves in the direction towards the bottom-left corner of the plot.

From arrival to Venus the GAMs are done with maximum deflection first pushing down the perihelion through the 4:3 and the 3:2 resonances, the second one exactly at the 0.28 AU constraint. Then the sequence 3:2-5:3-3:2 aims at maintaining a low perihelion, while increasing the final solar inclination. After the last GAM an infinite velocity with a right ascension of 180 deg is achieved, indicating that the maximum possible solar inclination is reached.

It must be pointed out that there is some flexibility for the end of the trajectory. If a shorter trajectory is preferred, the EMP can be declared finished at the end of the 5:3 resonant orbits. The final solar inclination of 31.3 deg is so reached in only 7.5 years from launch and the trajectory up to this point



includes 12 perihelions below 0.3 AU and 17 below 0.35 AU in 9.3 years. The last 3:2 resonance provides an additional 1.6 deg of inclination with respect to the previous 5:3 orbit, but also raises the perihelion to 0.38 AU and increases the duration of EMP.

An alternative to the final 3:2 resonance could be a 5:3 resonance with perihelion at 0.305 AU and solar inclination of 32.3 deg, or the selection of a non-resonant orbit at the closest perihelion of 0.28 AU and solar inclination of 31.9 deg. Thus, the penalty in final solar inclination with respect to the 3:2 option is 0.6 deg for the 5:3 and 1 deg for the non-resonant.

Another alternative for the end of the mission is to select a 3:2 resonance after GAM V6 raising the perihelion to about 0.363 AU and the inclination to 31.7 deg. The advantage of doing this is that the final maximum solar inclination after GAM V7 can be reached 1 Venus revolution faster, thus advancing it by 0.6 years or from launch in only 8.7 years. It will then be natural to go for a lower perihelion for the last science orbits of the mission, either in the 5:3 resonance or in a non-resonant orbit, but GAM-V7 would not produce a significant inclination gain. These alternatives are illustrated in the V-infinity diagram (Figure 3-2) with grey arrows.

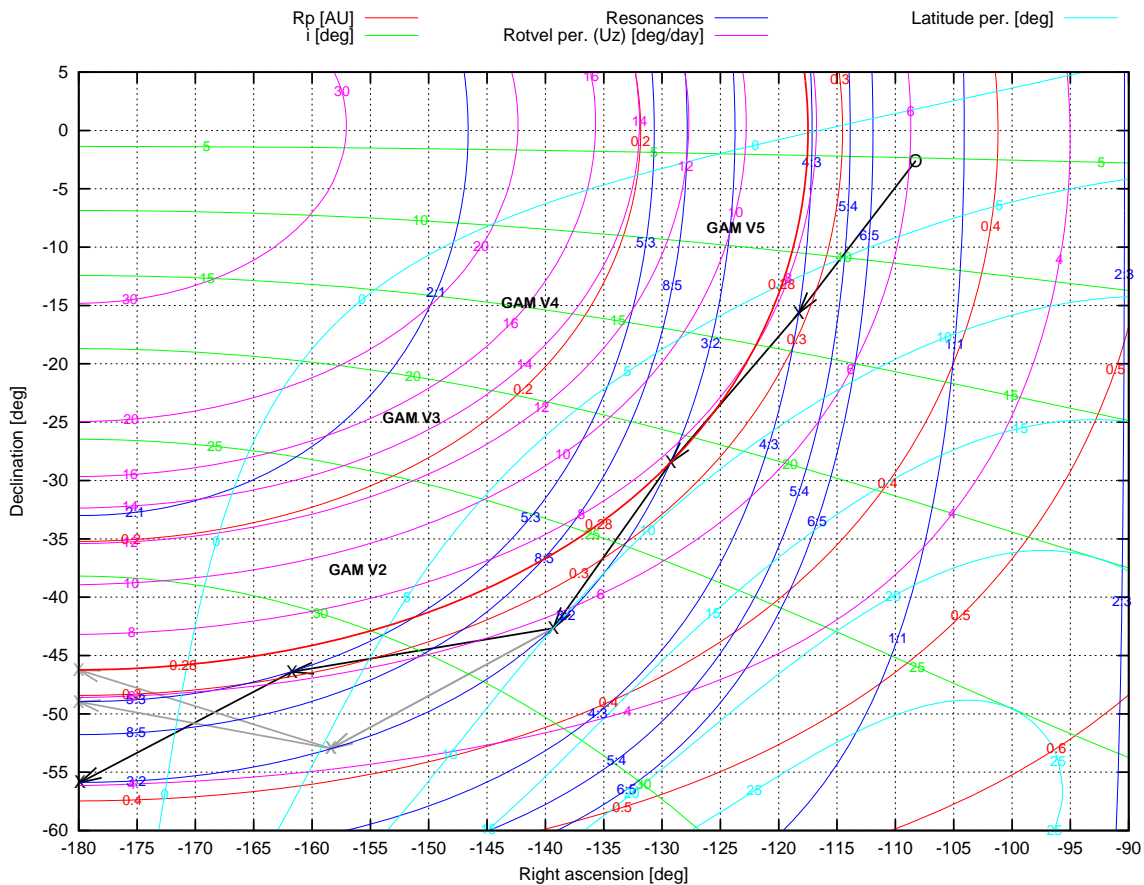


Figure 3-2 2018 Launch Option E: V-infinity diagram for the sequence of resonances



Trajectory Plots

Figure 3-3 shows the X-Y trajectory projection from launch until GAM-V4, which includes the cruise phase and the Earth-Venus arc until the first GAM at Venus initiating the sequence of resonances for the science phase. In this plot the green lines indicate the location of Venus that are optimal to increase the solar inclination of the heliocentric orbit, while the red lines indicate the points of Venus orbit that are the worst for a given hyperbolic velocity. Though GAM-V4 is not located at a particularly sweet point (but still closer to the optimal than to the worst case) and the moderate infinite velocity of 17.5 km/s, it is possible to reach a solar inclination of 33 deg by the end of the mission. This can be achieved because the longer science phase allows reaching the 3:2 resonance with the maximum solar inclination. Previous trajectories regarded for Solar Orbiter typically made use of higher infinite velocities (even > 20 km/s), which did not allow reaching the maximum possible solar inclination within the mission lifetime.

Figure 3-4 shows the X-Y projection of the entire trajectory on the ecliptic plane and the ecliptic rotating plane with Sun at the origin and the Earth always on the positive X-axis. Different colours have been used to represent the arcs of the trajectory between GAMs. Figure 3-5 shows the projection of the trajectory on the ecliptic system (X,Z)-plane and (Y,Z)-plane, respectively.

Figure 3-6 shows the projection of each of the science orbits in the Sun-Earth rotating frame. GAM-V3 at an Earth-Sun-Venus angle of -27° is close to a downlink best case for a 4:3 orbit: an aphelion at 0.45 AU from Earth comes immediately after the GAM and the second next aphelion is shifted to an inferior conjunction geometry getting as close as 0.15 AU from Earth. The maximum data rate can be sustained for about 4 months largely contributing to the remarkable 2.09 AU^{-2} DLI provided by this 4:3.

The first of the 3:2 resonances starts at ESV angle of 29° providing again good downlink conditions during the first aphelion after V4. The orbit then drifts to bad downlink geometry with minimum Earth distance at perihelion, but the DLI in the first 3:2 orbit is still 1.23. The second 3:2 orbit is well suited for downlink thanks to the Earth-close aphelion that provides a 2-month period with maximum data rate. Of the last two resonances, the 5:3 is less favourable for downlink and the last 3:2 resonance also provides an aphelion close to Earth and a period of about 45 days under the maximum data rate.

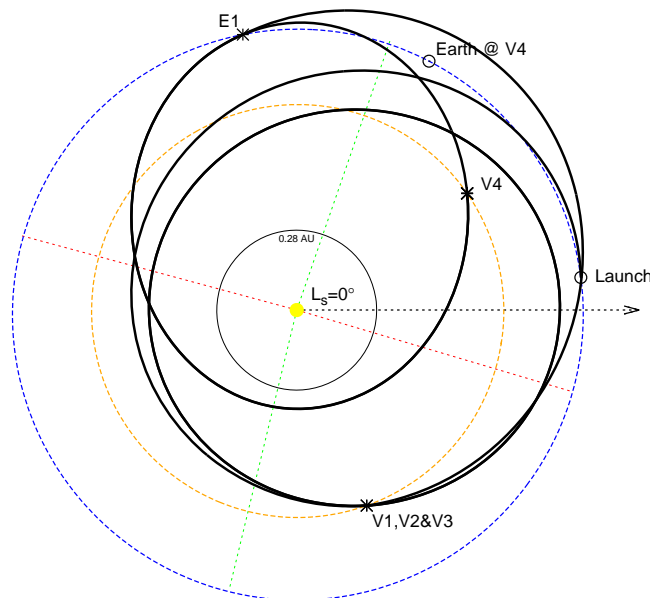
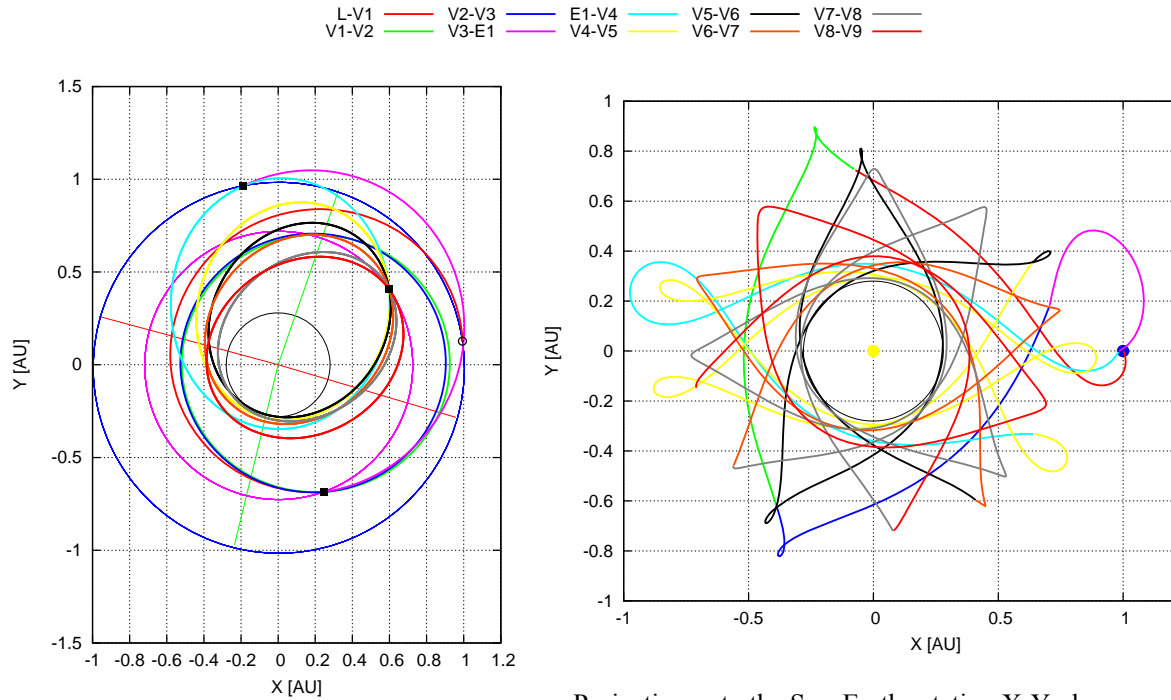


Figure 3-3 2018 Launch Option E: X-Y Trajectory projection from launch until GAM-V4



Projection onto the ecliptic X-Y plane

Projection onto the Sun-Earth rotating X-Y plane
The X-axis (Y=0) is the line from the Sun to the Earth

Figure 3-4 2018 Launch Option E: X-Y Trajectory projections from Launch to End of Mission

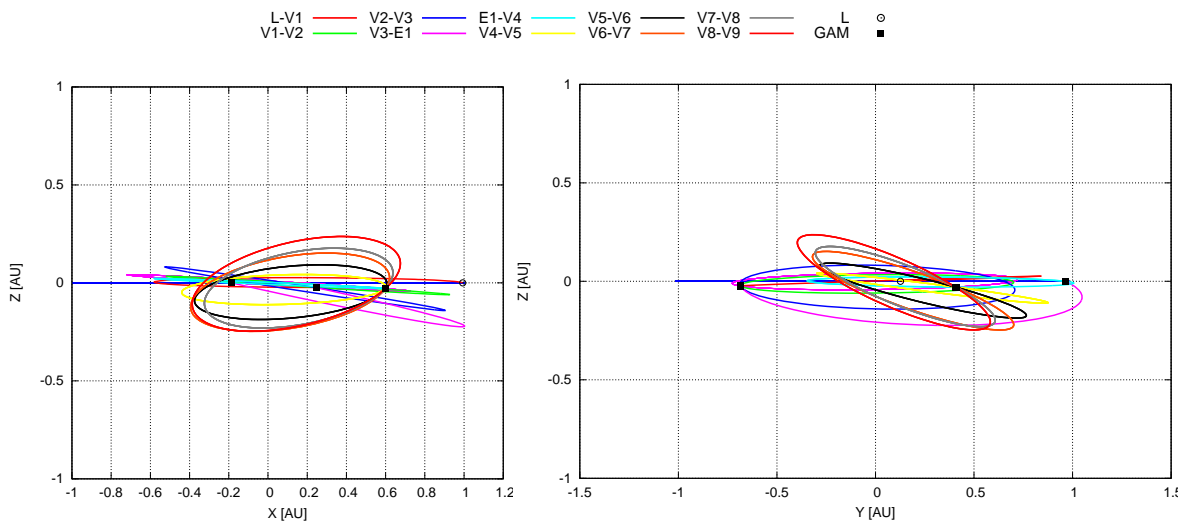


Figure 3-5 2018 Launch Option E: X-Z and Y-Z Trajectory projections

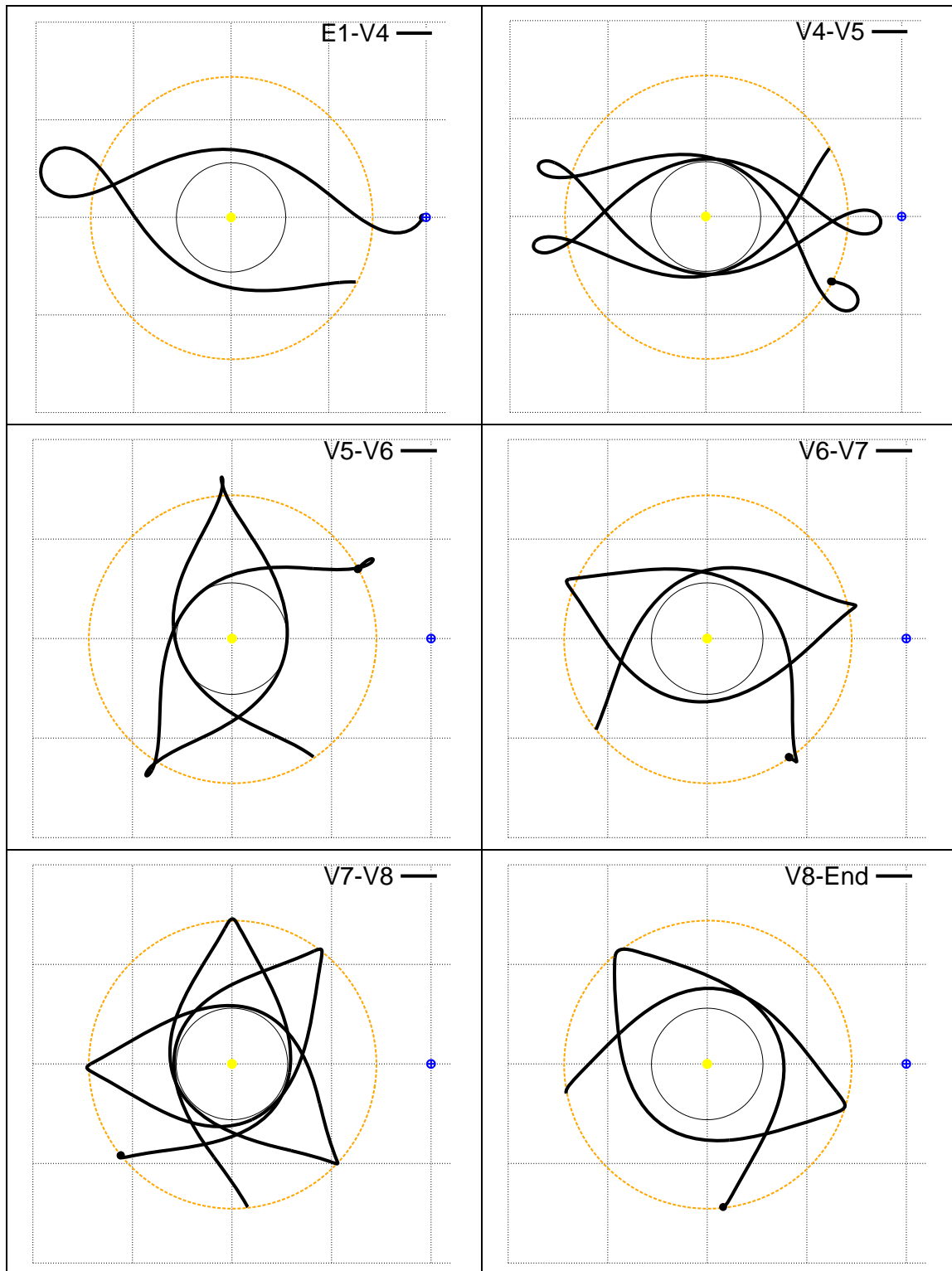


Figure 3-6 2018 Launch Option E: Science orbits projection on the Sun-Earth rotating frame



Figure 3-7 shows the evolution of the distance to the Sun, Earth and Venus and Figure 3-8 shows the evolution of the Sun-Spacecraft-Earth and Sun-Earth-Spacecraft angles. Figure 3-9 zooms on the region below 10 deg to show more clearly the solar conjunctions, which occur outside the GAM events. Table 3-4 provides a summary of the solar conjunction periods. For this trajectory 8 solar superior conjunctions are encountered, the longest of them lasting 25 days.

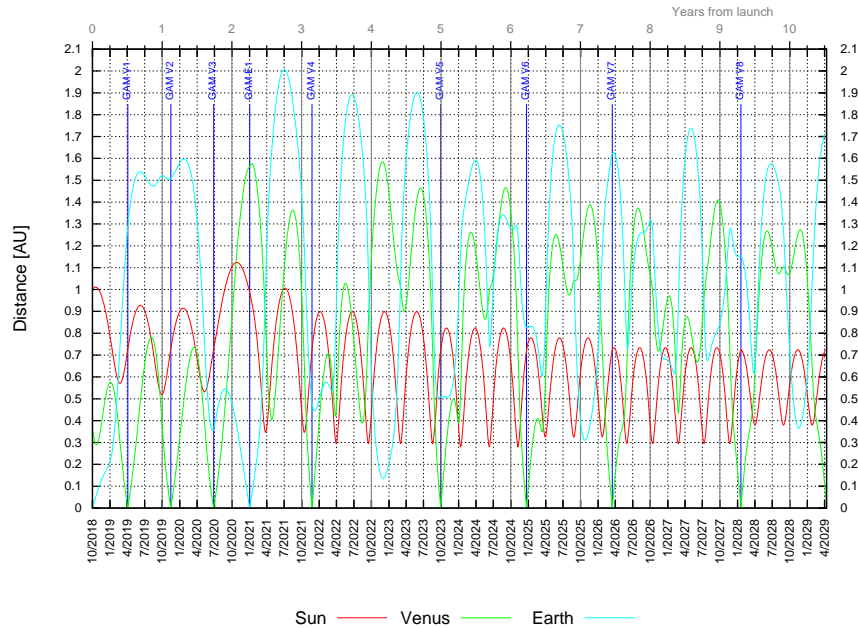


Figure 3-7 2018 Launch Option E: Spacecraft distance to Sun, Venus and Earth

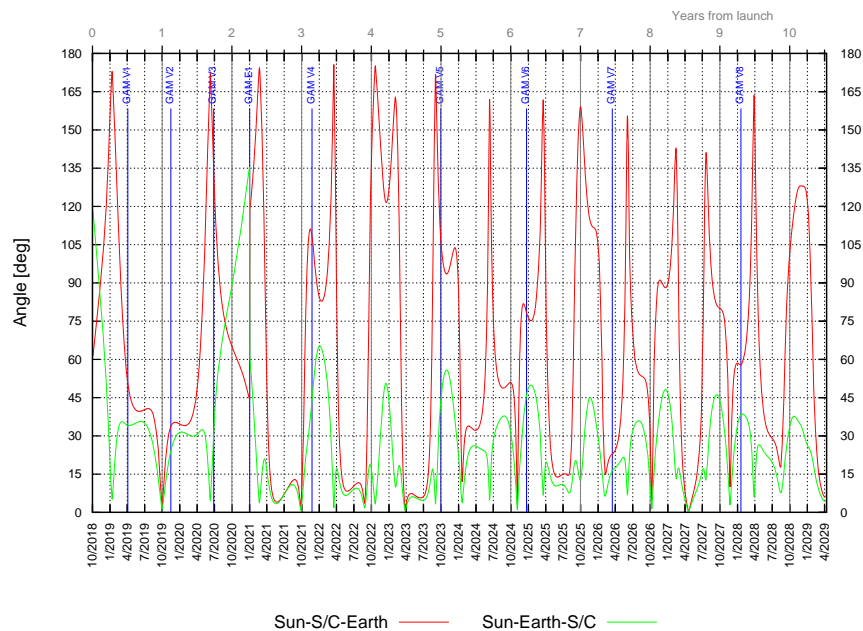


Figure 3-8 2018 Launch Option E: SSE and SES angles

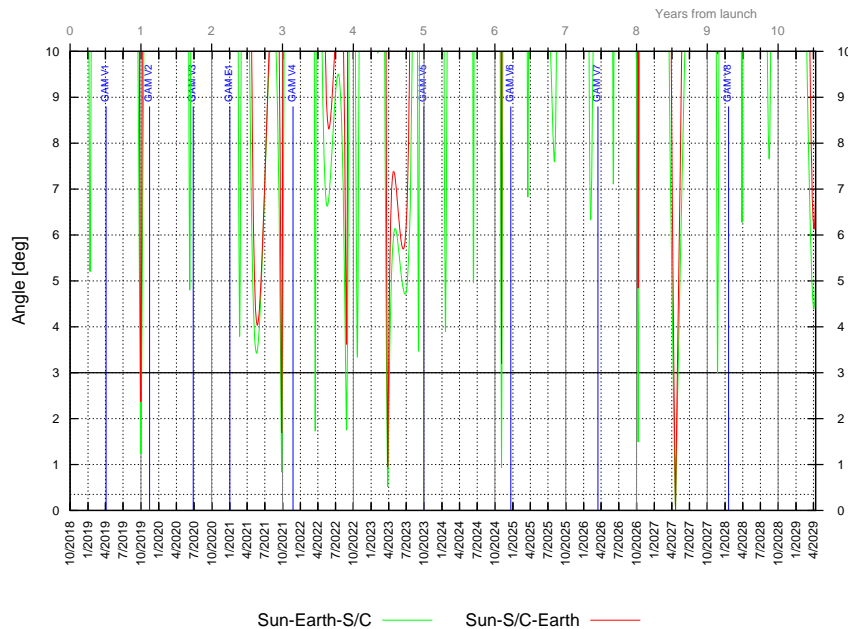


Figure 3-9 2018 Launch Option E: SSE and SES angles – Detail of conjunctions

Table 3-5 shows in addition the periods in which the S/C is not able to communicate via the MGA. If a safe mode is triggered during one of such periods there would be no communication with the S/C until the end of the period. The geometric condition considered for such safe mode blackouts is $SES \leq 5$ deg or $SSE \leq 3$ deg. This condition has been reviewed by Airbus DS after CDR and now reflects the expected spacecraft performance (MGA link-budget, blocking by the Sun-shield,...). The impact is very small with respect to the previous safe mode blackout condition used in older versions of this document. The longest communications blackout would occur if safe mode is entered exactly at the start of the MGA blackout. 10 of these periods longer than 7 days will occur during the mission. The two longest of these periods will occur in 2021 April-June and 2027 March-May with duration of 45 and 42 days, respectively. In 2023 another 2 of these periods extending barely a month will take place.

	Type	Start	End	Duration [days]	Min SES [deg]
1	Superior	2019-09-26	2019-10-04	8.1	1.23
2	Superior	2021-09-21	2021-09-30	9.2	0.83
3	Inferior	2022-03-17	2022-03-19	2.3	1.73
4	Superior	2022-08-22	2022-08-30	8.5	1.75
5	Superior	2023-03-21	2023-04-04	14.5	0.52
6	Superior	2024-11-01	2024-11-05	3.8	0.93
7	Superior	2026-10-07	2026-10-11	3.8	1.49
8	Superior	2027-04-07	2027-05-03	25.3	0.02
9	Superior	2027-11-22	2027-11-23	0.2	2.97

Table 3-4 2018 Launch Option E: Solar Conjunction Periods

Solar conjunctions are considered as the periods when the Sun-Earth-spacecraft angle is below 3 degrees.

	Start	End	Duration [days]
1	2019-09-23	2019-10-07	13.9
2	2021-04-29	2021-06-14	45.4
3	2021-09-17	2021-10-03	16.2
4	2022-08-16	2022-09-02	17.0
5	2022-10-17	2022-10-25	7.4
6	2023-03-18	2023-04-14	27.6
7	2023-06-09	2023-07-07	27.6
8	2026-10-05	2026-10-12	7.0
9	2027-03-31	2027-05-12	41.9
10	2029-03-24	2029-04-11	18.5

Table 3-5 2018 Launch Option E: Longest periods of communications blackout if S/C enters safe mode (longer than 7 days only)

Communications blackout in safe mode are considered as the periods when $SES \leq 5$ deg OR $SSE \leq 3$ deg.



Figure 3-10 shows the evolution of the Earth-Spacecraft range-rate. The range of variation for the entire mission is within ± 60 km/s.

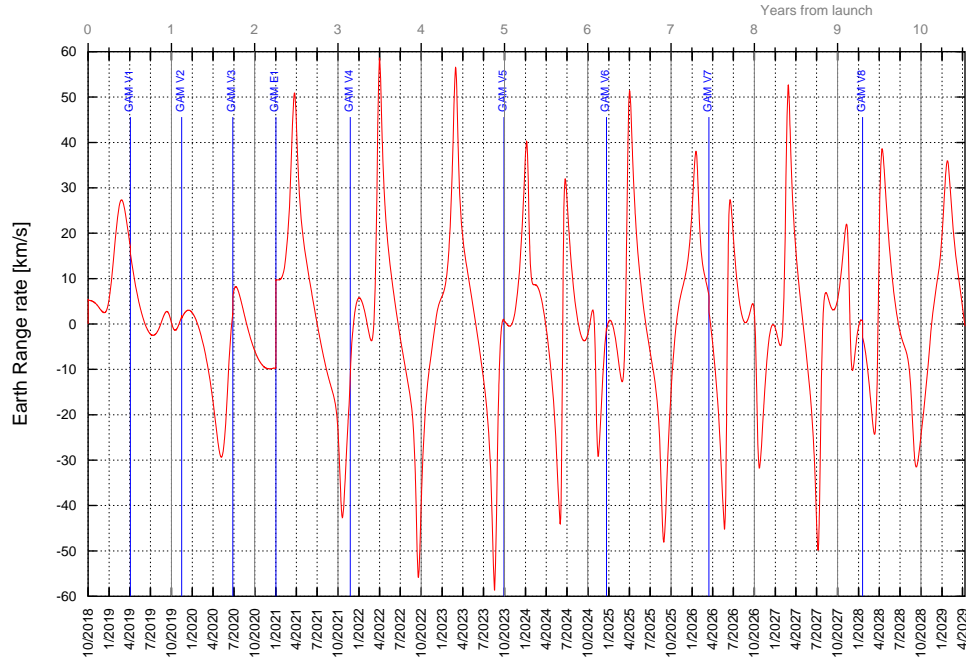


Figure 3-10 2018 Launch Option E: Variation of Earth-Spacecraft range-rate

Figure 3-11 shows the evolution of the Doppler effect due to the Earth-Spacecraft range-rate and Figure 3-12 shows the evolution of the Doppler rate. The formulation to obtain these parameters from the trajectory Earth range-rate and range-acceleration is as follows:

$$\text{Doppler: } F_{RX} = F_{TX} \cdot \sqrt{\frac{1 - \frac{v}{c}}{1 + \frac{v}{c}}}$$

$$\text{Doppler-rate: } F_{RX}(t) = F_{TX} \cdot \left(\frac{1 - \frac{v}{c}}{1 + \frac{v}{c}} \right)^{-1/2} \cdot \frac{-2 \cdot \frac{a}{c}}{\left(1 + \frac{v}{c}\right)^2} \cdot \frac{1}{2} = F_{TX} \cdot \left(\frac{1 + \frac{v}{c}}{1 - \frac{v}{c}} \right)^{1/2} \cdot \frac{-2 \cdot \frac{a}{c}}{\left(1 + \frac{v}{c}\right)^2} \cdot \frac{1}{2}$$

Where:

c = speed of light

v = relative velocity or range-rate

a = relative acceleration or range-acceleration

F_{TX} = frequency of the carrier (downlink/uplink)



The computations of Doppler and Doppler-rate have been performed for the downlink frequency of 8.42 GHz. The Doppler varies from -1.64 MHz to 1.69 MHz during the entire mission. The Doppler seen from the ground stations will be slightly different due to the rotation velocity of the Earth.

Doppler varies very rapidly at the GAMs and so Figure 3-12 shows Doppler-rate peaks extending beyond the limits of the graph, which have been chosen to show the variations of Doppler-rate in the heliocentric phases of the order of a few Hz/s, while peaks at the GAMs can largely exceed 500 Hz/s. The detail analysis of the Doppler-rates reached at the GAMs is presented in Section 3.1.4.

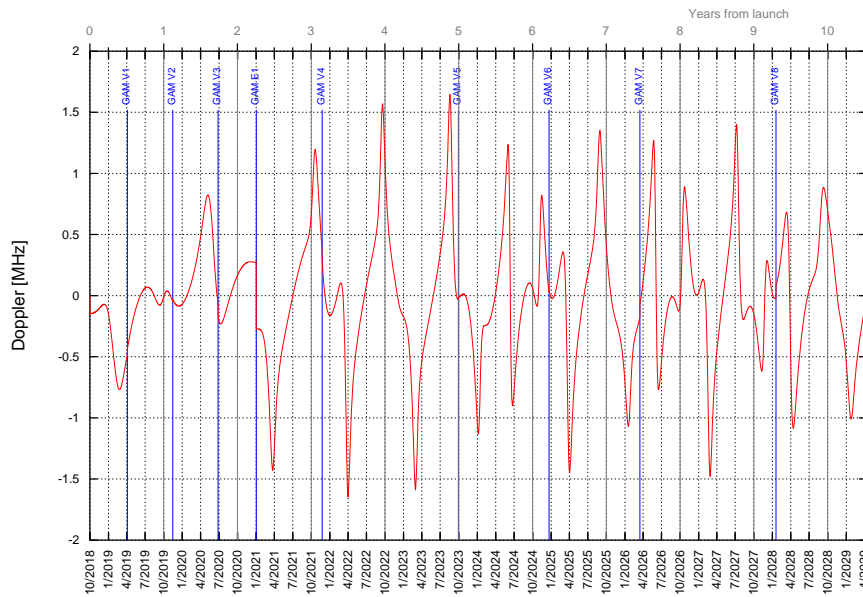


Figure 3-11 2018 Launch Option E: Variation of Earth-Spacecraft Doppler

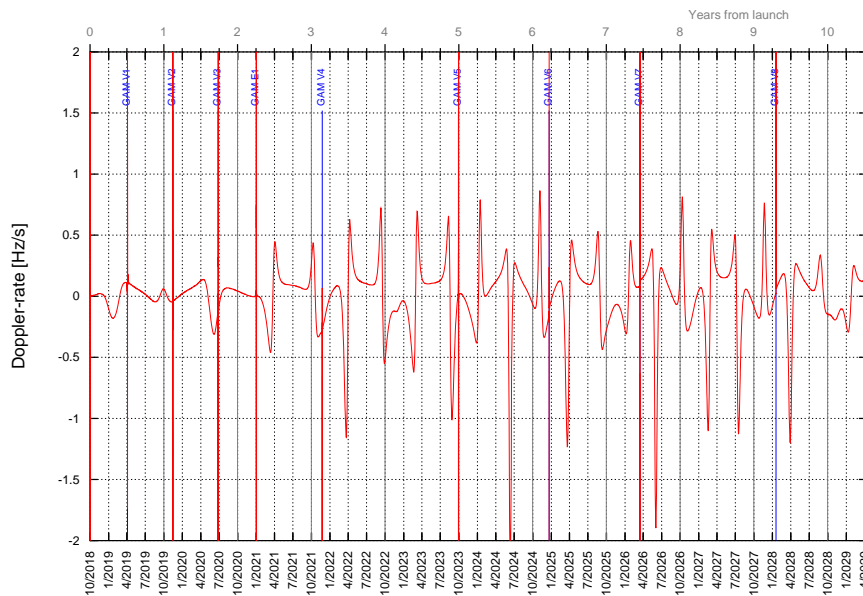


Figure 3-12 2018 Launch Option E: Variation of Earth-Spacecraft Doppler-rate



3.1.2 SCIENCE PROPERTIES

Figure 3-13 combines the evolution of the solar latitude with the distance to the Sun. During the science mission the solar latitude is positive at the perihelions and negative at the aphelions. The highest solar latitude is achieved short before the perihelion and the lowest solar latitude between the perihelion and the aphelion.

Figure 3-14 provides a representation of the science orbits during NMP and EMP. The X-axis gives the projection of the spacecraft position vector on the Sun Equator plane, while the Y-axis gives the projection on the Sun North's Pole. Thus the Sun is located at the origin of these coordinates. Orange straight lines from the Sun represent the points of same solar latitude, while grey circles represent the points with the same Sun distance. The 0.28 AU constraint appears highlighted. This plot is useful to identify very quickly the location of perihelion and the points of minimum and maximum solar latitude that will be used for the remote sensing windows. It includes as well the location of the TCMs used for the Venus GAMs navigation following the timeline provided in Section 5.1.

It also provides a nice overview of the evolution of the orbit during both parts of the science phase. All orbits intersect at the point at which the Venus GAMs are performed. The solar inclination of the orbit is increased at each GAM. Since the Venus GAMs are encountered outbound, in the arc going from perihelion to aphelion, the orbits are described by the spacecraft in the clockwise direction. After a Venus GAM, first the point of minimum latitude is encountered, then the perihelion and then the point of maximum latitude. The 3 10-day remote sensing windows per orbit are also represented in the plot.

Figure 3-15 shows the evolution of the perihelion and aphelion and the points of maximum and minimum solar latitude as a function of the date. This information is superimposed to the spacecraft to Sun distance.

Table 3-6 provides information about the events during the science mission at which remote sensing observations will take place: during perihelion passes and at the points of minimum and maximum solar latitude of each orbit. The table considers only the period of science including both the nominal and the extended science missions.

Table 3-7 provides information of the number and duration of the passes close to the Sun separating cruise phase and science phase (NMP+EMP) and for distances below 0.3 AU, 0.4 AU, 0.5 AU and 0.6 AU. The spacecraft will approach the Sun 9 times below 0.3 AU and 16 times below 0.4 AU, and will stay below these distances is 71 and 490 days, respectively. In addition, Figure 3-17 shows the evolution of the time spent below given Sun ranges. This time increases abruptly at every perihelion pass below the given Sun range. The stays below 0.295 AU reach their maximum by GAM-V6, about 6 years after launch.

Figure 3-18 shows the spacecraft rotation velocity around the Sun. The maximum rotation velocity is achieved at the pericentre of the heliocentric orbit after GAM V5.

Figure 3-16 shows the evolution of the Earth distance together with the estimated downlink volume per day assuming a flat 8-hour daily pass. The plot clearly shows the periods in which the maximum data rate is provided (green shadowed), which are related to the close-Earth aphelions as shown before in Figure 3-6. This trajectory provides 4 of such periods. The first one right after GAM-V3 is rather short, but the next one in the 4:3 resonance lasts about 4 months. The following ones during 3:2 resonances last between 1.5 and 2 months.

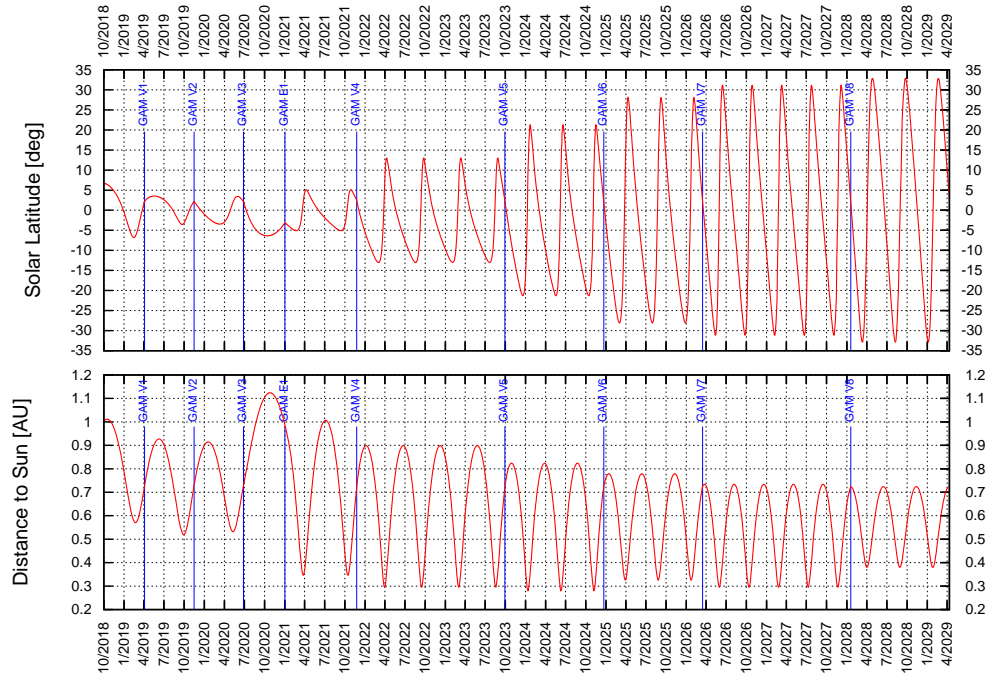


Figure 3-13 2018 Launch Option E: Spacecraft solar latitude + Spacecraft distance to the Sun

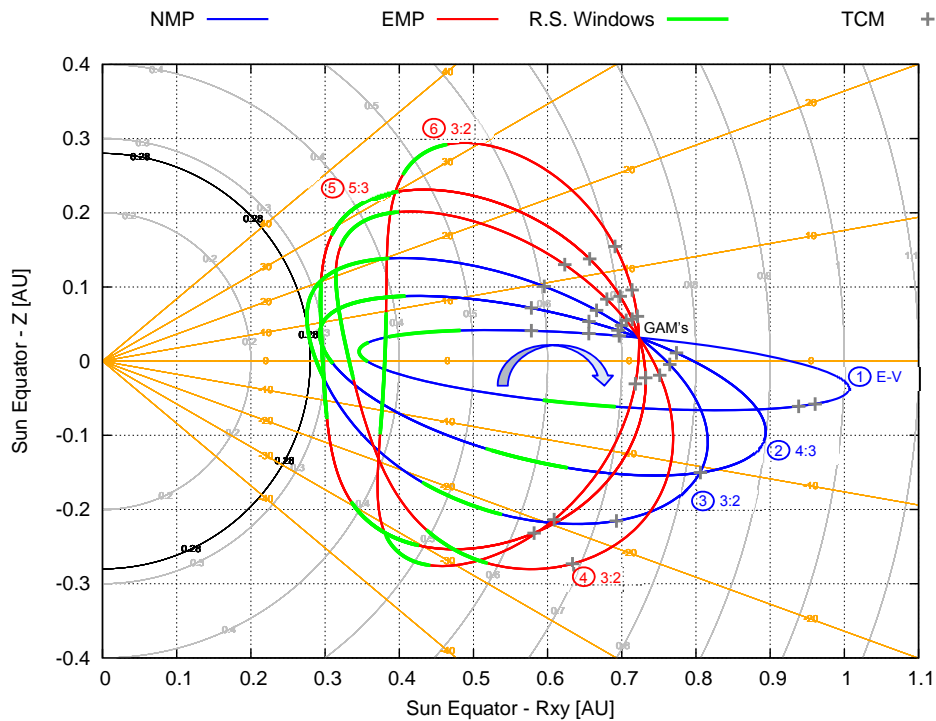


Figure 3-14 2018 Launch Option E: projection of science orbits wrt Sun Equator and North Pole

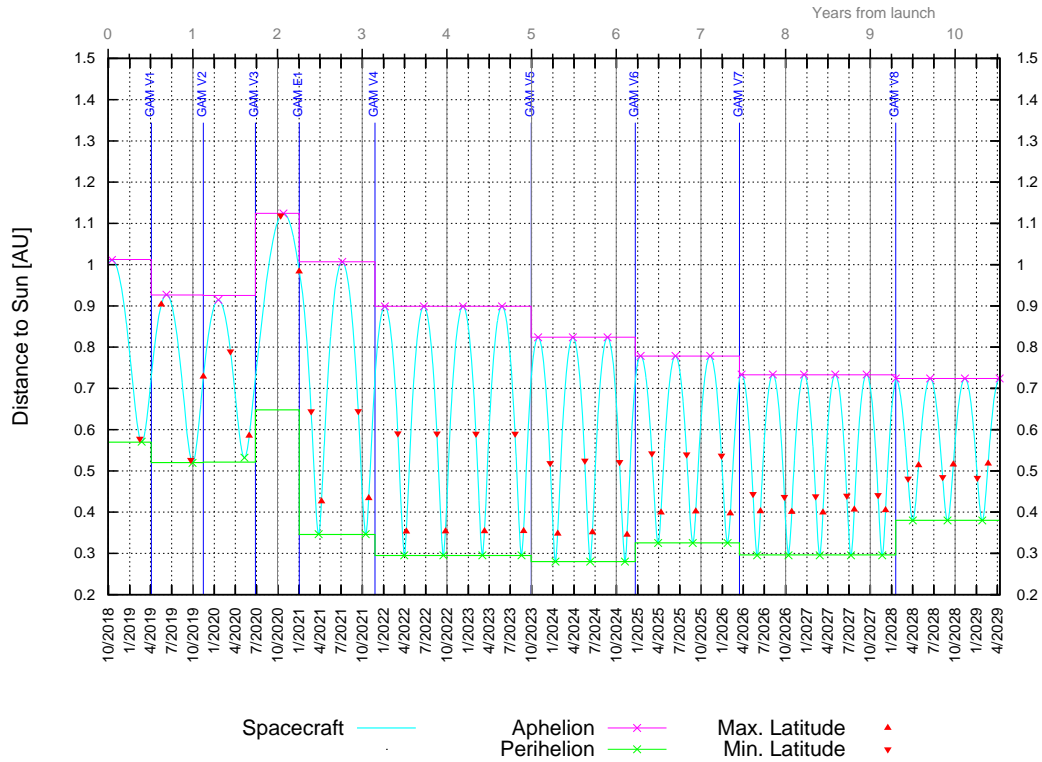


Figure 3-15 2018 Launch Option E: Evolution of apses and points of extreme solar latitude

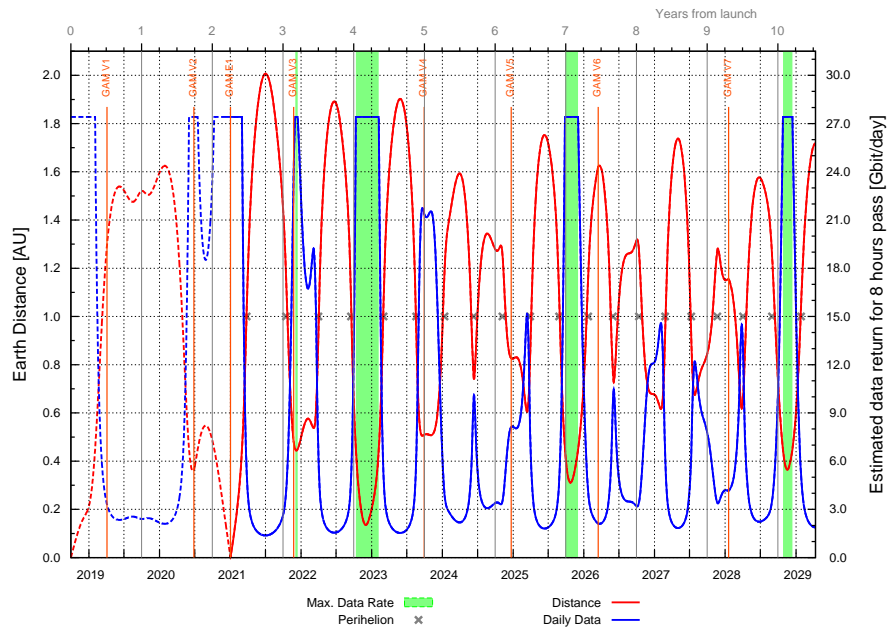


Figure 3-16 2018 Launch Option E: Evolution of Earth distance and potential downlink



Event	#	Date	Flight Time (y)	Sun Distance (AU)	Solar Latitude (deg)
GAM-E1		2020-05-22	2.26	NMP Start	
MINLAT	1	2021-02-22	2.40	0.644	-5.10
MINRP	1	2021-03-26	2.49	0.346	2.09
MAXLAT	1	2021-04-08	2.52	0.430	5.10
MINLAT	2	2021-09-13	2.95	0.644	-5.10
MINRP	2	2021-10-15	3.04	0.346	2.07
MAXLAT	2	2021-10-28	3.08	0.430	5.10
GAM-V4		2021-11-23	3.15		
MINLAT	3	2022-03-03	3.42	0.589	-13.03
MINRP	3	2022-03-31	3.50	0.295	6.29
MAXLAT	3	2022-04-09	3.52	0.357	13.03
MINLAT	4	2022-08-19	3.88	0.588	-13.03
MINRP	4	2022-09-15	3.96	0.295	6.23
MAXLAT	4	2022-09-25	3.99	0.358	13.03
MINLAT	5	2023-02-03	4.35	0.589	-13.02
MINRP	5	2023-03-03	4.42	0.295	6.27
MAXLAT	5	2023-03-12	4.45	0.357	13.02
MINLAT	6	2023-07-22	4.81	0.589	-13.02
MINRP	6	2023-08-19	4.88	0.295	6.30
MAXLAT	6	2023-08-28	4.91	0.357	13.02
GAM-V5		2023-09-28	5.00		
MINLAT	7	2023-12-20	5.22	0.523	-21.29
MINRP	7	2024-01-12	5.28	0.280	8.56
MAXLAT	7	2024-01-22	5.31	0.348	21.29
MINLAT	8	2024-05-18	5.63	0.523	-21.29
MINRP	8	2024-06-10	5.69	0.280	8.51
MAXLAT	8	2024-06-19	5.72	0.348	21.29
MINLAT	9	2024-10-14	6.04	0.523	-21.29
MINRP	9	2024-11-07	6.10	0.280	8.47
MAXLAT	9	2024-11-16	6.13	0.348	21.29
GAM-V6		2024-12-21	6.23		

Event	#	Date	Flight Time (y)	Sun Distance (AU)	Solar Latitude (deg)
GAM-V6		2024-12-21	6.23	EMP Start	
MINLAT	10	2025-03-03	6.42	0.541	-28.08
MINRP	10	2025-03-30	6.50	0.325	9.91
MAXLAT	10	2025-04-11	6.53	0.399	28.08
MINLAT	11	2025-07-31	6.83	0.540	-28.08
MINRP	11	2025-08-26	6.91	0.325	9.86
MAXLAT	11	2025-09-08	6.94	0.398	28.08
MINLAT	12	2025-12-28	7.24	0.540	-28.08
MINRP	12	2026-01-23	7.32	0.325	10.03
MAXLAT	12	2026-02-05	7.35	0.399	28.08
GAM-V7		2026-03-15	7.46		
MINLAT	13	2026-05-14	7.62	0.441	-31.14
MINRP	13	2026-05-31	7.67	0.295	3.06
MAXLAT	13	2026-06-15	7.71	0.403	31.14
MINLAT	14	2026-09-25	7.99	0.441	-31.13
MINRP	14	2026-10-13	8.04	0.295	3.21
MAXLAT	14	2026-10-28	8.08	0.403	31.13
MINLAT	15	2027-02-07	8.36	0.441	-31.13
MINRP	15	2027-02-25	8.41	0.295	3.07
MAXLAT	15	2027-03-11	8.44	0.403	31.13
MINLAT	16	2027-06-22	8.73	0.441	-31.14
MINRP	16	2027-07-10	8.77	0.295	3.22
MAXLAT	16	2027-07-24	8.81	0.403	31.13
MINLAT	17	2027-11-04	9.09	0.441	-31.14
MINRP	17	2027-11-22	9.14	0.295	3.09
MAXLAT	17	2027-12-06	9.18	0.403	31.14
GAM-V8		2028-01-18	9.30		
MINLAT	18	2028-03-12	9.45	0.482	-32.85
MINRP	18	2028-04-02	9.50	0.380	-3.32
MAXLAT	18	2028-04-27	9.57	0.515	32.85
MINLAT	19	2028-08-09	9.86	0.482	-32.85
MINRP	19	2028-08-29	9.92	0.380	-3.38
MAXLAT	19	2028-09-24	9.98	0.515	32.85
MINLAT	20	2029-01-06	10.27	0.483	-32.85
MINRP	20	2029-01-26	10.33	0.380	-3.25
MAXLAT	20	2029-02-20	10.39	0.516	32.85

Table 3-6 2018 Launch Option E: Characteristics of perihelion and extreme points of solar latitude



	# Times	Accumulated Duration (days)	Minimum Duration (days)	Maximum Duration (days)
Cruise Phase		824		
Below 0.3 AU	0	0.0	0.0	0.0
Below 0.4 AU	0	0.0	0.0	0.0
Below 0.5 AU	0	0.0	0.0	0.0
Below 0.6 AU	3	131.1	31.7	49.7
Science Mission		3022		
Below 0.3 AU	12	70.7	4.5	9.5
Below 0.4 AU	20	489.7	16.2	28.2
Below 0.5 AU	20	873.6	38.5	46.4
Below 0.6 AU	20	1282.7	55.8	74.1
Total Mission		3847		
Below 0.3 AU	12	70.7	4.5	9.5
Below 0.4 AU	20	489.7	16.2	28.2
Below 0.5 AU	20	873.6	38.5	46.4
Below 0.6 AU	23	1413.8	31.7	74.1

Table 3-7 2018 Launch Option E: Number and duration of passes close to the Sun

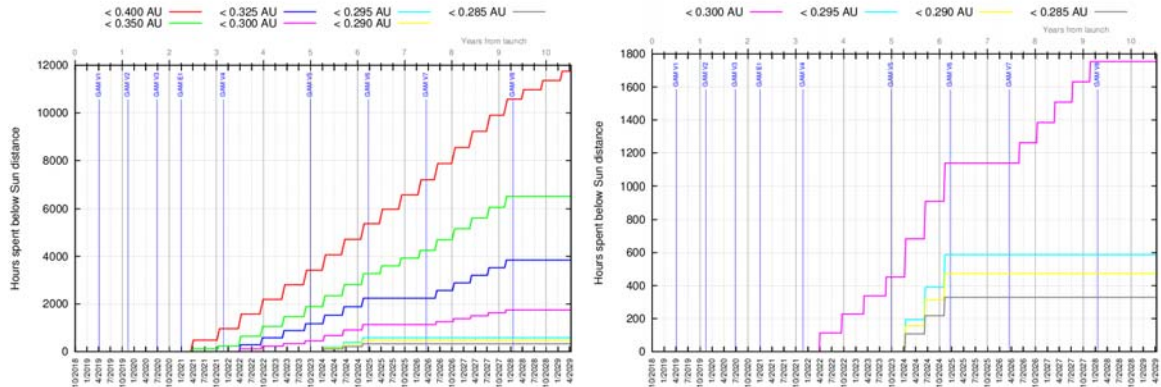


Figure 3-17 2018 Launch Option E: Evolution of time spent below different Sun ranges

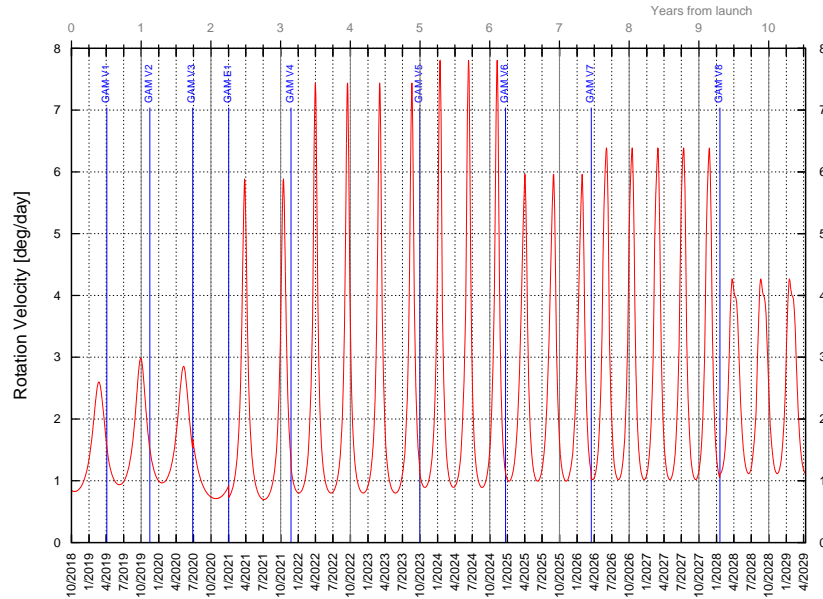


Figure 3-18 2018 Launch Option E: Spacecraft rotation velocity about the Sun

3.1.3 GROUND STATION VISIBILITY

The ground station visibility has been analysed from the 3 stations of the ESA Deep Space network: Cebreros (Spain), New Norcia (Australia) and the future station in Malargüe (Argentina). The operations plan foresees the use of Malargüe as baseline station for Solar Orbiter with Cebreros as backup. New Norcia will be used punctually to provide additional support, i.e. for Δ DOR measurements for the navigation of the GAMA. Table 3-8 provides the location assumed for these ground stations.

Ground Station	Malargüe (Baseline)	Cebreros (Backup)	New Norcia
Longitude [°]	69.40 W	4.37 W	116.19 E
Latitude [°]	35.78 S	40.45 N	31.05 S
Altitude [km]	1.554	0.794	0.252

Table 3-8 Location of ESA Deep Space Ground Stations

The visibility from the ground stations is associated with the equatorial declination of the Earth-to-spacecraft direction as presented in Figure 3-19. High positive declinations favour the visibility from the Northern hemisphere, hence increasing the duration of the visibility pass from Cebreros and decreasing it for Malargüe and New Norcia. Conversely, high negative declinations favour the visibility from the latter two stations.

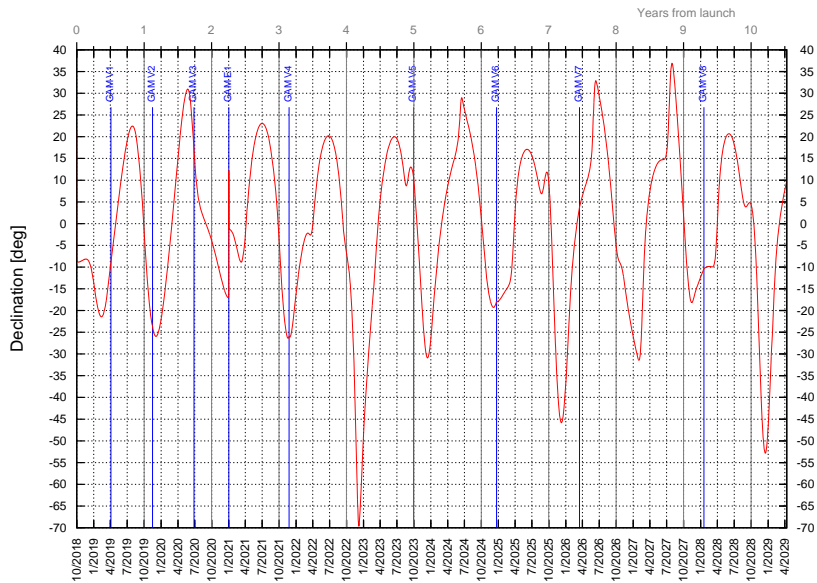


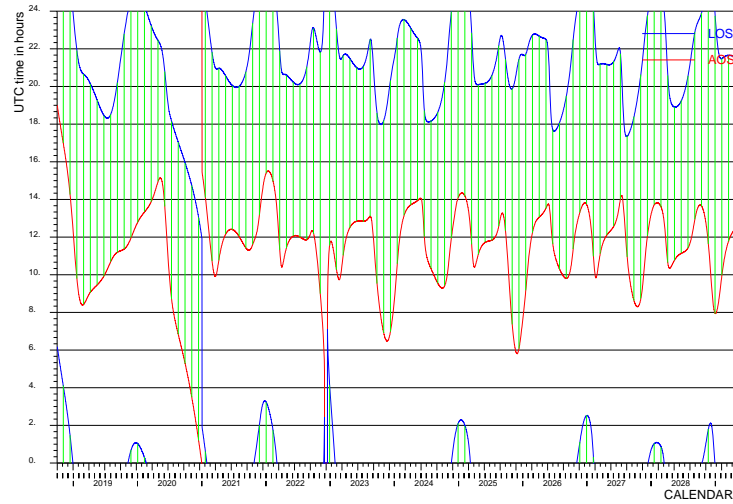
Figure 3-19 2018 Launch Option E: Spacecraft equatorial declination.

Figure 3-20 presents the daily period of visibility from each of the 3 ESA ground stations. The hours of the day when Acquisition Of Signal, AOS, and Loss Of Signal, LOS, take place is provided with a red and a blue line, respectively. Vertical black lines show the GAMs. The visibility is shown assuming 10° minimum elevation from the ground station. Daily visibility from Malargüe and New Norcia is guaranteed. However, for Cebreros there are 3 periods of no visibility due to very high negative-South declination: the first one just is in the middle of the 4:3 resonance between GAM-V4 and GAM-V5, the second is before GAM-V7 and the last one before encountering Venus again at the mission end. These periods have to be taken into account for the operations planning. They may affect the orbit determination activities, since during these periods the tracking data from the only station in the Northern hemisphere will be missing. In addition, it will not be possible to collect Δ DOR measurements from the Cebreros-New Norcia or the Cebreros-Malargüe baselines.

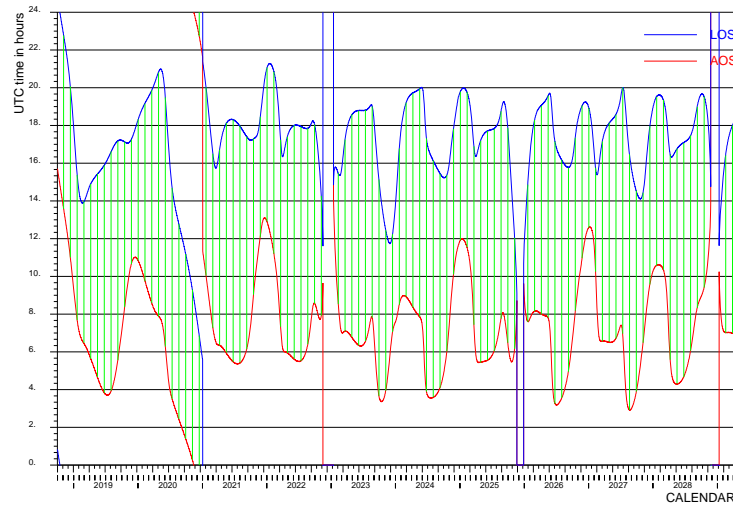
Figure 3-21 shows the duration of the visibility as a function of the date for all three ground stations. Figure 3-22 shows a combination of the daily period of visibility from the 3 stations.



Malargüe



Cebreros



New Norcia

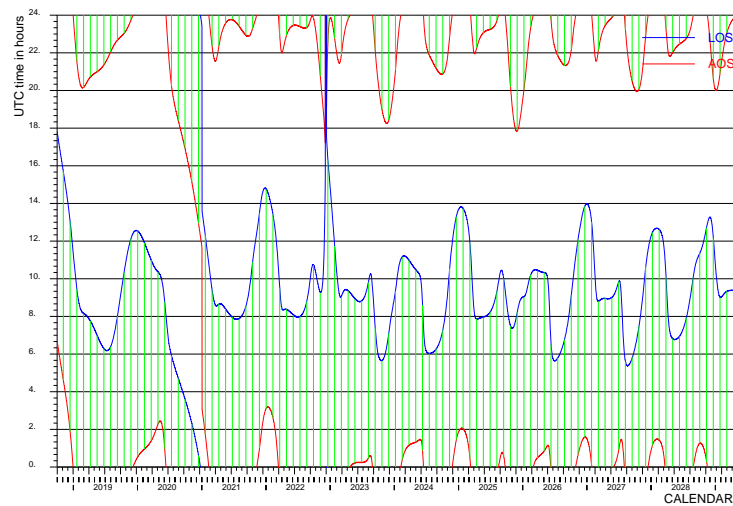


Figure 3-20 2018 Launch Option E: Daily period of visibility from ESA DS stations.

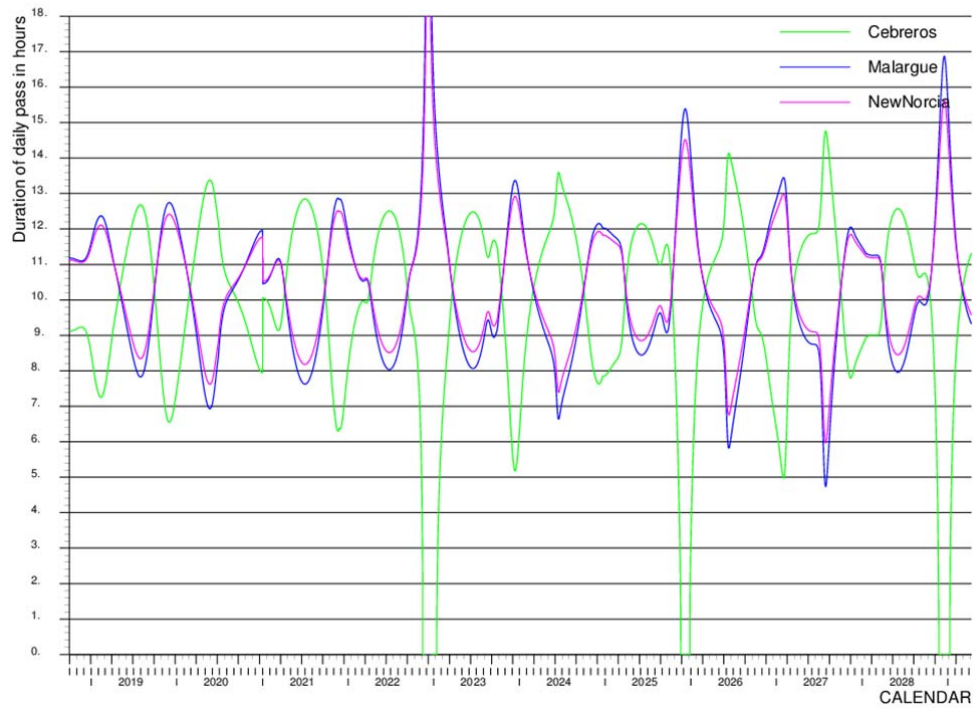


Figure 3-21 2018 Launch Option E: Daily duration of visibility from ESA Deep Space stations

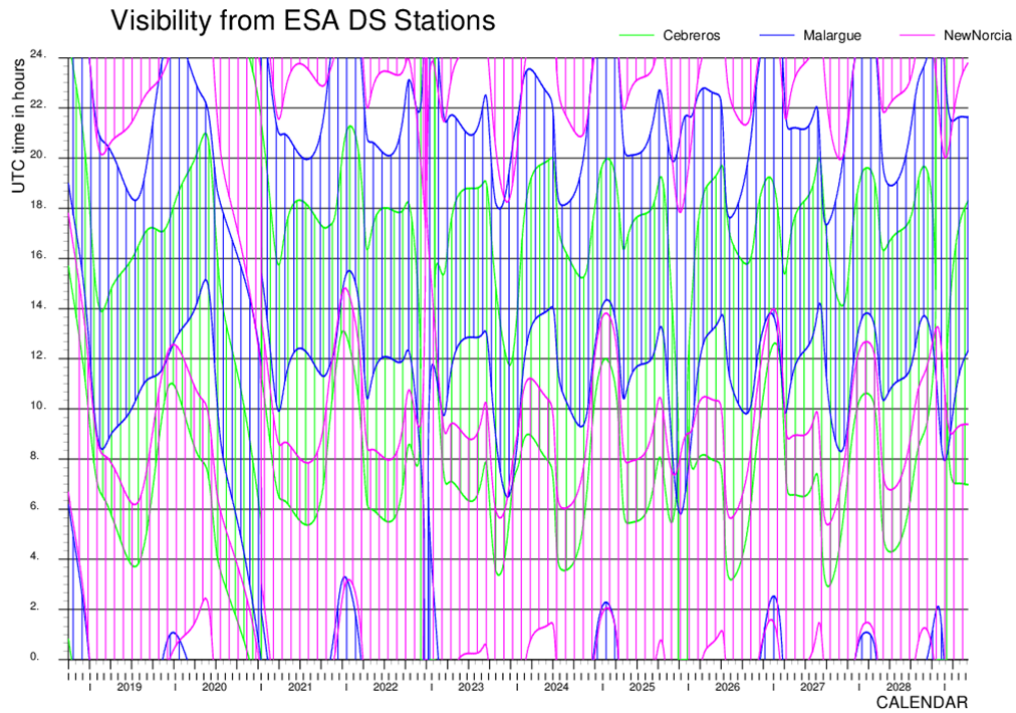


Figure 3-22 2018 Launch Option E: Daily period of visibility from ESA Deep Space stations.



3.1.4 GAMS DETAILS

Table 3-9 shows the characteristics of the GAMS including the duration of the eclipse and occultation events. For this trajectory eclipses are found during the Venus GAMS from V4 onwards. The worst-case eclipse is about 19 minutes at GAM-V4. Occultation of the Earth occurs only at the very last Venus GAMS and is limited to about 11 minutes.

GAM	Date	Re (AU)	Vinf (km/s)	Hmin (km)	Eclipse (min)	Occult. (min)	LST ¹ (h)	Ls (deg)	SSE (deg)	SES (deg)	ESV (deg)
V1	2019-04-04	1.300	9.823	15070	0	0	19.4	6.4	50.3	34.0	95.7
V2	2019-11-14	1.511	9.827	11000	0	0	21.2	289.5	33.6	24.0	-122.3
V3	2020-06-26	0.362	9.831	5831	0	0	6.4	289.4	135.3	30.2	14.5
E1	2021-01-01	0.006	9.692	387	0	0	20.4	289.2	-	-	-
V4	2021-11-23	0.478	17.463	363	18.7	0	15.5	100.9	108.5	44.1	-27.4
V5	2023-09-28	0.508	17.463	350	14.1	0	14.2	34.1	107.5	43.6	29.0
V6	2024-12-21	0.829	17.464	440	10.7	0	12.7	34.1	78.3	46.1	-55.5
V7	2026-03-15	1.621	17.464	561	10.6	10.0	13.2	34.1	22.9	16.4	-140.6
V8	2028-01-18	1.157	17.464	715	8.5	10.8	10.8	34.1	57.7	38.5	-83.7

Table 3-9 2018 Launch Option E: Characteristics of GAMS and eclipse/occultation durations

The minimum altitude of GAM E1 is close to the 350 km constraint. For GAM V4 to V8 the minimum altitude is also close to the limit. In this particular case the optimizer had freedom to choose slightly higher altitudes to adjust the trajectory. However, this can still be subject to fine tuning and it is likely that in the final real trajectory the GAMS V4 to V7 will be forced to the minimum altitude of 350 km, while the last V8 will be higher. This does not suppose any penalty for the science observations and has a minimal impact to the trajectory results shown in this section.

Table 3-10 provides the components of the infinite velocity vectors at each GAM and the incoming B-plane impact vector. The impact vectors are given in the ICRF/EME2000 reference frame. The 2 components of the impact vector are defined in the B-plane (perpendicular to the incoming velocity vector), with the X component contained in the Earth's Mean Equator of J2000.0 and the Y component perpendicular to it. The geometry of the GAM hyperbola can be exactly determined either by the use of the arrival infinite velocity vector and the B-plane impact vector or by both infinite velocity vectors.

The geometry of the GAM hyperbolas is given in Figure 3-23 for the Venus GAMS and Figure 3-24 for the Earth GAM. The representation makes use of the following reference frame defined at the time of closest approach (periapsis):

- X-Axis in the anti-Sun direction, thus the $-X$ axis points from the planet (Venus or Earth) to the Sun and the shadow of the planet is in the $+X$ direction.
- Y-Axis is contained in the orbit plane of the hyperbola and perpendicular to the X-Axis.
- Z-Axis completes a triorthogonal reference frame.

The projection presented is in the X-Y plane, which is different for each GAM, and the Z component is given color-coded (yellow-orange in $+Z$ direction, out of the paper/screen towards the viewer; purple-black in the $-Z$ direction). Several visual aids are included in the plots: markers for the initial point in the incoming arc of the hyperbola (full circle) and final point in the outgoing arc (empty circle);

¹ Local solar time (LST) at the pericentre of the GAM. The criterion for Venus LST is not related to the rotation of the planet and follows the same definition as for the Earth. Thus, 6 h local time is approximately in the direction of the planet velocity vector with respect to the Sun, and 18 h local time is in the opposite direction.



markers for the periapsis (triangle); tick-marks every 5 minutes from the periapsis; the planet with its terminator and the shadow region; and thicker line to show the eclipse period. The direction of movement goes from the incoming point to the outgoing point. In general ± 45 minutes around the periapsis are plotted, with the exception of GAM-V1, -V2 & V-3 for which ± 60 minutes are plotted. As seen in Figure 3-23 all the Venus GAMs are outbound as the incoming asymptote is on the Sun side and the direction of movement is from the 2nd quadrant to the 1st and 4th quadrants. It must be noticed that the projection passing through the shadow region does not immediately lead to an eclipse as the Z-component also plays a role. Eclipses can only occur if the spacecraft is close to the X-Y plane.

GAM	Arrival					Departure		
	$V_{\infty x}$ (km/s)	$V_{\infty y}$ (km/s)	$V_{\infty z}$ (km/s)	Bx (km)	By (km)	$V_{\infty x}$ (km/s)	$V_{\infty y}$ (km/s)	$V_{\infty z}$ (km/s)
V1	3.436	-8.967	-2.067	-11861.0	21158.2	1.908	-8.638	-4.271
V2	1.908	-8.642	-4.272	13.4	20137.3	1.507	-6.816	-6.917
V3	1.509	-6.820	-6.918	10786.6	10235.0	3.915	-3.495	-8.314
E1	4.675	-7.999	2.842	9549.4	3451.0	9.231	-2.941	-0.244
V4	16.710	5.062	0.365	-1590.8	7231.0	16.435	3.873	-4.457
V5	16.435	3.871	-4.457	-1440.1	7249.6	14.784	2.495	-8.952
V6	14.786	2.496	-8.951	120.3	7481.5	11.722	2.058	-12.780
V7	11.723	2.058	-12.780	-4402.6	6199.6	8.932	-1.253	-14.954
V8	8.933	-1.253	-14.955	-1255.3	7657.0	4.559	-1.408	-16.800

Table 3-10 2018 Launch Option E: infinite velocity vectors and B-plane target of GAMs

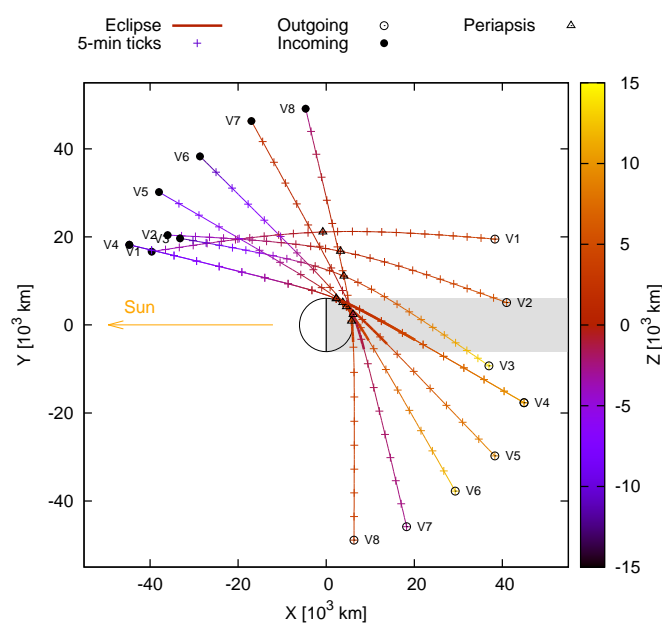


Figure 3-23 2018 Launch Option E: Projection of hyperbolas for Venus GAMs

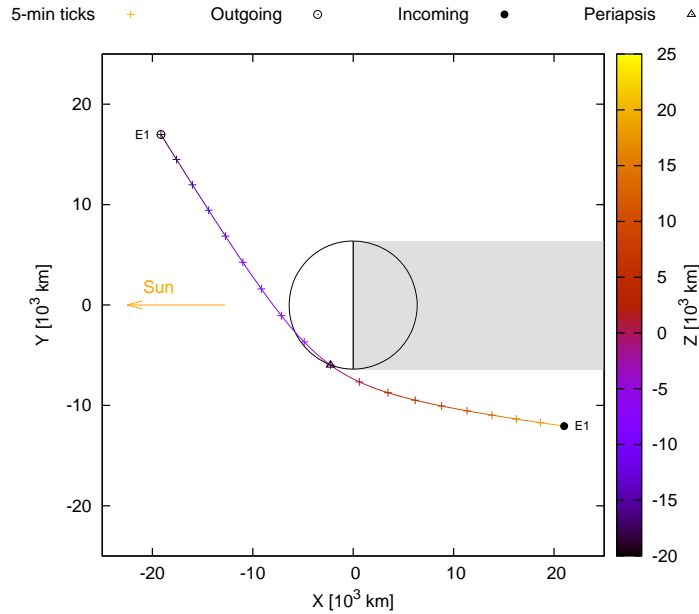


Figure 3-24 2018 Launch Option E: Projection of hyperbolas for Earth GAM

Figure 3-25 shows the evolution of the Doppler rate between the S/C and the centre of the Earth in the vicinity of the closest approach of each GAM. The Doppler rate varies abruptly for a period of about 30-60 min, especially for the Earth GAM. At the Earth GAM the peak value of -635 Hz/s is reached. For the Venus GAMs the limits are reached at +167 Hz/s for GAM-V8 and -137 Hz/s for GAM-V4. It must be pointed out that the Doppler rate that will be seen from the ground stations will be slightly different than these values due to the acceleration due to the Earth rotation.

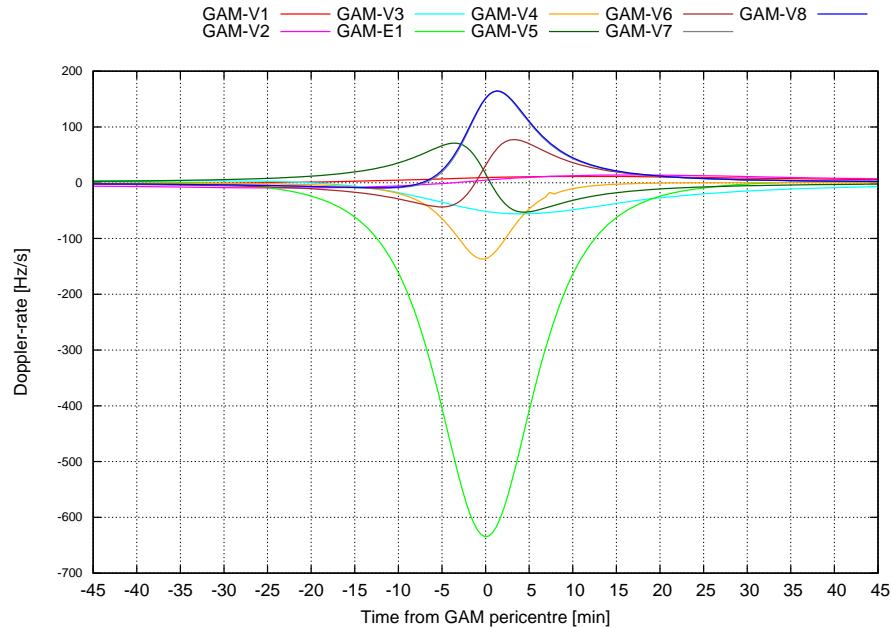


Figure 3-25 2018 Launch Option E: Doppler rate around GAM pericentres



Figure 3-26 shows the communication angles SSE and SES for a period extending from -60 to +30 days with respect to the GAM closest approach. It is seen that a superior solar conjunction occurs before several of the Venus GAMs, but in all the cases both communication angles are above 30 deg for at least the last 30 days before the GAM, so that no impact for the GAM navigation is expected. GAM-V1 and GAM-E1 are not provided, since both communication angles remain above 30 deg in the proximity of these GAMs.

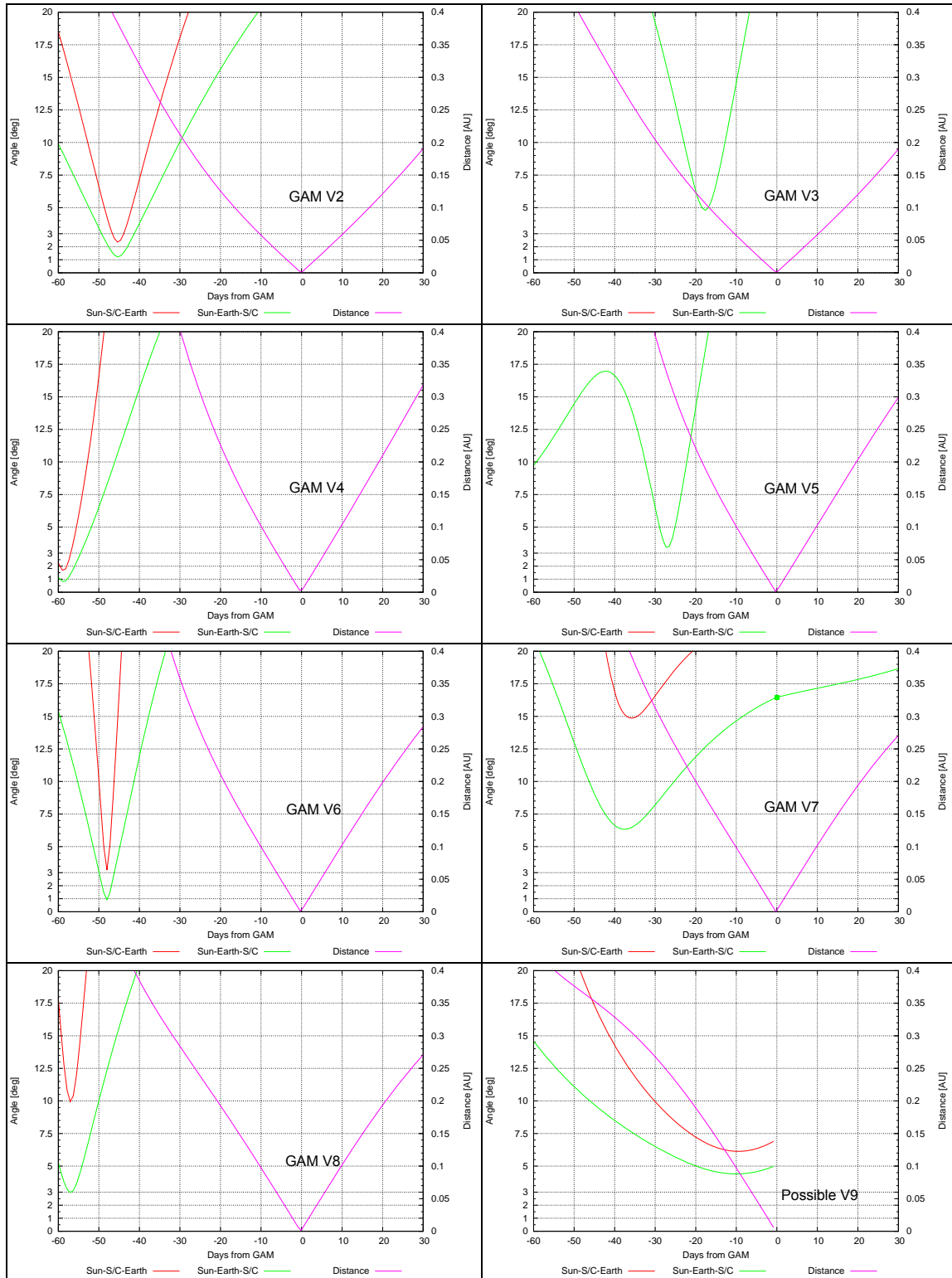


Figure 3-26 2018 Launch Option E: Communication angles in the proximity to GAMs



3.1.5 LEOP

A description of the Atlas V launch vehicle and the sequence of events during the ascent phase is provided in section 4.1. A dedicated analysis of the Atlas V 411 ascent trajectory required for the 2018 Option E launch targets has been performed by ULA. NASA has provided the detailed results of this analysis to ESA in April 2016 in [31]. This data has been used to produce the following analysis.

The trajectory selected for LEOP analysis corresponds to the first launch day of the launch window identified for this trajectory opportunity as presented in Table 4-2. Launch on 2018-09-22 requires an infinite velocity of 5.216 km/s, DLA of -12.09 deg and RLA of 304.96 deg (both angles in ICRF/EME2000). The lift-off time matching these escape conditions as calculated by ULA is 09:45:13 UTC and the spacecraft separation after a “short” coast phase takes place at 10:20:21 UTC.

Ground station visibility after separation of Solar Orbiter from the Atlas-V launch vehicle has been analysed ([17]). ESA/ESTRACK ground stations have been considered: Kourou and the 3 ESA-DSA as in Table 3-8: Malargüe, Cebreros and New Norcia (which includes the new 4.5-m NNO-2 antenna). In addition the coverage of some stations of the augmented/cooperative networks and NASA DSN station in Canberra has been included.

Figure 3-27 shows the ground track of Solar Orbiter for 1 day after separation from the launcher upper stage. From separation over South-Madagascar the Solar Orbiter spacecraft travels South East for about 50-60 minutes increasing the altitude and then the ground track turns towards West on the Indian Ocean. The spacecraft is then escaping from the Earth on the inertially fixed direction of the asymptote and so the latitude remains constant and equal to the target DLA while the longitude is swept west due to the rotation of the Earth. Separation occurs on the illuminated side of the Earth (nightside is shown at separation time) and numerical simulations show that there is no eclipse after separation.

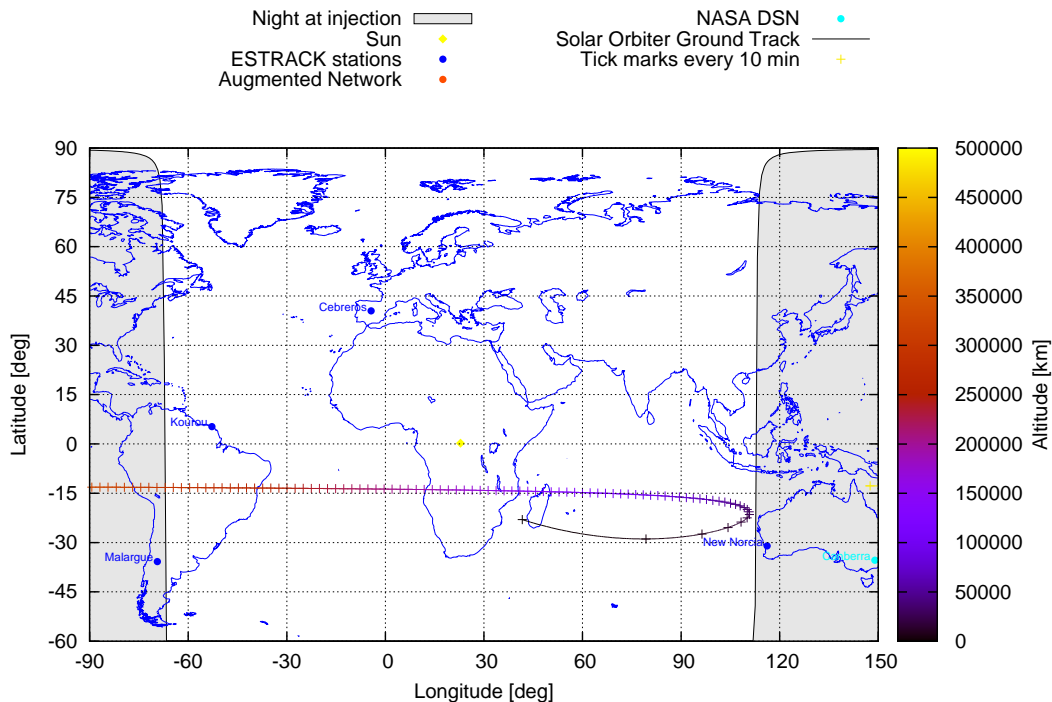


Figure 3-27 2018 Launch Option E: ground track for first LEOP day



Figure 3-28 shows the results of the ground station visibility analysis for the regarded scenario. The first station with spacecraft visibility is New Norcia. The new ESA 4.5-m NNO-2 antenna will support the initial acquisition. The spacecraft will be above the horizon 5 minutes and above an elevation of 10 degrees 7 minutes after separation. The next station to have visibility is Canberra, the spacecraft will be above the 10 degrees elevation 15 min after separation. The elevation from New Norcia reaches a maximum of 75 degrees 45 minutes after separation. Due to the South declination of the escape asymptote, during the LEOP the ESA stations in Malargüe and New Norcia can alternate tracking of the spacecraft to provide continuous 24-h coverage. Cebreros provides visibility only with low elevations and Kourou does not improve the coverage of Malargüe, but can be used as backup.

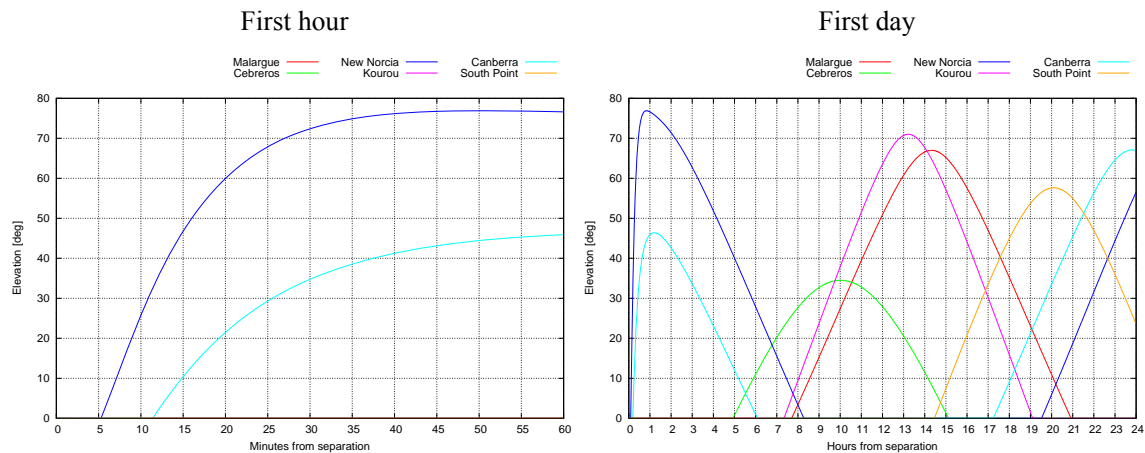


Figure 3-28 2018 Launch Option E: elevation from ground stations

Figure 3-29 shows the slant-range, the Doppler and the Doppler-rate from the considered ground stations during the first 100 minutes after separation, corresponding to the period of first acquisition. All these results take into account the actual locations of the ground stations in the rotating Earth. Only in the very first minutes from New Norcia there is a positive Doppler as the spacecraft is actually approaching the ground station. Soon later and as well for the other stations the Doppler is negative, down to about -0.2 MHz, as the spacecraft is going away from the Earth. The Doppler-rate can be large at the very beginning of the visibility, down to about -400 Hz/s for New Norcia and -200 Hz/s for Canberra, before it then approaches a zero value.

The geometry of Earth, S/C and Sun short after departure is presented in the Figure 3-30. The plot on the left shows the evolution for the first 5 hours after separation of the SSE and SES angles along with the Earth distance. The spacecraft will be beyond the LEO protected region (2000 km altitude) in 3 minutes, beyond the geostationary orbit in less than 90 minutes and in about 18.5 hours it will be beyond Moon's orbit.

The plot on the right shows the projection of the departure hyperbola on the Sun-Earth rotating frame relative to Earth (thus at the centre; Sun on the left, far out the plot scale). Since the spacecraft will quickly achieve the Sun pointing attitude, the +X_{sc} axis will point towards the -X axis of the figure. It is thus possible to estimate from the plot the position of Earth with respect to the LGAs and the star tracker field of view. To illustrate the possible changes of the geometry with the launch date, 4 departure hyperbolas have been included.

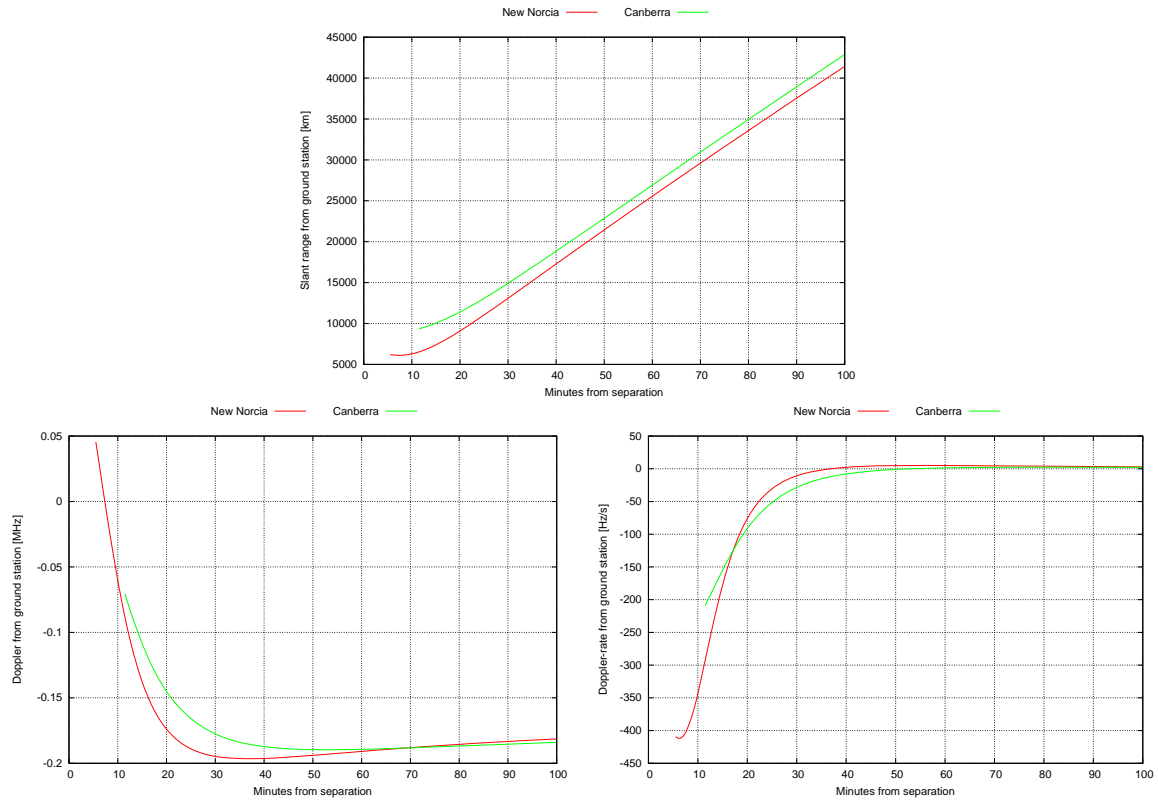


Figure 3-29 2018 Launch Option E: slant-range, Doppler and Doppler-rate at first acquisition

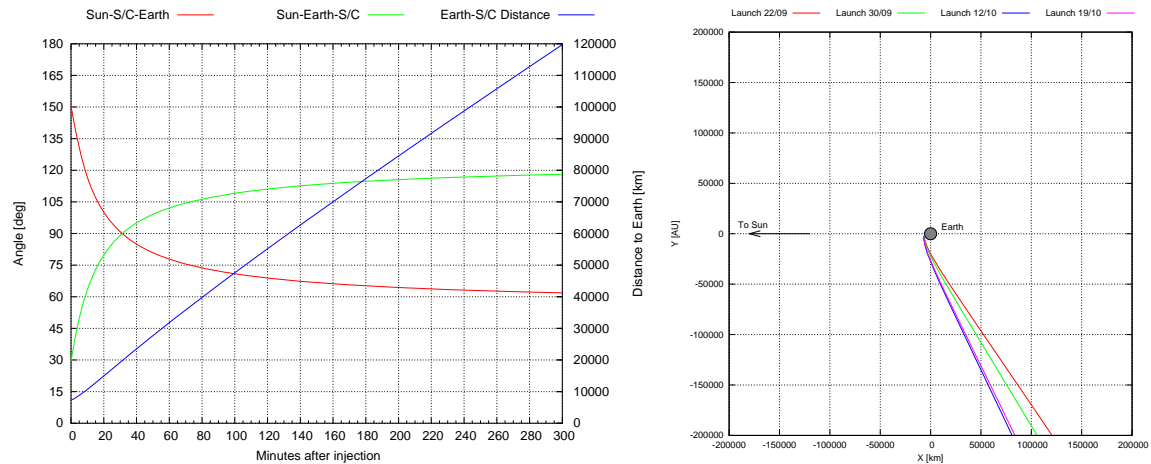


Figure 3-30 2018 Launch Option E: Earth, Sun & S/C relative geometry at early LEOP.

The following figure shows the evolution of SES, SSE and Sun-S/C-Moon angles during the first 24 hours after separation. The SES goes in 7 hours from about 30 deg to 120 deg, where it then stabilises as the spacecraft departs from the Earth in the asymptote direction. The SSE goes in the same time from about 150 deg to 60 deg. The Sun-S/C-Moon increases initially peaking at about 171 deg 9 hours after launch.



The last 2 phasing angles are relevant for possible blinding of the star trackers due to the Earth and/or Moon. The nominal spacecraft attitude is Sun pointing with the +Xsc panel. The star trackers are mounted in the opposite -Xsc panel with the bore sight canted about 26 deg from the -Xsc axis as shown in [30]. This design avoids the star trackers being blinded by the Sun. However, during LEOP the Earth and/or the Moon can be in the -Xsc hemisphere for some period of time, with the risk of blinding the star trackers. Earth and Moon, require an exclusion angle of 20 deg and 19 deg, respectively, with respect to their limb. The exclusion angle dependency with the distance to Earth and Moon is not known, so it is assumed constant at this point in time. The exclusion angle added to the 26 deg cant angle of the star trackers means that there is a certain risk of blinding until the Sun-S/C-Earth(or Moon) angle gets below about 135 deg. The figure shows that for this launch day this condition is satisfied very quickly for the Earth, but it takes 18 hours for the Moon.

Earth and Moon phasing angles experience significant changes with the launch day. Further analysis of the star tracking blinding as a function of the launch day is provided in the launch window analysis in Section 4.2 (pages 133-135).

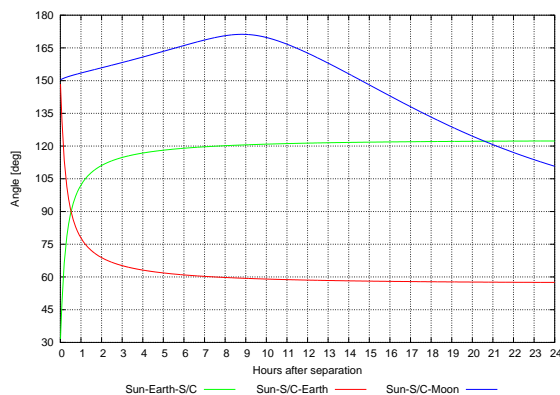


Figure 3-31 2018 Launch Option E: communication angles in the first 24 hours of LEOP

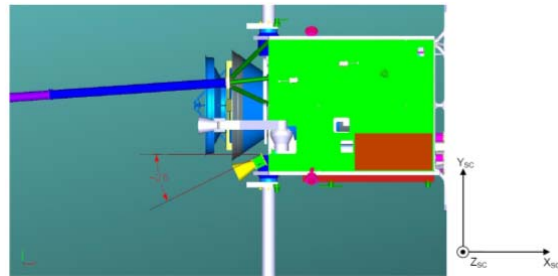


Figure 3-32 Solar Orbiter Star Tracker Configuration (extracted from [30])

On the ejection of the METIS cap

Solar Orbiter's METIS instrument needs a sealing cap to prevent contamination to the interior of the instrument. The current design concept foresees a sealing cap to be installed on-ground during early instrument integration and to be ejected in-orbit following the completion of the spacecraft activation activities that can produce particulate contamination.

The ejection of the METIS cap is planned to occur in general short after LEOP and during the 90-day NECP. Actual constraints imposed by METIS are:

- Cap ejection no earlier than 30 days after launch to avoid contamination
- Cap ejection before reaching a spacecraft-Sun distance of 0.6 AU (due to METIS cap design)

So the ejection has to occur when the spacecraft is travelling between the Earth and the first Venus GAM. The cap will then flyby Venus in a slightly different trajectory as the spacecraft and will reach a certain post-flyby orbit around the Sun. The direction in which the METIS cap is ejected will have to be carefully chosen such as to be compliant with the Planetary Protection Requirements (accidental impact on Mars) and Space Debris Mitigation Policies, as the cap might come back to the Earth.



On the selection of the ejection direction the spacecraft constraint to maintain Sun pointing attitude below 0.95 AU from the Sun plays a major role. Above this distance any orientation is allowed so that there is no constraint to the direction of cap ejection. Below this distance only a roll around the spacecraft-Sun line is allowed giving just 1 degree-of-freedom for the ejection direction, which will lie then in a cone around the spacecraft-Sun line due to the angle of 20-40 deg (TBD) between the cap ejection direction and the spacecraft +Xsc axis.

Figure 3-33 shows the evolution of Sun, Earth and Venus distances early in the mission. It permits to identify that the Sun distance to maintain the Sun pointing attitude is reached 55 days after launch. Thus ejection in any direction and respecting the METIS cap constraints is possible between 30 and 55 days after launch. The latest possible ejection before reaching the 0.6 AU constraint is 128 days after launch (57 days before GAM-V1).

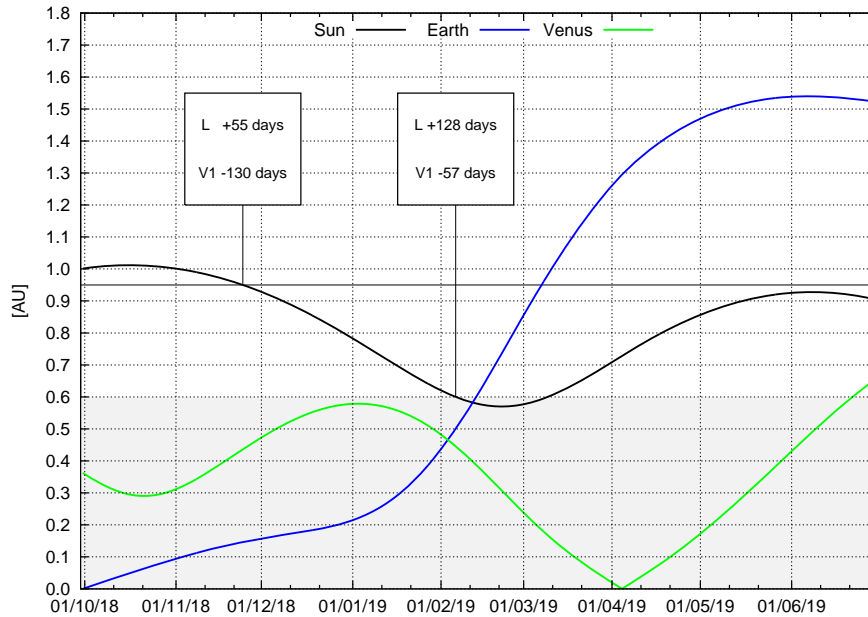


Figure 3-33 2018 Launch Option E: distances applicable to METIS cap ejection

A detailed analysis of the METIS cap trajectory after ejection and the selection of the ejection direction is reported in [32]. The conclusion is that the post-Venus-flyby aphelion radius can be limited below 0.96 AU for early ejection 30 days after launch and below 0.933 AU for late ejection 120 days after launch when the METIS cap is ejected within the spacecraft heliocentric orbital plane and opposite to the velocity (ejection cones from 20 to 40 degrees from the +Xsc direction were studied).



3.2 2018 Launch Option D

3.2.1 DESCRIPTION

This trajectory uses the same cruise scheme as the 2018 October trajectory of Section 3.3, but slightly modified to use a different sequence of resonances during the science phase that dramatically improve the data return. The modification of the cruise phase is based on shifting the GAM-E1 back from Ls 140° to Ls 127°, which reduces the relative velocity of the next Venus encounters (19.2 km/s instead of 20 km/s) and at the same time shifts the Venus GAMs closer to the optimum solar longitude (Ls 75°) to increase the solar inclination. With this modification GAM-V2 is encountered at an ESV angle of 147° that is close to a best case geometry in terms of data return for the next 5:4 resonant orbit.

The sequence of resonances used in this trajectory is 5:4–4:3–3:2–3:2. The NMP starts already with the E2-V2 leg with a perihelion pass at 0.31 AU. The next 5:4 resonance is considered the core science period of the NMP and will provide 5 perihelion passes at 0.29 AU, while the solar inclination has reached 12.7°. For the next 4:3 resonance the perihelion can be maintained at 0.3 AU and the inclination raises to 21°. During the EMP, the 3:2 resonances will provide a combination of perihelion radius and solar inclination of 0.292 AU – 27.5° and 0.34 AU – 32.4°. The overall duration of the trajectory as planned is 10.59 years.

The reference trajectory described here corresponds to launch on 7th November, which is on the close side of the identified Atlas V 411 launch window. The majority of possible launch days are actually on October 2018. The trajectory will be implemented as follows:

1. Launch with an escape velocity from the Earth of 5.62 km/s and declination of the escape velocity of -17.4°.
2. About 4.5 months after launch in March 2019, a Venus GAM with a pericentre height of 7400 km will put the spacecraft in a trajectory towards the Earth.
3. 10.5 months later in February 2020, an Earth GAM with a pericentre height of 4100 km inserts the spacecraft in an orbit with a period such that there is another Earth GAM 22 months later when the spacecraft has described more than 2.6 revolutions and the Earth has described a bit less than 2 revolutions about the Sun.
4. The second Earth GAM with a pericentre height of about 4700 km inserts the spacecraft into a heliocentric orbit in which Venus is encountered after about 1.4 revolutions. The perihelion radius of 0.31 AU allows for the start of the remote sensing observations already in this Earth-Venus arc.
5. The spacecraft arrives to the second Venus GAM with a hyperbolic velocity of 19.17 km/s and starts the sequence of resonances with Venus 5:4–4:3–3:2–3:2 of the science mission. This sequence requires 4 additional GAMs, from GAM-V2 to GAM-V5 that are performed at the maximum possible deflection compatible with a minimum altitude of 350 km at the Venus closest approach.

Table 3-11 and Table 3-12 present a summary of the main events/parameters of the mission. All results for this trajectory option have been obtained with the linked conics model.

Table 3-11 2018 Launch Option D: Trajectory SummaryTable 3-12 2018 Launch Option D: Mission Parameters

Figure 3-34 shows V-infinity direction diagram that summarizes the sequence of resonances 5:4-4:3-3:2-3:2 at Venus. In this case the Venus GAMs are inbound as shown by the positive right ascension of the infinite velocity. The sequence starts with the arrival velocity of GAM-V2 at the top-left corner. The solar inclination is maximized by decreasing the declination of the infinite velocity, thus going towards the bottom-right corner of the plot. At the last 3:2 resonance the solar inclination has not reached its potential maximum for this infinite velocity and solar longitude of Venus. A hypothetical GAM-V6 performed after mission end could increase the solar inclination beyond 35 deg, even in a shorter period orbit like the 5:3 resonance.

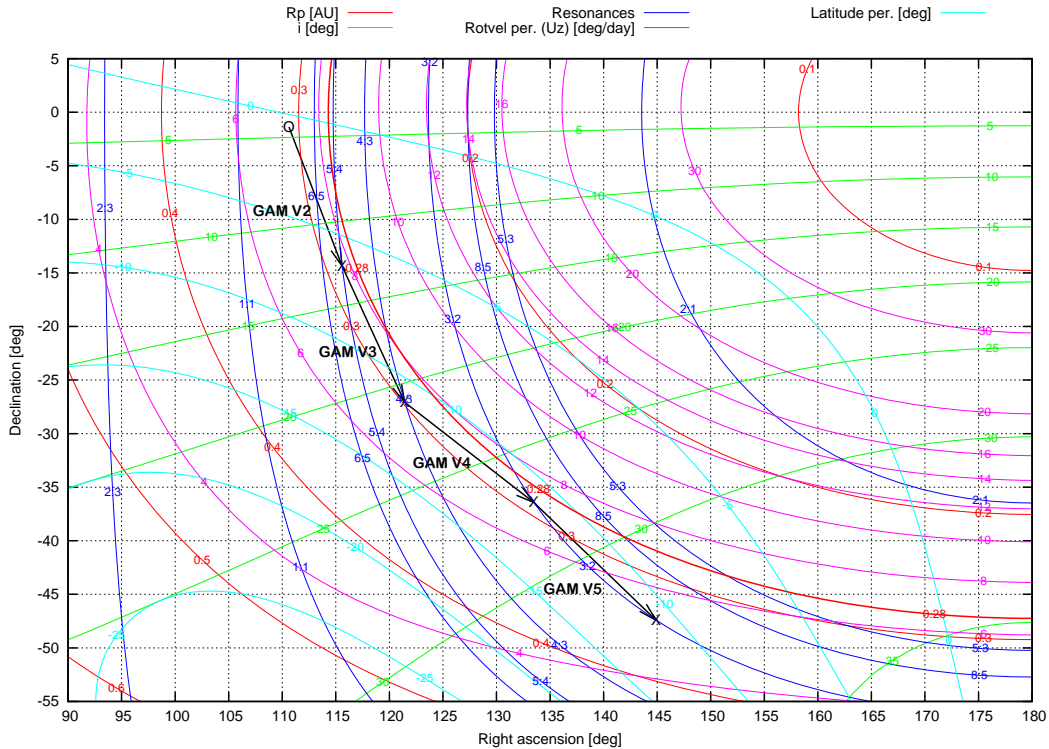


Figure 3-34 2018 Launch Option D: V-infinity diagram

Trajectory Plots

Figure 3-35 shows the X-Y trajectory projection from launch until GAM-V2, which includes the cruise phase and the Earth-Venus arc until the first GAM at Venus initiating the sequence of resonances for the science phase. In this plot the green lines indicate the location of Venus that are optimal to increase the solar inclination of the heliocentric orbit, while the red lines indicate the points of Venus orbit that are the worst for a given hyperbolic velocity. GAM-V2 is not located at a particularly favourable point for the inclination increase, thus a relatively high infinite velocity is required. It is however a better location than in the 2018 October trajectory (see Section 3.3.1) due to the small shift towards the optimal solar longitude produced by the 1 week earlier arrival to Venus.

Figure 3-36 and Figure 3-37 shows the projections of the entire trajectory either on the ecliptic reference frame or on the XY plane of the Sun-Earth rotating plane.

Figure 3-38 shows separately the projection of each of the science orbits in the Sun-Earth rotating frame. The initial 5:4 resonance provides a huge capability for data return with DLI of 2.43. The favourable phasing of the orbit with the Earth provides 3 aphelia properly oriented for downlink and drifting gradually closer to Earth with minimum distances from 0.35 down to 0.2 AU. Thus during the V2-V3 leg three long periods provide the maximum data rate.

The 4:3 resonance starting at V3 with a favourable ESV angle of -21° is also close to a best case for downlink providing a DLI of 1.89 AU^{-2} . Overall for NMP from V2 to V4 an outstanding DLI of 2.18 AU^{-2} is provided. The data return capability of this part of the trajectory is huge: from E2 the spacecraft



Figure 3-39 shows the evolution of the distance to the Sun, Earth and Venus and Figure 3-40 shows the evolution of the Sun-Spacecraft-Earth and Sun-Earth-Spacecraft angles. Figure 3-41 zooms on the region below 10 deg to show more clearly the solar conjunctions, which occur outside the GAM events. Table 3-13 provides a summary of the solar conjunction periods and MGA safe-mode blackouts. For this trajectory 6 solar superior conjunctions are encountered, the longest of them lasting 21 days on August 2025. The longest safe-mode blackout occurs also during the same solar conjunction and can last as much as 44 days.

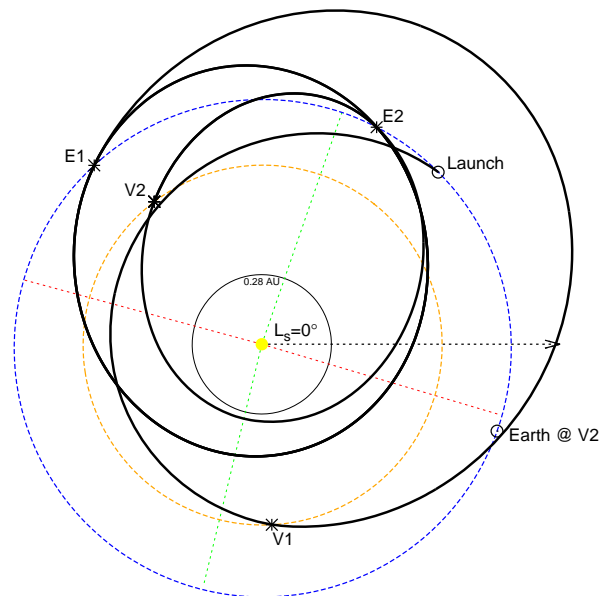
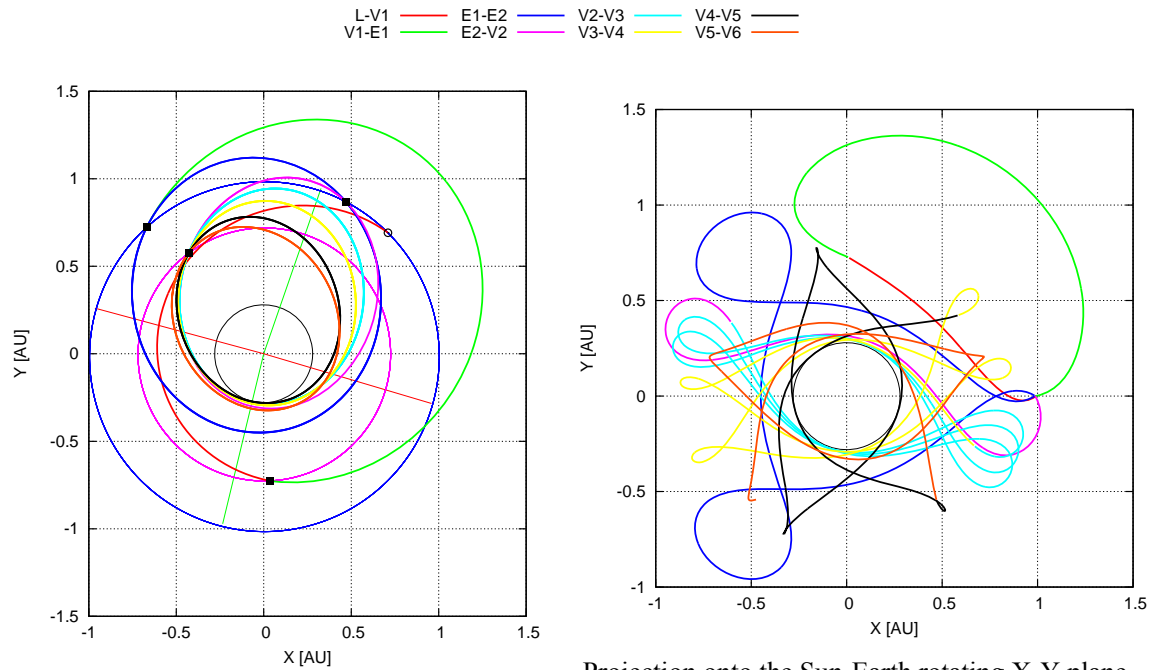


Figure 3-35 2018 Launch Option D: X-Y Trajectory projection from launch until GAM-V2



Projection onto the ecliptic X-Y plane

Projection onto the Sun-Earth rotating X-Y plane
The X-axis (Y=0) is the line from the Sun to the Earth

Figure 3-36 2018 Launch Option D: X-Y Trajectory projections from Launch to End of Mission

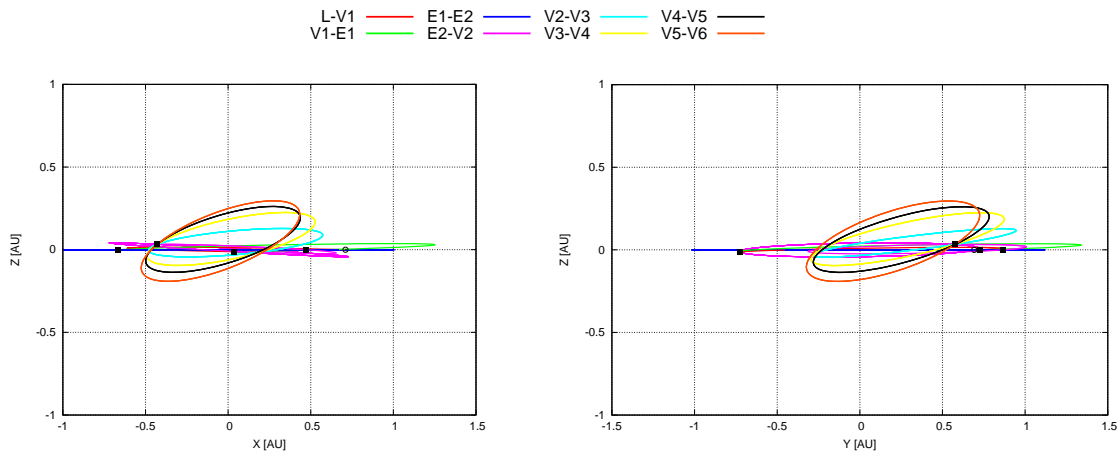


Figure 3-37 2018 Launch Option D: X-Z and Y-Z Trajectory projections

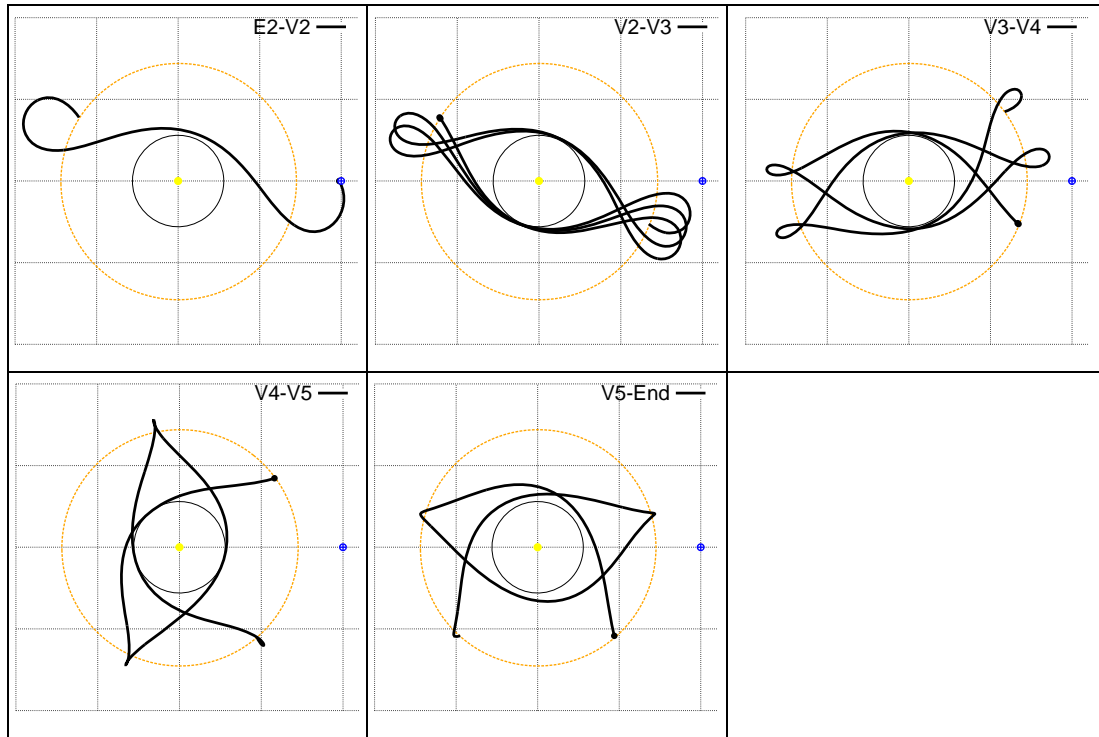


Figure 3-38 2018 Launch Option D: Science orbits projection in the Sun-Earth rotating frame

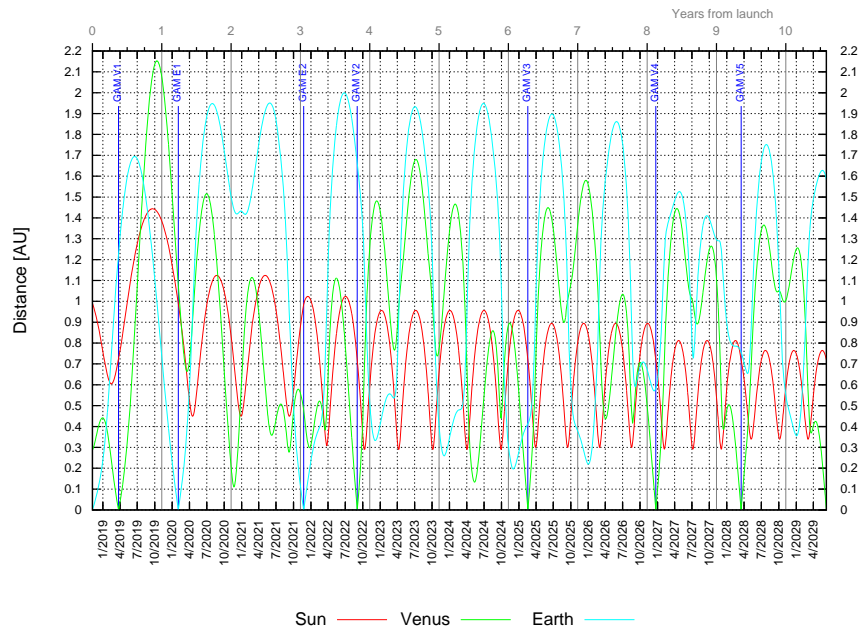


Figure 3-39 2018 Launch Option D: Spacecraft distance to Sun, Venus and Earth

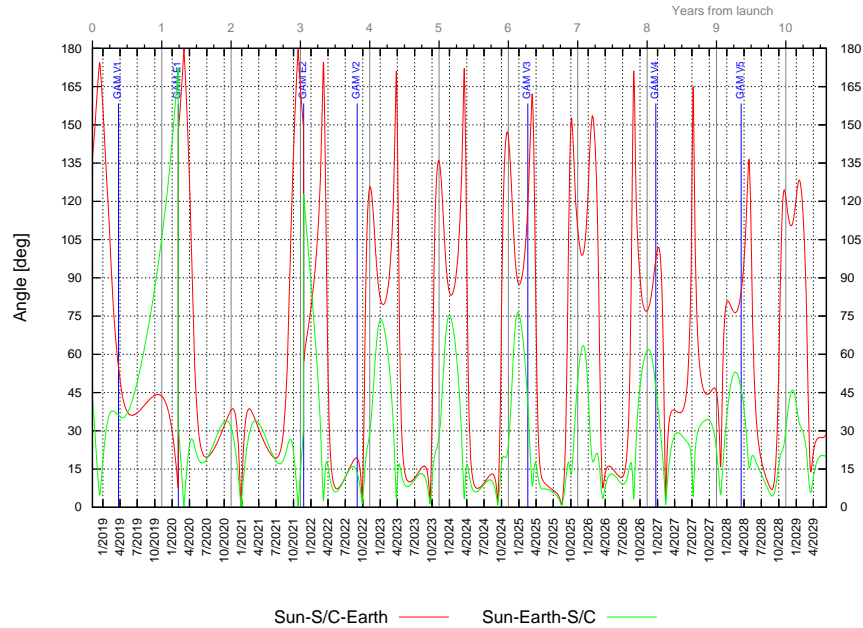


Figure 3-40 2018 Launch Option D: SSE and SES angles

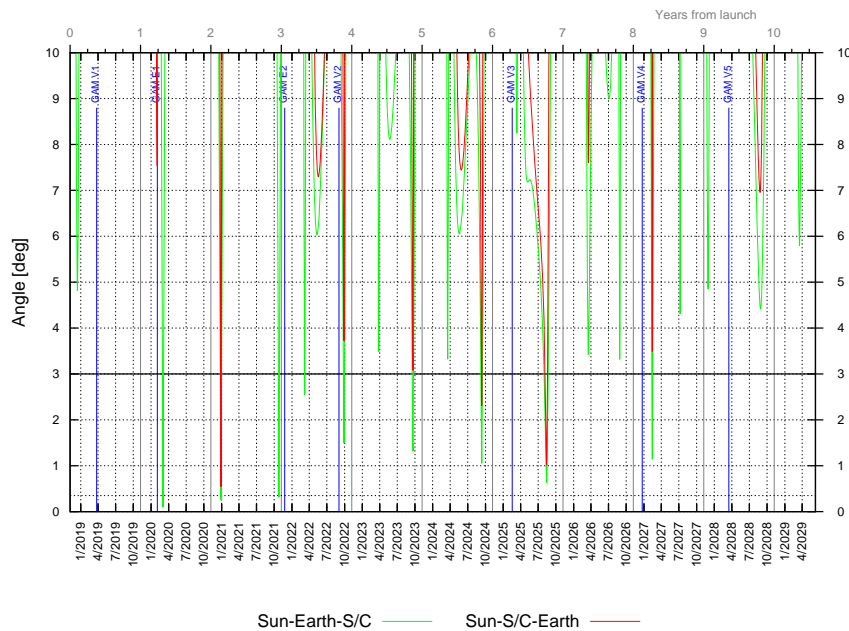


Figure 3-41 2018 Launch Option D: SSE and SES angles – Detail of conjunctions



Solar Conjunction Periods SES<3 deg

	Type	Start	End	Duration [days]	Min SES [deg]
1	Inferior	2020-02-29	2020-03-05	5.5	0.10
2	Superior	2020-12-25	2020-12-31	6.6	0.25
3	Inferior	2021-10-22	2021-10-28	5.6	0.31
4	Inferior	2022-03-07	2022-03-08	1.7	2.55
5	Superior	2022-09-24	2022-09-30	5.9	1.49
6	Superior	2023-09-16	2023-09-23	6.9	1.32
7	Superior	2024-09-07	2024-09-15	8.4	1.05
8	Superior	2025-07-31	2025-08-22	21.3	0.63
9	Superior	2027-02-10	2027-02-15	4.4	1.14

Safe Mode Blackout Periods SES<=5 deg OR SSE<=3 deg (longer than 7 days)

	Start	End	Duration [days]
1	2020-02-27	2020-03-07	9.2
2	2020-12-22	2021-01-03	11.1
3	2021-10-20	2021-10-29	9.3
4	2022-09-21	2022-10-02	11.0
5	2023-09-13	2023-09-26	12.7
6	2024-09-02	2024-09-18	15.2
7	2025-07-13	2025-08-26	43.9
8	2026-03-13	2026-03-23	10.2
9	2027-02-09	2027-02-17	7.7
10	2028-08-19	2028-09-04	16.0

Table 3-13 2018 Launch Option D: Solar Conjunctions

Figure 3-42 shows the evolution of the Earth-Spacecraft range-rate. The range of variation for the entire mission goes from -57.5 km/s to 59.9 km/s.

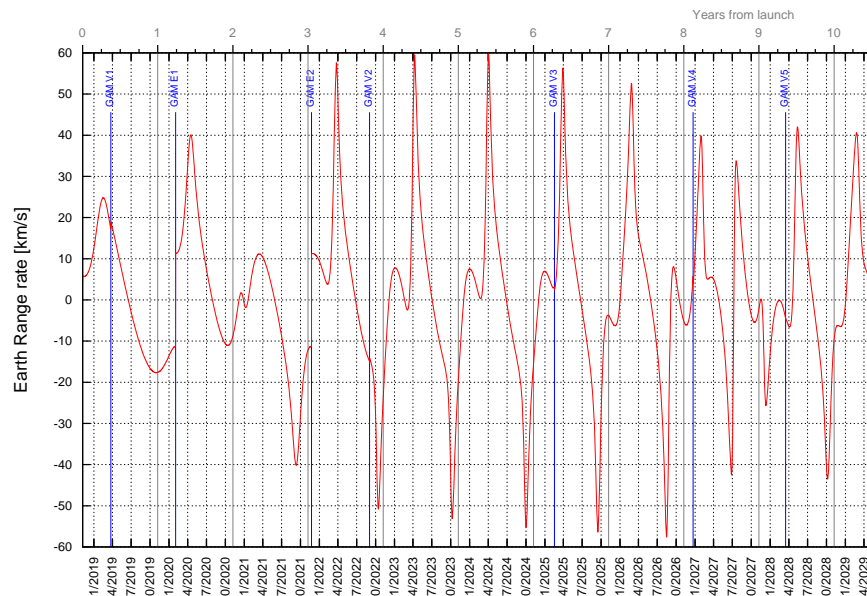


Figure 3-42 2018 Launch Option D: Variation of Earth-Spacecraft range-rate

Figure 3-43 shows the evolution of the Doppler effect due to the Earth-Spacecraft range-rate and Figure 3-44 shows the evolution of the Doppler rate. The Doppler varies from -1.68 MHz to 1.62 MHz during the entire mission. The Doppler seen from the ground stations will be slightly different due to the rotation velocity of the Earth.

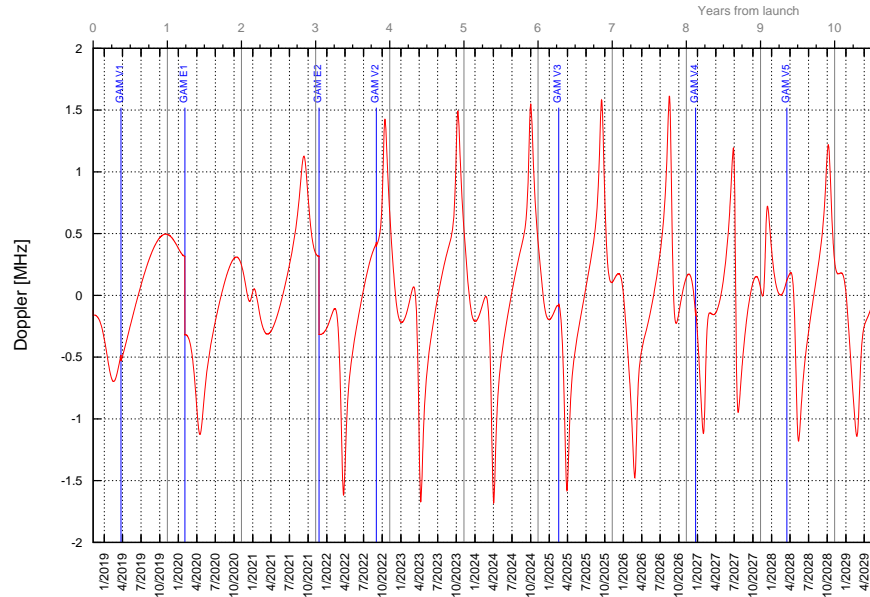


Figure 3-43 2018 Launch Option D: Variation of Earth-Spacecraft Doppler

The Doppler varies very rapidly at the GAMs and so Figure 3-44 shows Doppler-rate peaks extending beyond the limits of the graph. The limits of this figure have been chosen to allow representing the variations of the Doppler-rate in the heliocentric phases which are of the order of a few Hz/s, while peaks at the GAMs can largely exceed 500 Hz/s. The detail analysis of the Doppler-rates reached at the GAMs is presented in Section 3.2.4.

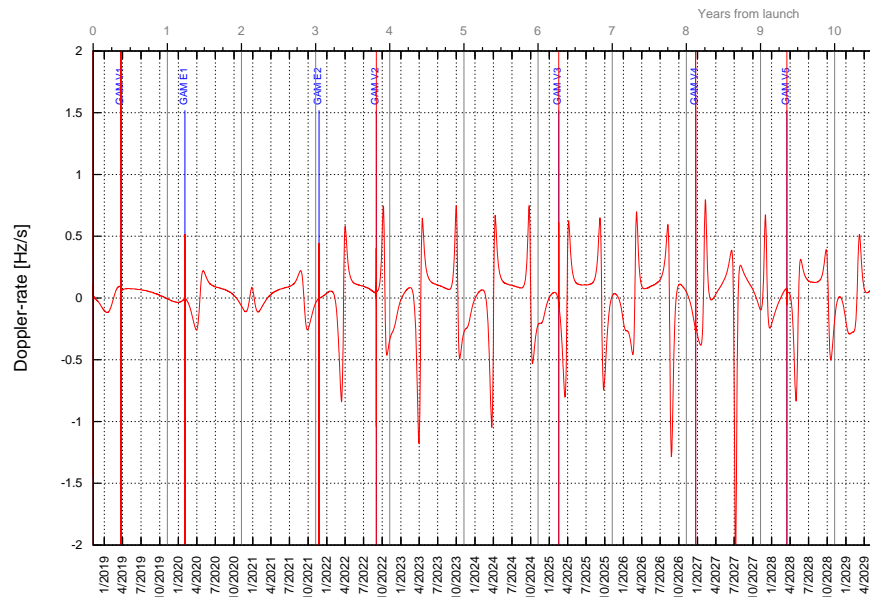


Figure 3-44 2018 Launch Option D: Variation of Earth-Spacecraft Doppler-rate



3.2.2 SCIENCE PROPERTIES

The following set of figures and tables provide details of the characteristics of the trajectory relevant for the mission science.

Figure 3-45 shows together the evolution of the solar latitude with the distance to the Sun. Contrarily to 2018 Option E trajectory, the perihelion of the science orbit goes on the Southern Sun hemisphere and thus the solar latitude is negative at the perihelion. For each science orbit the spacecraft passes the point of minimum latitude first, shortly later the perihelion and then the highest latitude.

Figure 3-46 provides a Sun-centric representation of the science orbits during the NMP and EMP. The plot shows the 5 orbits that are used in the science phase of this trajectory, including the second Earth-Venus leg. This figure also shows how the perihelions are below the Sun Equator and the Venus GAMs are encountered after the perihelion. The spacecraft describes the orbits in the clockwise direction of the plot.

Figure 3-47 shows the evolution of the perihelion and aphelion and the points of maximum and minimum solar latitude as a function of the date and Table 3-14 provides data about the minimum/maximum latitude and perihelion events of each science orbit.

Table 3-15 provides the number and duration of the passes close to the Sun for different distances. For this trajectory the spacecraft will approach the Sun 10 times below 0.3 AU with stays between 0.2 and 6.5 days and 16 times below 0.4 AU with an average stay of 25 days. The accumulated duration below these distances to the Sun is 52 and 404 days, respectively. 3 additional perihelions between 0.4 and 0.5 AU will be provided during the cruise phase.

Figure 3-49 shows the spacecraft rotation velocity around the Sun. The maximum rotation velocity is achieved at perihelion of the orbit achieved after GAM V2.

Figure 3-50 shows the evolution of the Earth distance together with the estimated downlink volume per day assuming a flat 8-hour daily pass. The plot shows the periods in which the maximum data rate is provided (green shadowed), which are related to the close-Earth aphelions as shown before in Figure 3-38. This trajectory provides 5 of such periods. 4 of them occur during NMP between GAM-V2 and GAM-V4. The last period occurs near the end of the mission.

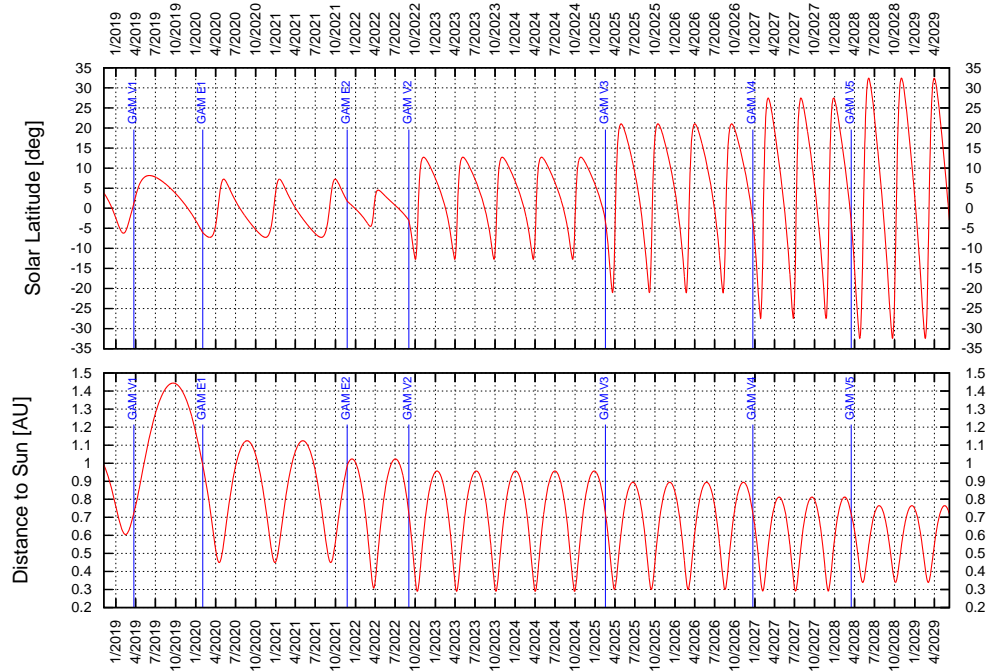


Figure 3-45 2018 Launch Option D: Spacecraft solar latitude + Spacecraft distance to the Sun

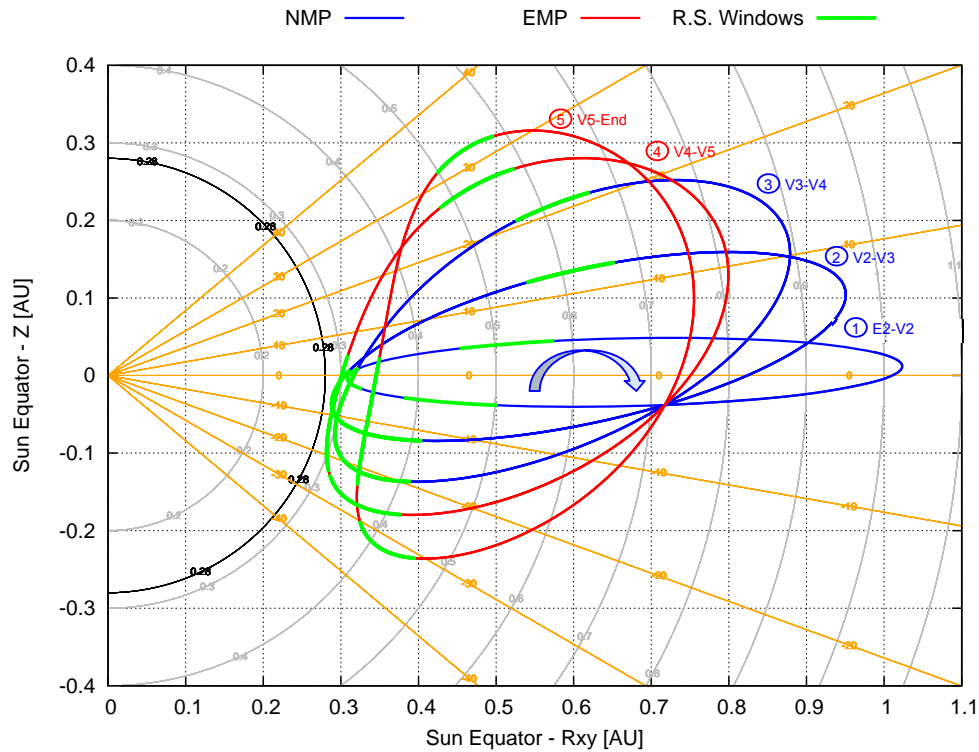


Figure 3-46 2018 Launch Option D: projection of science orbits wrt Sun Equator and North Pole

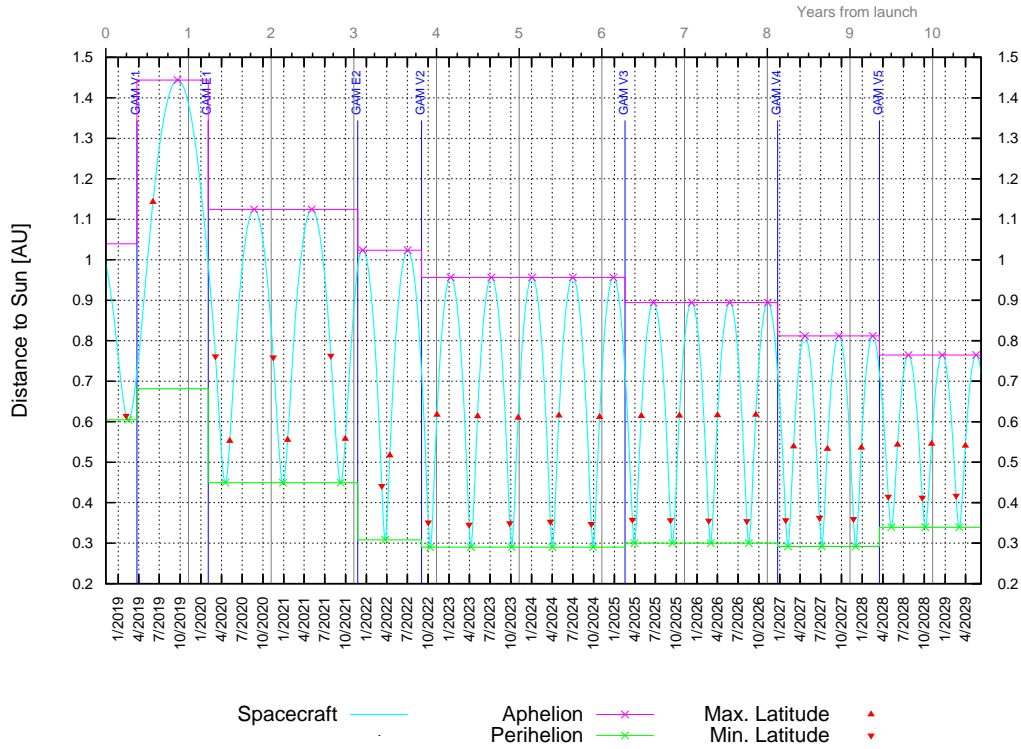


Figure 3-47 2018 Launch Option D: Evolution of apses and points of extreme solar latitude

Event	#	Date	Flight Time (y)	Sun Distance (AU)	Solar Latitude (deg)
GAM-E2		2021-11-24	3.05		NMP Start
MINLAT	1	2022-03-10	3.34	0.438	-4.53
MINRP	1	2022-03-25	3.38	0.309	-0.70
MAXLAT	1	2022-04-14	3.43	0.517	4.53
GAM-V2		2022-09-02	3.82		
MINLAT	2	2022-10-02	3.90	0.350	-12.73
MINRP	2	2022-10-10	3.92	0.290	-6.48
MAXLAT	2	2022-11-08	4.00	0.614	12.73
MINLAT	3	2023-03-31	4.39	0.350	-12.73
MINRP	3	2023-04-08	4.42	0.290	-6.54
MAXLAT	3	2023-05-07	4.50	0.613	12.73
MINLAT	4	2023-09-26	4.89	0.350	-12.73
MINRP	4	2023-10-05	4.91	0.290	-6.50
MAXLAT	4	2023-11-03	4.99	0.614	12.73
MINLAT	5	2024-03-24	5.38	0.350	-12.73
MINRP	5	2024-04-02	5.40	0.290	-6.47
MAXLAT	5	2024-05-01	5.48	0.614	12.73
MINLAT	6	2024-09-20	5.87	0.350	-12.73
MINRP	6	2024-09-28	5.89	0.290	-6.44
MAXLAT	6	2024-10-27	5.97	0.613	12.73
GAM-V3		2025-02-16	6.28		
MINLAT	7	2025-03-21	6.37	0.355	-21.03
MINRP	7	2025-03-30	6.39	0.300	-11.15
MAXLAT	7	2025-04-29	6.48	0.615	21.03
MINLAT	8	2025-09-06	6.83	0.354	-21.03
MINRP	8	2025-09-14	6.85	0.300	-11.23
MAXLAT	8	2025-10-15	6.94	0.614	21.03
Event	#	Date	Flight Time (y)	Sun Distance (AU)	Solar Latitude (deg)
MINLAT	9	2026-02-21	7.29	0.355	-21.03
MINRP	9	2026-03-02	7.32	0.300	-11.14
MAXLAT	9	2026-04-01	7.40	0.615	21.04
MINLAT	10	2026-08-09	7.75	0.354	-21.04
MINRP	10	2026-08-17	7.78	0.300	-11.21
MAXLAT	10	2026-09-17	7.86	0.614	21.04
GAM-V4		2026-12-22	8.13		EMP Start
MINLAT	11	2027-01-27	8.22	0.359	-27.46
MINRP	11	2027-02-06	8.25	0.292	-11.18
MAXLAT	11	2027-03-03	8.32	0.536	27.46
MINLAT	12	2027-06-26	8.63	0.358	-27.46
MINRP	12	2027-07-06	8.66	0.292	-11.24
MAXLAT	12	2027-07-31	8.73	0.535	27.46
MINLAT	13	2027-11-23	9.04	0.359	-27.46
MINRP	13	2027-12-03	9.07	0.292	-11.04
MAXLAT	13	2027-12-27	9.14	0.535	27.46
GAM-V5		2028-03-16	9.36		
MINLAT	14	2028-04-25	9.46	0.415	-32.42
MINRP	14	2028-05-08	9.50	0.340	-10.78
MAXLAT	14	2028-06-05	9.58	0.543	32.42
MINLAT	15	2028-09-21	9.87	0.415	-32.42
MINRP	15	2028-10-05	9.91	0.340	-10.84
MAXLAT	15	2028-11-02	9.99	0.544	32.42
MINLAT	16	2029-02-18	10.28	0.414	-32.42
MINRP	16	2029-03-04	10.32	0.340	-10.90
MAXLAT	16	2029-03-31	10.40	0.544	32.42

Table 3-14 2018 Launch Option D: Characteristics of perihelion and extreme points of solar latitude



	# Times	Accumulated Duration (days)	Minimum Duration (days)	Maximum Duration (days)
Cruise Phase		1112		
Below 0.3 AU	0	0.0	0.0	0.0
Below 0.4 AU	0	0.0	0.0	0.0
Below 0.5 AU	3	80.0	26.7	26.7
Below 0.6 AU	3	152.6	50.9	50.9
Science Mission		2754		
Below 0.3 AU	10	52.1	0.2	6.5
Below 0.4 AU	16	403.8	23.6	26.9
Below 0.5 AU	16	668.1	38.7	45.3
Below 0.6 AU	16	952.0	54.2	67.9
Total Mission		3867		
Below 0.3 AU	10	52.1	0.2	6.5
Below 0.4 AU	16	403.8	23.6	26.9
Below 0.5 AU	19	748.1	26.7	45.3
Below 0.6 AU	19	1104.6	50.9	67.9

Table 3-15 2018 Launch Option D: Number and duration of passes close to the Sun

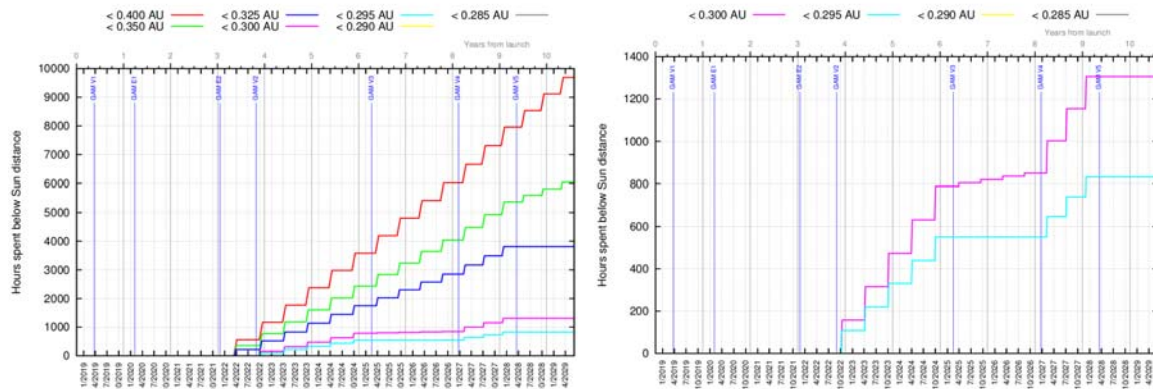


Figure 3-48 2018 Launch Option D: Evolution of time spent below different Sun ranges

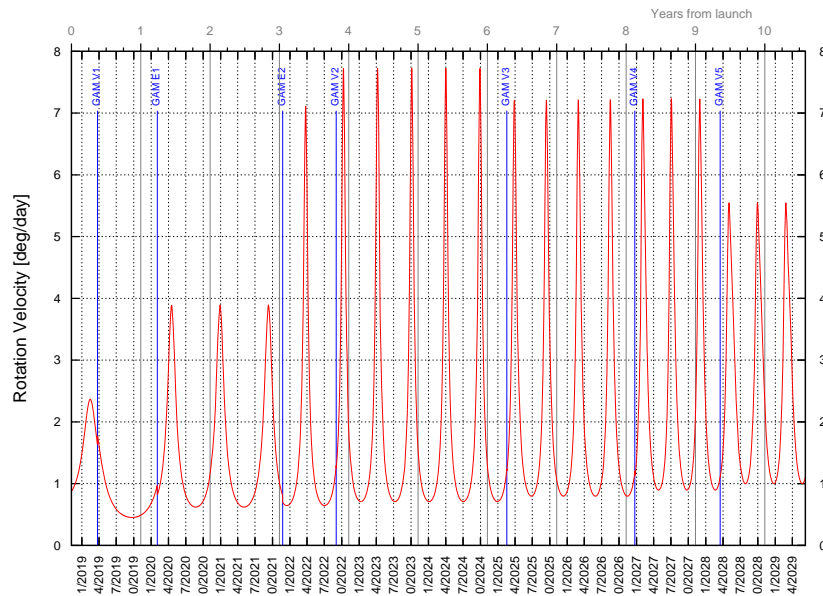


Figure 3-49 2018 Launch Option D: Spacecraft rotation velocity about the Sun

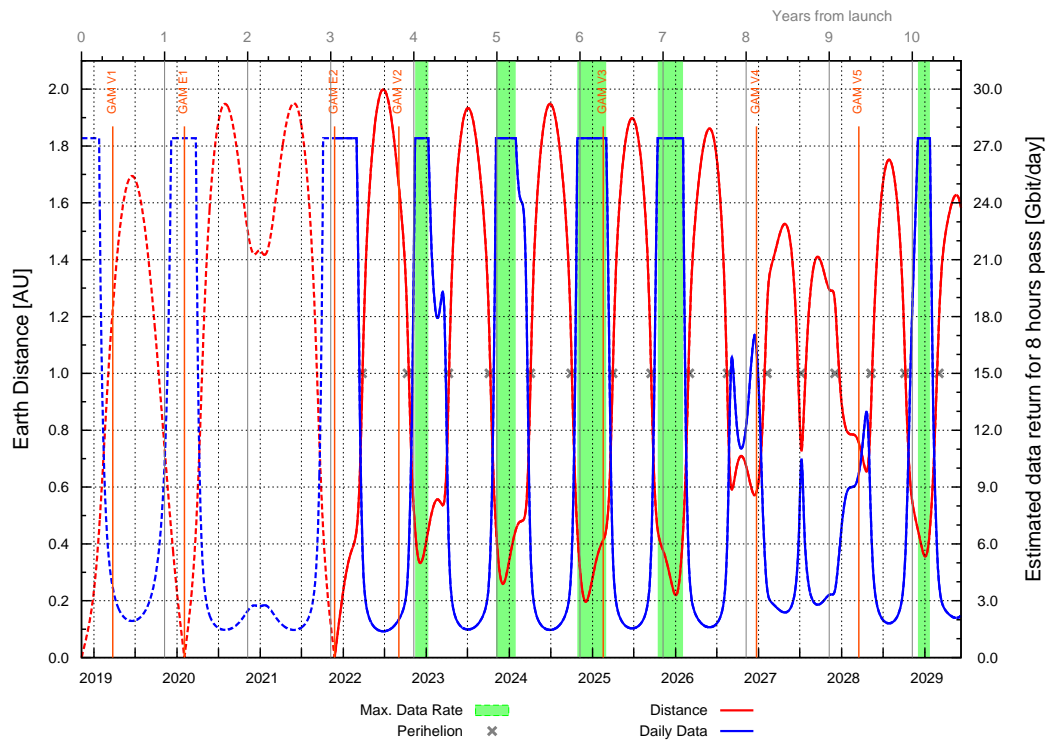


Figure 3-50 2018 Launch Option D: Evolution of Earth distance and potential downlink



3.2.3 GROUND STATION VISIBILITY

Figure 3-51 shows the evolution of the equatorial declination of the Earth-to-spacecraft direction.

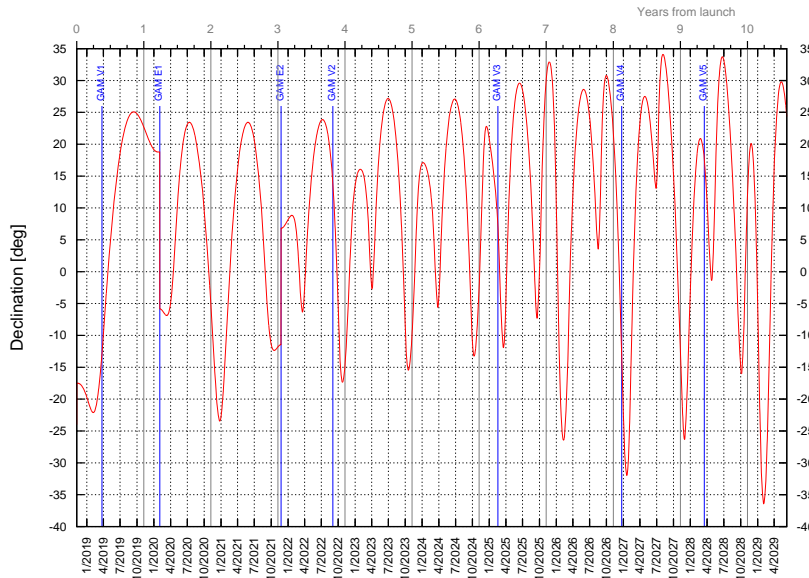


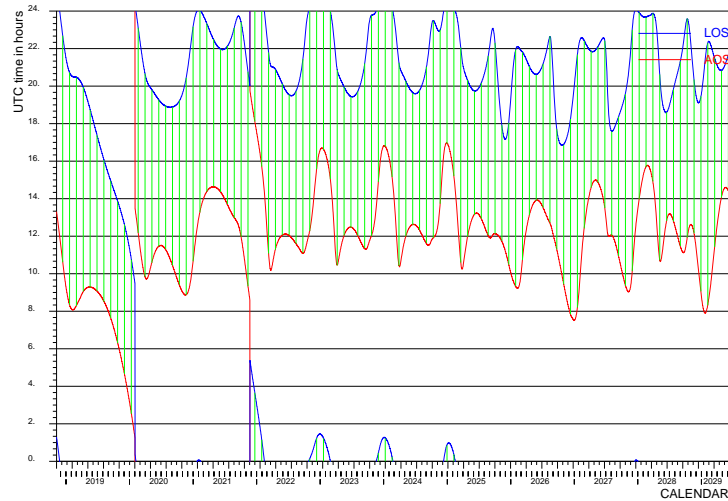
Figure 3-51 2018 Launch Option D: Spacecraft equatorial declination.

Figure 3-52 presents the daily period of visibility from each of the 3 ESA ground stations. The hours of the day when Acquisition Of Signal, AOS, and Loss Of Signal, LOS, take place is provided with a red and a blue line, respectively. Vertical black lines show the GAMs. The visibility is shown assuming 10° minimum elevation from the ground station. Daily visibility from any of the ground stations is guaranteed.

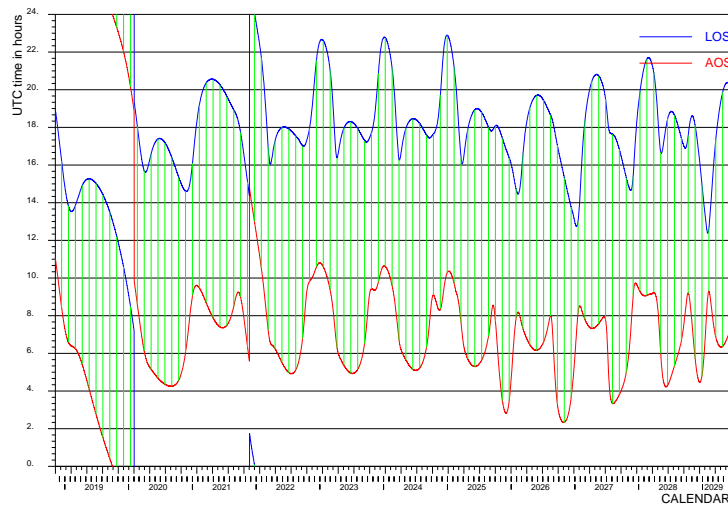
Figure 3-53 shows the duration of the visibility as a function of the date for all three ground stations. Figure 3-54 shows a combination of the daily period of visibility from the 3 stations.



Malargüe



Cebreros



New Norcia

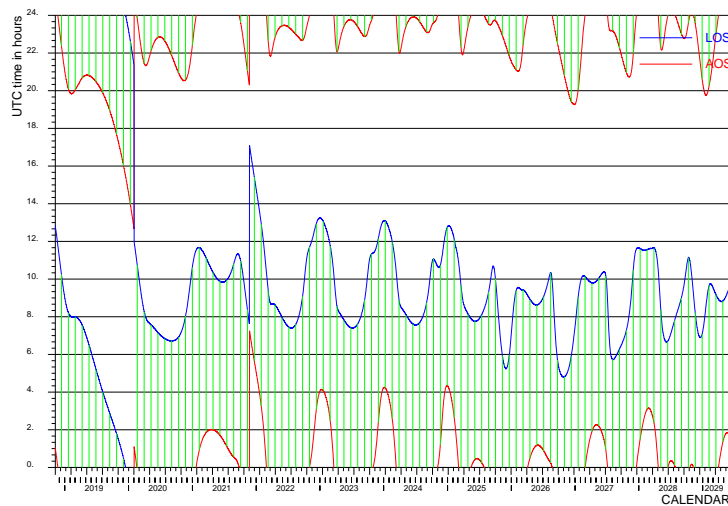


Figure 3-52 2018 Launch Option D: Daily period of visibility from ESA DS stations.

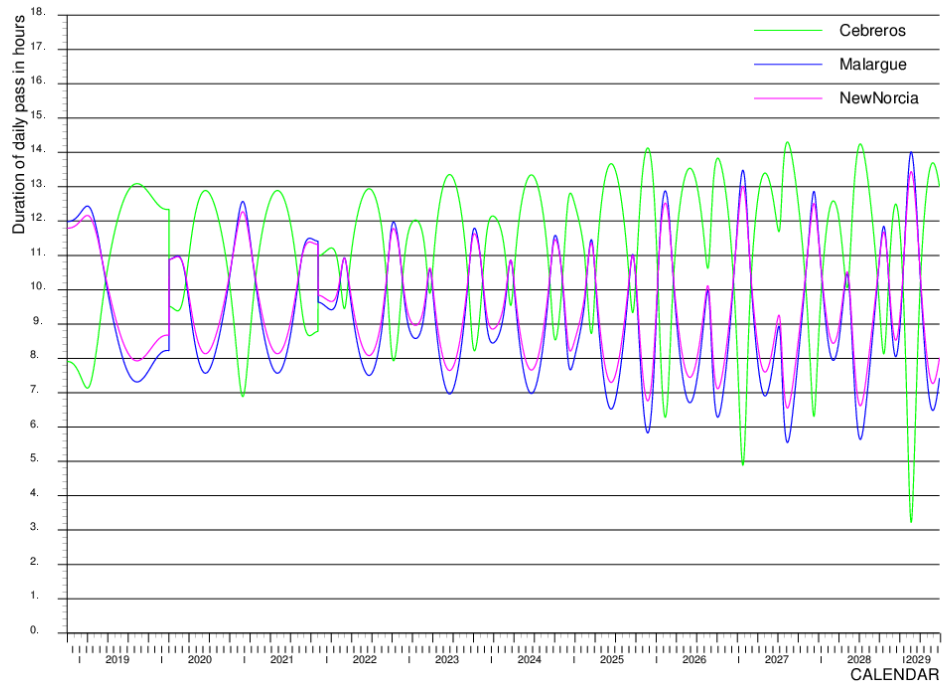


Figure 3-53 2018 Launch Option D: Daily duration of visibility from ESA Deep Space stations

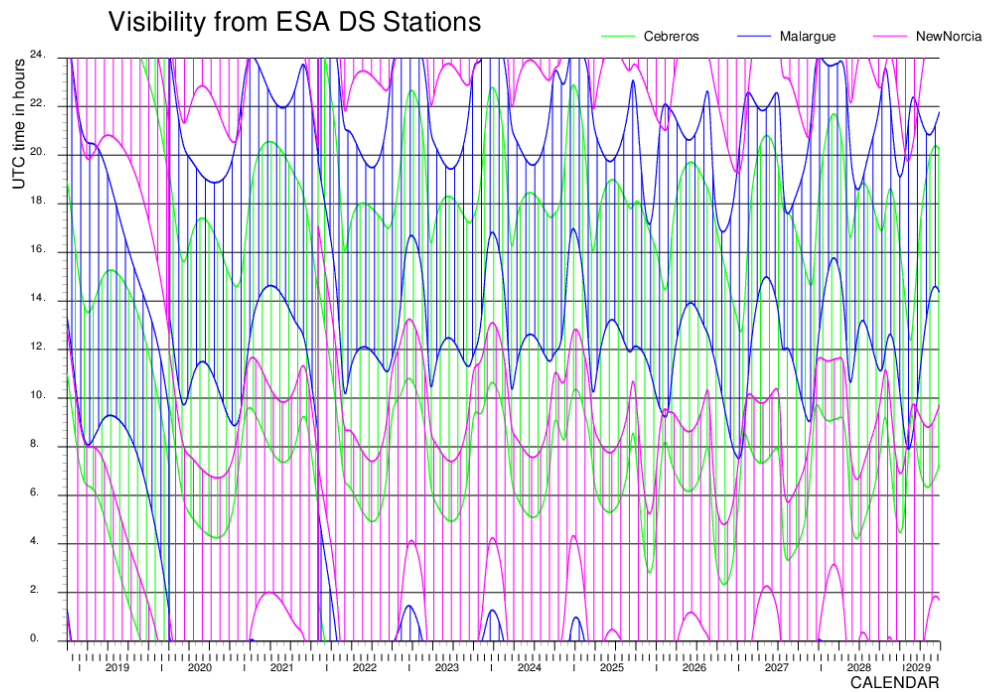


Figure 3-54 2018 Launch Option D: Daily period of visibility from ESA Deep Space stations.



3.2.4 GAMS DETAILS

Table 3-16 shows the characteristics of the GAMS including the duration of the eclipse and occultation events. The GAMS during the cruise phase are all performed at comfortable altitudes from 4000 to 7000 km. The Venus GAMS during the science phase are all performed at maximum deflection at the minimum altitude of 350 km.

For this trajectory eclipse will occur only at GAM-V1 and GAM-E2, being the longest eclipse about 31 min. Occultation occurs only at GAM-V4 for about 5 min.

GAM	Date	Re (AU)	Vinf (km/s)	Hmin (km)	Eclipse (min)	Occult. (min)	LST ¹ (h)	Ls (deg)	SSE (deg)	SES (deg)	ESV (deg)
V1	2019-03-24	1.227	8.867	7437	30.8	0	19.6	273.2	54.2	36.3	89.5
E1	2020-02-02	0	11.266	4143	0	0	6.8	133.2	-	-	-
E2	2021-11-24	0	11.269	4712	19.4	0	3.1	62.1	-	-	-
V2	2022-09-02	1.660	19.171	350	0	0	9.2	127.0	19.0	13.4	147.5
V3	2025-02-16	0.414	19.169	350	0	0	10.7	127.0	119.3	39.4	21.3
V4	2026-12-22	0.585	19.169	350	0	4.8	10.3	127.0	97.4	46.4	36.2
V5	2028-03-16	0.756	19.169	350	0	0	12.0	127.0	84.9	46.0	49.1

Table 3-16 2018 Launch Option D: GAM Properties

Table 3-17 provides the components of the infinite velocity vectors at each GAM (in the ICRF/EME2000 reference frame) and the incoming B-plane impact vector. These vectors completely define the geometry of the GAM hyperbola.

GAM	Arrival					Departure		
	V _{∞x} (km/s)	V _{∞y} (km/s)	V _{∞z} (km/s)	Bx (km)	By (km)	V _{∞x} (km/s)	V _{∞y} (km/s)	V _{∞z} (km/s)
V1	1.456	-8.456	-2.235	15455.1	-7387.8	4.965	-7.340	-0.302
E1	8.428	-6.526	-3.645	11947.3	-5834.7	10.877	-2.693	-1.167
E2	9.800	5.106	2.214	-13734.9	1991.6	11.185	0.416	1.316
V2	16.067	-8.872	-5.536	4646.8	5542.2	16.134	-5.520	-8.760
V3	16.132	-5.520	-8.760	5088.5	5139.7	15.290	-1.798	-11.420
V4	15.290	-1.800	-11.420	6854.3	2308.5	14.479	2.702	-12.268
V5	14.480	2.701	-12.268	6570.0	3024.0	12.070	6.518	-13.390

Table 3-17 2018 Launch Option D: infinite velocity vectors and B-plane target of GAMS

¹ Local solar time (LST) at the pericentre of the GAM. The criterion for Venus LST is not related to the rotation of the planet and follows the same definition as for the Earth. Thus, 6 h local time is approximately in the direction of the planet velocity vector with respect to the Sun, and 18 h local time is in the opposite direction.



Figure 3-55 and Figure 3-56 show the projections of the Venus and Earth GAMs hyperbolas, respectively. For the details on how this projection is obtained refer to Section 3.1.4 (page 44). In this trajectory GAM-V1 during the cruise is outbound (going from 2nd to 4th quadrant) and all the Venus GAMs during the science phase are clearly identified as inbound (going from 4th to 2nd quadrant).

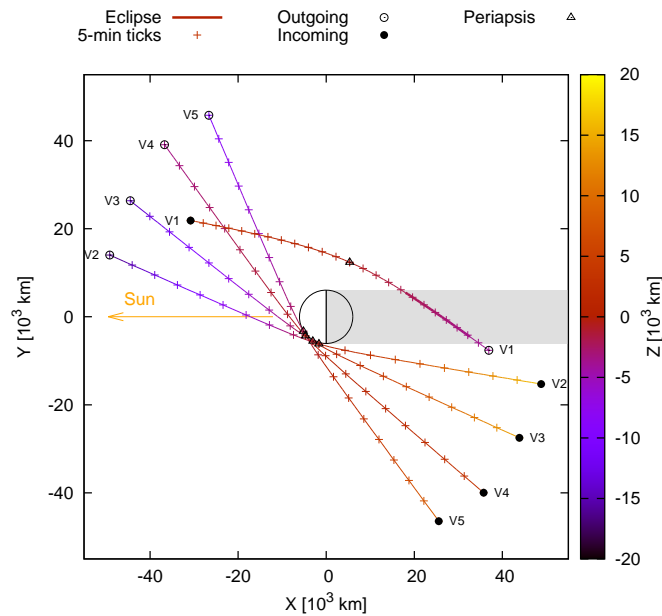


Figure 3-55 2018 Launch Option D: Projection of hyperbolas for Venus GAMs

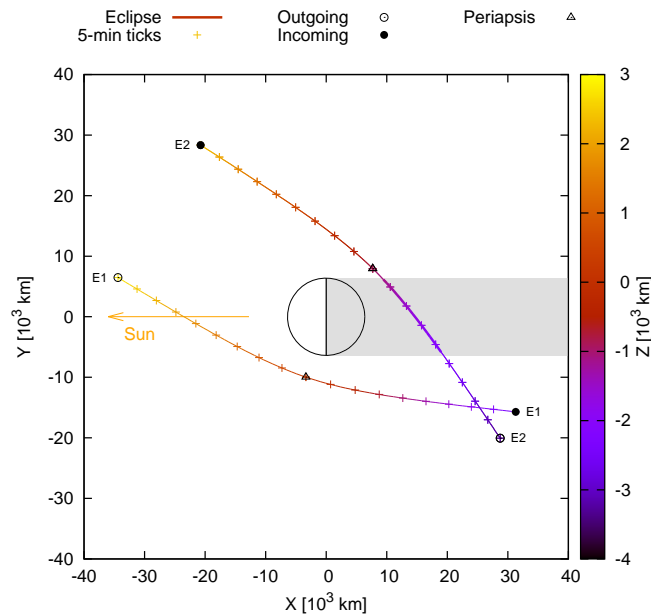


Figure 3-56 2018 Launch Option D: Projection of hyperbolas for Earth GAMs



Figure 3-57 shows the evolution of the Doppler rate between the S/C and the centre of the Earth in the vicinity of the closest approach of each GAM. The Doppler rate varies abruptly for a period of about 30-60 min, especially for the Earth GAMs. Both Earth GAMs reach peak values of below -400 Hz/s: for GAM-E1 the lowest value is -438 Hz/s and for GAM-E2 -411 Hz/s. For the Venus GAMs the limits are reached at +119 Hz/s for GAM-V4 and -113 Hz/s for GAM-V2. It must be pointed out that the Doppler rate that will be seen from the ground stations will be slightly different than these values due to the acceleration due to the Earth rotation.

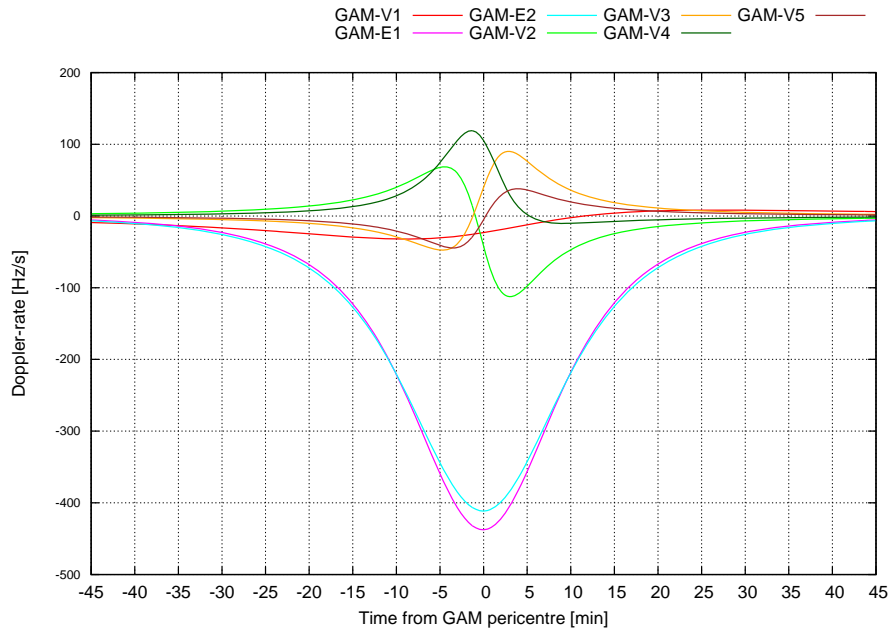


Figure 3-57 2018 Launch Option D: Doppler rate around GAM pericentres

3.2.5 LEOP

A dedicated analysis from NASA/ULA of the Atlas V 411 ascent trajectory for the launch targets required for this trajectory is not available at this point in time. The following describes preliminary results obtained at ESOC by a first approximation of the separation conditions. Several assumptions were required to model the geometry at separation: inclination, perigee radius and longitude of the ascending node of the escape hyperbola, as well as the true anomaly at separation. The values used for such parameters are consistent with the results of the Preliminary Launch Vehicle Performance & Trajectory assessment [20] performed by NASA KSC.

The trajectory selected for LEOP analysis corresponds to the first launch day of the launch window identified for this trajectory opportunity as presented in Table 4-2. Launch on 2018-10-08 requires an infinite velocity of 3.997 km/s, DLA of -15.58 deg and RLA of -72.31 deg (both angles in ICRF/EME2000). The separation time matching the escape conditions is 08:38:56 UTC. Assuming a short coast phase is possible; the lift-off will take place about 35 minutes earlier.



Figure 3-27 shows the ground track of Solar Orbiter for 1 day after separation from the launcher upper stage. From separation over Africa the Solar Orbiter spacecraft travels South East for about 50-60 minutes increasing the altitude and then the ground track turns towards West on the Indian Ocean. The spacecraft is then escaping from the Earth on the inertially fixed direction of the asymptote and so the latitude remains constant and equal to the target DLA while the longitude is swept west due to the rotation of the Earth. Separation occurs on the illuminated side of the Earth (nightside is provided at time of separation) and there is no eclipse after separation.

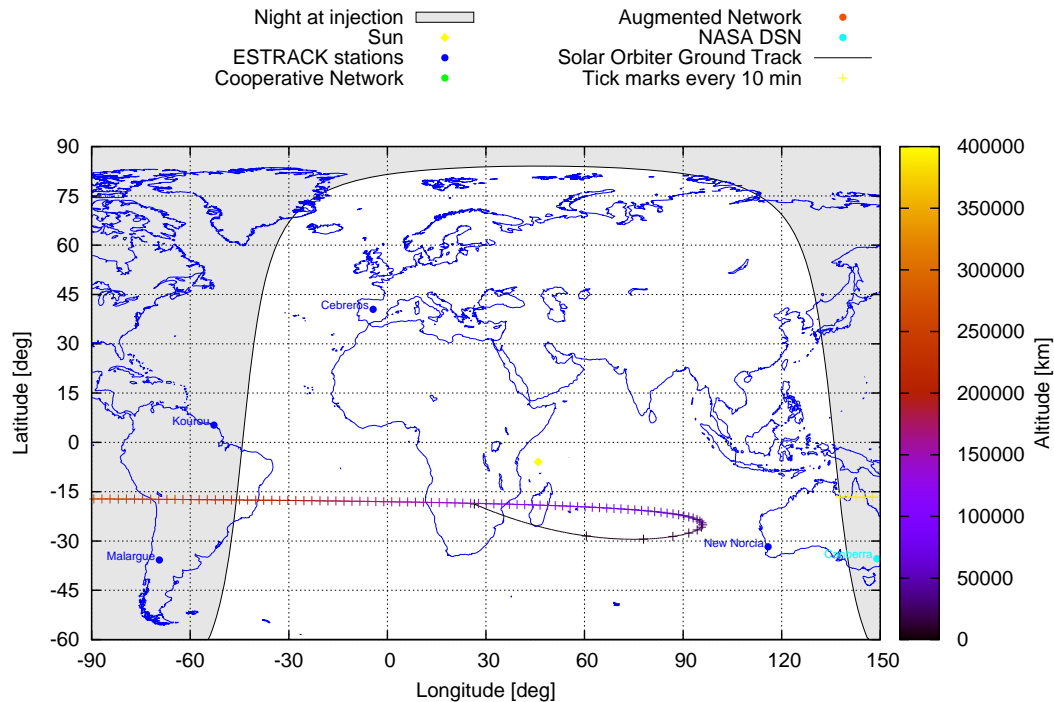


Figure 3-58 2018 Launch Option D: ground track for first LEOP day

Figure 3-28 show the results of the ground station visibility analysis for the regarded scenario. The first station with spacecraft visibility is New Norcia. The spacecraft will be above the horizon 8 minutes and above an elevation of 10 degrees 12 minutes after separation. The next station to have visibility is Canberra, the spacecraft will be above the 10 degrees elevation 23 min after separation. The elevation from New Norcia reaches a maximum around 65 degrees about 1 hour after separation. Due to the South declination of the escape asymptote, during the LEOP the ESA stations in Malargüe and New Norcia can alternate tracking of the spacecraft to provide continuous 24-h coverage. Cebreros provides visibility only with low elevations and Kourou does not improve the coverage of Malargüe, but can be used as backup.

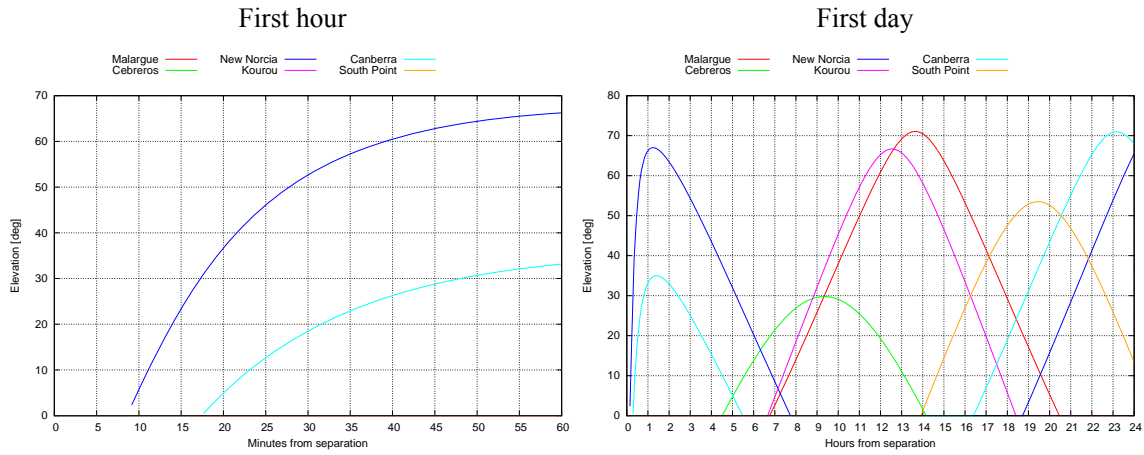


Figure 3-59 2018 Launch Option D: elevation from ground stations

The previous results are preliminary and based on ESOC assumptions of the separation conditions. Once a dedicated analysis by NASA/ULA is available, the LEOP analysis will be recomputed with the exact separation conditions.

The geometry of Earth, S/C and Sun short after departure is presented in Figure 3-60. The plot on the left shows the evolution for the first 5 hours after separation of the SSE and SES angles along with the Earth distance. The plot on the right shows the projection of the departure hyperbola on the Sun-Earth rotating frame relative to Earth (thus at the centre; Sun on the left, far out the plot scale).

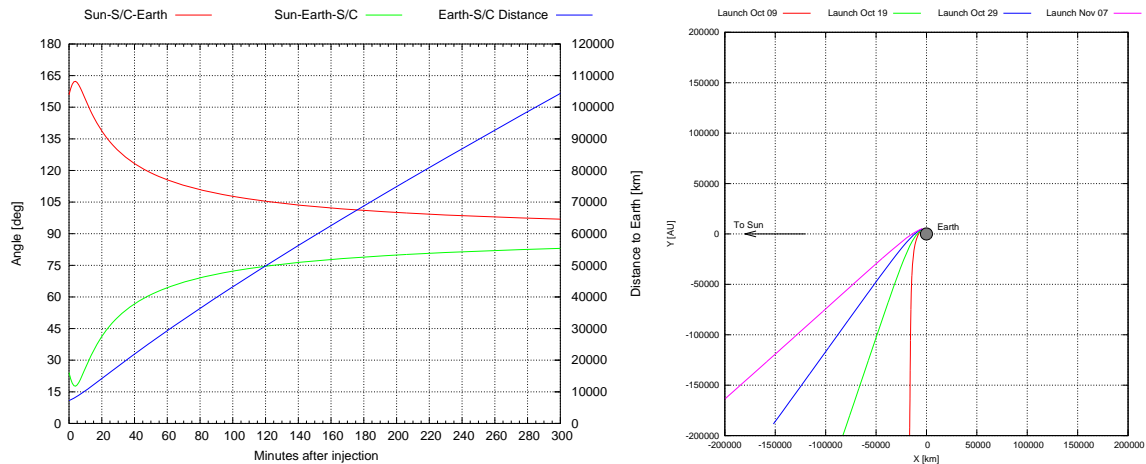


Figure 3-60 2018 Launch Option D: Earth, Sun & S/C relative geometry at early LEOP



On the ejection of the METIS cap

For a description of METIS cap ejection details and constraints refer to Section 3.1.5 (page 52). Figure 3-61 shows that Solar Orbiter must start maintaining the Sun pointing attitude 39 days after launch. Thus ejection in any direction is only possible for 2 days, between 30 and 39 days after launch. In this trajectory the 0.6 AU constraint is not reached before the first Venus GAM. However, it is recommended to eject the METIS cap before GAM-V1 as accurate B-plane targeting will allow a better control of the cap trajectory. A detailed analysis of the METIS cap trajectory shows that by an early ejection (30 days after launch) the aphelion radius can be limited below 0.89 AU and by late ejection (later than 90 days after launch) Venus impact can be targeted (full analysis in [32]).

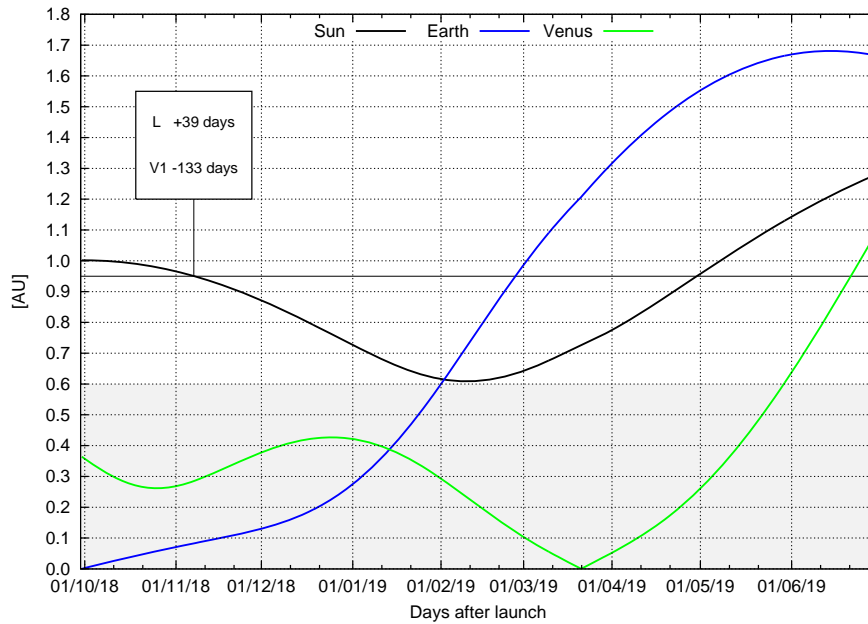


Figure 3-61 2018 Launch Option D: distances applicable to METIS cap ejection



3.3 2018 October Launch

3.3.1 DESCRIPTION

The trajectory with launch in October 2018 is based on an Earth-Venus-Earth-Earth-Venus transfer identical to the old 2017 March trajectory option described in the previous issue of this document, but with launch on the next Earth-Venus synodic period. The cruise phase is similar to the 2018 Option D trajectory, but a different sequence of resonances is implemented. This trajectory is described by:

1. Launch in with an escape velocity from the Earth of about 4.83 km/s, and declination of the escape velocity of -7° .
2. About 6 months after launch, a Venus GAM, with a pericentre height of more than 3800 km, will put the spacecraft in a trajectory towards the Earth.
3. 11 months later, an Earth GAM with a pericentre height of 3000 km inserts the spacecraft in an orbit with a period such that there is another Earth GAM 22 months later when the spacecraft has described more than 2.6 revolutions and the Earth has described a bit less than 2 revolutions about the Sun.
4. The second Earth GAM with a pericentre height of about 3000 km inserts the spacecraft into a heliocentric orbit in which Venus is encountered after about 1.4 revolutions. The minimum radius of 0.285 AU of the entire trajectory is achieved at the perihelion of this orbit. Therefore the nominal mission phase will start after GAM-E2 and this perihelion will be used to start the close Sun science observations with the remote sensing instruments.
5. The spacecraft arrives to the second Venus GAM with a large hyperbolic velocity of 20.06 km/s and starts the sequence of resonances with Venus in order to increase the solar inclination while staying as close as possible to the Sun. In this trajectory a sequence of 5 Venus GAM is implemented with the resonances 1:1-1:1-4:3-3:2-3:2.
6. The first resonances at 1:1 are forced by the perihelion constraint of 0.28 AU and imply a gradual increase of the perihelion radius to 0.338 and 0.368 AU, while the solar inclination increases quickly from 9.9 to 17.6 deg.
7. Then the 4:3 and the 3:2 resonances reduce again the perihelion below 0.3 AU providing a long series of 7 close approaches to the Sun with solar inclinations at 21.9 and 28.1 deg, respectively.
8. Finally, the last 3:2 resonance is used to increase the solar inclination to the final value of 33 deg, while the perihelion radius increases to 0.33 AU.

During the sequence of resonances with Venus all the GAMs are performed with maximum deflection at a minimum altitude of 350 km.

Table 3-18 and Table 3-19 present a summary of the main events/parameters of the mission.

Figure 3-62 shows V-infinity direction diagram that summarizes the sequence of resonances 1:1-1:1-4:3-3:2-3:2 at Venus of the October 2018 trajectory.



Mission Phase Duration (days)	Event	Date	Flight Time (days)	Ra (AU)	Rp (AU)	i_{ecl} (deg)	i_s (deg)	Perih. Solar Latitude (deg)	ω (deg/day)
LEOP (7)	LAUNCH	2018-10-10	0	1.002	0.573	2.11	6.41	-5.90	2.575
	LEOP end	2018-10-17	7	1.002	0.573	2.11	6.41	-5.90	2.575
NECP (90)	NECP end	2019-01-15	97	1.002	0.573	2.11	6.41	-5.90	2.575
Cruise (1061)	GAM V1	2019-04-07	179	1.470	0.676	3.44	8.73	-3.84	2.061
	GAM E1	2020-02-21	499	1.139	0.439	0.00	7.25	4.70	4.068
	GAM E2 - Cruise end	2021-12-11	1158	1.020	0.285	3.49	3.78	1.35	8.079
Science Nominal Mission (1396)	Perihelion	2022-04-07	1275	1.020	0.285	3.49	3.78	1.35	8.079
	GAM V2	2022-09-10	1431	1.109	0.338	6.93	9.94	-6.05	6.187
	Perihelion	2022-10-16	1467	1.109	0.338	6.93	9.94	-6.05	6.187
	GAM V3	2023-04-23	1655	1.079	0.368	14.49	17.59	-13.29	5.432
	Perihelion	2023-05-31	1694	1.079	0.368	14.49	17.59	-13.29	5.432
	GAM V4	2023-12-03	1880	0.901	0.293	18.82	21.93	-11.26	7.375
	Perihelion	2024-01-13	1921	0.901	0.293	18.82	21.93	-11.26	7.375
	Perihelion	2024-06-30	2090	0.901	0.293	18.82	21.93	-11.26	7.375
	Perihelion	2024-12-15	2258	0.901	0.293	18.82	21.93	-11.26	7.375
	Perihelion	2025-02-06	2427	0.901	0.293	18.82	21.93	-11.26	7.375
Science Extended Mission (899)	GAM V5 - ENM	2025-10-08	2554	0.819	0.285	25.05	28.15	-11.17	7.220
	Perihelion	2025-11-21	2599	0.819	0.285	25.05	28.15	-11.17	7.220
	Perihelion	2026-04-20	2748	0.819	0.285	25.05	28.15	-11.17	7.220
	Perihelion	2026-09-17	2898	0.819	0.285	25.05	28.15	-11.17	7.220
	GAM V6	2026-12-31	3004	0.772	0.332	29.91	33.01	-11.21	5.302
	Perihelion	2027-02-21	3055	0.772	0.332	29.91	33.01	-11.21	5.302
	Perihelion	2027-07-20	3205	0.772	0.332	29.91	33.01	-11.21	5.302
	Perihelion	2027-12-17	3355	0.772	0.332	29.91	33.01	-11.21	5.302
	Arrival V7 – EEM	2028-03-24	3453						

Table 3-18 2018 October Launch: Mission Summary

Absolute Minimum Sun Distance (AU)	Absolute Maximum Sun Distance (AU)	Absolute Maximum Earth Distance (AU)	Maximum Solar Latitude (deg)	Maximum Angular Rate (deg/day)
0.285 First achieved after GAM E2 2022-04-07 3.49 years after launch	1.470 2019-10-05 ~1 year after launch	2.015 2022-07-08 3.7 years after launch	33.0 First achieved after GAM V5 2027-03-19 8.44 years after launch	8.079 First achieved after GAM E2 2022-04-07 3.49 years after launch

Table 3-19 2018 October Launch: Mission Parameters

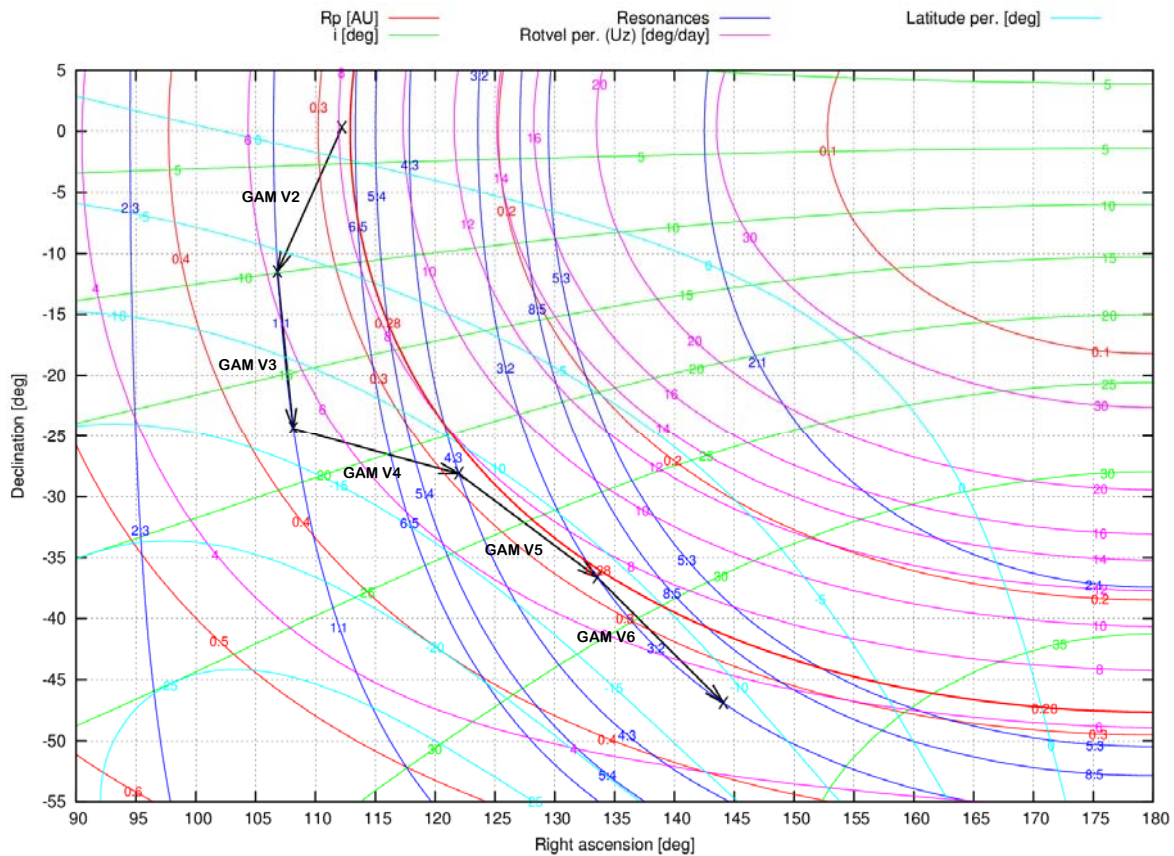


Figure 3-62 2018 October Launch: V-infinity diagram for the sequence of resonances

Trajectory Plots

Figure 3-63 to Figure 3-64 show the projections of the trajectory on the planes of the ecliptic reference system and XY projection onto the Sun-Earth rotating frame. Figure 3-65 shows the evolution of the distance of the spacecraft with respect to the Sun, Earth and Venus.

Figure 3-66 shows the evolution of the angle Sun-Spacecraft-Earth and Sun-Earth-Spacecraft. Table 3-20 provides a summary of the solar conjunction periods, for which the SES is below 3 deg and communications with the HGA are not guaranteed. This trajectory presents overall 8 solar conjunctions (5 of them superior) and the longest conjunction is 11.6 days.

There is an inferior conjunction before GAM-E2 in which the Sun-Earth-Spacecraft angle gets below 0.37 deg. This will have to be considered during the operations, but it is not viewed as a problem since the SES angle increases rapidly after the conjunction and reaches a value higher than 5 deg 24 days before GAM-E2. The last week before the GAM the SES angle is over 25 deg.

Table 3-21 gives the “safe-mode blackout periods” in which communications via MGA are not possible. Six of these periods will occur during the mission for this trajectory, the longest one in May-June 2022 for 46 days.

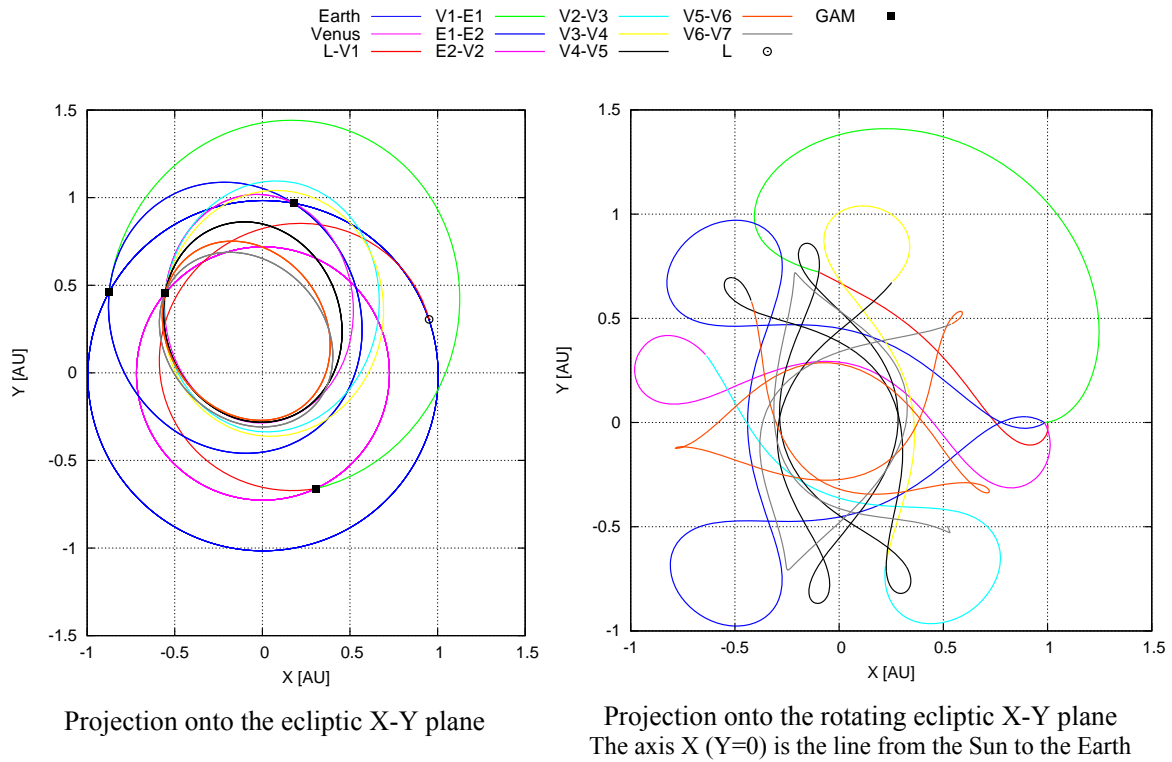


Figure 3-63 2018 October Launch: X-Y Trajectory projections from Launch to End of Mission

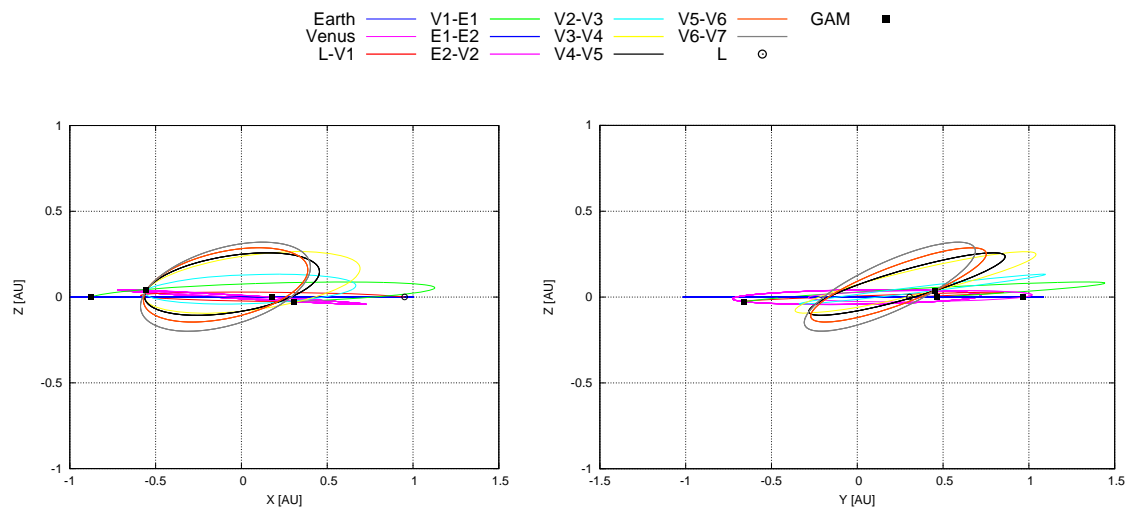


Figure 3-64 2018 October Launch: X-Z and Y-Z Trajectory projections

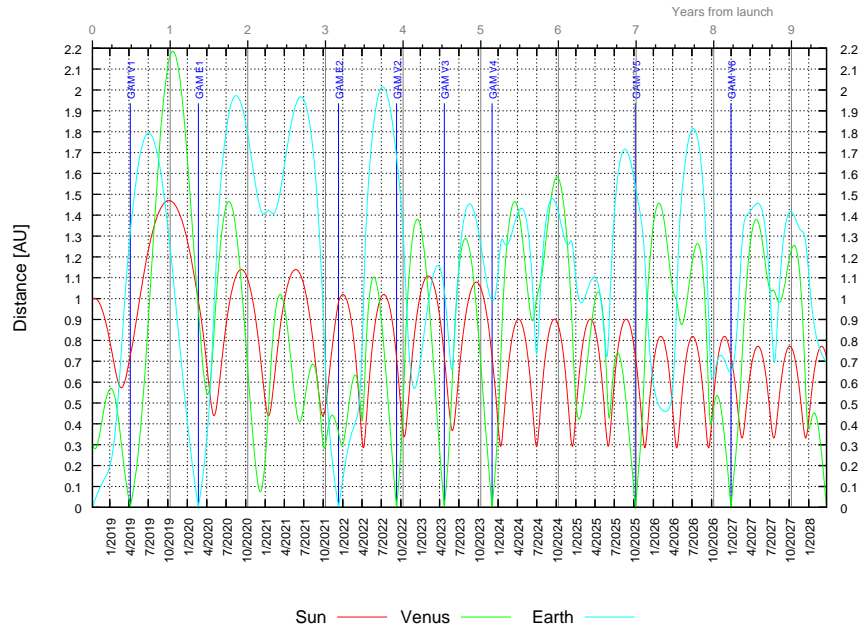


Figure 3-65 2018 October Launch: Spacecraft distance to Sun, Venus and Earth

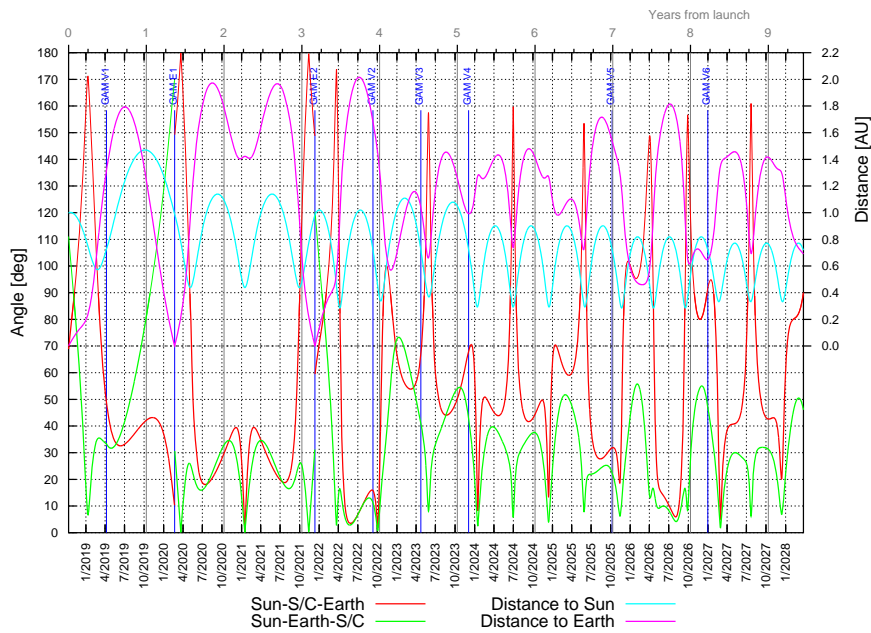


Figure 3-66 2018 October Launch: SSE and SES angles

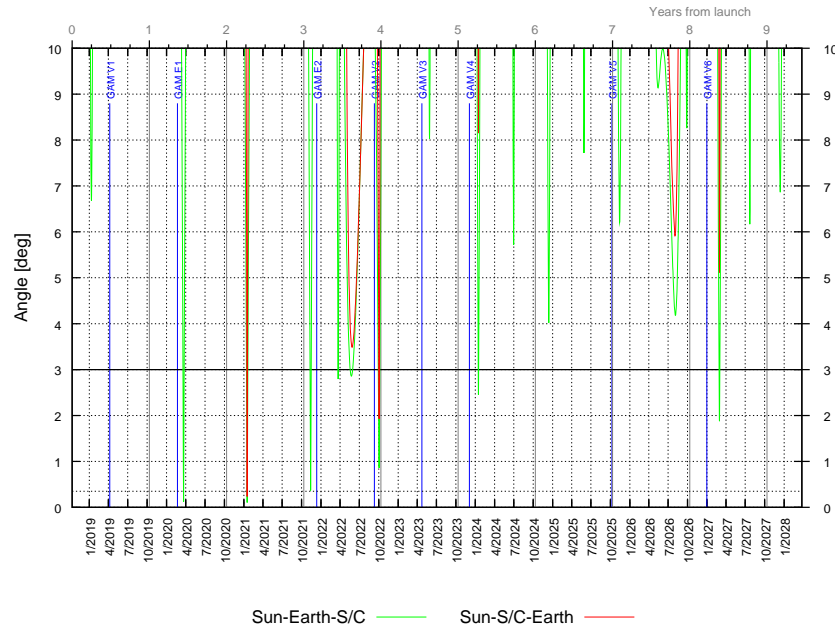


Figure 3-67 2018 October Launch: SSE and SES angles – Detail of conjunctions

	Type	Start	End	Duration [days]	Min SES [deg]
1	Inferior	2020-03-18	2020-03-24	5.6	0.12
2	Superior	2021-01-13	2021-01-19	6.4	0.10
3	Inferior	2021-11-10	2021-11-15	5.5	0.37
4	Inferior	2022-03-22	2022-03-23	1.0	2.79
5	Superior	2022-05-19	2022-05-30	11.6	2.86
6	Superior	2022-09-28	2022-10-06	7.4	0.86
7	Superior	2024-01-14	2024-01-17	2.3	2.46
8	Superior	2027-02-27	2027-03-03	4.1	1.88

Table 3-20 2018 October Launch: Solar Conjunction Periods

Solar conjunctions are considered as the periods when the Sun-Earth-spacecraft angle is below 3 degrees.

	Start	End	Duration [days]
1	2020-03-17	2020-03-26	9.4
2	2021-01-11	2021-01-22	10.7
3	2021-11-08	2021-11-17	9.2
4	2022-05-04	2022-06-20	46.8
5	2022-09-25	2022-10-08	12.8
6	2026-07-24	2026-08-13	19.8
7	2027-02-24	2027-03-04	8.2

Table 3-21 2018 October Launch: periods of MGA safe mode blackout

MGA communications blackout in safe mode are considered as the periods when SES < 5 deg OR SSE < 3 deg. Only blackouts longer than 7 days are provided.



Figure 3-68 shows the evolution of the Earth-Spacecraft range-rate. The range of variation for the entire mission goes from -58.7 km/s to 61.5 km/s.

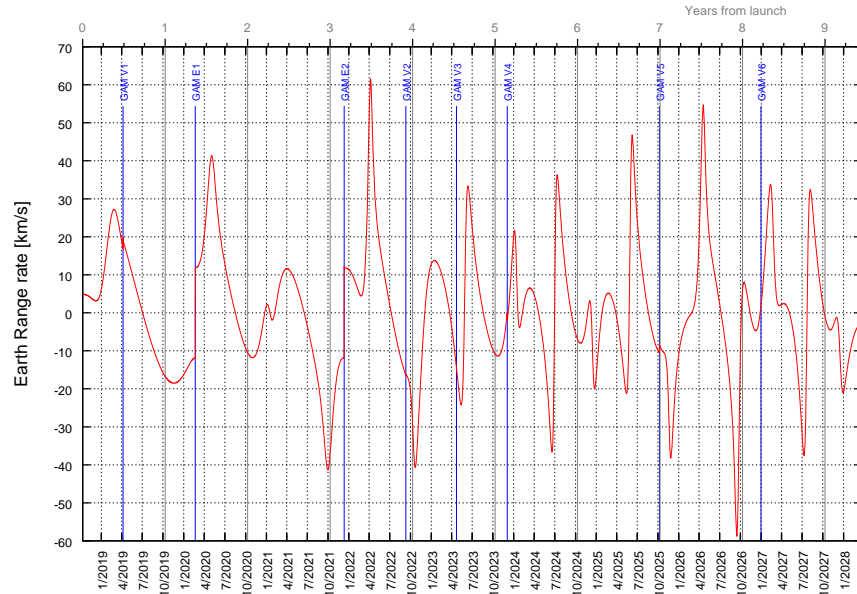


Figure 3-68 2018 October Launch: Variation of Earth-Spacecraft range-rate

Figure 3-69 shows the evolution of the Doppler effect due to the Earth-Spacecraft range-rate and Figure 3-70 shows the evolution of the Doppler rate. The Doppler varies from -1.73 MHz to 1.65 MHz during the entire mission. The Doppler seen from the ground stations will be slightly different due to the rotation velocity of the Earth.

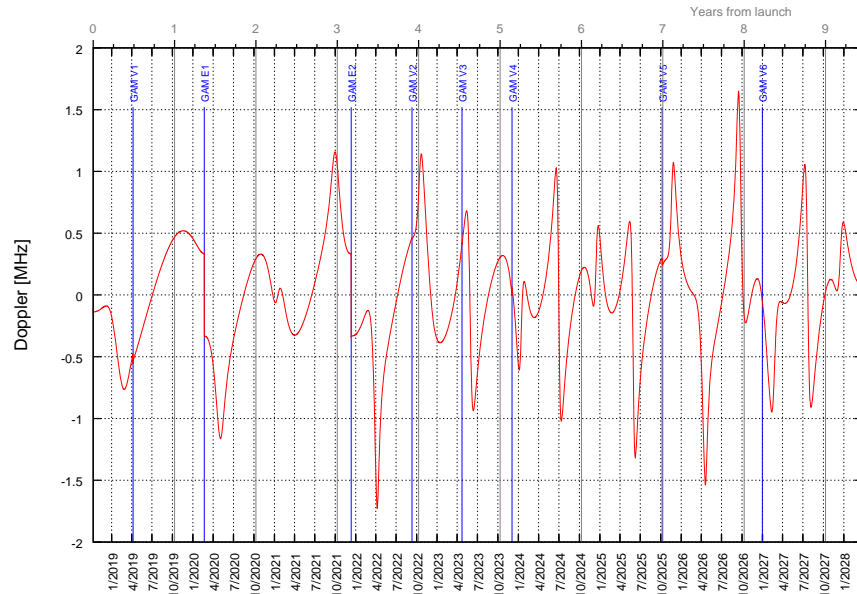


Figure 3-69 2018 October Launch: Variation of Earth-Spacecraft Doppler



The Doppler varies very rapidly at the GAMs and so Figure 3-70 shows Doppler-rate peaks extending beyond the limits of the graph. The limits of this figure have been chosen to allow representing the variations of the Doppler-rate in the heliocentric phases which are of the order of a few Hz/s, while peaks at the GAMs can largely exceed 500 Hz/s. The detail analysis of the Doppler-rates reached at the GAMs is presented in Section 3.3.4.

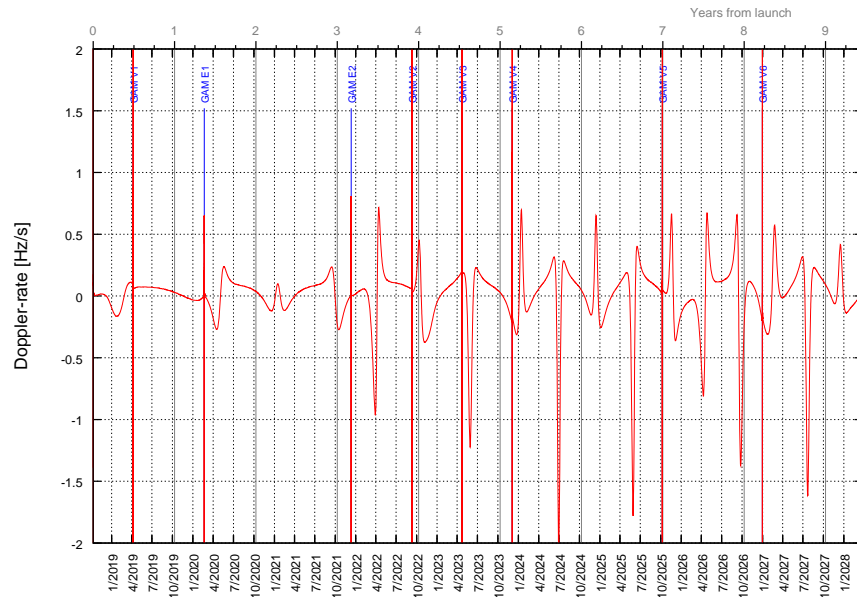


Figure 3-70 2018 October Launch: Variation of Earth-Spacecraft Doppler-rate

3.3.2 SCIENCE PROPERTIES

Figure 3-71 combines the evolution of the solar latitude with the distance to the Sun and Figure 3-73 shows the evolution of the perihelion and aphelion and the points of maximum and minimum solar latitude as a function of the date. During the science mission the solar latitude is negative at the perihelions and positive at the aphelions. The lowest solar latitude is achieved short before the perihelion so that both remote sensing windows will build a continuous science period of 20 days. The highest solar latitude is reached then between the perihelion and the aphelion.

Figure 3-69 provides a Sun-centric representation of the science orbits during the NMP and EMP. The plot shows the 6 orbits that are used in the science phase of this trajectory, including the first orbit that goes from the second Earth GAM to the second Venus GAM describing more than one revolution around the Sun and having a perihelion close to the 0.28 AU constraint. In this trajectory the perihelions are below the Sun Equator and the Venus GAMs are encountered after the perihelion. Therefore the spacecraft describes the orbits in the clockwise direction.

Table 3-22 provides information about the events during the science mission when the remote sensing instruments will be operative: during perihelion passes and at the points of minimum and maximum solar latitude of each orbit. The table considers the period of science after GAM E2 including both the nominal and the extended science missions.



Table 3-23 provides information of the number and duration of the passes close to the Sun. For this trajectory the spacecraft will approach the Sun 8 times below 0.3 AU and 13 times below 0.4 AU in an overall duration of 9.45 years. The duration that the spacecraft will stay below these distances is 56 and 319 days, respectively. 3 additional perihelions below 0.5 AU will be provided during the cruise phase.

Figure 3-75 shows the spacecraft rotation velocity around the Sun. The maximum rotation velocity is achieved at perihelion of the orbit achieved after GAM V2.

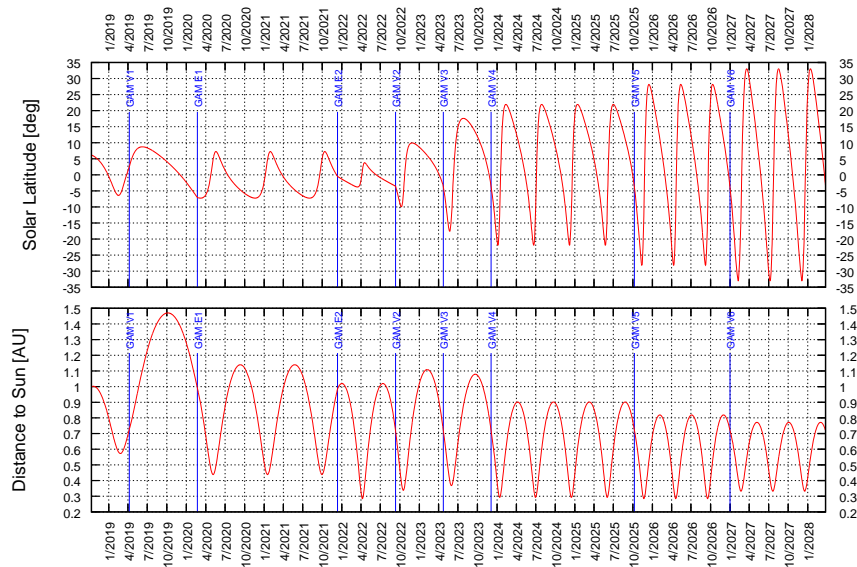


Figure 3-71 2018 October Launch: Spacecraft solar latitude + Spacecraft distance to the Sun

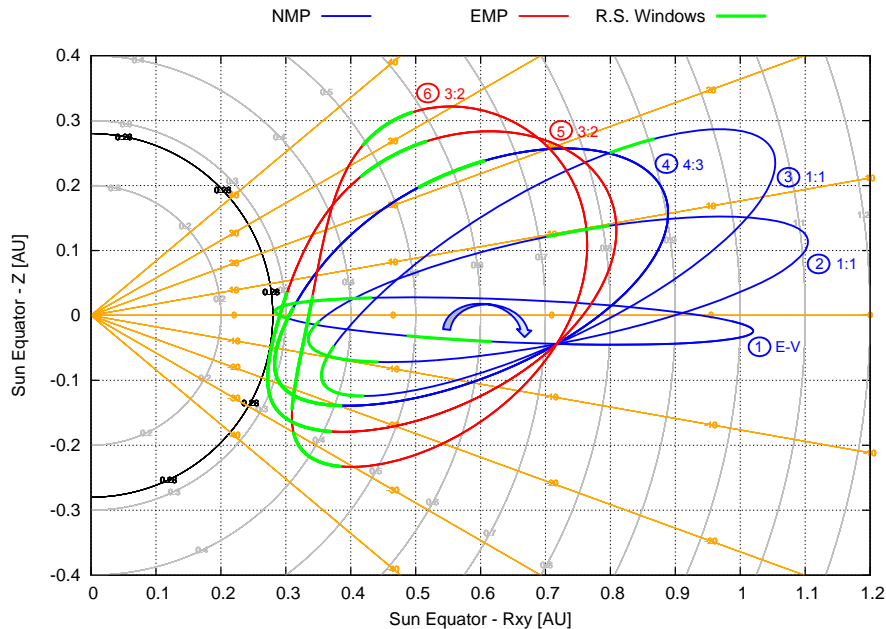


Figure 3-72 2018 October Launch: projection of science orbits wrt Sun Equator and North Pole

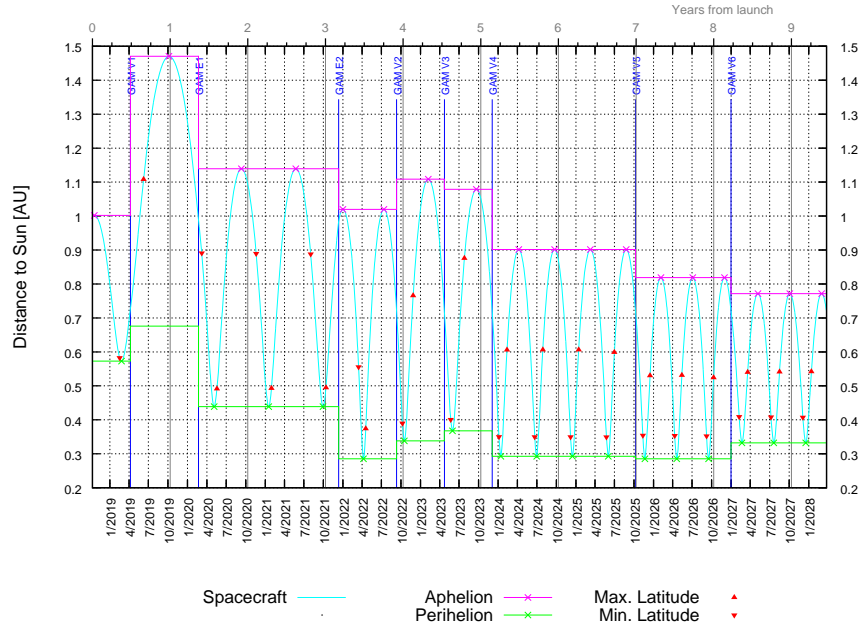


Figure 3-73 2018 October Launch: Evolution of apses and points of extreme solar latitude

Event	#	Date	Flight Time (days)	Sun Distance (AU)	Solar Latitude (deg)
GAM-E2		2021-12-11	1158	NMP Start	
Min. Lat	1	2022-03-15	1252	0.556	-3.78
Perihelion	1	2022-04-07	1275	0.285	1.35
Max. Lat	1	2022-04-18	1285	0.374	3.78
GAM-V2		2022-09-10	1431		
Min. Lat	2	2022-10-07	1458	0.390	-9.94
Perihelion	2	2022-10-16	1467	0.338	-6.05
Max. Lat	2	2022-11-27	1509	0.766	9.94
GAM-V3		2023-04-23	1655		
Min. Lat	3	2023-05-23	1685	0.401	-17.59
Perihelion	3	2023-05-31	1694	0.368	-13.29
Max. Lat	3	2023-07-26	1750	0.876	17.59
GAM-V4		2023-12-03	1880		
Min. Lat	4	2024-01-04	1912	0.350	-21.93
Perihelion	4	2024-01-13	1921	0.293	-11.26
Max. Lat	4	2024-02-11	1950	0.606	21.93
Min. Lat	5	2024-06-21	2081	0.350	-21.93
Perihelion	5	2024-06-30	2090	0.293	-11.26
Max. Lat	5	2024-07-29	2119	0.606	21.93
Min. Lat	6	2024-12-06	2249	0.350	-21.93
Perihelion	6	2024-12-15	2258	0.293	-11.26
Max. Lat	6	2025-01-13	2287	0.606	21.93
Min. Lat	7	2025-05-24	2418	0.350	-21.93
Perihelion	7	2025-06-02	2427	0.293	-11.26
Max. Lat	7	2025-06-30	2455	0.606	21.93
GAM-V5		2025-10-08	2554	EMP Start	
Min. Lat	8	2025-11-11	2589	0.353	-28.15
Perihelion	8	2025-11-21	2599	0.285	-11.17
Max. Lat	8	2025-12-15	2623	0.530	28.15
Min. Lat	9	2026-04-10	2739	0.353	-28.15
Perihelion	9	2026-04-20	2748	0.285	-11.17
Max. Lat	9	2026-05-14	2773	0.530	28.15
Min. Lat	10	2026-09-07	2889	0.353	-28.15
Perihelion	10	2026-09-17	2898	0.285	-11.17
Max. Lat	10	2026-10-10	2922	0.530	28.15
GAM-V6		2026-12-31	3004		
Min. Lat	11	2027-02-07	3042	0.408	-33.01
Perihelion	11	2027-02-21	3055	0.332	-11.21
Max. Lat	11	2027-03-19	3082	0.541	33.01
Min. Lat	12	2027-07-07	3192	0.408	-33.01
Perihelion	12	2027-07-20	3205	0.332	-11.21
Max. Lat	12	2027-08-16	3232	0.541	33.01
Min. Lat	13	2027-12-04	3342	0.408	-33.01
Perihelion	13	2027-12-17	3355	0.332	-11.21
Max. Lat	13	2028-01-13	3382	0.541	33.01

Table 3-22 2018 October Launch: Characteristics of perihelion and extreme points of solar latitude



	# Times	Accumulated Duration (days)	Minimum Duration (days)	Maximum Duration (days)
Cruise		1157		
0.3	0	0.0	0.0	0.0
0.4	0	0.0	0.0	0.0
0.5	3	85.4	28.5	28.5
0.6	4	183.8	30.5	51.1
Science		2295		
0.3	8	56.0	5.8	8.4
0.4	13	319.2	16.1	27.1
0.5	13	539.9	36.4	45.1
0.6	13	773.3	52.9	66.9
Total		3452		
0.3	8	56.0	5.8	8.4
0.4	13	319.2	16.1	27.1
0.5	16	625.3	28.5	45.1
0.6	17	957.0	30.5	66.9

Table 3-23 2018 October Launch: Number and duration of passes close to the Sun

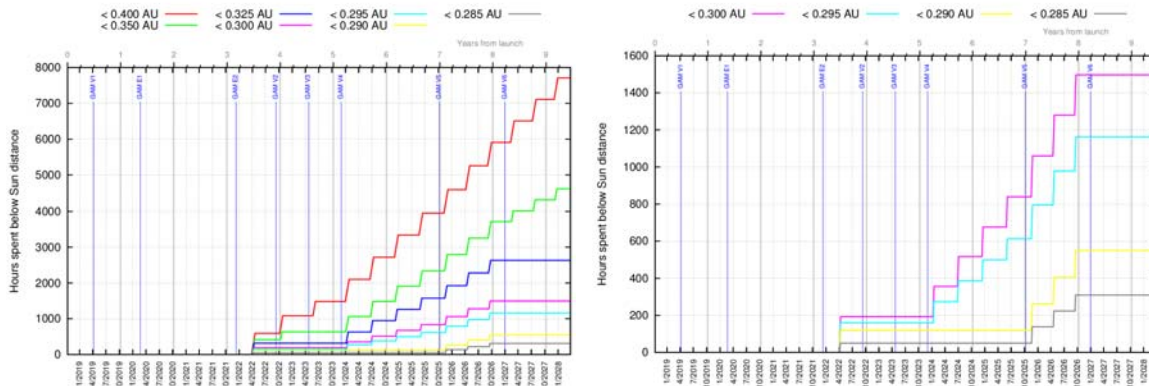


Figure 3-74 2018 October Launch: Evolution of time spent below different Sun ranges

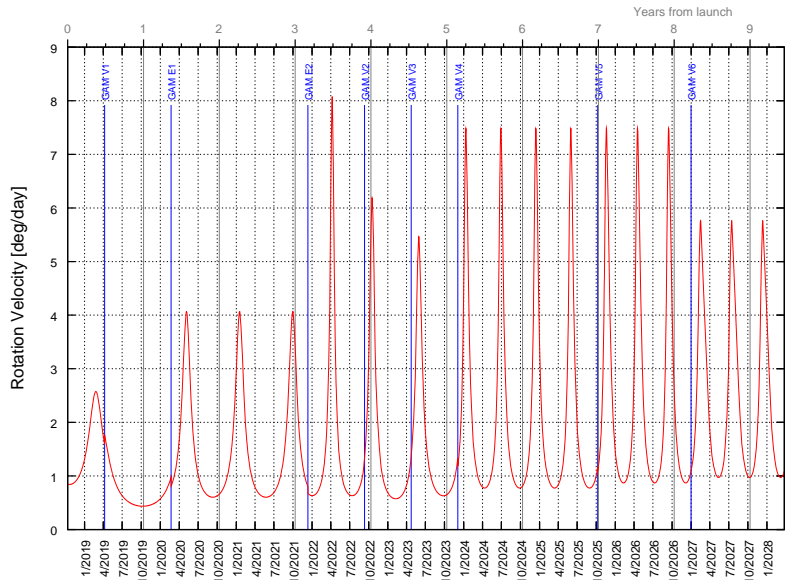


Figure 3-75 2018 October Launch: Spacecraft rotation velocity about the Sun

Figure 3-76 shows the evolution of the Earth distance together with the potential downlink volume per day assuming a flat 8-hour daily pass. Compared to 2018 Option E & D it is clear the absence of periods with the highest downlink capability during NMP+EMP. Instead the potential downlink remains rather low for the entire science phase, with small peaks that reach about half the maximum potential downlink and only one period between V4 and V5 in which the downlink rate almost reaches the maximum.

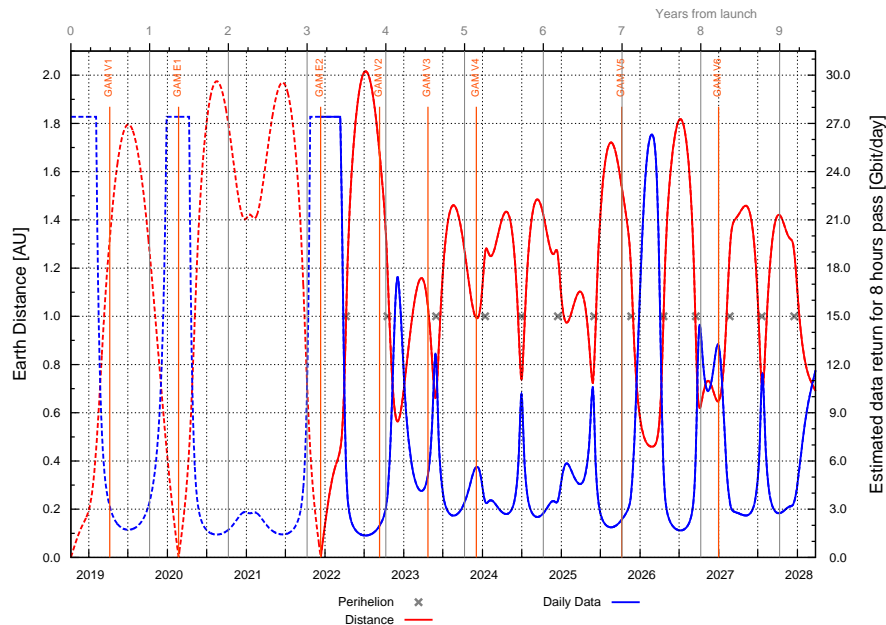


Figure 3-76 2018 October Launch: Evolution of Earth distance and potential downlink



Figure 3-77 shows the evolution of the equatorial declination of the Earth-to-spacecraft direction.

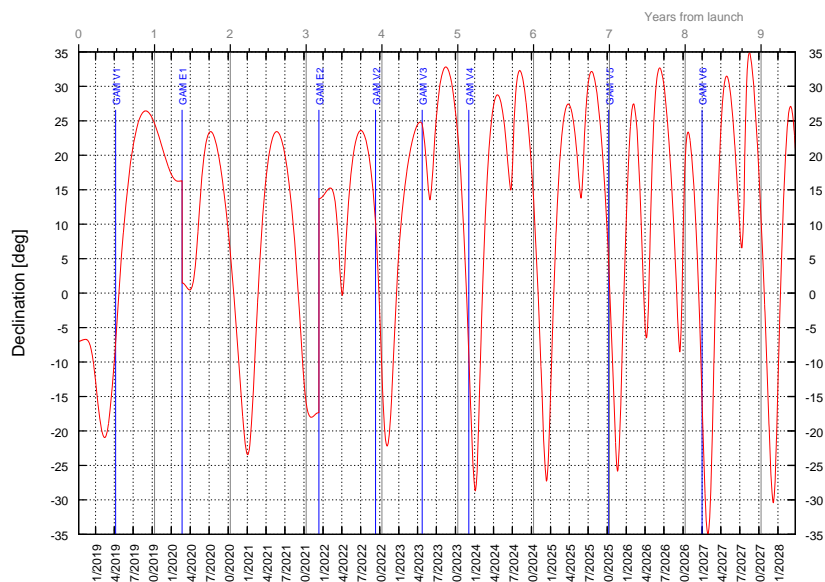


Figure 3-77 2018 October Launch: Spacecraft equatorial declination.

Figure 3-78 to Figure 3-80 present the daily period of visibility from each of the 3 ESA ground stations assuming 10° minimum elevation from the ground station. Daily visibility from any of the ground stations is guaranteed except for first 2 months after launch, when there is no visibility from Cebreros due to the very high negative-South declination.

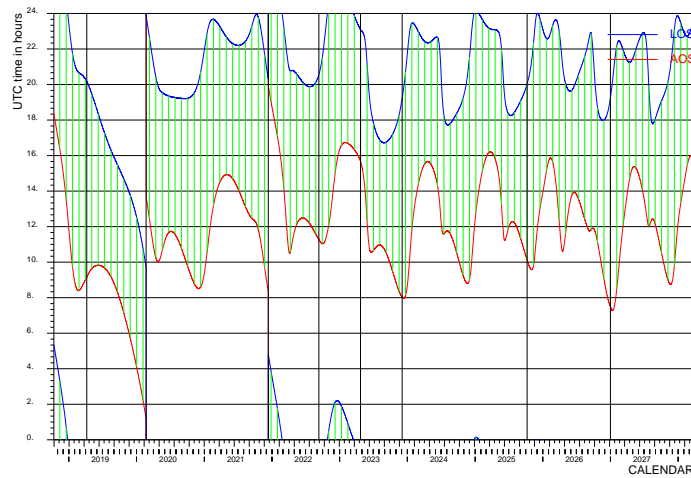


Figure 3-78 2018 October Launch: Daily period of visibility from Malargüe.

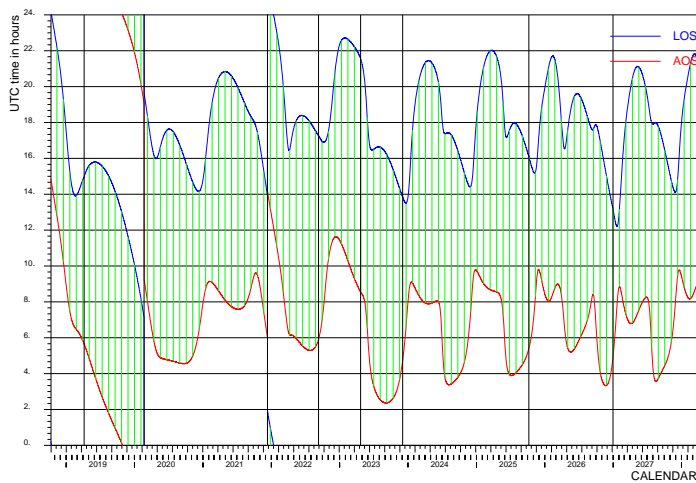


Figure 3-79 2018 October Launch: Daily period of visibility from Cebreros.

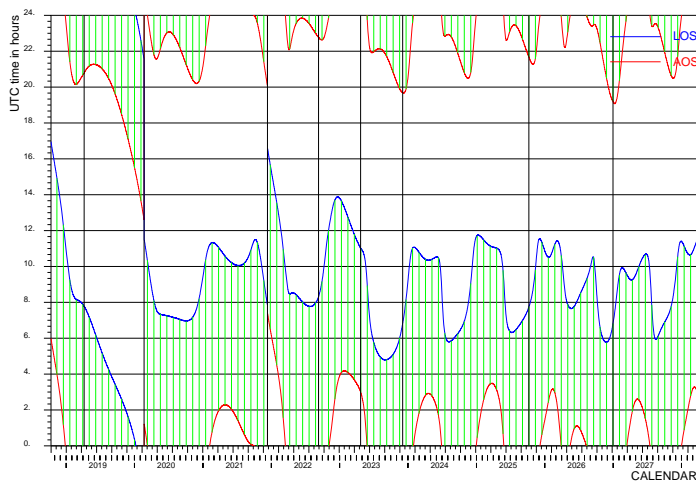


Figure 3-80 2018 October Launch: Daily period of visibility from New Norcia.



Figure 3-81 shows the duration of the visibility as a function of the date for all three ground stations. Figure 3-82 shows a combination of the daily period of visibility from the 3 stations.

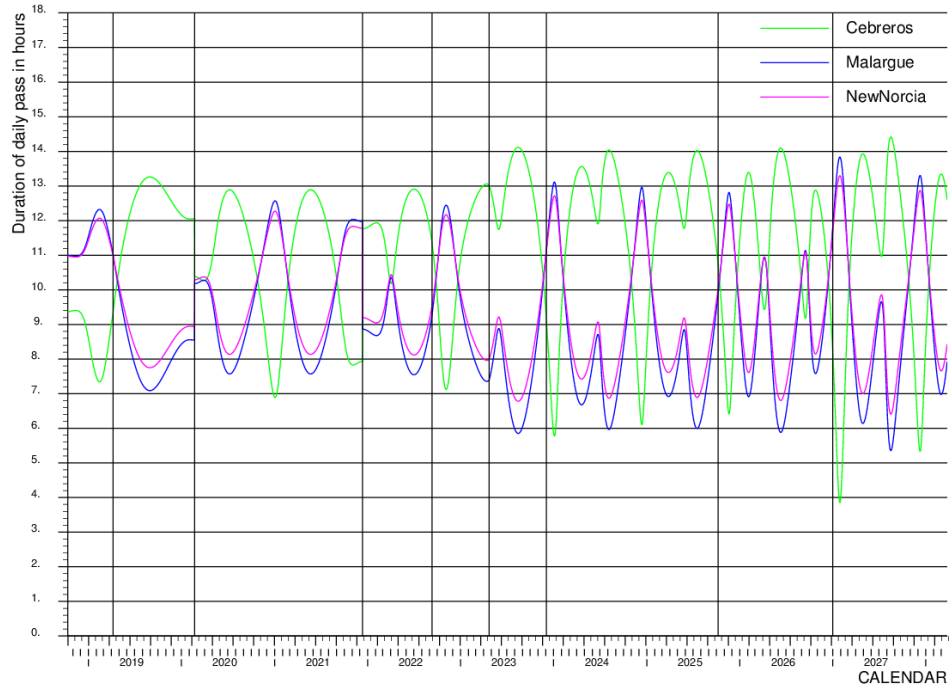


Figure 3-81 2018 October Launch: Daily duration of visibility from ESA Deep Space stations

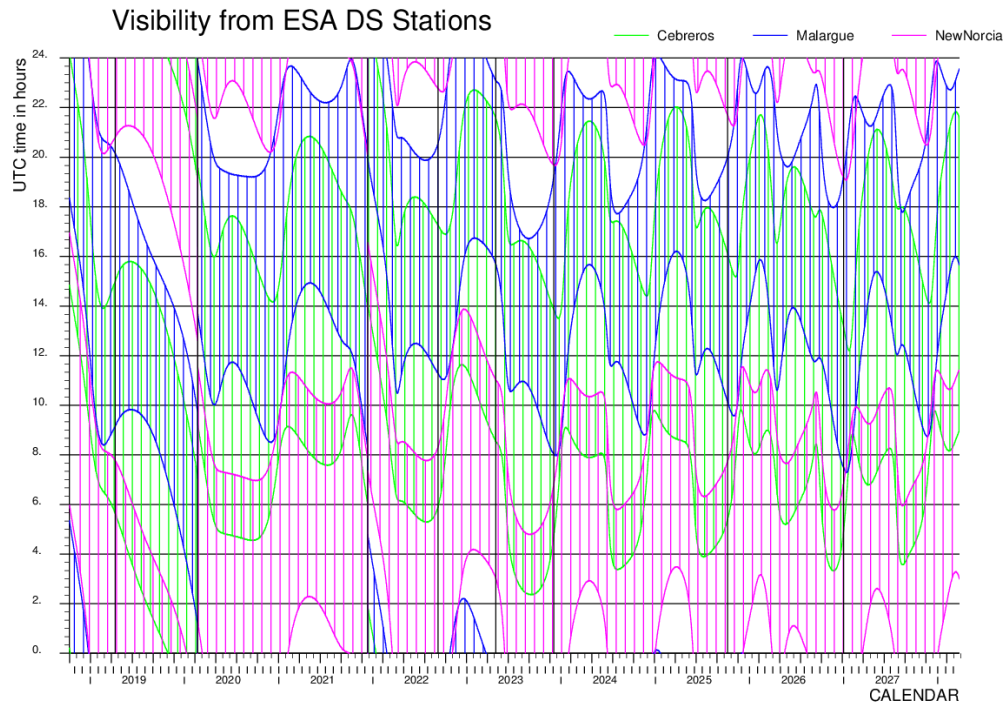


Figure 3-82 2018 October Launch: Daily period of visibility from ESA Deep Space stations.



3.3.4 GAMS DETAILS

Table 3-24 shows the characteristics of the GAMS including the duration of the eclipse and occultation events. The GAMS during the cruise phase are all performed at comfortable altitudes above 2000 to 3000 km. The Venus GAMS during the science phase are all performed at maximum deflection at the minimum altitude of 350 km.

For this trajectory eclipse will occur at GAM-V1 and GAM-E2, being the longest eclipse about 28 min. Occultation occurs only at GAM-V4 for about 9 min.

GAM	Date	Re (AU)	Vinf (km/s)	Hmin (km)	Eclipse (min)	Occult. (min)	LST ¹ (h)	Ls (deg)	SSE (deg)	SES (deg)	ESV (deg)
V1	2019-04-08	1.317	9.727	3730	27.4	0	19.4	295.7	48.8	33.2	98.0
E1	2020-02-21	0.000	11.912	3017	0	0	6.8	152.3	-	-	-
E2	2021-12-11	0.000	11.892	2409	18.2	0	3.0	79.6	-	-	-
V2	2022-09-10	1.679	20.130	350	0	0	18.1	140.6	15.8	11.2	152.9
V3	2023-04-23	1.039	20.130	350	0	0	12.1	140.6	66.9	41.1	72.0
V4	2023-12-03	0.995	20.128	350	0	8.8	8.2	140.6	68.0	42.5	69.4
V5	2025-10-08	1.535	20.131	350	0	0	10.2	140.6	31.8	22.3	125.9
V6	2026-12-31	0.649	20.129	350	0	0	12.0	140.6	91.8	46.9	41.3

Table 3-24 2018 October Launch: Characteristics of GAMS and eclipse/occultation durations

Table 3-25 provides the components of the infinite velocity vectors at each GAM (in the ICRF/EME2000 reference frame) and the incoming B-plane impact vector. These vectors completely define the geometry of the GAM hyperbola.

	Arrival					Departure		
	$V_{\infty x}$ [km/s]	$V_{\infty y}$ [km/s]	$V_{\infty z}$ [km/s]	Bx [km]	By [km]	$V_{\infty x}$ [km/s]	$V_{\infty y}$ [km/s]	$V_{\infty z}$ [km/s]
GAM V1	4.286	-8.477	-2.090	10419.1	-7370.8	7.537	-6.076	0.945
GAM E1	10.933	-3.283	-3.402	9018.7	-7727.5	11.890	0.661	0.286
GAM E2	7.911	8.146	3.532	-11237.5	675.1	11.060	3.360	2.794
GAM V2	19.208	-5.000	-3.356	-280.3	7153.8	17.970	-4.858	-7.660
GAM V3	17.970	-4.859	-7.660	3377.7	6312.4	16.631	-2.321	-11.101
GAM V4	16.630	-2.320	-11.100	7106.4	-869.6	17.124	2.074	-10.374
GAM V5	17.126	2.073	-10.375	6868.9	2017.8	15.547	6.185	-11.193
GAM V6	15.545	6.185	-11.192	6375.4	3257.2	12.648	9.299	-12.599

Table 3-25 2018 October Launch: infinite velocity vectors and B-plane target of GAMS

¹ Local solar time (LST) at the pericentre of the GAM. The criterion for Venus LST is not related to the rotation of the planet and follows the same definition as for the Earth. Thus, 6 h local time is approximately in the direction of the planet velocity vector with respect to the Sun, and 18 h local time is in the opposite direction.



Figure 3-83 and Figure 3-84 show the projections of the Venus and Earth GAMs hyperbolas, respectively. For the details on how this projection is obtained refer to Section 3.1.4 (page 44). The GAM geometries are similar to those of the 2018 Option D trajectory in Section 3.2.4.

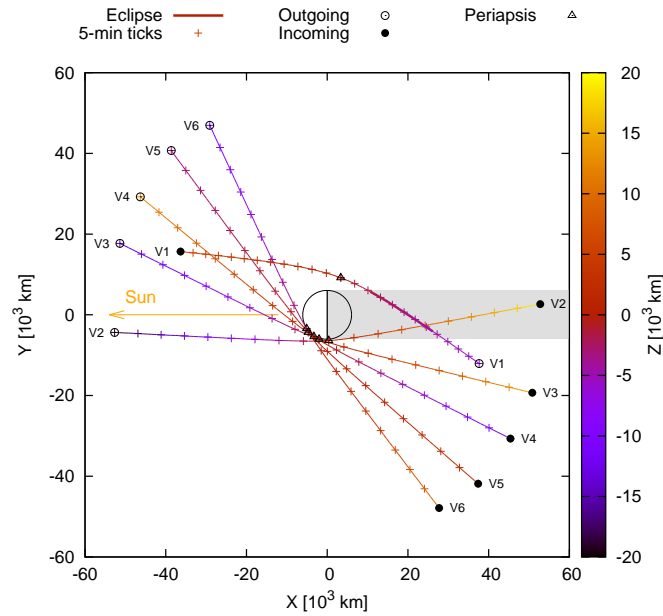


Figure 3-83 2018 October Launch: Projection of hyperbolas for Venus GAMs

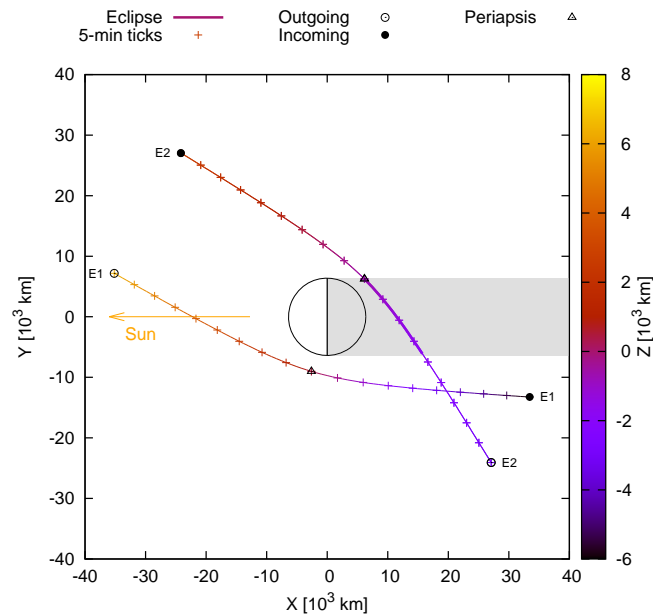


Figure 3-84 2018 October Launch: Projection of hyperbolas for Earth GAMs

Figure 3-85 shows the evolution of the Doppler rate between the S/C and the centre of the Earth in the vicinity of the closest approach of each GAM. The Doppler rate varies abruptly for a period of about 30-60 min, especially for the Earth GAMs. The Earth GAMs reach the largest peak values with -542 Hz/s at GAM E1 and -586 Hz/s at GAM E2. For the Venus GAMs the limits are reached at +151 Hz/s for GAM V4 and -102 Hz/s for GAM V2. It must be pointed out that the Doppler rate that will be seen from the ground stations will be slightly different than these values due to the acceleration due to the Earth rotation.

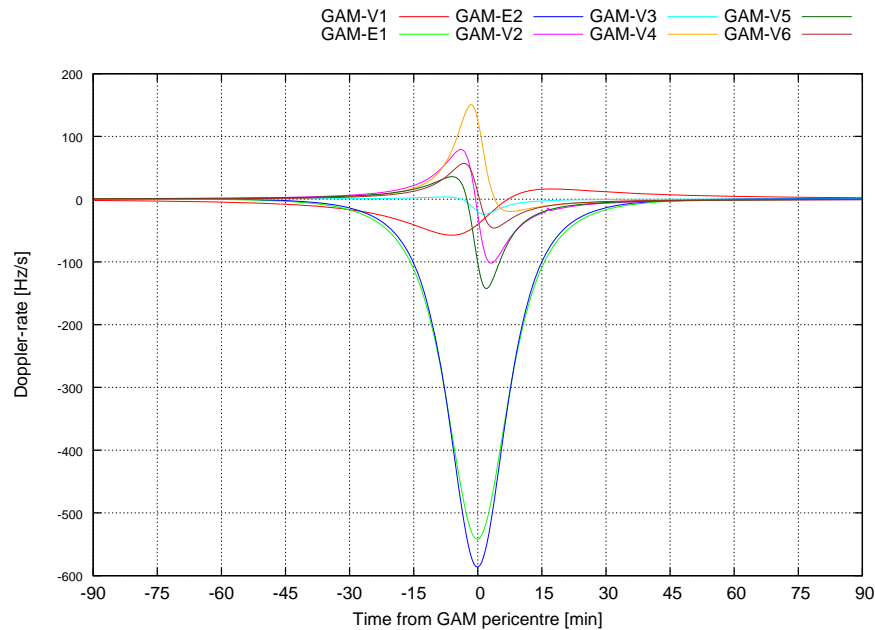


Figure 3-85 2018 October Launch: Doppler rate around GAM pericentres

3.3.5 LEOP

Given the high hyperbolic velocity required for the 2018 October trajectory, the performance of the Atlas V launcher is compatible with the Solar Orbiter spacecraft only from version 411 onwards. Reference Atlas V 411 ascent trajectories have been obtained by NASA/KSC as part of the Preliminary Launch Vehicle Performance & Trajectory assessment [20]. These trajectories are based on NLS-2 contract performance and trajectory design ground rules, including the assumption of a 185-km circular parking orbit, which might be sub-optimal from the performance point of view.

2 launch dates have been regarded in this LEOP analysis [21], covering the extreme cases in terms of required infinite velocity: 2018-10-22 with 4.285 km/s and 2018-11-14 with 5.567 km/s. The ascent trajectory makes use of the short coast phase leading to a launch duration from lift-off to separation between 35.3 and 36.2 minutes. Lift-off time is 06:57 UTC for the first launch date and 04:47 UTC for the latter launch date. In both cases the spacecraft experiences no eclipse after separation.

Figure 3-86 shows the ground track of Solar Orbiter for 1 day after separation from the launcher upper stage. The separation occurs over the Indian Ocean, between the African West coast and Madagascar. The spacecraft sub-satellite point travels to the East and in about 60 min reaches the furthest point before the Australian coast and starts travelling West as the spacecraft escapes from Earth at the target asymptotic declination. Separation occurs on the illuminated side of the Earth (nightside on the plot is given at time of separation) and therefore there is no eclipse after separation.

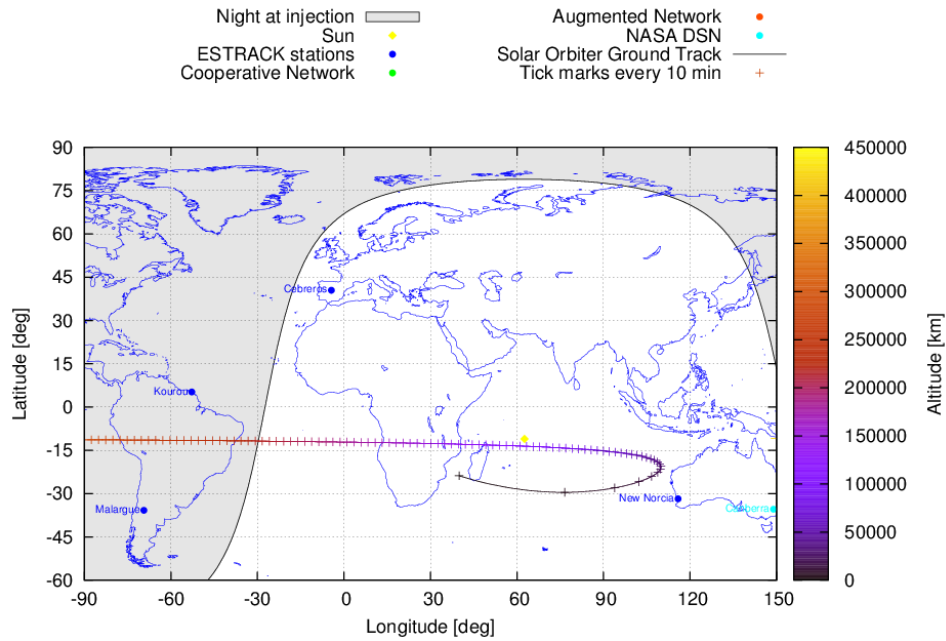


Figure 3-86 2018 October Launch: ground track for first LEOP day

Figure 3-87 shows the results of the ground station visibility analysis for the regarded scenario. The first station with spacecraft visibility is New Norcia with an elevation over 10 deg 3 minutes after separation. The elevation from New Norcia has a maximum around 75 deg 25 minutes after separation. During the LEOP the ESA stations in Malargüe and New Norcia can alternate to provide almost continuous 24-h tracking of the spacecraft.

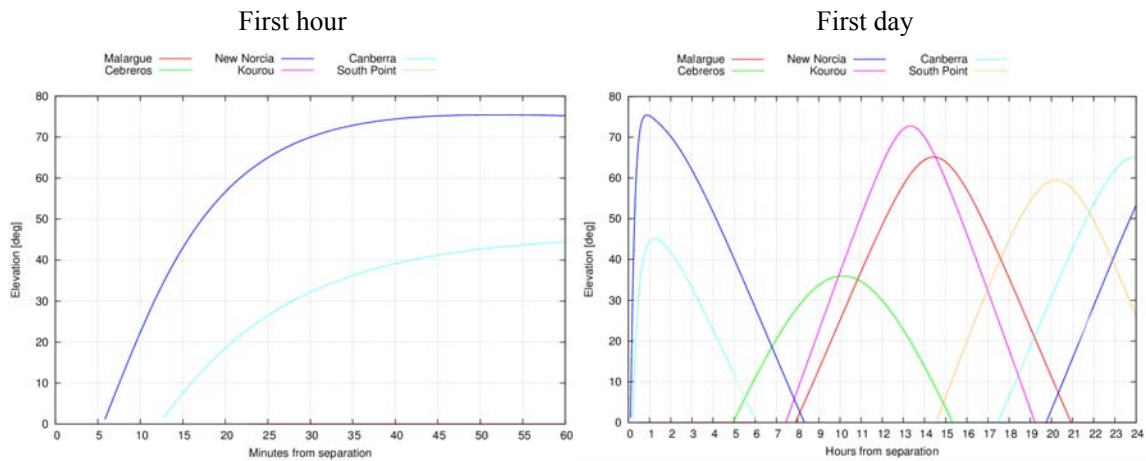


Figure 3-87 2018 October Launch: elevation from ground stations



The geometry of Earth, S/C and Sun short after departure is presented in Figure 3-88. The plot on the left shows the evolution for the first 5 hours after separation of the SSE and SES angles along with the Earth distance. The plot on the right shows the projection of the departure hyperbola on the Sun-Earth rotating frame relative to Earth (thus at the centre; Sun on the left, far out the plot scale).

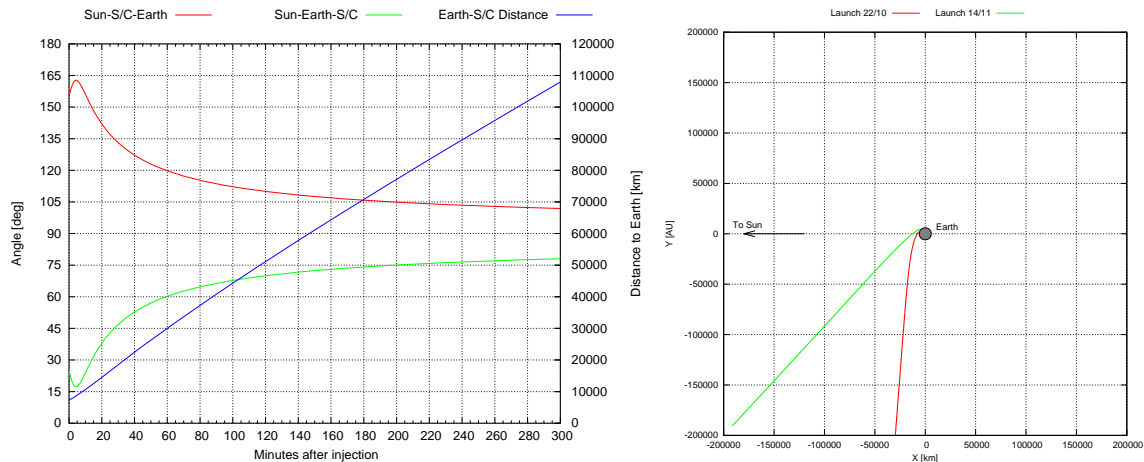


Figure 3-88 2018 October Launch: Earth, Sun & S/C relative geometry at early LEOP.

On the ejection of the METIS cap

For a description of METIS cap ejection details and constraints refer to Section 3.1.5 (page 52). Figure 3-89 shows that Solar Orbiter must start maintaining the Sun pointing attitude 32 days after launch. Thus ejection in any direction is only possible for 2 days, between 30 and 32 days after launch. Latest possible ejection is 114 days after launch. A detailed analysis of the METIS cap trajectory shows that by an early ejection the aphelion radius can be limited below 0.9 AU and by late ejection Venus impact can be targeted (full analysis in [32]).

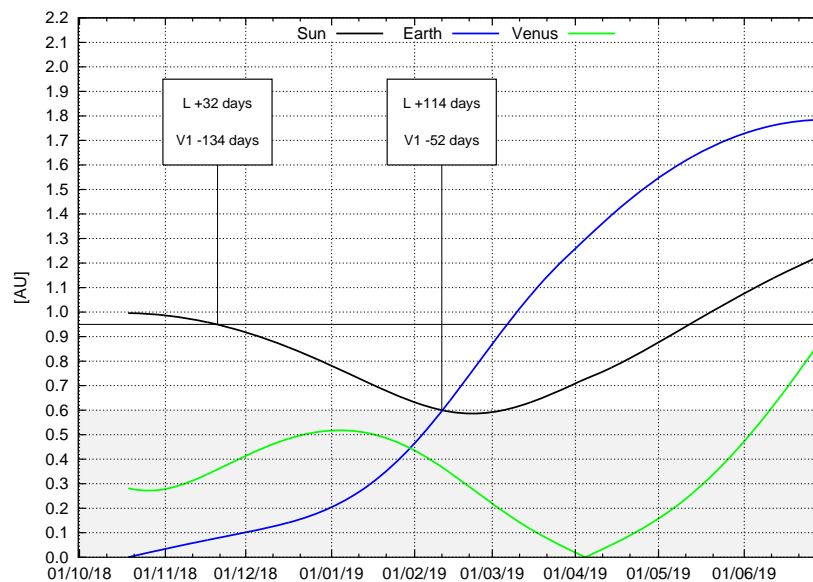


Figure 3-89 2018 October Launch: distances applicable to METIS cap ejection



3.4 2019 & 2020 February Launch

3.4.1 DESCRIPTION

This trajectory is based on a short EVVEV cruise profile departing from Earth on February 2020 and it was referred as February Option B in a previous technical note [25]. The cruise phase until start of the remote sensing observations below 0.35 AU takes roughly 2 years. This fast cruise allows also launching on February 2019 by adding a 1:1 Earth resonant “parking orbit” in which the spacecraft spends 1 year before performing an Earth GAM that connects with the rest of the trajectory as if launched in 2020. The penalty for the 2019 launch is a 1-year longer cruise, an increased maximum Sun distance and the truncation of the trajectory at end of mission to comply with the lifetime requirement so that a lower solar inclination is reached. This chapter describes the trajectory properties of both launch options. Whenever possible, for instance the science phase, a common description is given using 2020 as reference.

The spacecraft is launched in 2020 with high infinite velocity and positive DLA (or is launched in 2019 and after an Earth GAM 1 year later is injected) into a delayed transfer to Venus describing more than one revolution about the Sun in 0.9 years. The next orbit is in 1:1 Venus resonance (0.6 years) and provides the proper phasing for the rest of the trajectory. Because of the resonance there is flexibility to select the altitude of the first 2 Venus GAMs. In order to avoid long eclipses, the altitude of GAM-V2 is constrained to 8000 km resulting in no eclipse for any of the first two Venus GAMs and a rather high altitude also at GAM-V1.

Venus-Earth arc is direct and the Earth is encountered before the aphelion pass. The Earth GAM injects the spacecraft into a heliocentric science orbit with perihelion at 0.32 AU in which the first remote sensing observations will take place. NMP starts then just after the Earth GAM only 1.8 years after launch in 2020 (2.8 years after launch in 2019).

Maximum Sun distance for 2020 launch occurs in this Earth-Venus arc at only 1.02 AU. For 2019 launch the maximum Sun distance occurs earlier in the 1-year Earth-Earth parking orbit at about 1.18 AU. In both cases there should be no need to send the spacecraft into a hibernation mode.

Venus is encountered inbound for GAM-V3 with a hyperbolic velocity of 18.56 km/s at a L_s of roughly 129° , which is about half way from Venus optimal ($L_s \sim 75^\circ$) and worst positions to increase the solar inclination. The sequence of resonances 5:4 4:3 3:2 3:2 3:2 is selected primarily for its excellent downlink properties. Indeed the science mission after GAM-V3 follows the same profile as 2018 Option D at the same Venus location for the GAMs, but a slightly different hyperbolic velocity.

- The 5:4 resonance is reached 2.57 years after 2020 launch and puts the perihelion down to 0.292 AU. The orbits start with an excellent phasing at an Earth-Sun-Venus angle of 148° that provides 3 aphelia gradually closer to Earth. The downlink index of this orbit is a remarkable 2.42 AU^{-2} .
- The 4:3 resonance maintains perihelion at 0.294 AU. It has a first aphelion close to inferior conjunction and provides as well an excellent downlink capability with index 1.87 AU^{-2} .
- The first 3:2 resonance lowers perihelion to 0.284 AU and raises the solar inclination for the first time above 20° . This is considered the start of the EMP in both launch cases, 2019 and 2020. The downlink capability of this resonance is however limited.
- The second 3:2 resonance raises perihelion to 0.331 AU and the solar inclination for the first time above 30° . The downlink capability is again excellent with index 1.66 AU^{-2} . In a 2019 launch the mission would normally end after the 3rd orbit in this resonance after an overall mission duration of 10.34 years.



- For launch in 2020 a last GAM-V7 can be used for injecting the spacecraft again into a 3:2 resonance with an even larger solar inclination of 33.4 deg. Perihelion needs to be raised as well to 0.373 AU.

Alternatively, the inclination increase could be accelerated by slightly raising the perihelia of the 3 first resonances. The resulting orbits would be grazing 0.3 AU, with the 5:4 orbit already at a solar inclination of 12.5 deg, the next 4:3 at 21 deg, the first 3:2 at 27 deg and the second 3:2 at 31.8 deg. This is an interesting variant for launch in 2019 as within an overall duration of 10.2 years a solar inclination of roughly 32 deg would be achieved, although a penalty would be paid in science as the perihelion would not go below 0.3 AU.

A reference trajectory corresponding to launch on 7th February is described in detail next. Table 3-26 and Table 3-27 present a summary of the main events/parameters of the mission. All results for this trajectory option have been obtained with the linked conics model.



Phase	Cruise				NMP			EMP		
Trajectory arc - 2019 launch	L-E1	E1-V1	V1-V2	V2-E2	E2-V3	V3-V4	V4-V5	V5-V6	V6-End	
Trajectory arc - 2020 launch		L-V1	V1-V2	V2-E1	E1-V3	V3-V4	V4-V5	V5-V6	V6-V7	V7-End
Start	2019-02-07	2020-02-07	2020-12-26	2021-08-08	2021-11-26	2022-09-03	2025-02-18	2026-12-24	2028-03-17	2029-06-10
Flight time (years) – 2019 launch	0.00	1.00	1.89	2.50	2.80	3.57	6.03	7.88	9.11	10.34
Flight time (years) – 2020 launch		0.00	0.89	1.50	1.80	2.57	5.03	6.88	8.11	9.34
Duration (days)	365	324	225	110	281	899	674	449	449	449
Number of revolutions Venus Resonance	1	1	1 1:1	0	1	5 5:4	4 4:3	3 3:2	3 3:2	3 3:2
Period (days)	365.25	238.1	224.7	310.0	199.7	179.8	168.5	149.8	149.8	149.8
R at aphelion (AU)	1.176	0.990	0.955	(1.208)	1.017	0.955	0.900	0.820	0.773	0.731
R at max. latitude (AU)	0.845	0.514	0.532	0.724	0.518	0.567	0.596	0.527	0.543	0.523
R at min. latitude (AU)	1.137	0.988	0.832	0.864	0.461	0.369	0.352	0.352	0.405	0.468
R at perihelion (AU)	0.824	0.513	0.492	0.585	0.321	0.292	0.294	0.284	0.331	0.373
Perihelion latitude (deg)	8.621	6.54	1.53	0.59	-0.49	-3.44	-8.61	-9.75	-10.54	-5.41
ω at perih. (deg/day)	1.437	3.098	3.285	2.556	6.671	7.673	7.426	7.436	5.466	4.196
Ecliptic inclination (deg)	4.62	1.86	5.52	5.31	2.97	4.62	12.91	20.10	25.88	29.05
Solar inclination (deg)	10.28	6.57	2.23	2.33	4.39	8.66	17.22	24.43	30.21	33.39
Heliolatitude > 25 deg (days/orbit)									30.0	32.8
Heliolatitude < -25 deg (days/orbit)									16.9	26.5
Downlink index (1/AU ²)	4.13	2.03	0.47	3.32	2.10	2.42	1.87	0.93	1.66	0.94

Color Legend: Only 2019 Both 2019&2020 Only 2020

Table 3-26 2019 & 2020 February Launch: Trajectory Summary

Absolute Minimum Sun Distance (AU)	Absolute Maximum Sun Distance (AU)	Absolute Maximum Earth Distance (AU)	Maximum Solar Latitude (deg)	Maximum Angular Rate (deg/day)
0.284 First achieved after GAM V5 2022-10-10	1.176 Achieved after launch 2019-05-24	1.992 Achieved after GAM E1/E2 2022-06-27	30.21 First achieved after GAM V6 2028-04-26	7.673 First achieved after GAM V3 2022-10-12
	1.017 Achieved after GAM E2 2021-12-15		33.39 First achieved after GAM V7 2029-07-24	

Table 3-27 2019 & 2020 February Launch: Mission Parameters



Figure 3-90 shows V-infinity direction diagram that summarizes the sequence of resonances 5:4-4:3-3:2-3:2-3:2 at Venus of this trajectory. In this case the Venus GAMs are inbound as shown by the positive right ascension of the infinite velocity vector. The sequence starts with the arrival velocity of GAM-V3 at the top-left corner. The solar inclination is maximized by decreasing the declination of the infinite velocity, thus going towards the bottom-right corner of the plot. At the last 3:2 resonance the solar inclination has not reached yet its potential maximum for this infinite velocity and solar longitude of Venus.

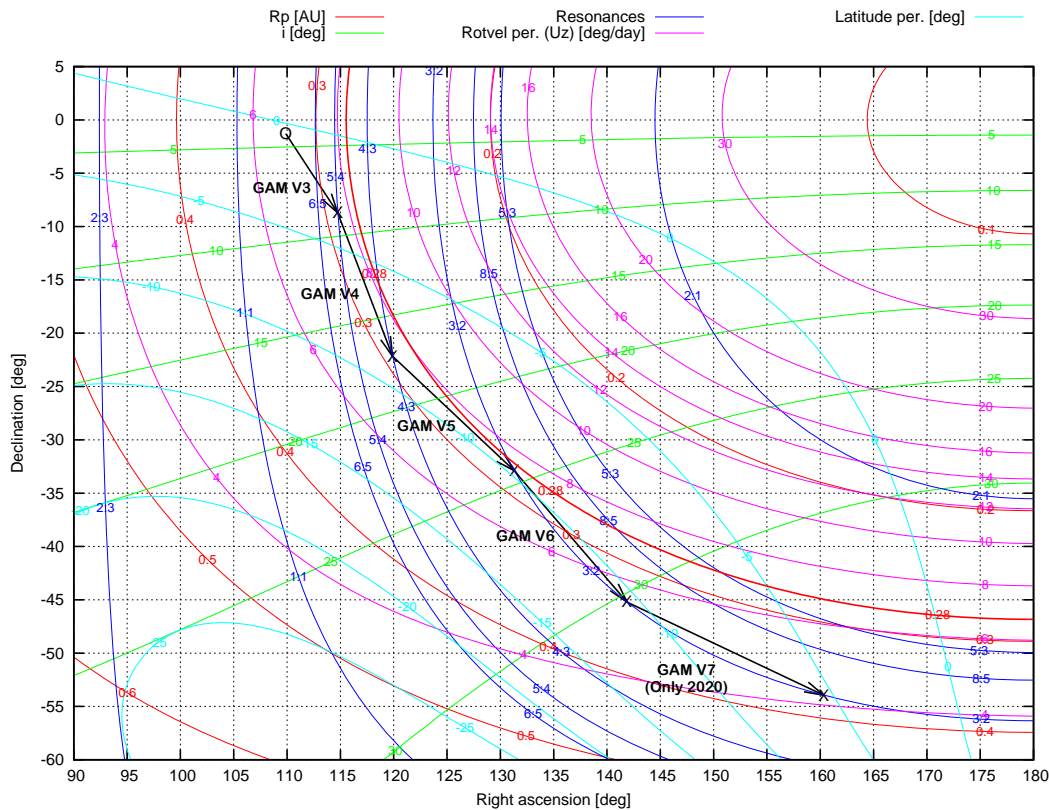


Figure 3-90 2019 & 2020 February Launch: V-infinity diagram

Trajectory Plots

Figure 3-91 shows the X-Y trajectory projection from launch until GAM-V3, which includes the cruise phase (also a sample outbound 1-year Earth-Earth parking orbit for 2019 launch) and the Earth-Venus arc until the first GAM at Venus initiating the sequence of resonances for the science phase. In this plot the green lines indicate the location of Venus that are optimal to increase the solar inclination of the heliocentric orbit, while the red lines indicate the points of Venus orbit that are the worst for a given hyperbolic velocity. As seen GAM-V3 is not located at a particularly favourable point.

Figure 3-92 and Figure 3-93 shows the projections of the entire trajectory either on the ecliptic reference frame or on the XY plane of the Sun-Earth rotating plane.



Figure 3-94 shows separately the projection of each of the science orbits in the Sun-Earth rotating frame in which the phasing with Earth gives a clear indication of the downlink capability.

Figure 3-95 shows the evolution of the distance to the Sun, Earth and Venus and Figure 3-96 shows the evolution of the Sun-Spacecraft-Earth and Sun-Earth-Spacecraft angles. Figure 3-97 zooms on the region below 10 deg to show more clearly the solar conjunctions, which occur outside the GAM events. Table 3-28 provides a summary of the solar conjunction periods and MGA safe-mode blackouts. For this trajectory 7 solar superior conjunctions are encountered, the longest of them lasting 24 days on end July-August 2025. The longest safe-mode blackout occurs also during the same solar conjunction and can last up to about 64 days, which is close to the current spacecraft capability.

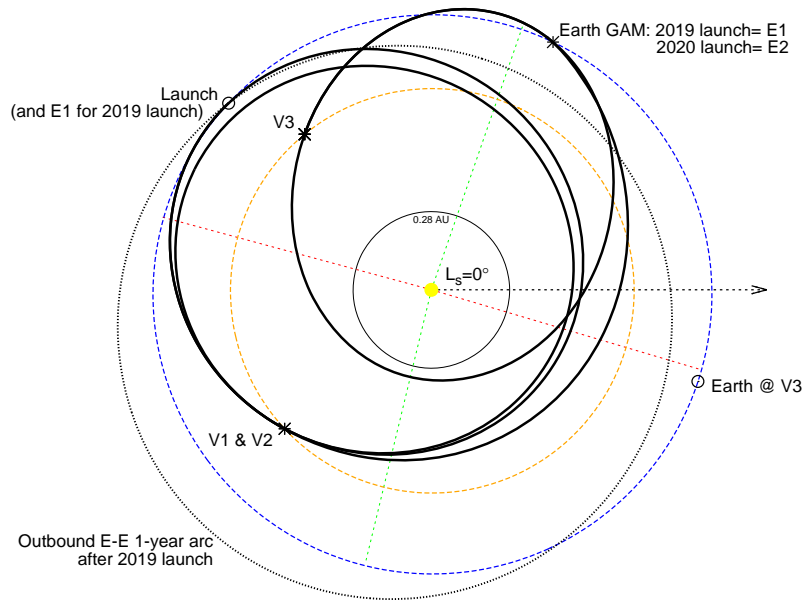


Figure 3-91 2019 & 2020 February Launch: X-Y Trajectory projection from launch until GAM-V2

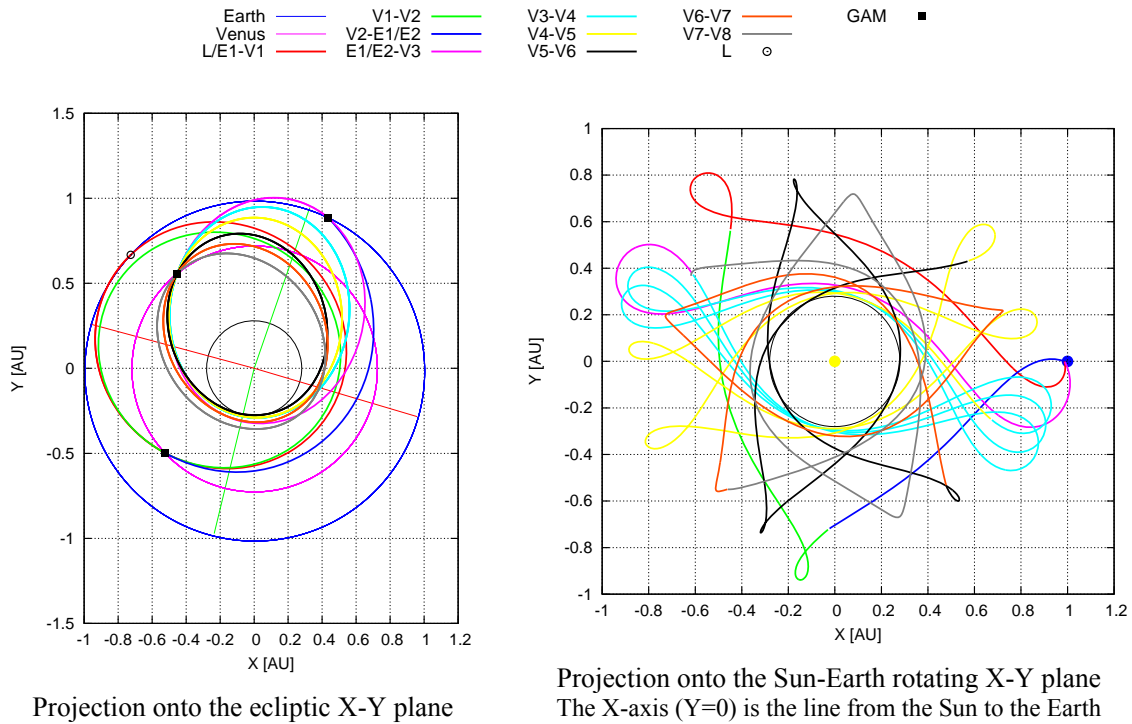


Figure 3-92 2019 & 2020 February Launch: X-Y Trajectory projections

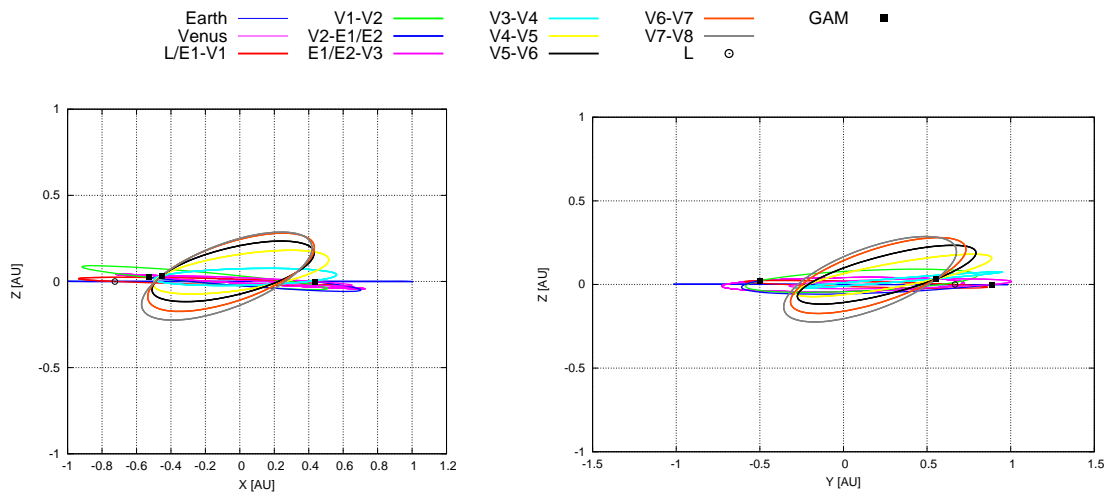


Figure 3-93 2019 & 2020 February Launch: X-Z and Y-Z Trajectory projections

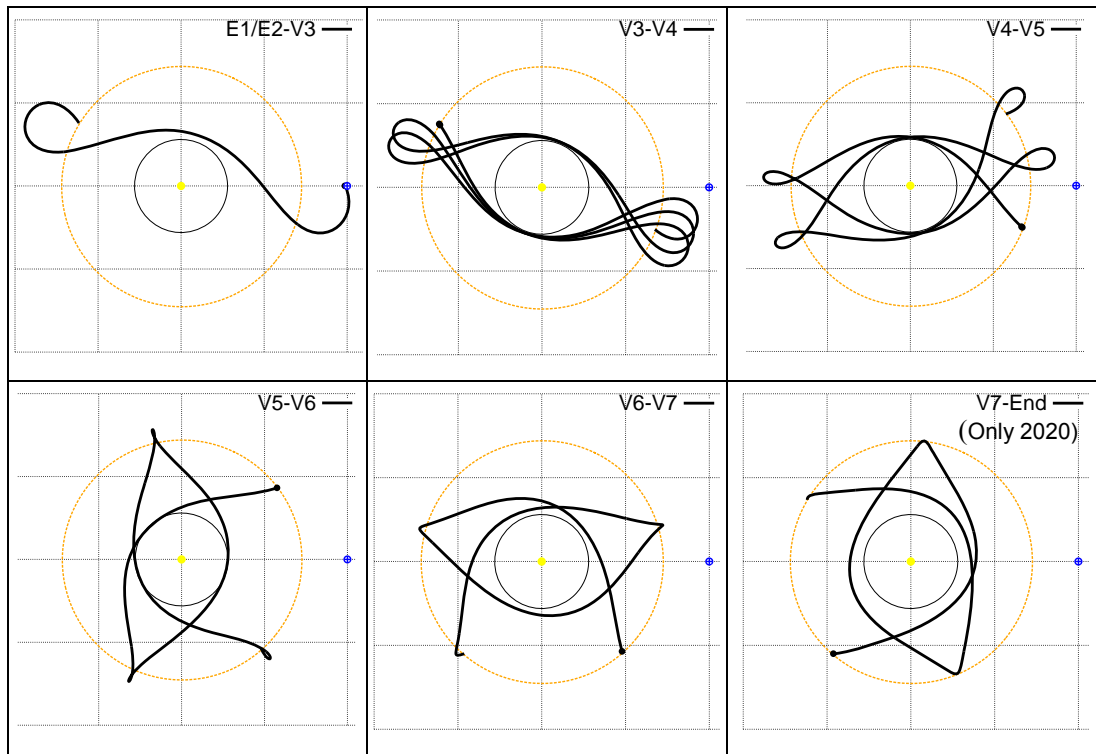


Figure 3-94 2019 & 2020 February Launch: Science orbits projection in the Sun-Earth rotating frame

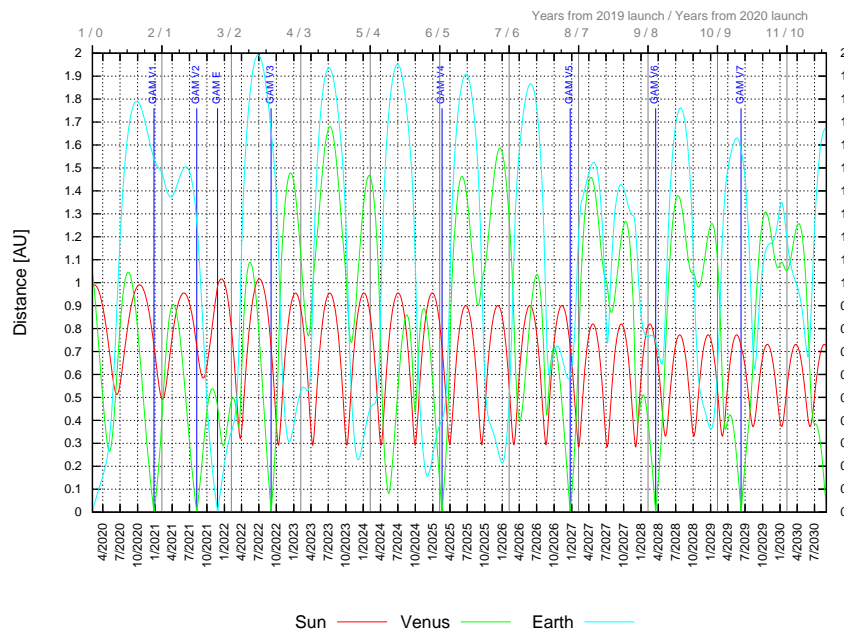


Figure 3-95 2019 & 2020 February Launch: Spacecraft distance to Sun, Venus and Earth

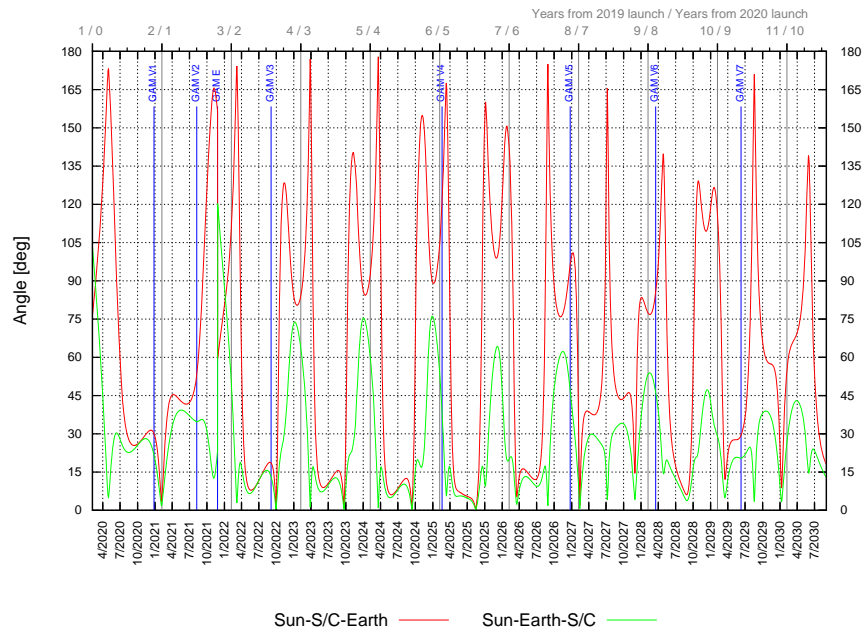


Figure 3-96 2019 & 2020 February Launch: SSE and SES angles

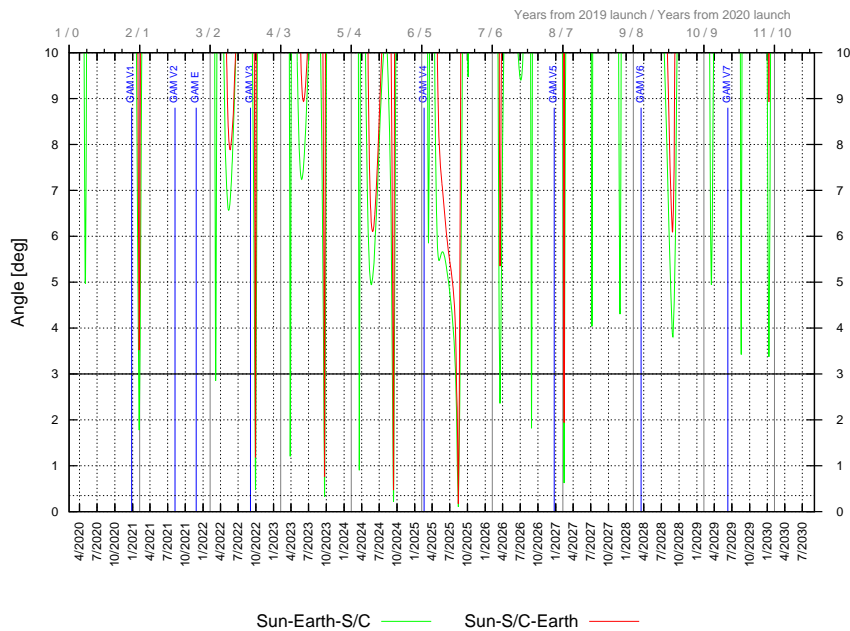


Figure 3-97 2019 & 2020 February Launch: SSE and SES angles – Detail of conjunctions



Solar Conjunction Periods SES<3 deg

	Type	Start	End	Duration [days]	Min SES [deg]
1	Superior	2021-01-31	2021-02-07	6.6	1.78
2	Inferior	2022-03-06	2022-03-07	0.8	2.85
3	Superior	2022-09-25	2022-10-02	6.8	0.48
4	Inferior	2023-03-27	2023-03-29	2.6	1.21
5	Superior	2023-09-17	2023-09-25	7.8	0.33
6	Inferior	2024-03-18	2024-03-21	2.9	0.90
7	Superior	2024-09-07	2024-09-17	9.3	0.22
8	Superior	2025-07-30	2025-08-23	24.0	0.11
9	Superior	2026-03-16	2026-03-21	4.9	2.36
10	Inferior	2026-08-27	2026-08-29	2.1	1.82
11	Superior	2027-02-10	2027-02-15	4.4	0.62

Safe Mode Blackout Periods SES<=5 deg OR SSE<=3 deg (longer than 7 days)

	Start	End	Duration [days]
1	2021-01-28	2021-02-10	12.8
2	2022-09-22	2022-10-04	11.7
3	2023-09-14	2023-09-27	13.4
4	2024-05-17	2024-05-25	8.1
5	2024-09-03	2024-09-19	16.0
6	2025-06-25	2025-08-27	63.6
7	2026-03-13	2026-03-25	12.0
8	2027-02-09	2027-02-17	7.6
9	2028-08-17	2028-09-07	21.7

Table 3-28 2019 & 2020 February Launch: Solar Conjunctions

Figure 3-98 shows the evolution of the Earth-Spacecraft range-rate. The range of variation for the entire mission goes from -56.3 km/s to 58.5 km/s.

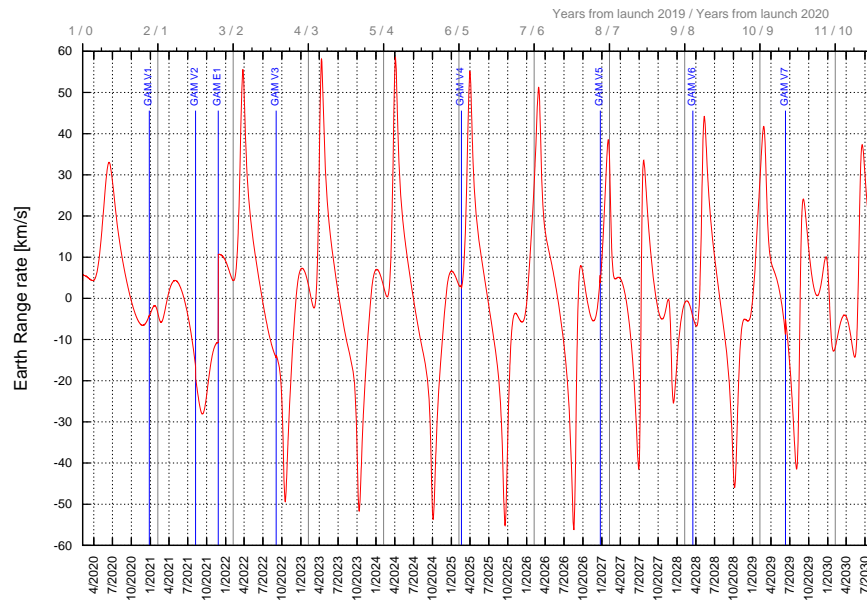


Figure 3-98 2019 & 2020 February Launch: Variation of Earth-Spacecraft range-rate

Figure 3-99 shows the evolution of the Doppler effect due to the Earth-Spacecraft range-rate and Figure 3-100 shows the evolution of the Doppler rate. The Doppler varies from -1.64 MHz to 1.58 MHz during the entire mission. The Doppler seen from the ground stations will be slightly different due to the rotation velocity of the Earth.

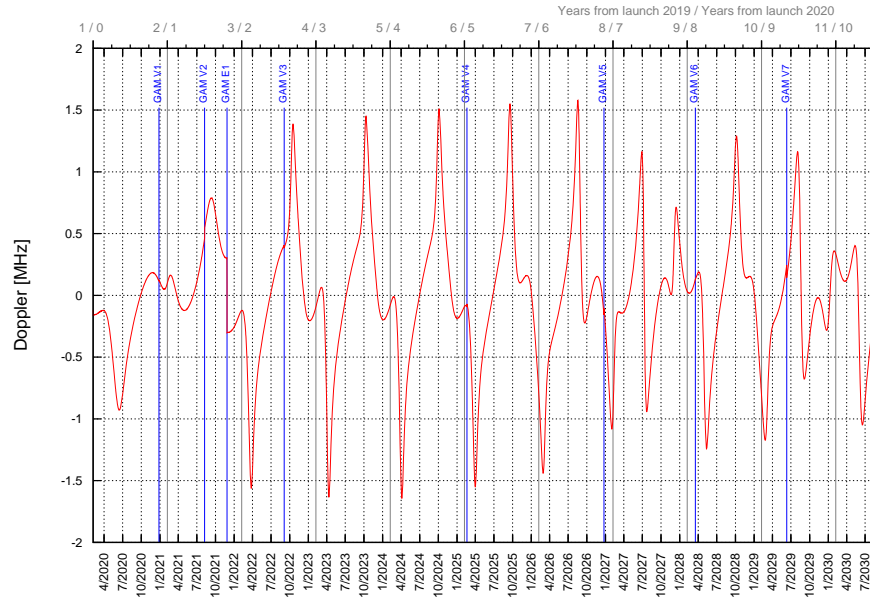


Figure 3-99 2019 & 2020 February Launch: Variation of Earth-Spacecraft Doppler

The Doppler varies very rapidly at the GANs and so Figure 3-100 shows Doppler-rate peaks extending beyond the limits of the graph. The limits of this figure have been chosen to allow representing the variations of the Doppler-rate in the heliocentric phases which are of the order of a few Hz/s, while peaks at the GANs can largely exceed 500 Hz/s. The detail analysis of the Doppler-rates reached at the GANs is presented in Section 3.4.4.

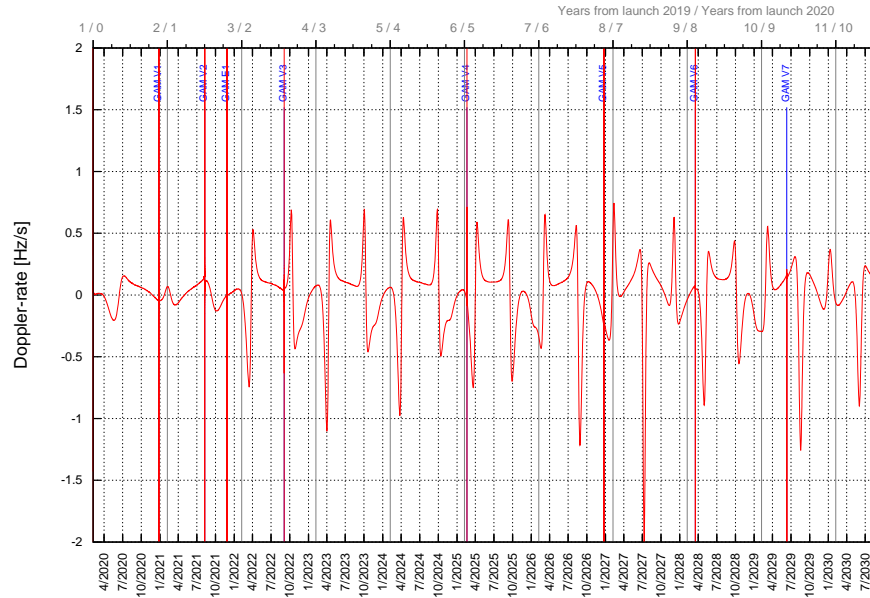


Figure 3-100 2019 & 2020 February Launch: Variation of Earth-Spacecraft Doppler-rate



3.4.2 SCIENCE PROPERTIES

The following set of figures and tables provide details of the characteristics of the trajectory relevant for the mission science.

Figure 3-101 shows together the evolution of the solar latitude with the distance to the Sun. The perihelion of the science orbit is located on the Southern Sun hemisphere. For each science orbit the spacecraft passes the point of minimum latitude first, shortly later the perihelion and then the maximum latitude, which typically occurs farther away from the Sun as the minimum latitude.

Figure 3-102 provides a Sun-centric representation of the 6 science orbits used during the NMP and EMP, including the second Earth-Venus leg. The spacecraft describes the orbits in the clockwise direction of the plot. This figure shows how the perihelions are below the Sun Equator and the Venus GAMs are encountered inbound after the aphelion. In addition, the location of the expected TCM to navigate the Earth and Venus GAMs has been included. The assumed TCM timeline considers targeting manoeuvres 30, 14, 7 and 3 days before the GAM, and a clean-up TCM 7 days after the GAM.

Figure 3-103 shows the evolution of the perihelion and aphelion and the points of maximum and minimum solar latitude as a function of the date and Table 3-29 provides data about the minimum/maximum latitude and perihelion events of each science orbit.

Table 3-30 provides the number and duration of the passes close to the Sun for different distances. For launch in 2019 the mission is assumed to end just before GAM-V7, therefore it has 3 science orbits less than for launch in 2020. In both cases the spacecraft will approach the Sun 12 times below 0.3 AU with stays between 5.3 and 8.6 days. For 2019 launch it will approach the Sun 16 times below 0.4 AU, while for 2020 launch it will have 3 additional approaches for a total of 19 times. The stay below 0.4 AU lasts from 18 to 27 days. During the cruise phase only one short approach below 0.5 AU will occur.

Figure 3-105 shows the spacecraft rotation velocity around the Sun. The maximum rotation velocity is achieved at perihelion of the orbit achieved after GAM-V3.

Figure 3-106 shows the evolution of the Earth distance together with the estimated downlink volume per day assuming a flat 8-hour daily pass. The plot shows the periods in which the maximum data rate is provided (green shadowed), which are related to the close-Earth aphelions. This trajectory provides 5 of such periods. 4 of them occur during NMP between GAM-V3 and GAM-V5 and are long and almost equally distributed. The last period occurs around the middle of the second 3:2 resonance during EMP.

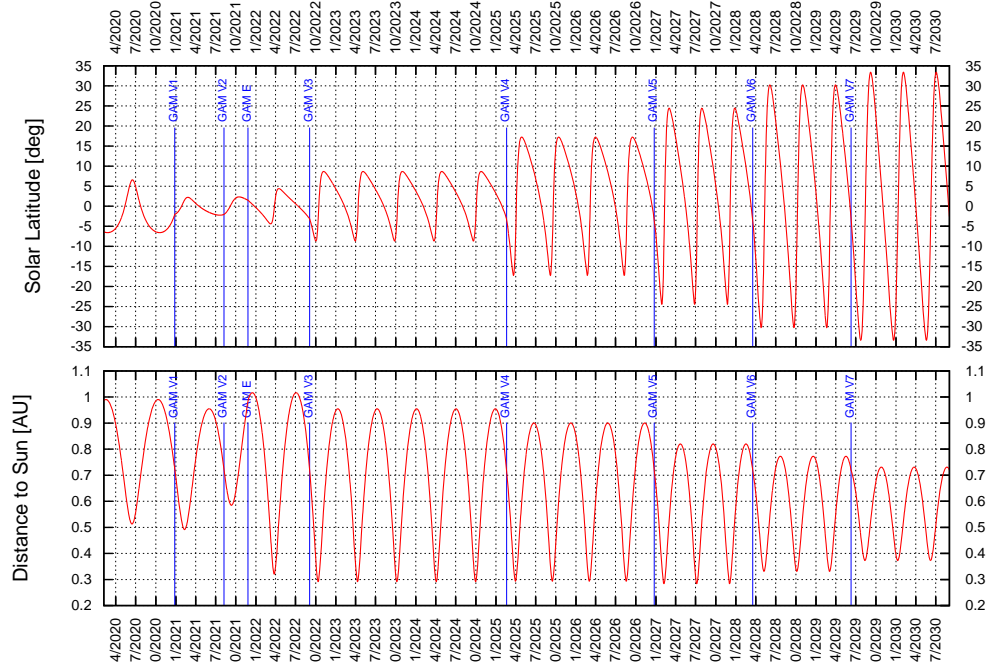


Figure 3-101 2019 & 2020 February Launch: Spacecraft solar latitude + distance to Sun

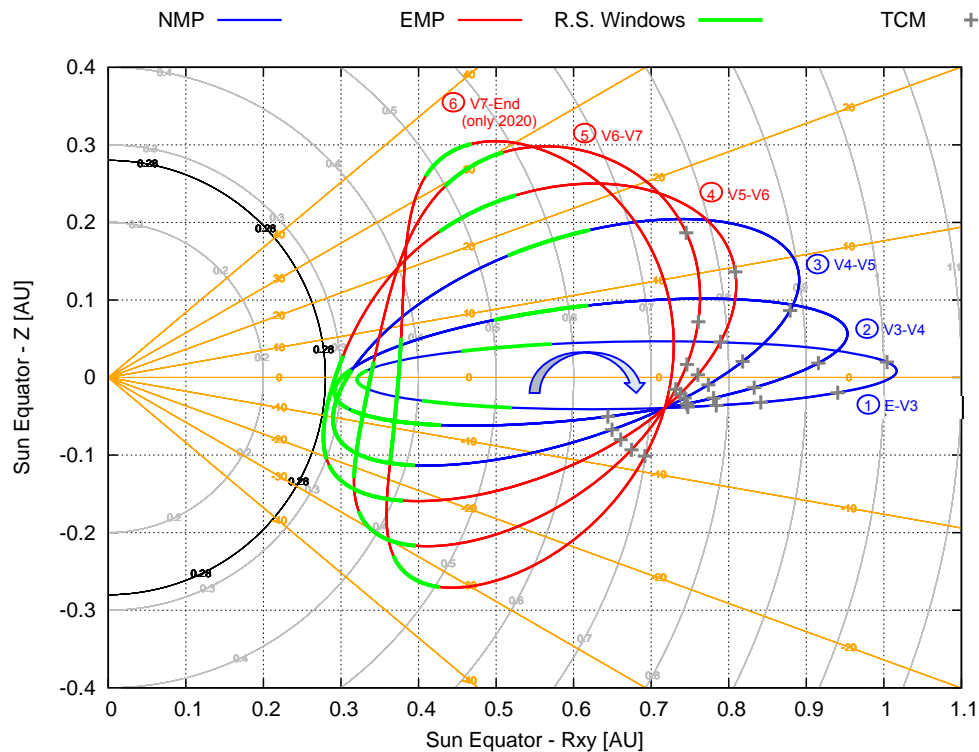


Figure 3-102 2019 & 2020 February Launch: projection of science orbits wrt Sun Equator and North Pole

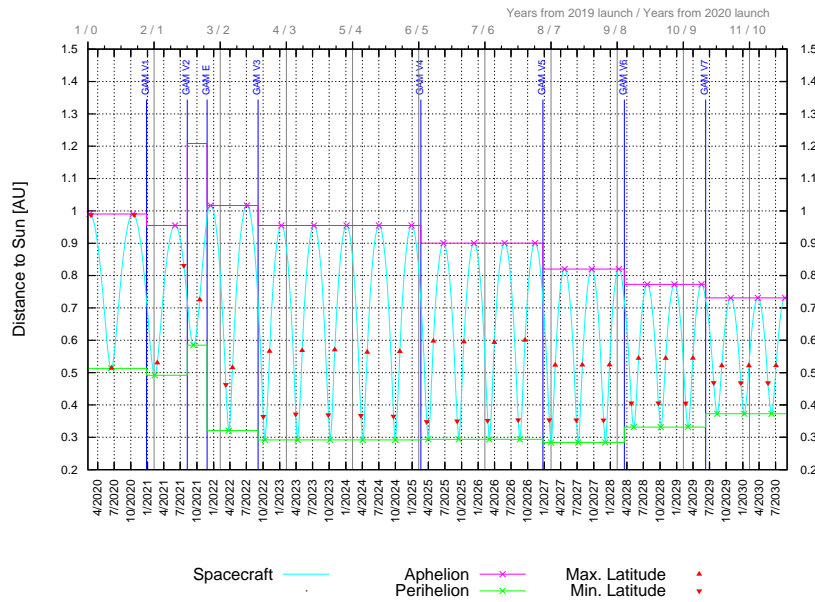


Figure 3-103 2019 & 2020 February Launch: Evolution of apsides and points of extreme solar latitude

Event	#	Date yy-mm-dd	Flight Time (y)	Sun Distance (AU)	Solar Latitude (deg)
GAM-E		21-11-26	1.80		
MINLAT	1	22-03-10	2.09	0.461	-4.39
MINRP	1	22-03-26	2.13	0.321	-0.49
MAXLAT	1	22-04-16	2.19	0.518	4.39
GAM-V3		22-09-03	2.57		
MINLAT	2	22-10-02	2.65	0.369	-8.66
MINRP	2	22-10-12	2.68	0.292	-3.43
MAXLAT	2	22-11-06	2.75	0.567	8.66
MINLAT	3	23-03-31	3.14	0.369	-8.66
MINRP	3	23-04-10	3.17	0.292	-3.44
MAXLAT	3	23-05-05	3.24	0.567	8.66
MINLAT	4	23-09-27	3.64	0.369	-8.66
MINRP	4	23-10-07	3.66	0.292	-3.45
MAXLAT	4	23-11-01	3.73	0.567	8.66
MINLAT	5	24-03-24	4.13	0.369	-8.66
MINRP	5	24-04-03	4.15	0.292	-3.45
MAXLAT	5	24-04-29	4.22	0.567	8.66
MINLAT	6	24-09-20	4.62	0.369	-8.66
MINRP	6	24-09-30	4.65	0.292	-3.46
MAXLAT	6	24-10-25	4.71	0.567	8.66
GAM-V4		25-02-18	5.03		
MINLAT	7	25-03-22	5.12	0.352	-17.22
MINRP	7	25-03-31	5.14	0.294	-8.63
MAXLAT	7	25-04-28	5.22	0.596	17.22
MINLAT	8	25-09-07	5.58	0.353	-17.22
MINRP	8	25-09-16	5.61	0.294	-8.57
MAXLAT	8	25-10-14	5.68	0.596	17.22
MINLAT	9	26-02-22	6.04	0.352	-17.22
MINRP	9	26-03-03	6.07	0.294	-8.66
MAXLAT	9	26-03-31	6.14	0.596	17.22
MINLAT	10	26-08-10	6.51	0.353	-17.22
MINRP	10	26-08-19	6.53	0.294	-8.59
MAXLAT	10	26-09-16	6.61	0.596	17.22
GAM-V5		26-12-24	6.88		
MINLAT	11	27-01-28	6.97	0.352	-24.43
MINRP	11	27-02-07	7.00	0.284	-9.78
MAXLAT	11	27-03-02	7.06	0.527	24.43
MINLAT	12	27-06-27	7.38	0.352	-24.43
MINRP	12	27-07-07	7.41	0.284	-9.79
MAXLAT	12	27-07-30	7.47	0.527	24.43
MINLAT	13	27-11-24	7.79	0.352	-24.43
MINRP	13	27-12-03	7.82	0.284	-9.80
MAXLAT	13	27-12-27	7.89	0.527	24.43
GAM-V6		28-03-17	8.11		
MINLAT	14	28-04-25	8.21	0.405	-30.21
MINRP	14	28-05-08	8.25	0.331	-10.43
MAXLAT	14	28-06-04	8.32	0.543	30.21
MINLAT	15	28-09-22	8.62	0.405	-30.21
MINRP	15	28-10-05	8.66	0.331	-10.46
MAXLAT	15	28-11-01	8.73	0.542	30.21
MINLAT	16	29-02-19	9.03	0.405	-30.21
MINRP	16	29-03-04	9.07	0.331	-10.48
MAXLAT	16	29-03-31	9.14	0.542	30.21
GAM-V7		29-06-10	9.34		
(Mission end if 2019 launch)					
MINLAT	17	29-07-24	9.46	0.468	-33.39
MINRP	17	29-08-12	9.51	0.373	-5.46
MAXLAT	17	29-09-07	9.58	0.523	33.39
MINLAT	18	29-12-21	9.87	0.468	-33.39
MINRP	18	30-01-09	9.92	0.373	-5.47
MAXLAT	18	30-02-04	9.99	0.523	33.39
MINLAT	19	30-05-20	10.28	0.468	-33.39
MINRP	19	30-06-08	10.33	0.373	-5.47
MAXLAT	19	30-07-04	10.40	0.523	33.39

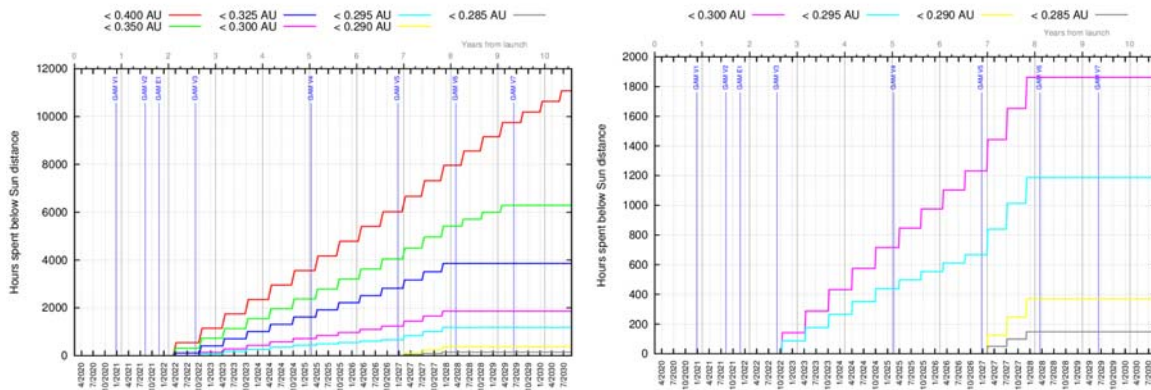
Note: Assumed launch in 2020, launch in 2019 adds +1 year to all flight times

Table 3-29 2019 & 2020 February Launch: Characteristics of perihelion and extreme points of solar latitude



	Launch in 2019				Launch in 2020			
	# Times	ACC (days)	MIN (days)	MAX (days)	# Times	ACC (days)	MIN (days)	MAX (days)
Cruise Phase		1023				658		
Below 0.3 AU	0	0	0	0	0	0	0	0
Below 0.4 AU	0	0	0	0	0	0	0	0
Below 0.5 AU	1	13.2	13.2	13.2	1	13.2	13.2	13.2
Below 0.6 AU	3	121.4	20.3	52.8	3	121.4	20.3	52.8
Science Mission		2753				3202		
Below 0.3 AU	12	77.1	5.3	8.6	12	77.1	5.3	8.6
Below 0.4 AU	16	406.4	22.8	27.1	19	461.5	18.4	27.1
Below 0.5 AU	16	665.5	38.8	45.0	19	803.6	38.8	46.0
Below 0.6 AU	16	944.9	54.8	66.8	19	1163.7	54.8	72.9
Total Mission		3776				3861		
Below 0.3 AU	12	77.1	5.3	8.6	12	77.1	5.3	8.6
Below 0.4 AU	16	406.4	22.8	27.1	19	461.5	18.4	27.1
Below 0.5 AU	17	678.7	13.2	45.0	20	816.8	13.2	46.0
Below 0.6 AU	19	1066.2	20.3	66.8	22	1285.1	20.3	72.9

Table 3-30 2019 & 2020 February Launch: Number and duration of passes close to the Sun



Note: assumes launch in 2020. For 2019 launch add +1 year to flight times

Figure 3-104 2019 & 2020 February Launch: Evolution of time spent below different Sun ranges

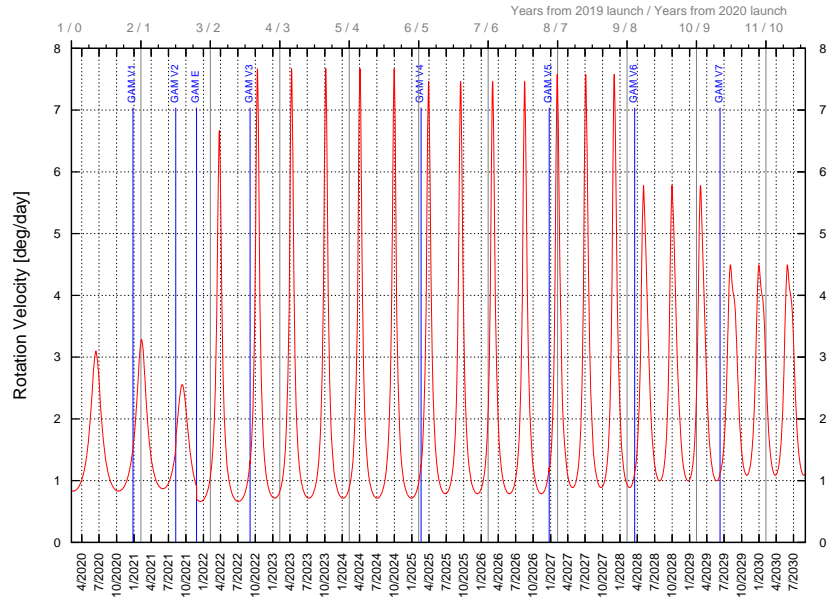


Figure 3-105 2019 & 2020 February Launch: Spacecraft rotation velocity about the Sun

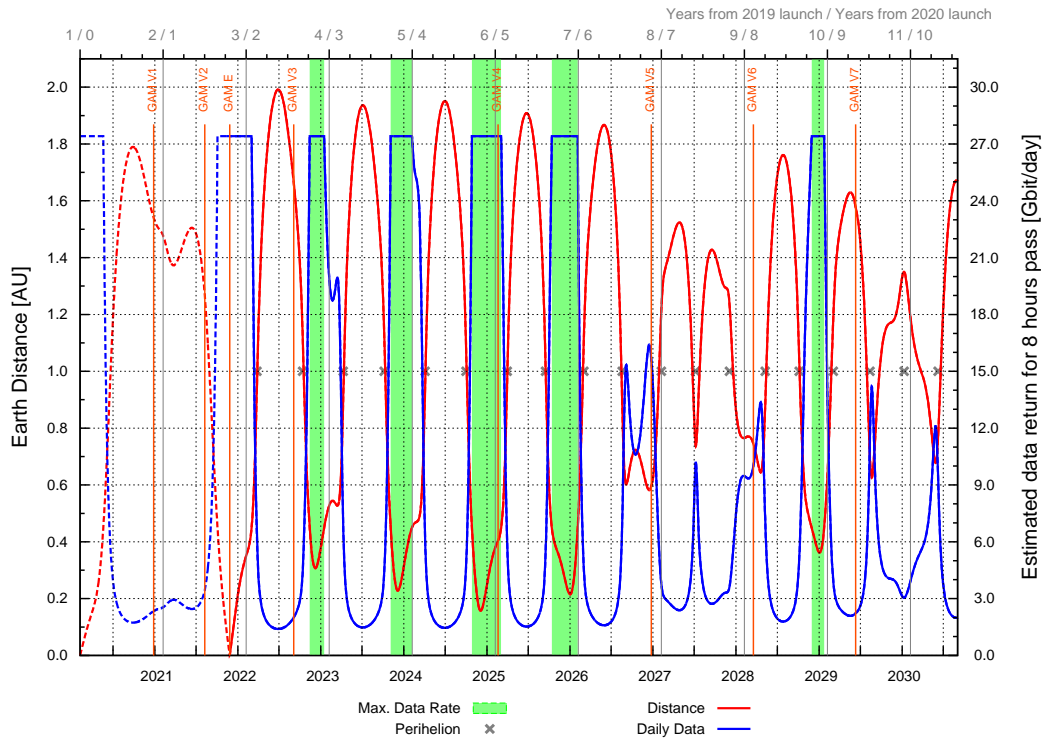


Figure 3-106 2019 & 2020 February Launch: Earth distance and potential daily downlink



3.4.3 GROUND STATION VISIBILITY

Figure 3-107 shows the evolution of the equatorial declination of the Earth-to-spacecraft direction.

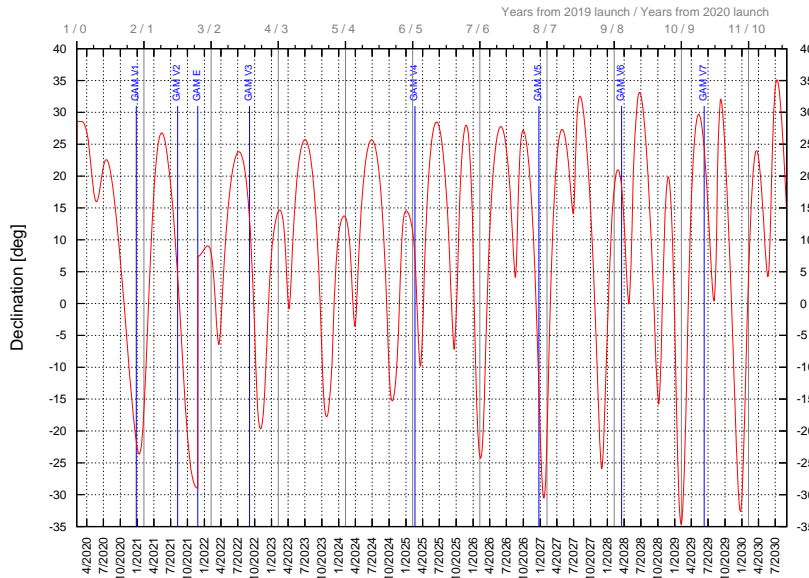


Figure 3-107 2019 & 2020 February Launch: Spacecraft equatorial declination.

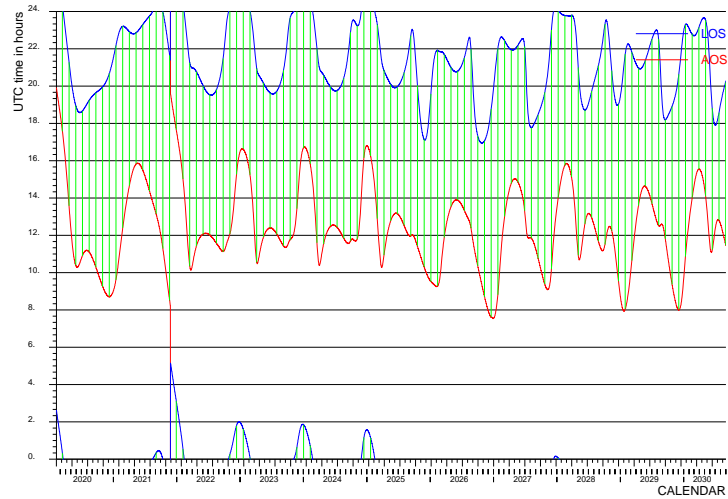
Figure 3-108 presents the daily period of visibility from each of the 3 ESA ground stations. The hours of the day when Acquisition Of Signal, AOS, and Loss Of Signal, LOS, take place is provided with a red and a blue line, respectively. Vertical black lines show the GAMs. The visibility is shown assuming 10° minimum elevation from the ground station. Daily visibility from any of the ground stations is guaranteed.

Figure 3-109 shows the duration of the visibility as a function of the date for all three ground stations. Figure 3-110 shows a combination of the daily period of visibility from the 3 stations.

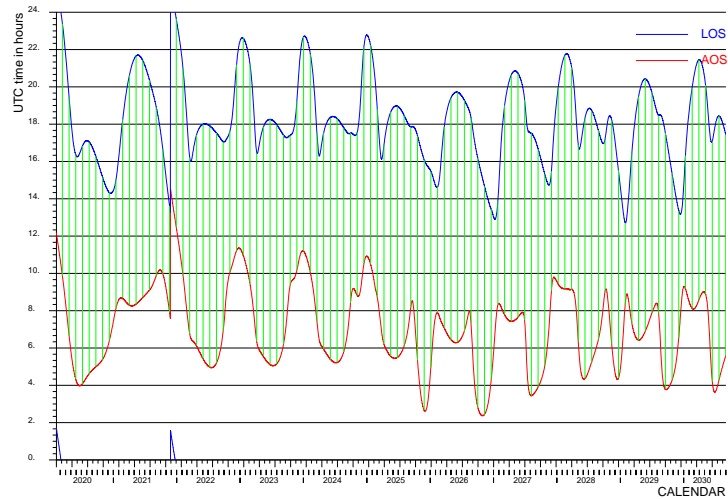
The previous 3 figures give the visibility evolution for the common part of the trajectories independently of the launch year covering until the end of the February 2020 mission. For launch in 2019, the visibility during the 1-year parking orbit from launch until the first Earth GAM and the corresponding results are provided in Figure 3-111, Figure 3-112 and Figure 3-113. In this case the reference launch date is February 15th 2019 so that both launch options, inwards and outwards, are feasible. The results of both options are presented next to each other.



Malargüe



Cebreros



New Norcia

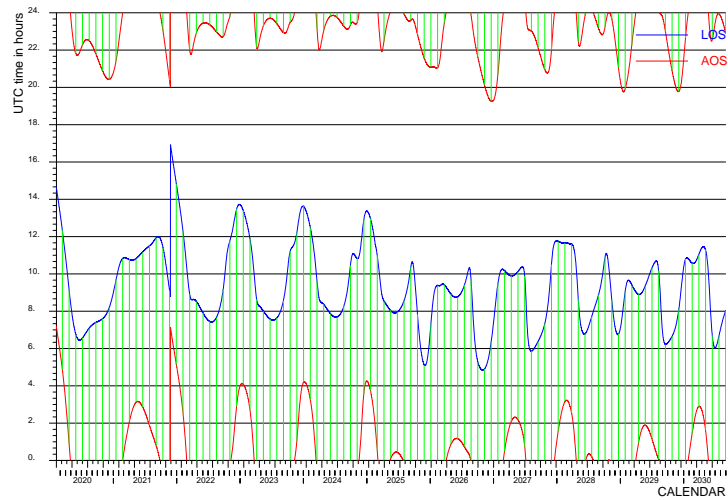


Figure 3-108 2019 & 2020 February Launch: Daily period of visibility from ESA DS stations.

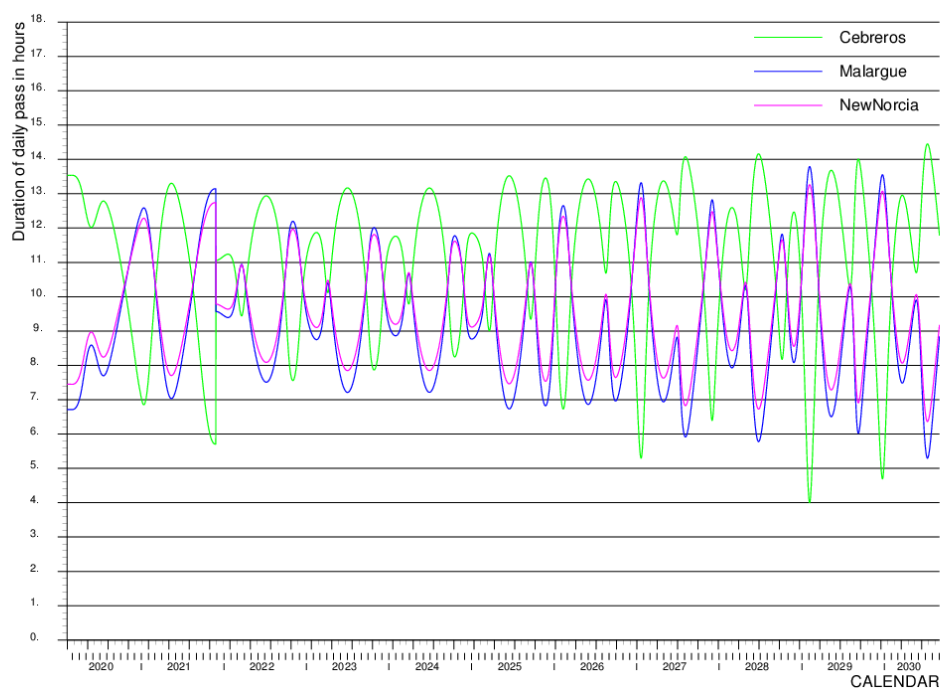


Figure 3-109 2019 & 2020 February Launch: Daily duration of visibility from ESA DS stations.

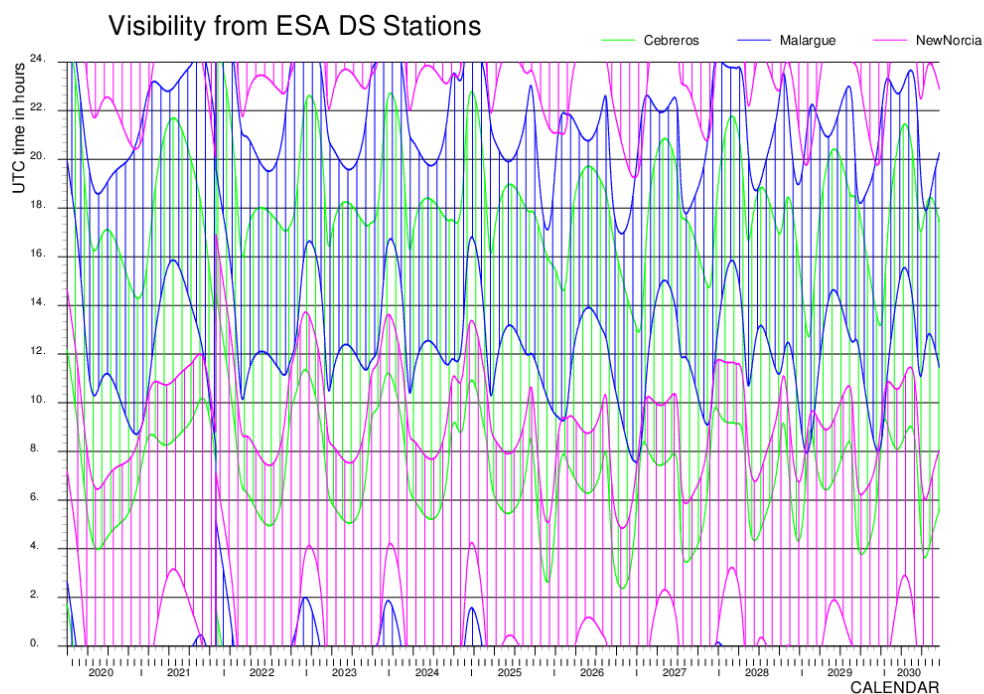


Figure 3-110 2019 & 2020 February Launch: Daily period of visibility from ESA DS stations.



Outwards

Inwards

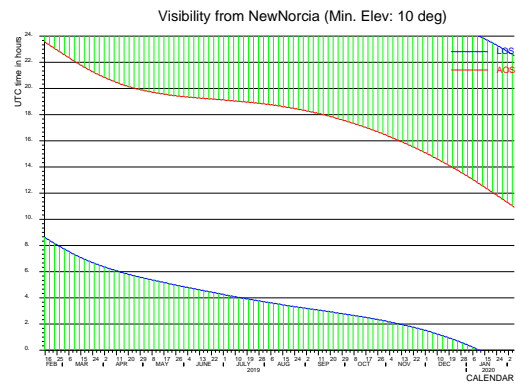
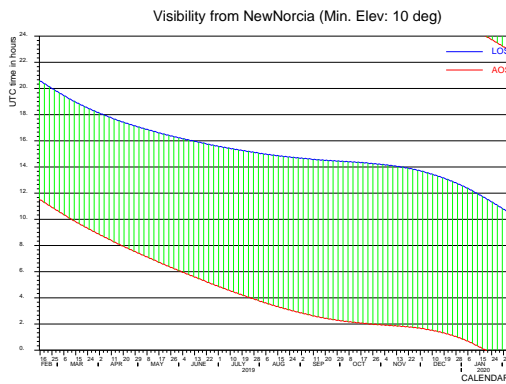
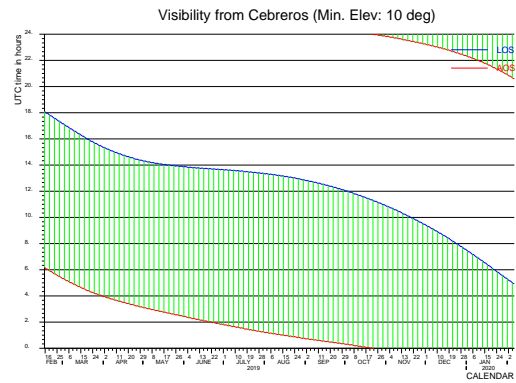
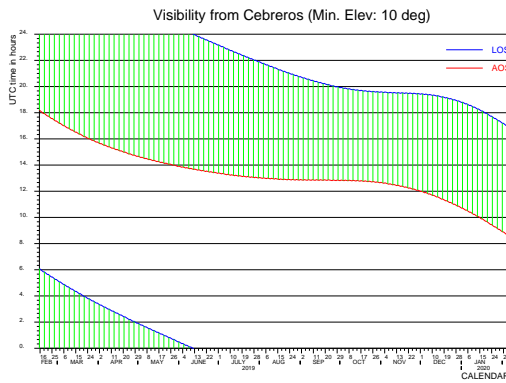
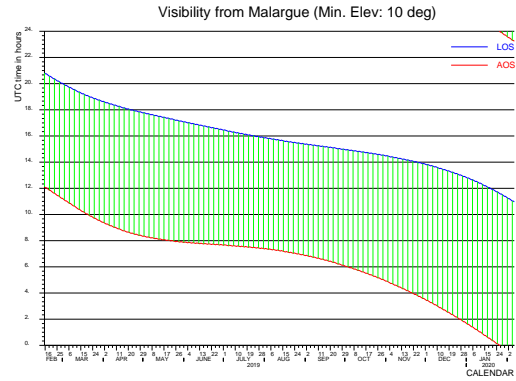
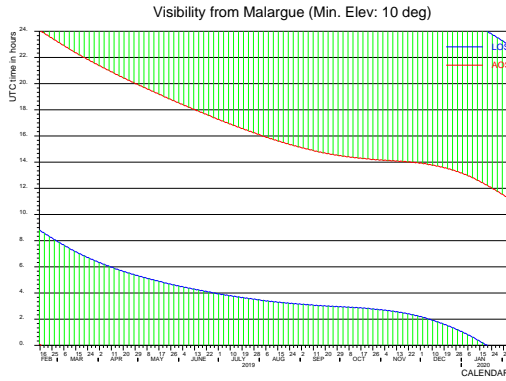


Figure 3-111 2019 February Launch: Daily period of visibility during 1-year parking orbit.

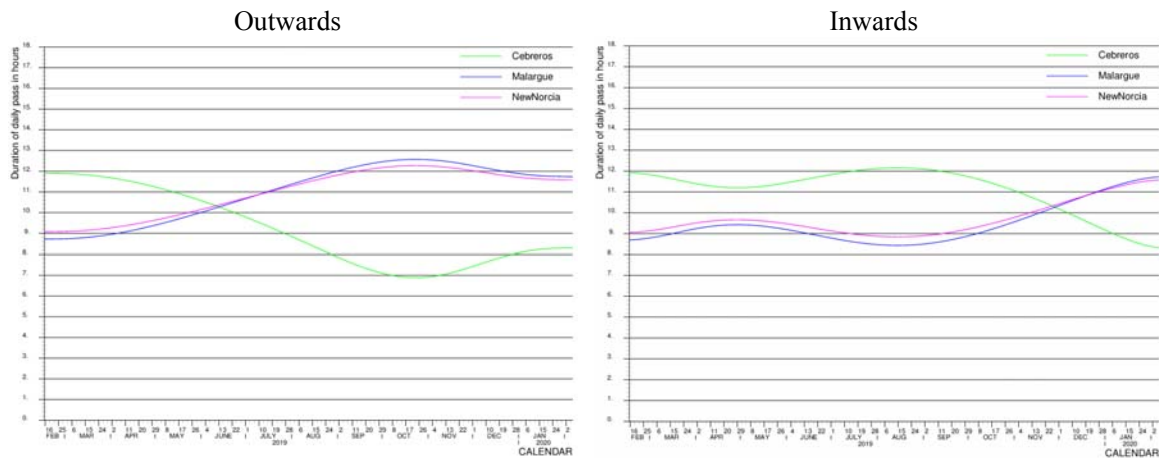


Figure 3-112 2019 February Launch: Daily duration of visibility during 1-year parking orbit.

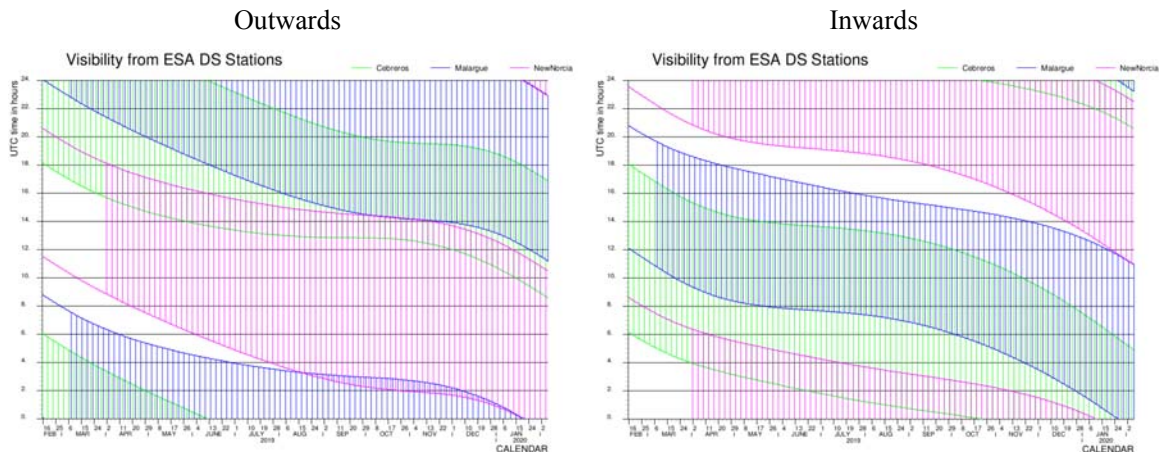


Figure 3-113 2019 February Launch: Daily period of visibility during 1-year parking orbit.

3.4.4 GAMS DETAILS

Table 3-31 shows the characteristics of the GAMS including the duration of the eclipse and occultation events. The table includes also the Earth GAM 1-year after a 2019 launch with both trajectory options: inwards and outwards from Earth (reference launch date for this case is February 15th so that both options are feasible for the same launch day). The Venus GAMS during the cruise phase are performed at altitudes of several thousand km, while the Earth GAM has to be performed at low altitude of about 440 km. Most of the Venus GAMS during the science phase are performed at maximum deflection at the minimum altitude of 350 km.

For this trajectory eclipses are only possible at the Earth GAMS. In a 2019 launch, only the inwards option leads to eclipse at the first Earth GAM. The Earth GAM at the end of the cruise phase always presents an eclipse. Occultation occurs only at GAM-V2 and GAM-V5.



GAM	Date	Re (AU)	V _{inf} (km/s)	Hmin (km)	Eclipse (min)	Occult. (min)	LST ¹ (h)	Ls (deg)	SSE (deg)	SES (deg)	ESV (deg)
2019 E1 In	2020-02-15	0.988	5.361	752	22.6	0	2.49	145.5	-	-	-
2019 E1 Out	2020-02-15	0.988	5.361	628	0	0	8.83	145.5	-	-	-
V1	2020-12-26	1.540	11.686	9005	0	0	6.34	223.4	30.1	21.6	128.3
V2	2021-08-08	1.269	11.686	8000	0	17.0	18.06	223.4	53.0	34.7	92.3
2020 E1 2019 E2	2021-11-26	0.000	10.705	439	18.6	0	3.93	63.8	-	-	-
V3	2022-09-03	1.664	18.560	5213	0	0	8.26	129.2	18.5	13.1	148.4
V4	2025-02-18	0.404	18.558	572	0	0	10.47	129.2	120.8	38.6	20.5
V5	2026-12-24	0.596	18.558	350	0	4.6	10.22	129.2	96.4	46.5	37.0
V6	2028-03-17	0.744	18.558	350	0	0	12.05	129.2	85.7	46.0	48.2
V7	2029-06-10	1.576	18.558	354	0	0	12.02	129.2	29.6	20.4	130.0
V8	2030-09-02	1.668	18.558	-	-	-	6.34	129.2	18.0	12.7	149.3

Table 3-31 2019 & 2020 February Launch: GAM Properties

Table 3-32 provides the components of the infinite velocity vectors at each GAM (in the ICRF/EME2000 reference frame) and the incoming B-plane impact vector. These vectors completely define the geometry of the GAM hyperbola.

GAM	Arrival					Departure		
	V _{∞x} (km/s)	V _{∞y} (km/s)	V _{∞z} (km/s)	B _x (km)	B _y (km)	V _{∞x} (km/s)	V _{∞y} (km/s)	V _{∞z} (km/s)
2019 E1 In	-4.092	3.173	1.388	-14131.8	-6994.4	2.880	3.796	2.455
2019 E1 Out	4.125	-3.134	1.377	13967.0	-6955.9	2.881	3.796	2.455
V1	7.613	7.455	4.800	9105.0	14678.7	6.952	9.138	2.173
V2	6.952	9.139	2.174	-15447.5	5067.2	9.310	6.984	1.057
2020 E1 2019 E2	7.461	5.678	5.165	-8700.0	4266.3	10.611	0.394	1.360
V3	15.872	-8.143	-5.124	9680.0	7378.8	16.294	-5.804	-6.729
V4	16.293	-5.804	-6.728	4963.4	5633.6	15.629	-2.346	-9.729
V5	15.628	-2.346	-9.729	6660.7	2950.2	14.762	2.154	-11.038
V6	14.762	2.154	-11.038	6306.7	3645.9	12.292	5.929	-12.576
V7	12.291	5.931	-12.576	7200.0	1134.2	9.410	9.722	-12.702

Table 3-32 2019 & 2020 February Launch: infinite velocity vectors and B-plane target of GAMs

¹ Local solar time (LST) at the pericentre of the GAM. The criterion for Venus LST is not related to the rotation of the planet and follows the same definition as for the Earth. Thus, 6 h local time is approximately in the direction of the planet velocity vector with respect to the Sun, and 18 h local time is in the opposite direction.



Figure 3-114 and Figure 3-115 show the projections of the Venus and Earth GAMs hyperbolas, respectively. For the details on how this projection is obtained refer to Section 3.1.4 (page 44). All the Venus GAMs are inbound incoming in the 4th quadrant and outgoing in the 3rd quadrant during the cruise phase and in the 2nd quadrant during NMP&EMP. The figure for the Earth GAMs shows together the GAM-E1 for a 2019 launch, both for inwards and outwards launch, and the GAM-E2 for 2019 launch (GAM-E1 for 2020 launch).

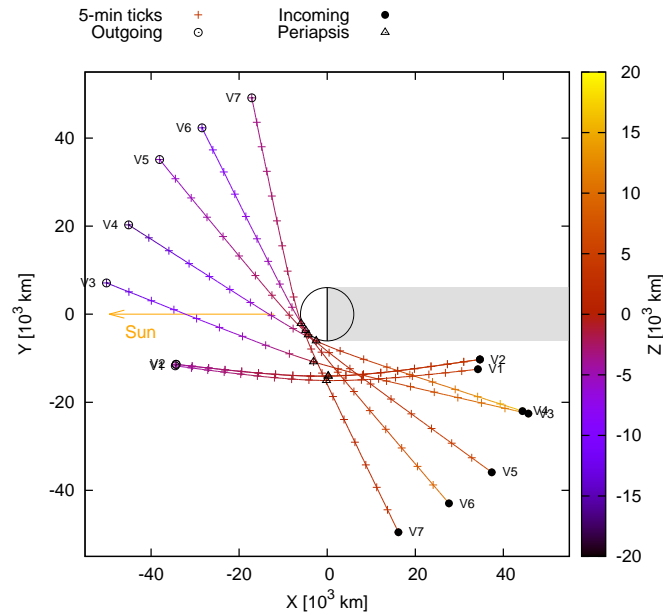


Figure 3-114 2019 & 2020 February Launch: Projection of hyperbolas for Venus GAMs

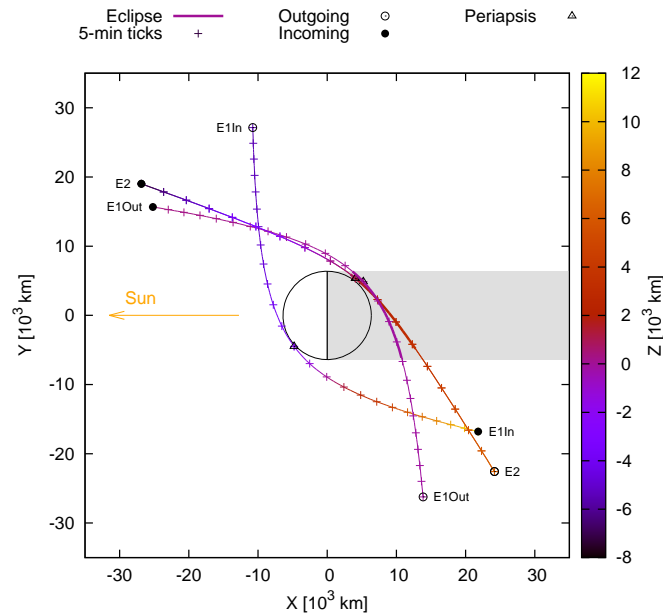


Figure 3-115 2019 & 2020 February Launch: Projection of hyperbolas for Earth GAMs



Figure 3-116 shows the Doppler rates around the Venus and Earth GAMs.

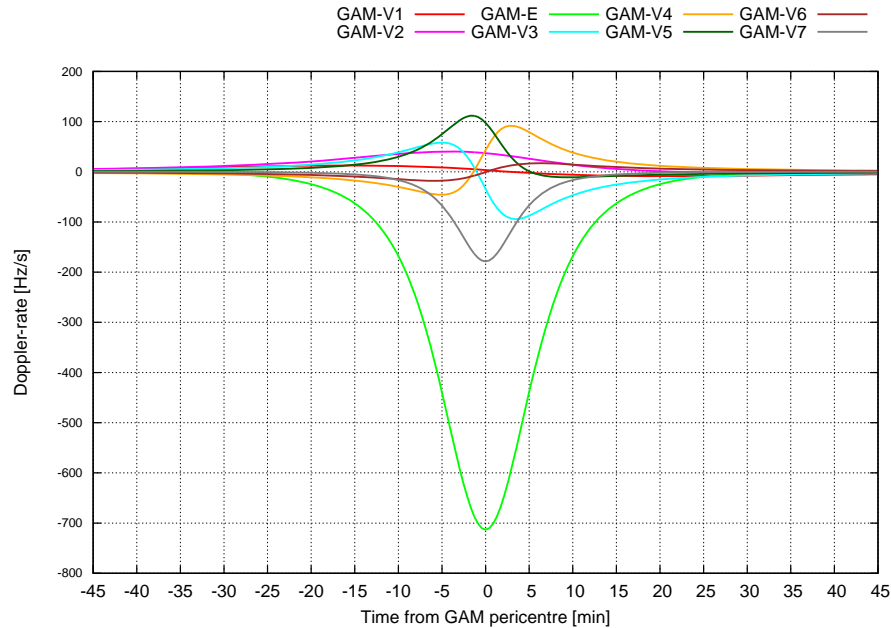


Figure 3-116 2019 & 2020 February Launch: Doppler rate around GAM pericentres

3.4.5 LEOP

A dedicated analysis from NASA/ULA of the Atlas V 411 ascent trajectory for the launch targets required for this trajectory is not available at this point in time. The following describes preliminary results obtained at ESOC by a first approximation of the separation conditions. Several assumptions were required to model the geometry at separation: inclination, perigee radius and longitude of the ascending node of the escape hyperbola, as well as the true anomaly at separation. The values used for such parameters are consistent with the results of the Preliminary Launch Vehicle Performance & Trajectory assessment [20] performed by NASA KSC.

For the analysis of a 2020 LEOP the same reference trajectory with launch on February 7th is considered. Launch on 2020-02-07 requires an infinite velocity of 5.585 km/s, DLA of 28.584 deg and RLA of 57.40 deg (both angles in ICRF/EME2000). This case is an extreme case in which the DLA is very close to the assumed inclination of the parking orbit and departure hyperbola. This leads to a very far East separation point on the Pacific Ocean and consequently a longer Atlas V 411 mission from lift-off to separation. However, for this particular case the models used by ESOC could not be fully representative of the real Atlas V ascent trajectory for such a target. A way to reduce the duration of the Atlas V flight and shift the separation point westwards could be to increase the inclination of the hyperbola, if possible within the performance capability of the launcher. The analysis will have to be redone once more detailed data from the launcher is available.

The separation time matching the escape conditions is 01:43:55 UTC (ESOC estimation).

Figure 3-117 shows the ground track of Solar Orbiter for 1 day after separation from the launcher upper stage. Separation occurs over the Pacific Ocean, North East of Australia. Solar Orbiter spacecraft travels North East for about 50-60 minutes increasing the altitude and then the ground track turns towards West. The spacecraft is then escaping from the Earth on the inertially fixed direction of the asymptote and so the latitude remains constant and equal to the target DLA while the longitude is



swept west due to the rotation of the Earth. Separation occurs on the illuminated side of the Earth (given in the plot at time of separation) and there is no eclipse after separation.

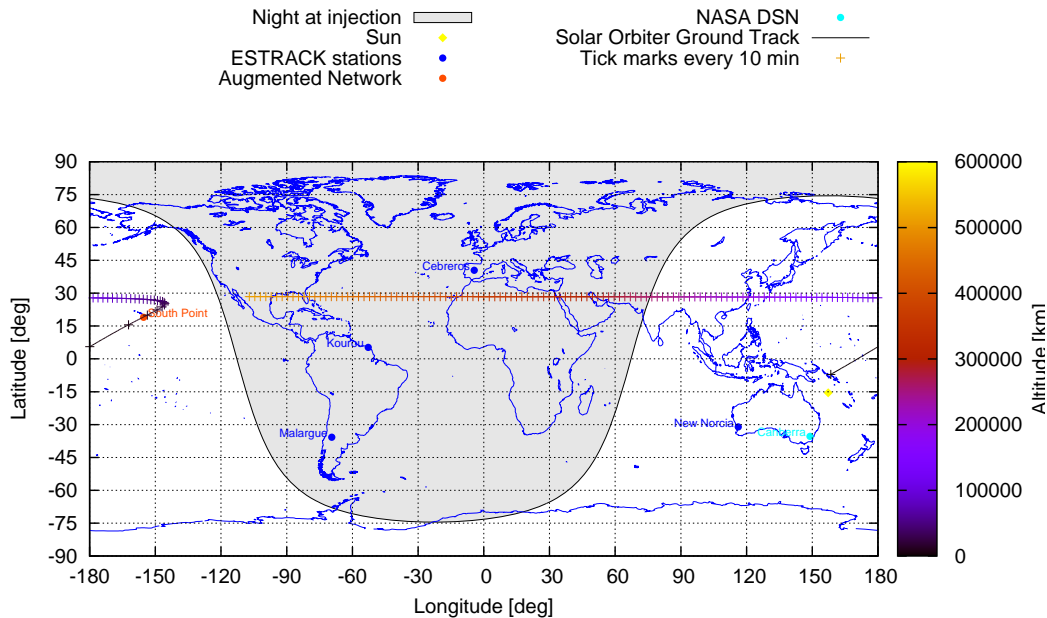


Figure 3-117 2020 February Launch: ground track for first LEOP day

Figure 3-118 shows the results of the ground station visibility analysis for the regarded scenario. The only station with visibility during the first hour after separation is South Point. The spacecraft will be above the horizon 4 minutes and the elevation will rise quickly even passing close to the Zenith of the station about 24 minutes after separation. Visibility from the ground stations in Australia is delayed several hours until the spacecraft is high enough to be seen. Canberra will acquire the signal first, about 2 hours after separation, while the first ESA station to acquire signal more than 4 hours after separation will be New Norcia. Therefore the visibility for this launch conditions is rather different from the 2018 launch options and it will be necessary to take operational measures such as to include additional ground stations to ensure coverage early during the LEOP.

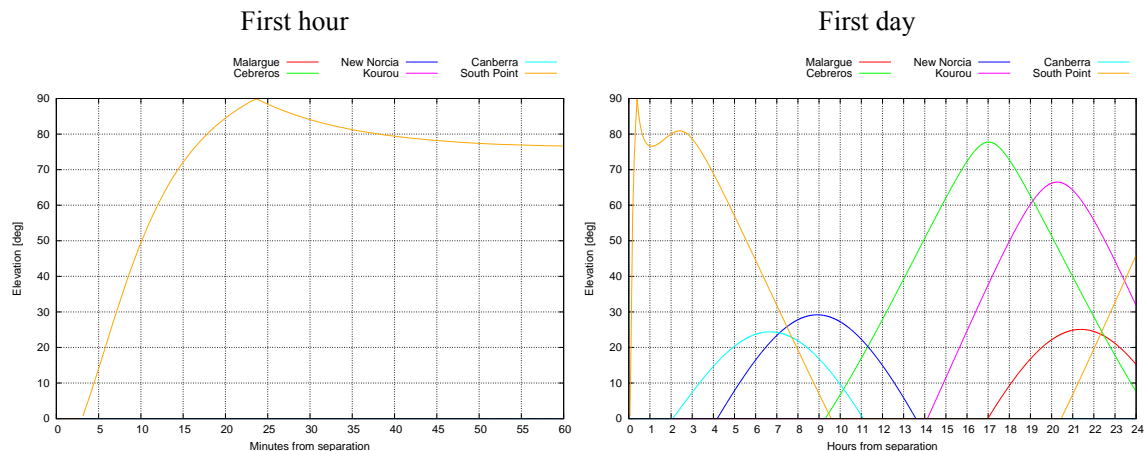


Figure 3-118 2020 February launch: elevation from ground stations



The geometry of Earth, S/C and Sun short after departure is presented in Figure 3-119. The plot on the left shows the evolution for the first 5 hours after separation of the SSE and SES angles along with the Earth distance. The plot on the right shows the projection of the departure hyperbola on the Sun-Earth rotating frame relative to Earth (thus at the centre; Sun on the left, far out the plot scale).

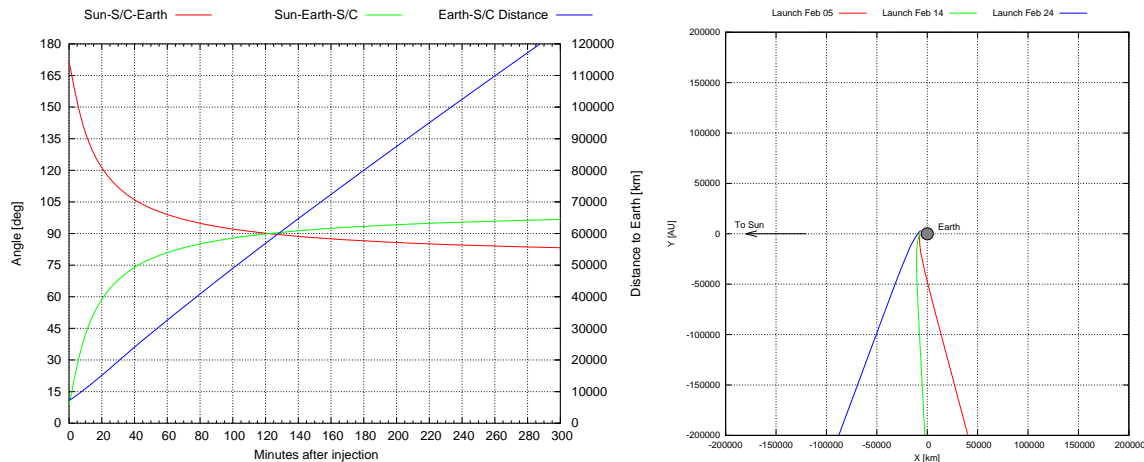


Figure 3-119 2020 February launch: Earth, Sun & S/C relative geometry at early LEOP.

For the analysis of the 2019 LEOP two launch options have to be considered: inwards and outwards from Earth. In both cases the Atlas V ascent trajectory with respect to the rotating Earth should be the same (except for the effect of a minor mismatch of the infinite velocity and DLA targets), but the lift-off time and separation times are different. The launch date considered is February 15th 2019, for which the 2 launch options are feasible as shown in Section 4.5. The launch targets are as follows:

- Outwards: V-infinity 5.382 km/s, DLA +15 deg, RLA 142.56 deg (ICRF/EME2000)
- Inwards: V-infinity 5.340 km/s, DLA +15 deg, RLA -37.02 deg (ICRF/EME2000)

Figure 3-120 shows the ground track of Solar Orbiter for the first day after separation for both solutions, inwards and outwards. Separation occurs over the Indian Ocean, West of Australia. Solar Orbiter travels North East for about 50-60 minutes increasing altitude. As the spacecraft escapes from Earth on the inertially fixed direction of the asymptote the latitude remains constant and equal to the target DLA while the longitude is swept west due to the rotation of the Earth. Although separation occurs in both cases close to the Earth surface terminator (outwards on the illuminated side, inwards on the night side), the spacecraft is already at an altitude at which it is illuminated. Notice also that the plot appears to indicate that the spacecraft will traverse the shadow region, but this is not the case as the altitude keeps increasing (subsattellite point in shadow does not mean spacecraft in shadow, for instance at 1000 km altitude surface terminator and eclipse entry point differ already by about 30 deg). Numerical simulations confirm that no eclipse will be encountered after separation.

The separation times estimated by ESOC are the following:

- Outwards: 10:27:32 UTC
- Inwards: 22:25:36 UTC

Figure 3-121 shows the results of the ground station visibility analysis. The coverage is the same for both solutions, inwards and outwards; therefore only one case is presented. Separation will be under visibility from New Norcia with an elevation just above 35 deg. The elevation then peaks up to 55 deg 2-3 minutes after separation and goes down smoothly to 20 deg. Visibility from Canberra will start just a few minutes after separation, while South Point will have the spacecraft over the horizon at about 16 minutes after separation.

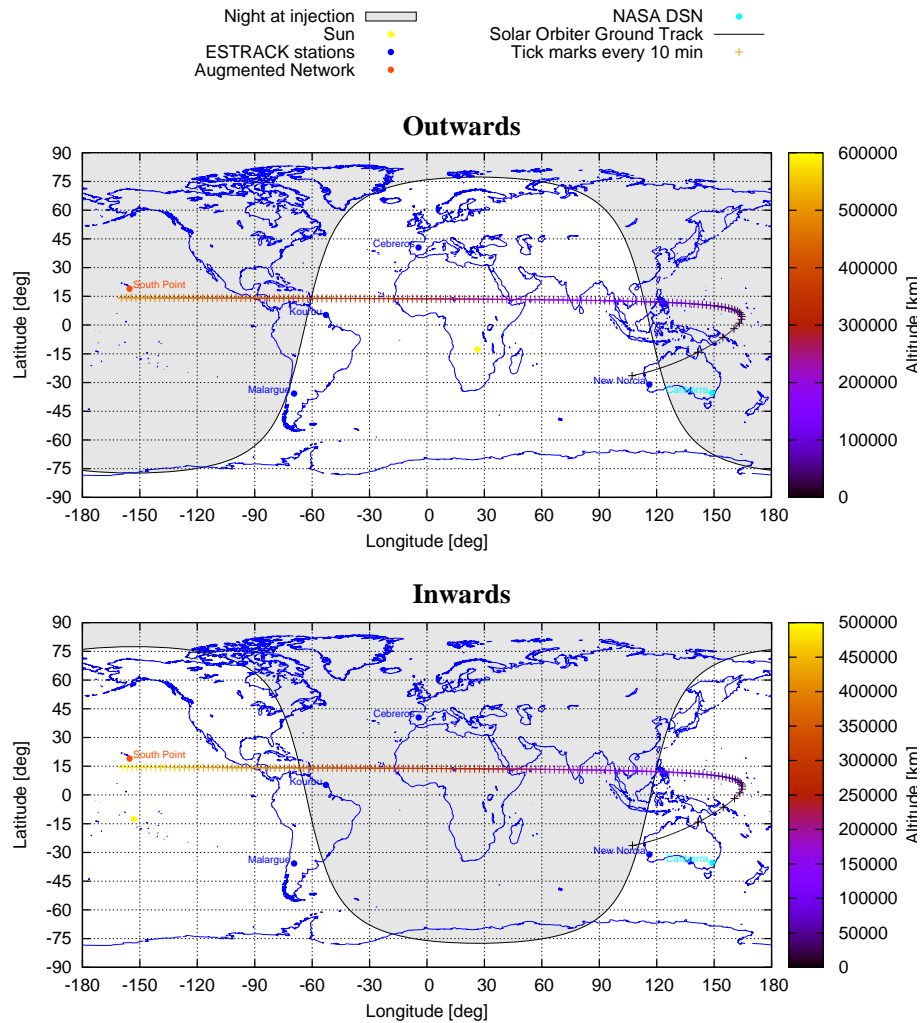


Figure 3-120 2019 February Launch: ground track for first LEOP day

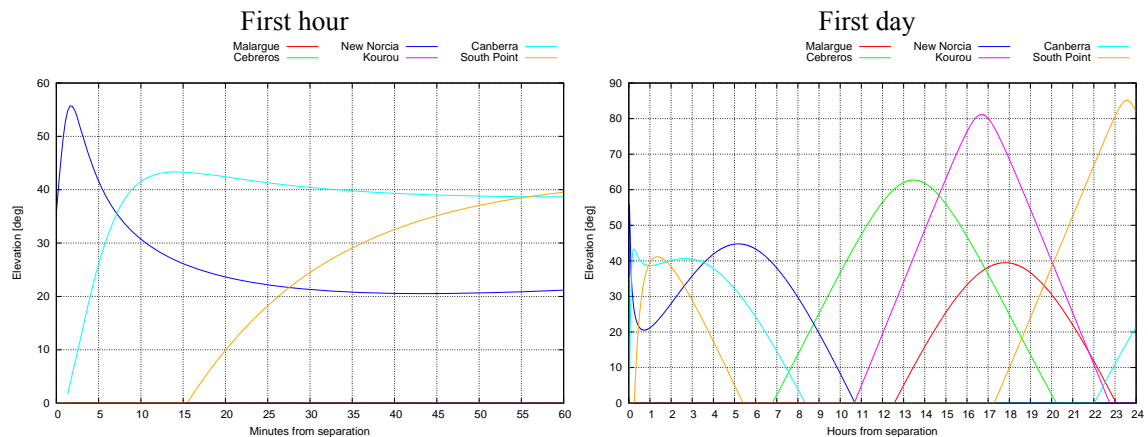


Figure 3-121 2019 February launch: elevation from ground stations



The geometry of Earth, S/C and Sun short after departure is presented in Figure 3-122 for both launch options, outwards and inwards from the Earth. The plot on the left shows the evolution for the first 5 hours after separation of the SSE and SES angles along with the Earth distance. The plot on the right shows the projection of the departure hyperbola on the Sun-Earth rotating frame relative to Earth (thus at the centre; Sun on the left, far out the plot scale).

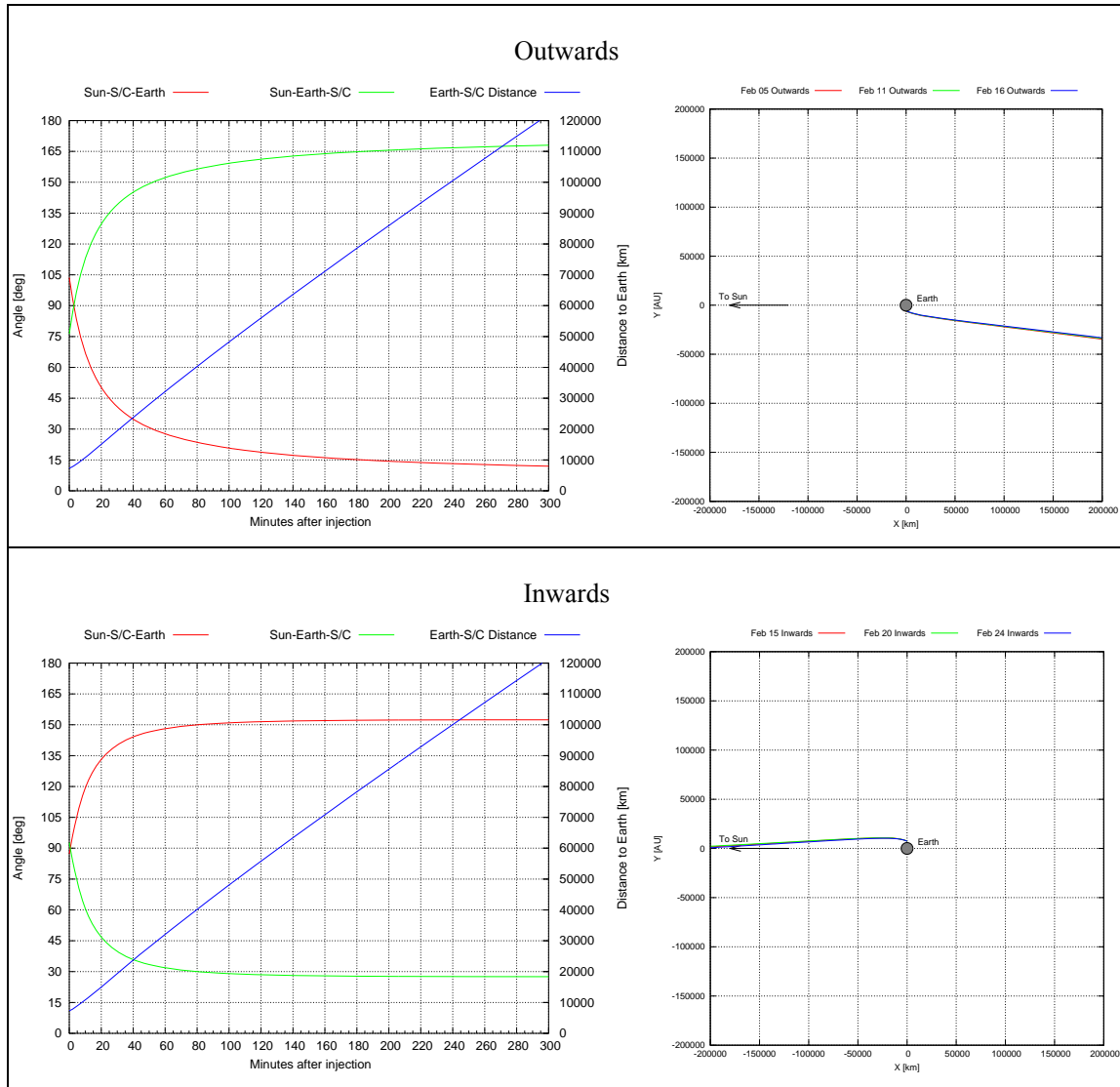


Figure 3-122 2019 February launch: Earth, Sun & S/C relative geometry at early LEOP.

The previous results are preliminary and based on ESOC assumptions of the separation conditions. Once a dedicated analysis by NASA/ULA is available, the LEOP analysis will be recomputed with exact separation conditions.



On the ejection of the METIS cap

For a description of METIS cap ejection details and constraints refer to Section 3.1.5 (page 52). Figure 3-123 shows the evolution of distances for a 2020 February launch. Solar Orbiter must start maintaining the Sun pointing attitude 38 days after launch, thus ejection in any direction is only possible for a period of 8 days. Latest possible ejection is 104 days after launch, still 219 before the first Venus GAM.

For 2019 launch the perihelion of the 1-year “parking orbit” after launch can be as low as 0.8 AU for the outwards option. Thus the METIS cap can be kept during the entire “parking orbit” and the ejection delayed after the first Earth GAM. In this case the same plot as below applies, just adding 1 year to the times from launch.

A detailed analysis of the METIS cap trajectory for the 2019/2020 launch opportunities needs to be carried out.

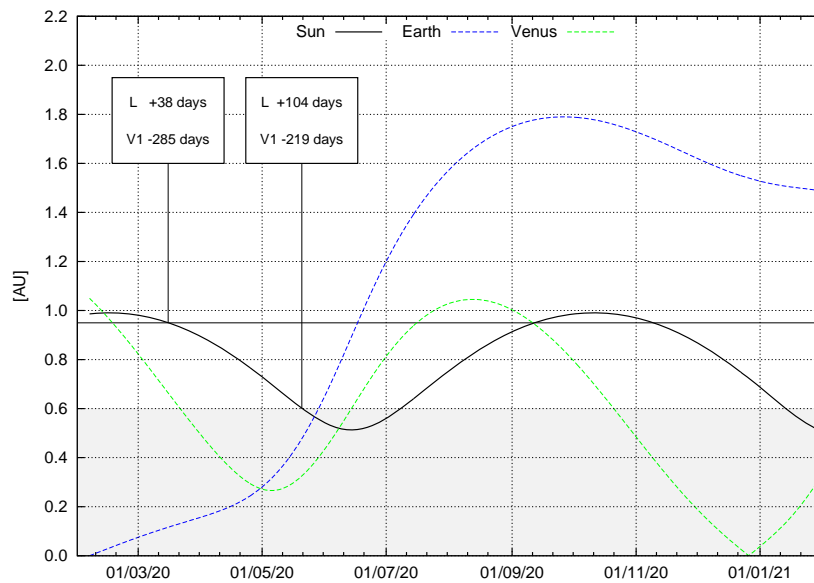


Figure 3-123 2020 February Launch: distances applicable to METIS cap ejection



3.5 *Summary*

As a recap of the trajectories presented in the previous sections, Figure 3-124 and Figure 3-125 show the evolution of perihelion radius and solar inclination over the mission, respectively.

Of the trajectories with 2018 launch, Option E is the only one that allows starting NMP and remote sensing observations below 0.35 AU in early 2021, almost 1 year before all other trajectory options. Option E and 2018 October get the perihelion below 0.3 AU at the same time, but 2018 October has only 1 perihelion pass whereas 2018 Option E maintains the perihelion below 0.3 AU for 7 consecutive orbits. Option D and the 2019/2020 February stay slightly above 0.3 AU in the Earth-Venus arc and are the last in reaching a perihelion below 0.3 AU, but it then maintains continuously the low perihelions during 12 orbits. The 2019/2020 February launch option reaches a perihelion below 0.35 AU in 2022 at the same time as the 2018 October and Option D, thus the short cruise phase allows it to recover from the launch delay with almost no penalty to start the science operations. Afterwards the 2019/2020 follows a very similar profile as 2018 Option D staying a bit closer to the Sun.

Regarding the solar inclination, each Venus GAM during the science phase produces an increase of typically 5 to 8 deg except when getting close to the final solar inclination, in which case the gain can be around 2-3 deg. All trajectory options initiate the science phase with a low solar inclination of 4-5 deg during the Earth-Venus arc. Option E has the advantage of starting earlier the inclination increase and is the first going beyond 30 deg already in 2026, just 7.5 years after launch. 2018 October recover part of the initial disadvantage with the 2 fast jumps using the 1:1 resonance, but still for the last inclination jumps is 1 Venus orbit (0.6 years) behind Option E. Due to the long stay in the 5:4 resonance, Option D provides a slower rate of inclination raise and achieves a >30 deg inclination 2 years after Option E. Launch in the 2019/2020 backups implies a penalty in the evolution of solar inclination as these trajectories follow the same profile as Option D, but the inclination at each step is lower. An inclination over 20 degrees is not reached until 2027 and like in Option D an inclination over 30 degrees is not reached until 2028. The highest solar inclination over 33 deg is not reached until the last 3:2 resonance in 2029.

In addition Figure 3-126 shows the evolution of the potential data return, on the left for the entire mission and on the right starting with NMP. These plots assume an 8-hour daily pass completely used for science data downlink. The actual bit rate based on the S/C-Earth distance as explained in Section 2.4 has been considered (max. bit rate 998 kb for SC-Earth < 0.45 AU, bit rate 202 kb at 1 AU). The effect of communication blackouts during solar conjunctions has also been included. However, the plots do not include any other operational constraint (i.e. actual visibility durations, ranging sessions preventing the data downlink,...) or consideration (i.e. additional ground station passes,...) to try to adjust the science data generation and storage rate with the downlink rate. This work is carried out by the Science Operations Centre in ESAC and the values provided here shall be understood as an indication only of how good the trajectory potentially is in terms of data downlink, but are not meant to be used for operational sizing. Any of the 2018 alternatives, Option E & D, and the 2019/2020 February backups outperform the 2018 October trajectory. Excluding the cruise phase, Option E begins performing better, but after 2025 is outperformed by any of Option D and the 2019/2020 February trajectories, all 3 with the same performance. The 1-year parking orbit close to Earth gives the 2019 February trajectory an advantage for the overall downlink, but during this period there will be no remote sensing measurements and the science relevance of the in-situ measurements will be limited as the spacecraft will stay close to 1 AU during this year. Otherwise Option E and D will have performed similarly by the end of mission, followed closely by the 2020 February backup.

Also of relevance for the spacecraft design is the accumulated level of Sun radiation seen along the mission. Since the radiation power density decreases with the inverse of the squared Sun distance, this magnitude has been integrated over the different trajectories and is shown in Figure 3-127. As a



reference, the 2017 January trajectory from the previous CReMA issue 3.1 (previous worst case) is also shown, together with the value accumulated at the end of this trajectory. Both 2018 Option E and 2020 February exceed this accumulated level by up to about 10% at end of mission, whereas 2018 Option D and 2019 February stay below this level.

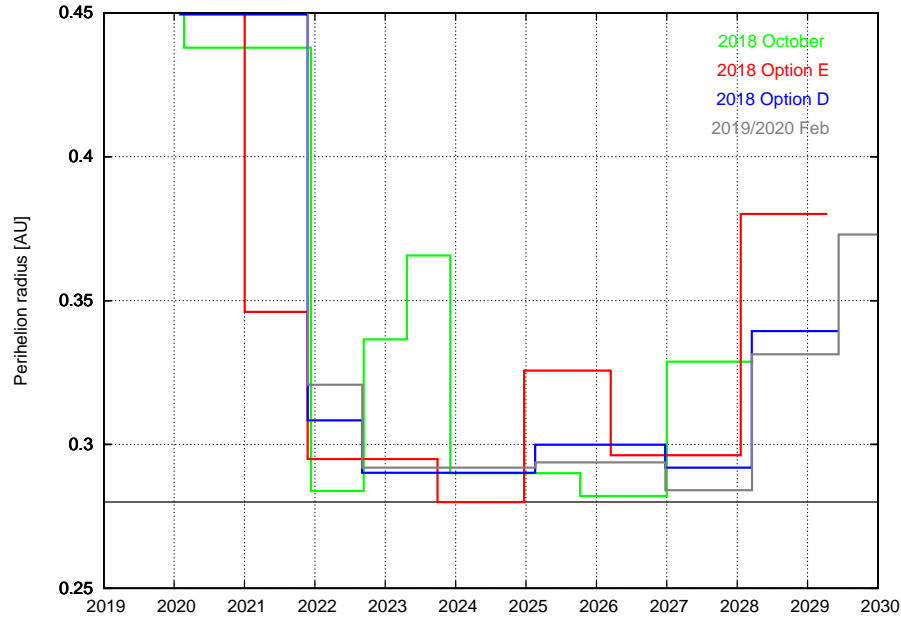


Figure 3-124 Evolution of perihelion radius

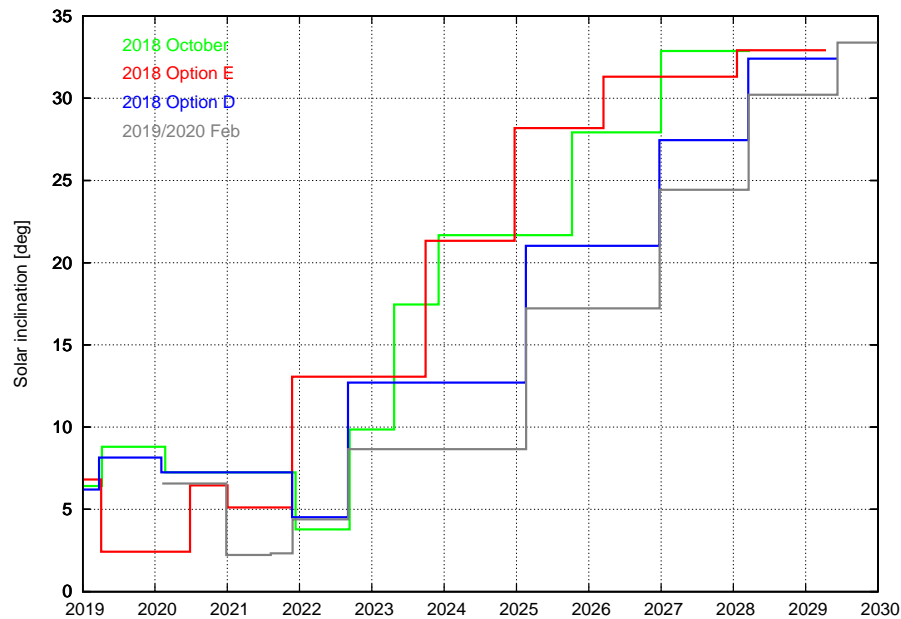


Figure 3-125 Evolution of solar inclination

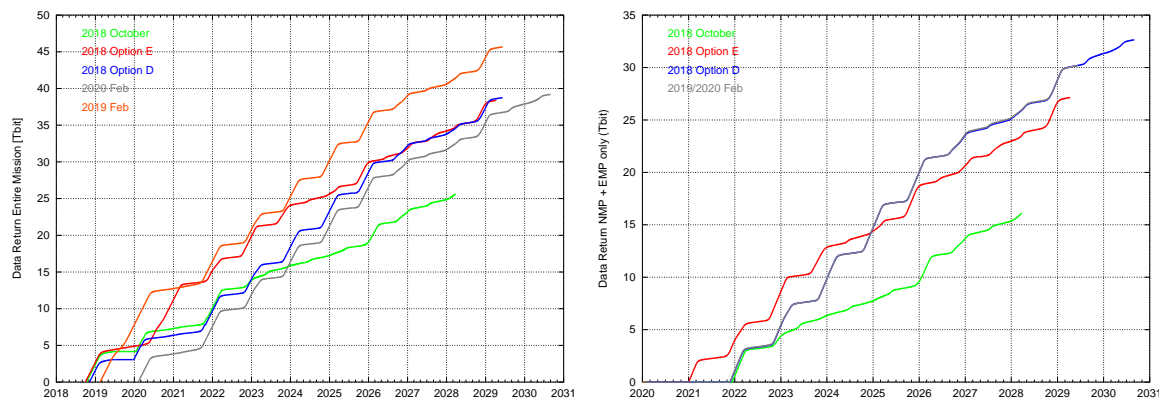


Figure 3-126 Evolution of potential science data return

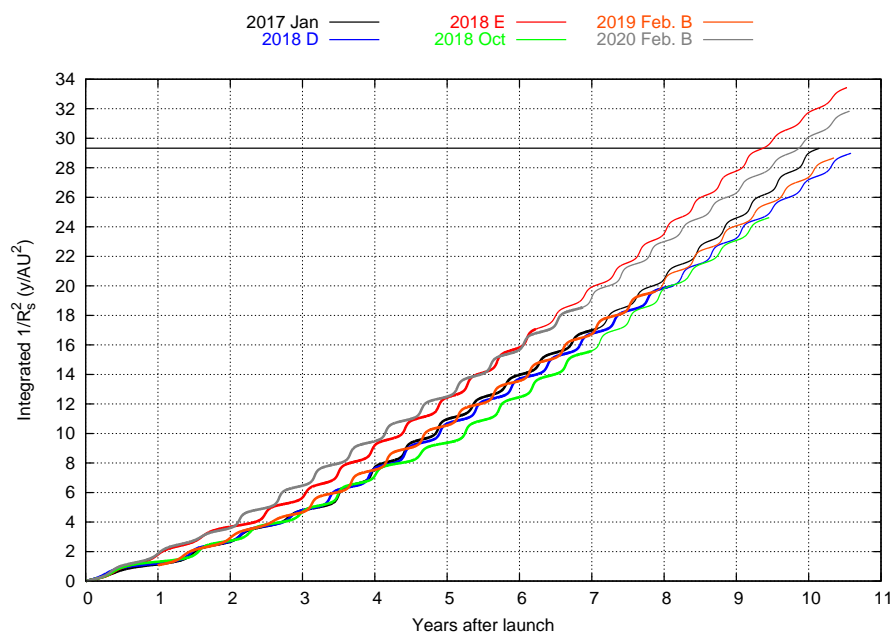


Figure 3-127 Evolution of integrated $(1/R_{\text{sun}})^2$



4 LAUNCH WINDOWS ANALYSIS

An analysis has been carried out to determine the duration and characteristics of the launch windows for each of the scenarios regarded for Solar Orbiter. This chapter contains relevant information about the launch vehicle and the launch event, and summarizes the results of the launch window analysis for all the regarded opportunities.

The computation of the launch window is based on constrained optimization of the trajectory for each launch day. The objective considered for this optimization process is the maximization of the final solar inclination after the last Venus GAM. The variables used are the dates of the Earth and Venus GAMs plus two direction angles of the relative outgoing velocity after the GAM per each resonant transfer. The minimum and maximum distances to the Sun allowed by the mission design are imposed as constraints in the trajectory optimization. The requirement of ballistic trajectories is also translated into constraints to neglect or minimize any intermediate deep space manoeuvre Delta-V.

The launch window computation process is initiated with the reference trajectory described in the previous section, which is feasible in terms of the constraints. The optimal parameters for the previous day are used as initial guess for the trajectory computation of the next day and so the solutions are extended by continuity to later launch dates. In a similar way the solutions are extended from the reference trajectory to earlier launch dates.

Although the variation of the optimization parameters provides a certain degree of flexibility in order to adjust the trajectory for a different launch day, it is in general not possible to fulfil the ballistic trajectory requirement indefinitely. Thus, after extending by continuity the solutions a given number of days the optimizer fails to obtain a ballistic trajectory and returns at least one non-zero Delta-V DSM in one of the trajectory arcs. By extending further such a solution the total Delta-V required for the trajectory experiences an increase. This behaviour can occur in any of the two directions in time: earlier or later launch dates and in the practice imposes a physical limit to the maximum extension of the launch window.

4.1 *Atlas V 411 Launch from KSC*

The baseline launch vehicle for the Solar Orbiter mission is a NASA provided Evolved Expendable Launch Vehicle (EELV). The NASA Solar Orbiter Project has awarded a contract for the procurement of an Atlas V launcher in its 411 version, which includes one additional strap-on booster to increase the launcher performance. A brief description of the launch with the Atlas V vehicle is provided next.

The launch with Atlas V 400 series consists of a booster first stage combined with zero to five Solid Rocket Boosters (SRB), a Centaur upper stage and the 4-m diameter payload fairing (PLF) protecting the satellite.

The ascent trajectory with Atlas V 400 series has two phases [8]:

- **Booster phase:** begins with the ignition of the RD-180 engine system followed by LV health checks before the booster release and SRB ignition, if applicable. After a short vertical rise away from the pad the LV pitches over to the prescribed ascent profile and direction and transitions to a nominal zero-alpha and zero-beta angle-of-attack orientation to minimize aerodynamic loads and engine angles.
A period with an alpha-bias angle-of-attack steering technique might follow to improve performance while maintaining aerodynamic loads within acceptable limits after which closed-loop guidance steering is enabled. SRB jettison is initiated after SRB burnout approximately 115 seconds after lift-off. Near the end of the booster phase, the RD-180 engine is



continuously throttled to maintain the axial acceleration below 5.0 g steady state level. The phase finally ends with booster engine cut-off (BECO) and booster shutdown. The Atlas V retains the PLF through the booster phase of flight.

- Centaur phase: the Atlas V Centaur can be configured as either a single or dual burn, whereas for Solar Orbiter the two burns with a 100-nm intermediate parking orbit will be used. The Centaur first burn Main Engine Start (MES1) occurs approximately 10 seconds after the Atlas booster is jettisoned and for a typical Atlas V 400 series mission the PLF is jettisoned 8 seconds after MES1, by which time the 3-sigma free molecular heat flux has fallen below 1,135 W/m² (worst case value).

After first burn Main Engine Cut-off (MECO1), the Centaur and SC enter a coast period. At a guidance calculated time the Centaur vehicle is aligned to the ignition attitude prior to the Centaur main engine re-ignition (MES2), which guides the vehicle to the desired orbit. After reaching the target orbit, the Centaur main engine is shut down (MECO2), and Centaur begins its alignment to the SC separation attitude.

After Centaur/SC separation, Centaur conducts a Collision and Contamination Avoidance Maneuver (CCAM) to prevent recontact and minimize contamination of the SC. A blowdown of remaining Centaur propellants follows after completion of the CCAM.

NASA & ULA have provided several batches of trajectory and performance information [9], [20], [26], [31] that confirm the feasibility of launching the Solar Orbiter spacecraft on an Atlas V 411.

The Atlas V launch vehicle has the capability to accommodate a finite launch slot for each launch day. Lift-off is possible at any moment within this slot and the guidance system of the vehicle is responsible to compensate the deviations with respect to the ascent trajectory at the optimal lift-off time. This implies a performance penalty in terms of injected mass with respect to instantaneous at the optimal lift-off time. The mass penalty for a 30-minute window as required by the Solar Orbiter mission has been characterised by NASA/KSC in [9] and the achieved performance is found compatible with the Solar Orbiter spacecraft mass. In addition, NASA & ULA have expressed their commitment to produce a flight program for each launch day within the launch period. This implies that for a given launch day the optimal escape conditions in terms of hyperbolic excess velocity and DLA will be provided by the launch vehicle and no correction will have to be performed by the spacecraft.

Currently the Atlas V 411 is assumed capable of launching the 1800-kg Solar Orbiter spacecraft up to a maximum infinite velocity of 5.64 km/s ($C3 = 31.8 \text{ km}^2/\text{s}^2$). This value takes into account the performance penalty for a 30-minute daily launch window and is valid for any DLA between -28.7 and 28.7 deg. For DLA values out of this interval, there will be a performance penalty that has to be analysed in a case basis.



4.2 2018 Option E Launch Window

The launch window analysis has been performed with the operational trajectory optimization software MANTRA. For every launch day a Solar Orbiter trajectory has been computed considering a high fidelity force model that includes all relevant orbit perturbations. The optimization process minimizes the size of the deterministic Delta-V manoeuvres under the condition that the 3:2 resonant orbits with the maximum possible solar inclination is reached after GAM-V8. The location of the deterministic Delta-V manoeuvres has been designed in agreement with the navigation analysis. The typical total Delta-V required for the entire trajectory is in the order of 5-6 m/s.

From the results of the computations, a 29-day feasible launch period has been identified from 22nd September to 20th October. Earlier launch days than 22nd September are unfeasible due to the appearance of a very long safe-mode blackout period over 100 days, which is not compatible with the spacecraft design in terms of autonomy. Later launch days than 20th October are not compatible with the Atlas V 411 launch performance.

Figure 4-1 shows the variation with the launch day of the infinite velocity at launch and the declination of the launch asymptote (DLA). The range considered in the figures show an extended period from 10th September to 25th October that includes the feasible launch window. The extended period is indicated with an orange shadow. The full-dynamics (MANTRA) results are given by the red crosses. Just for information the results of a simplified linked-conics launch window are shown as well with a green line. In general, both models are in good agreement.

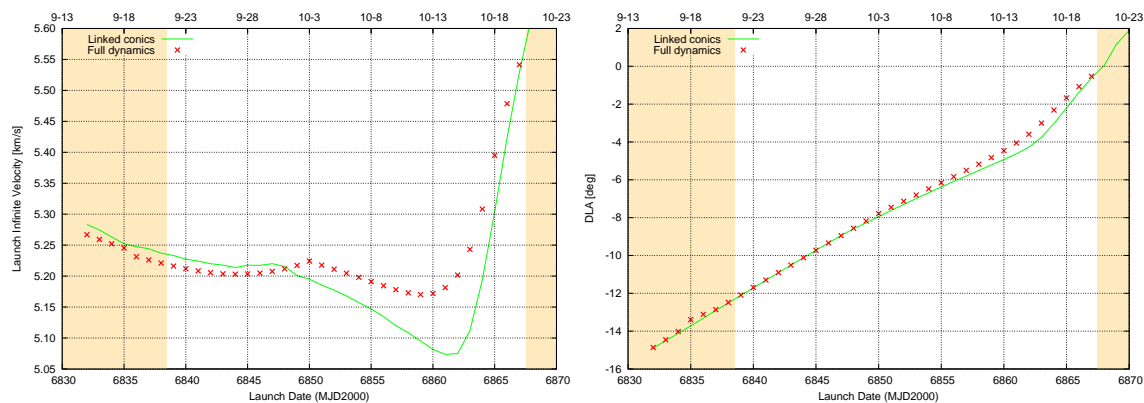


Figure 4-1 2018 Option E launch window: variation of launch infinite velocity and DLA

Figure 4-2 shows the final solar inclination reached at the end of mission, which grows from 32.4 deg at the launch window open to almost 34 deg at the launch window close.

Figure 4-3 shows the variation of the minimum and maximum distance to the Sun with the launch day. The minimum distance achieved at the perihelions after GAM-V5 has to be constrained at the minimum allowed value of 0.28 AU for most of the launch window. Only from 4th to 18th October the optimal trajectories require a slightly higher minimum Sun distance up to 0.2817 AU. The maximum distance to the Sun, reached at the aphelion between GAM-V3 and GAM-E1, grows steadily with the launch day reaching a highest value at the launch window close just below 1.15 AU.

Figure 4-4 provides the variation of the perihelion radius of each of the science orbits during NMP & EMP. Most of the perihelion radii remain almost constant across the launch period. Only the perihelion radius after GAM-E1 decreases constantly with the launch day.

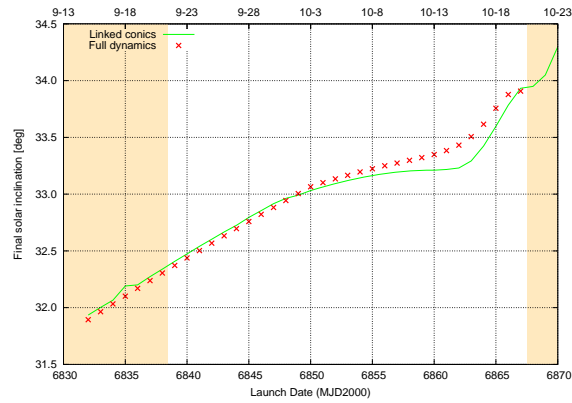


Figure 4-2 2018 Option E launch window: variation of Venus infinite velocity and final solar inclination

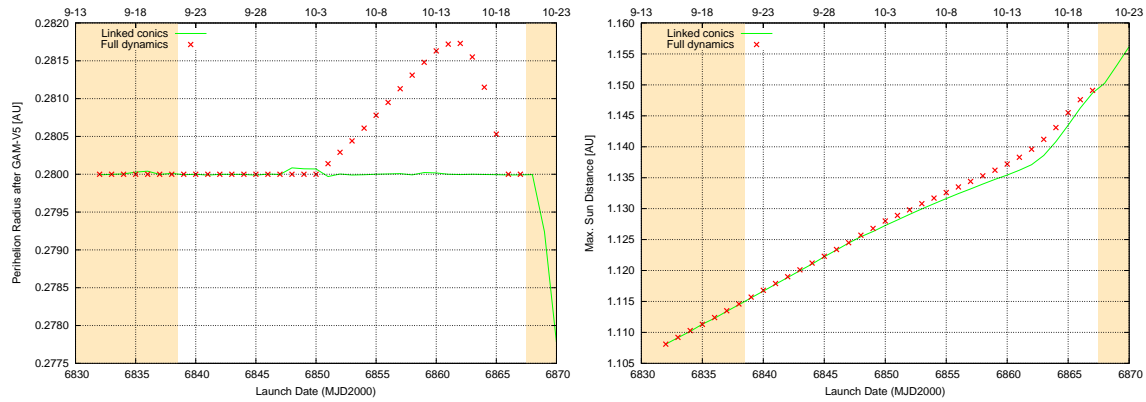


Figure 4-3 2018 Option E launch window: variation of minimum and maximum Sun distances.

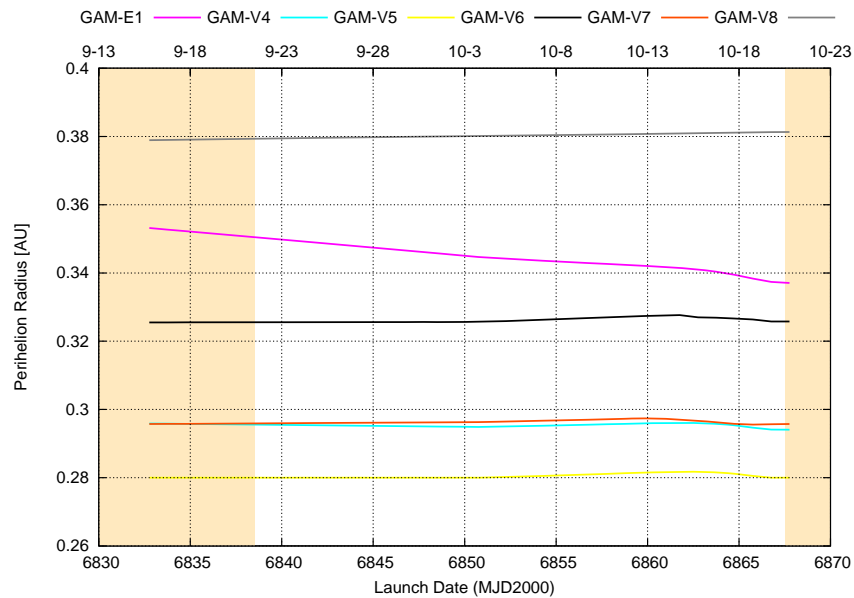


Figure 4-4 2018 Option E launch window: variation of perihelion radius of science orbits



Figure 4-5 shows the eclipse durations of all the GAMs as a function of the launch day (left), as well as the variation of the maximum eclipse encountered during the entire mission (right). Only the MANTRA high fidelity full-dynamics results are provided. The eclipse periods remain rather constant, with the exception of GAM-V3 which can reach up to about 19 minutes at the launch window open, but then gets shorter and even vanishes for later launch days. The longest eclipse at GAM-V4 does not exceed 20 min.

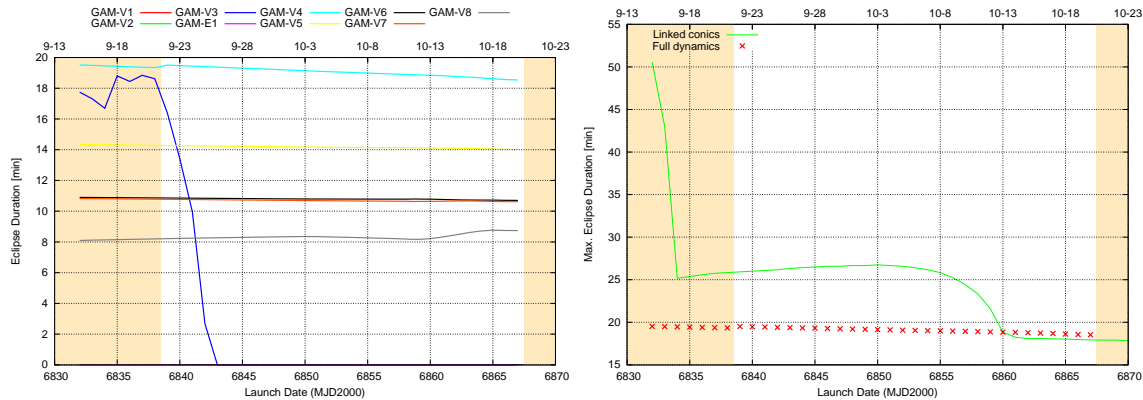


Figure 4-5 2018 Option E launch window: variation of eclipses duration and longest eclipse

Figure 4-6 shows the variation of the longest safe-mode blackout period (left; condition used: $SES < 5$ deg AND $SSE < 10$ deg) and the longest solar superior conjunction (right, condition used: $SES < 3$ deg). It can be seen that the longest safe-mode blackout period exceeds 120 days until 21st September. Such very long period would be encountered between March and June 2023, in the NMP between GAM-V4 and GAM-V5, and would pose a severe risk to the spacecraft in the case that a safe mode occurs. From September 22nd until October 20th the longest safe-mode blackout is within 40 and 65 days, compatible with the spacecraft design requirements. As per the figure to the right, the longest solar superior conjunction lasts between 20 and 37 days. This longest solar conjunction is encountered in the EMP around April 2027.

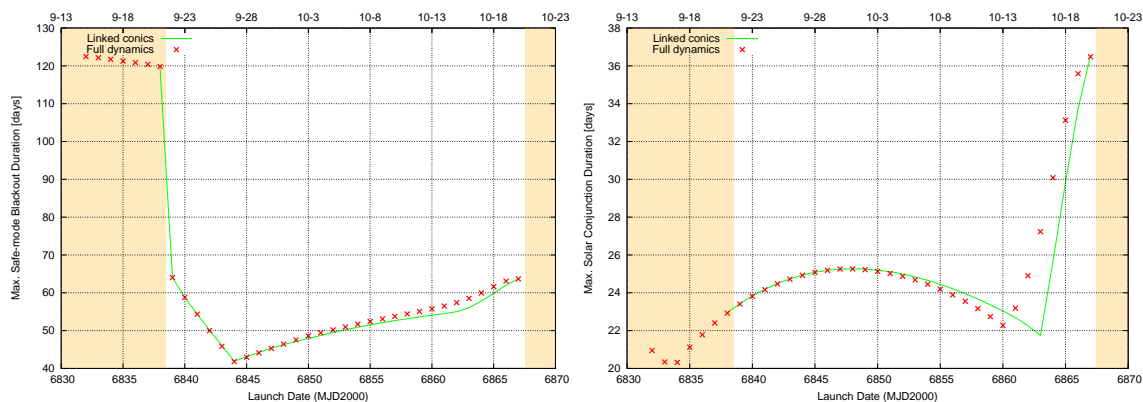


Figure 4-6 2018 Option E launch window: variation of longest safe-mod blackout and solar conjunction periods

Figure 4-7 shows the variation of the altitude at closest approach for all the GAMs for the MANTRA – full-dynamics results. The first 3 Venus GAMs have been designed at relatively large altitudes: GAM-V1 altitude varies between 13000 and 19000 km, GAM-V2 between 11000 and 14000 km and GAM-V3, the closest of all three, varies from 3500 to 10000 km. The rest of the GAMs, including GAM-E1,



require generally the maximum deflection achievable at the minimum altitude of 350 km, with the exception of GAM-V8 that rises up to about 900-1200 km.

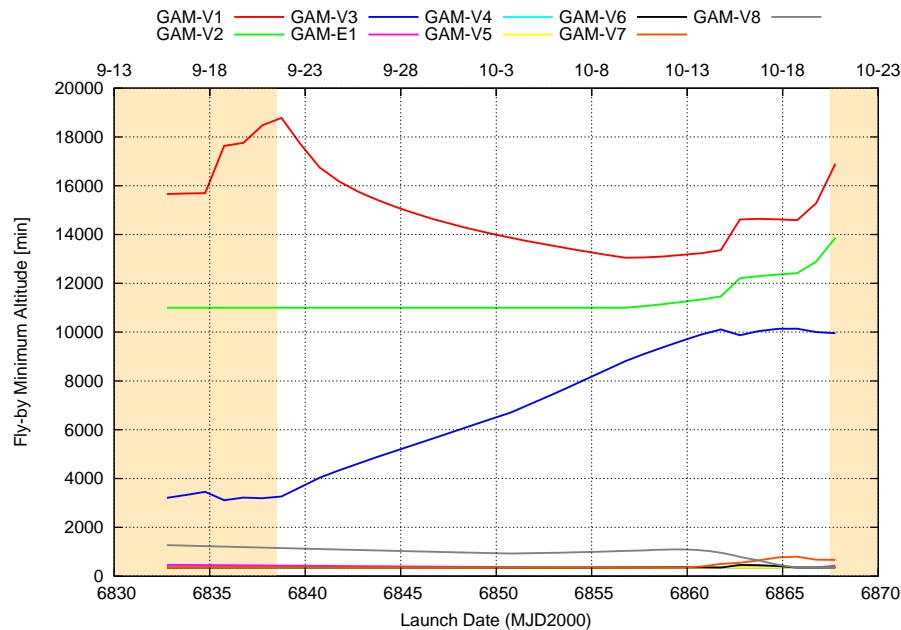


Figure 4-7 2018 Option E launch window: variation of minimum altitude at all GAMs

The blinding of star trackers during the LEOP has been analysed as a function of the launch day. For this analysis the star tracker configuration is assumed as given in Figure 3-32 [30], with both star trackers mounted in the $-X_{sc}$ panel and their bore sight canted 26 deg from the $-X_{sc}$ axis in the X_{sc} - Y_{sc} plane. The exclusion angles for the Earth and the Moon (measured from the limb, not from the center) are assumed constant and equal to 20 deg and 19 deg, respectively.

Two spacecraft attitudes have been regarded:

- Nominal attitude: $+X_{sc}$ axis points to the Sun and $+Y_{sc}$ axis is maintained in the orbital plane (with respect to the Sun) and the direction opposite to the heliocentric velocity vector.
- Alternative attitude: $+X_{sc}$ axis points to the Sun and $+Y_{sc}$ axis perpendicular to the heliocentric orbital plane (towards the celestial North).

The spacecraft trajectory has been propagated from the separation point for a period of 3 days and the geometry with respect to the Earth and Moon has been analysed. Figure 4-8 shows the evolution of the angle from the star tracker bore sight to the Earth and Moon limb for the launch days between September 22nd and October 19th. This angle is computed as the difference of angles between the angle Earth centre-S/C-star tracker bore sight and the half angle of the Earth as seen from the spacecraft (thus Earth centre-S/C-Earth limb angle). The corresponding angle difference is computed for the Moon. Because of the proximity to the Earth at separation, the Earth-S/C-limb angle can be large resulting in a negative angle. Star tracker blinding is assumed to start whenever the corresponding angle gets below the exclusion zone represented by the orange shadow. The nominal attitude is considered in these figures, whereas for the Earth the first 12 hours after separation are shown and for the Moon the first 3 days are shown (Moon orbit radius is crossed about 18.5 hours after launch). The star tracker will be initially blinded by Earth after separation for the first about 20 minutes. Blinding by the Moon is possible for launches earlier than September 29th and last hours.



Figure 4-9 show the corresponding analysis assuming the alternative spacecraft attitude with the +Ysc axis pointing towards the celestial North. Blinding by the Earth though shorter is not eliminated, while Moon blinding occurs only to the first 2 considered launch days, September 22nd and 23rd.

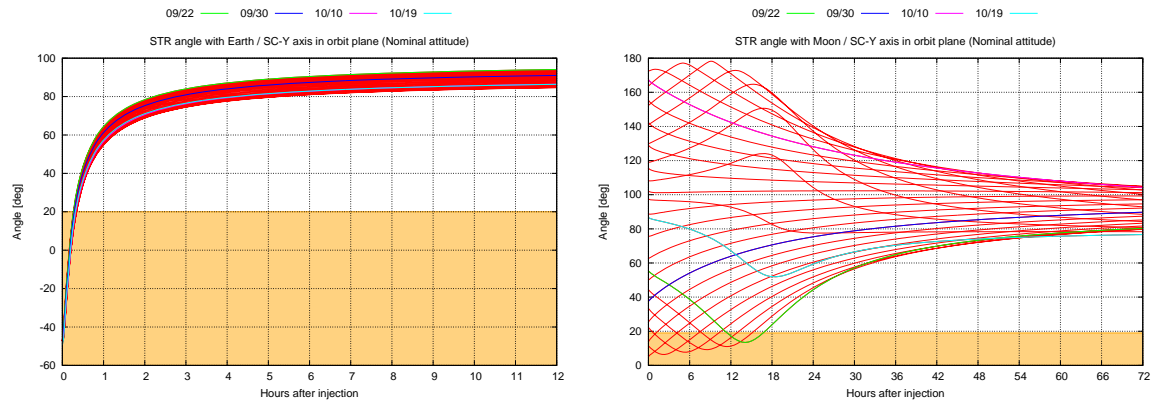


Figure 4-8 2018 Option E launch window: evolution of angles from Star Tracker bore sight to Earth and Moon limbs in the nominal attitude

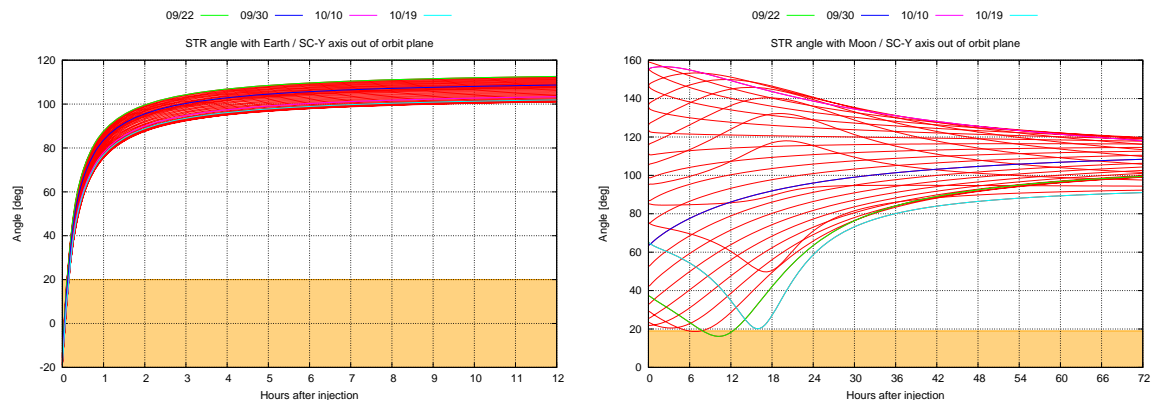


Figure 4-9 2018 Option E launch window: evolution of angles from Star Tracker bore sight to Earth and Moon limbs in the alternative attitude

Table 4-1 shows a summary of the star tracker blinding analysis as a function of the launch day. Separation always occurs under Earth blinding and so only the duration is given. Maximum duration is about 21 minutes in nominal attitude and below 10 minutes in the alternative attitude. Moon blinding can occur only for the first launch days. In the nominal attitude, the S/C is separated under Moon blinding for launches between September 26th and 28th and a later entry into Moon blinding occurs only for earlier launch days. The longest Moon blinding is 9.5 hours in the nominal attitude and 4.4 hours in the alternative attitude.

A follow on of this analysis will be to establish the range of roll angles around the spacecraft-Sun line for which the star tracker is not blinded for any launch day. From the current preliminary results, it appears possible to avoid the blinding by the Moon, but it will be hard to avoid the blinding by Earth early after separation.



	Nominal S/C attitude				Alternative S/C attitude			
	Earth Duration min	Moon Start h	Moon End h	Moon Duration h	Earth Duration min	Moon Start h	Moon End h	Moon Duration h
09-22	16.2	11.45	16.71	5.3	6.6	7.90	12.30	4.4
09-23	16.4	7.79	15.08	7.3	6.7	5.86	7.68	1.8
09-24	16.5	4.11	12.88	8.8	6.8			
09-25	16.7	0.73	10.24	9.5	6.9			
09-26	16.9	0	7.29	7.3	7.0			
09-27	17.0	0	4.17	4.2	7.1			
09-28	17.2	0	1.11	1.1	7.2			
09-29	17.4				7.3			
09-30	17.5				7.5			
10-01	17.7				7.6			
10-02	17.8				7.7			
10-03	18.0				7.8			
10-04	18.2				7.9			
10-05	18.5				8.0			
10-06	18.8				8.2			
10-07	19.0				8.4			
10-08	19.3				8.5			
10-09	19.6				8.7			
10-10	19.8				8.9			
10-11	20.1				9.0			
10-12	20.4				9.2			
10-13	20.6				9.3			
10-14	20.7				9.5			
10-15	20.8				9.6			
10-16	20.7				9.6			
10-17	20.3				9.5			
10-18	19.8				9.4			
10-19	19.3				9.2			

Table 4-1 2018 Option E launch window: Star tracker blinding events during LEOP

4.2.1 LAUNCH TARGETS

This section provides the launch conditions in terms of the modulus and declination of the infinite velocity that the launcher must provide for each launch day. ESOC has also performed an estimation of the separation time that is based on assumptions for the inclination, perigee radius, longitude of the ascending node of the escape hyperbola and the true anomaly at separation. The actual lift-off and separation times will be defined by ULA.

The process to obtain these launch targets has involved a refinement of targets and separation times in a double iteration with the MANTRA trajectory software in order to obtain a good accuracy and eliminate interpolation/extrapolation errors. Thus MANTRA was used to validate the final targets in a full dynamics model (all relevant perturbations included) such that there is no need for a Delta-V manoeuvre after separation to connect exactly with the desired heliocentric trajectory.

Table 4-2 show the launch targets and the solar inclination reached at the last 3:2 science orbit. DLA and RLA are expressed in the ICRF/EME2000 frame.



Date 2018 mm-dd	Separation (UTC)	V_{∞} (km/s)	DLA ¹ (deg)	RLA (deg)	Final i_s (deg)
09-22	10:20:53	5.218	-12.20	304.86	32.37
09-23	10:15:51	5.213	-11.81	305.40	32.44
09-24	10:10:46	5.207	-11.42	305.91	32.50
09-25	10:05:42	5.205	-11.02	306.43	32.57
09-26	10:00:36	5.201	-10.64	306.92	32.63
09-27	09:55:33	5.200	-10.25	307.42	32.70
09-28	09:50:31	5.200	-9.86	307.92	32.76
09-29	09:45:30	5.201	-9.47	308.42	32.82
09-30	09:40:32	5.203	-9.08	308.92	32.88
10-01	09:35:37	5.207	-8.70	309.42	32.94
10-02	09:30:44	5.212	-8.31	309.94	33.01
10-03	09:25:55	5.218	-7.92	310.46	33.07
10-04	09:21:04	5.217	-7.57	310.91	33.10
10-05	09:16:12	5.210	-7.24	311.30	33.14
10-06	09:11:22	5.204	-6.92	311.69	33.17
10-07	09:06:32	5.197	-6.59	312.08	33.20
10-08	09:01:44	5.191	-6.27	312.47	33.22
10-09	08:56:57	5.184	-5.95	312.87	33.25
10-10	08:52:10	5.178	-5.62	313.27	33.27
10-11	08:47:25	5.172	-5.29	313.68	33.30
10-12	08:42:42	5.170	-4.94	314.13	33.32
10-13	08:38:00	5.169	-4.59	314.59	33.35
10-14	08:33:27	5.178	-4.19	315.18	33.38
10-15	08:28:58	5.194	-3.75	315.86	33.43
10-16	08:24:40	5.230	-3.20	316.77	33.51
10-17	08:20:17	5.282	-2.55	317.85	33.62
10-18	08:16:46	5.362	-1.87	319.20	33.76
10-19	08:14:23	5.455	-1.25	320.73	33.88
10-20	08:11:17	5.507	-0.76	321.83	33.91

Table 4-2 2018 Option E launch window: Launch Targets

4.3 2018 Option D Launch Window

The full launch window analysis for the 2018 Option D trajectory is reported in [25]. This analysis has been performed using the linked conics model.

For the launch window analysis the perihelion of the 5:4 resonant orbit after GAM-V2 is fixed at 0.29 AU, the same value used for the trajectory described in Section 3.2.1 (see Table 3-11). A lower perihelion would penalize the solar inclination at the end of mission.

The following figures provide the variation of several relevant parameters with the launch day. Feasible trajectories can be found for a long period extending from end of August to early November. The results are shown for launch days starting mid-September, although schedule constraints will make very difficult to meet launch days before September 30th. The last launch day compatible with the Atlas V 411 performance is October 7th.

In general all the trajectory parameters have smooth variations. The maximum Sun distance presents the peak value of 1.4485 AU around October 18th. Eclipse duration at GAM-V1 increases with the launch day getting slightly above 30 min for launches later than November 4th.

¹ DLA and RLA are in the ICRF/EME2000 reference frame

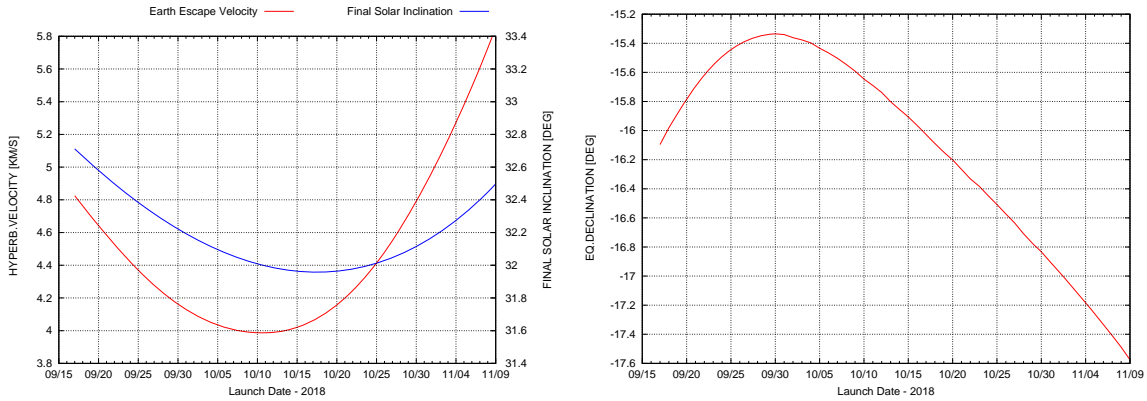


Figure 4-10 2018 Option D launch window: Launch targets and solar inclination

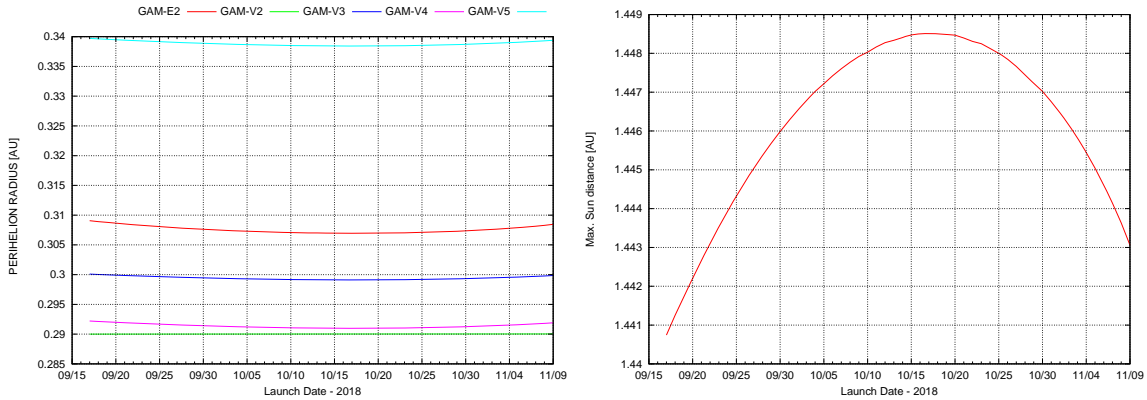


Figure 4-11 2018 Option D launch window: Perihelion of science orbits and maximum Sun distance

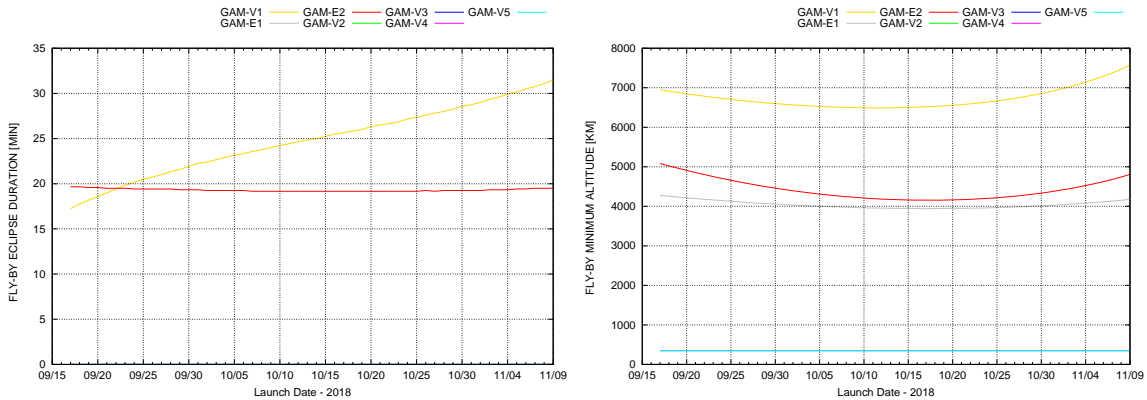


Figure 4-12 2018 Option D launch window: GAM eclipse duration and minimum altitude

The blinding of star trackers during the first 3 days of LEOP after separation has been analysed as a function of the launch day as in Section 4.2 (page 130), assuming two orientations of the spacecraft: Nominal (+Xsc Sun pointing and +Ysc in the orbital plane and opposite to heliocentric velocity) and Alternative (+Xsc axis points to the Sun and +Ysc axis perpendicular to the heliocentric orbital plane).



Figure 4-13 shows the evolution of the angle from the star tracker bore sight to the Earth and Moon limb for the regarded launch days between October 9th and November 7th for the nominal attitude. The star tracker is always blinded by the Earth at separation. For October 9th the blinding with Earth lasts 52 minutes. The blinding duration increases for later launch days, becoming very long, as seen in the figure. For launches after November 2nd the star tracker stays blinded by Earth for the whole 3 days of this simulation. Blinding by the Moon (Moon orbit radius crossed about 18.5 hours after launch) occurs for launch days in the middle of the considered period and can last up to 1.5 days.

Figure 4-14 shows the corresponding analysis assuming the alternative spacecraft attitude. This attitude permits to reduce both blindings. The Earth blinding after separation is limited to about 40 minutes and the Moon blinding occurs for less number of launch days and up to a maximum duration of 7.6 hours.

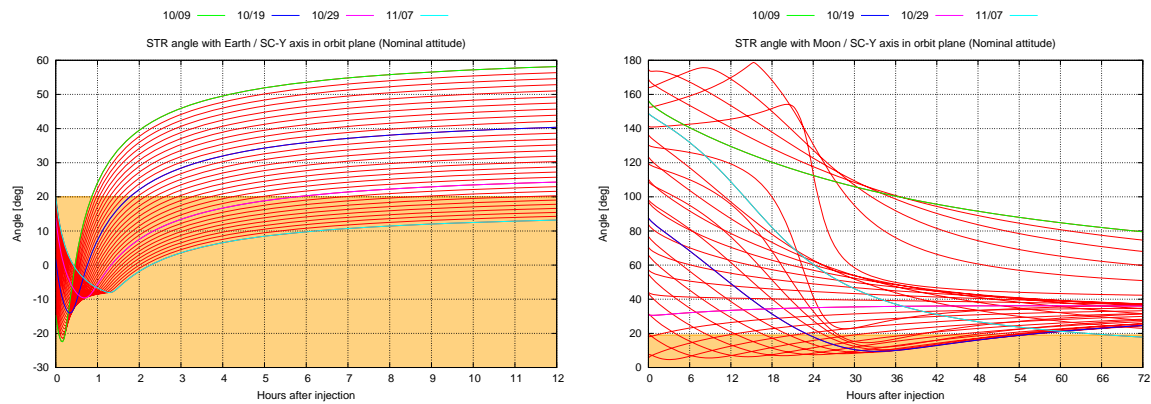


Figure 4-13 2018 Option D launch window: evolution of angles from Star Tracker bore sight to Earth and Moon limbs in the nominal attitude

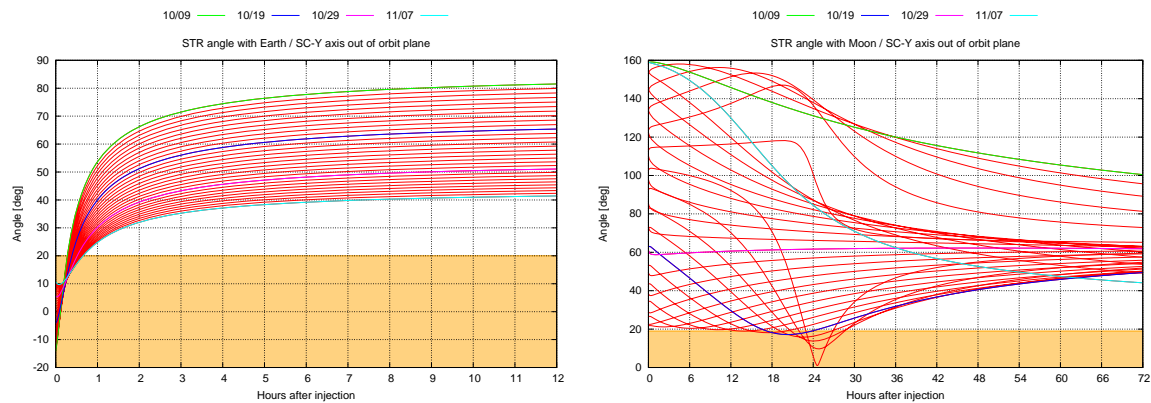


Figure 4-14 2018 Option D launch window: evolution of angles from Star Tracker bore sight to Earth and Moon limbs in the alternative attitude



Table 4-3 shows a summary of the star tracker blinding analysis as a function of the launch day.

	Nominal S/C attitude				Alternative S/C attitude			
	Earth Duration min	Moon Start h	Moon End h	Moon Duration h	Earth Duration min	Moon Start h	Moon End h	Moon Duration h
10-09	51.7				16.7			
10-10	55.0				17.3			
10-11	58.6				17.9			
10-12	62.5				18.5			
10-13	67.0				19.1			
10-14	71.9				19.8			
10-15	77.3				20.4	22.93	26.88	3.9
10-16	83.4	27.72	38.91	11.2	21.1	21.93	28.60	6.7
10-17	90.3	27.07	46.90	19.8	21.8	20.76	28.33	7.6
10-18	98.0	25.65	51.96	26.3	22.5	19.18	26.66	7.5
10-19	106.7	23.42	54.40	31.0	23.2	17.22	23.82	6.6
10-20	116.6	20.49	54.51	34.0	23.9	15.04	19.95	4.9
10-21	128.1	16.97	52.67	35.7	24.6	13.44	14.50	1.1
10-22	141.3	12.99	49.07	36.1	25.4			
10-23	156.4	8.70	43.88	35.2	26.1			
10-24	174.4	4.30	37.43	33.1	26.9			
10-25	195.6	0.23	29.79	29.6	27.7			
10-26	221.6	0	21.14	21.1	28.4			
10-27	252.9	0	11.52	11.5	29.3			
10-28	293.5	0	1.10	1.1	30.1			
10-29	345.2				30.9			
10-30	412.5				31.7			
10-31	511.6				32.6			
11-01	666.4				33.5			
11-02	959.6				34.4			
11-03	4320.0				35.3			
11-04	4320.0				36.3			
11-05	4320.0				37.3			
11-06	4320.0				38.3			
11-07	4320.0	67.23	72.00	4.8	39.4			

Table 4-3 2018 Option D launch window: Star tracker blinding events during LEOP

4.3.1 LAUNCH TARGETS

The next table shows the launch targets together with the separation time as estimated by ESOC and the achieved solar inclination at the end of mission. The presented launch period starts on October 8th and extends for 33 days until November 9th. The last day compatible with the Atlas V 411 performance is November 7th. Therefore the last 2 launch days (grey font colour) are not feasible and are only included for information to indicate how fast the infinite velocity increases in this region. Note that DLA and RLA targets are in ICRF/EME2000.

The trajectories for the launch targets presented hereafter have been computed with the MANTRA software including a full-dynamics model. An iteration process has been performed in order to match departure infinite velocity vector and separation time. Refinement of these launch targets might still be needed after cross-check/iteration with ULA.



Date 2018 (dd/mm)	Separation UTC	Vinf (km/s)	DLA ICRF (deg)	RLA ICRF (deg)	Final is (deg)
08/10	08:39:33	4.008	-15.40	288.26	32.04
09/10	08:32:53	4.001	-15.44	287.49	32.02
10/10	08:26:11	3.996	-15.48	286.70	32.01
11/10	08:19:27	3.994	-15.52	285.90	32.00
12/10	08:12:42	3.996	-15.55	285.10	31.98
13/10	08:05:49	4.003	-15.56	284.35	31.98
14/10	07:55:44	4.015	-15.17	283.68	31.97
15/10	07:48:10	4.012	-15.54	281.94	31.96
16/10	07:43:28	4.034	-15.75	281.25	31.96
17/10	07:37:02	4.057	-15.83	280.43	31.96
18/10	07:30:18	4.083	-15.90	279.57	31.96
19/10	07:23:31	4.114	-15.96	278.71	31.96
20/10	07:16:44	4.150	-16.03	277.84	31.96
21/10	07:09:59	4.191	-16.09	276.98	31.97
22/10	07:03:19	4.236	-16.16	276.14	31.98
23/10	06:56:43	4.287	-16.22	275.32	31.99
24/10	06:50:15	4.343	-16.29	274.53	32.00
25/10	06:43:54	4.403	-16.35	273.77	32.01
26/10	06:37:42	4.469	-16.41	273.05	32.03
27/10	06:31:40	4.540	-16.48	272.36	32.05
28/10	06:25:48	4.616	-16.55	271.71	32.07
29/10	06:20:07	4.696	-16.62	271.11	32.09
30/10	06:14:37	4.781	-16.69	270.55	32.11
31/10	06:09:17	4.869	-16.76	270.03	32.14
01/11	06:04:06	4.962	-16.83	269.54	32.17
02/11	05:59:06	5.059	-16.90	269.10	32.20
03/11	05:54:15	5.159	-16.98	268.69	32.24
04/11	05:49:32	5.263	-17.05	268.31	32.27
05/11	05:44:56	5.371	-17.13	267.96	32.31
06/11	05:40:29	5.483	-17.20	267.64	32.35
07/11	05:36:09	5.598	-17.27	267.37	32.40
08/11	05:31:58	5.718	-17.35	267.13	32.45
09/11	05:27:57	5.844	-17.40	266.97	32.50

Table 4-4 2018 Option D launch window: Launch targets

4.4 2018 October Launch Window

This section provides details of the variation of main trajectory parameters as a function of the launch day. The main results are given in Figure 4-15 to Figure 4-18. The Earth escape velocity and the final solar inclination decrease initially with the launch day, but then increase again in the second half of the window. Based on the Atlas V 411 performance launch is feasible from October 1st to November 17th, a period of 48 consecutive days. This period is presented in the figures.

The maximum distance to the Sun reaches its maximum of 1.475 AU at about November 1st. The longest eclipse occurs at GAM V1 and its duration increases slowly with the launch day, but stays in any case below 32 minutes.

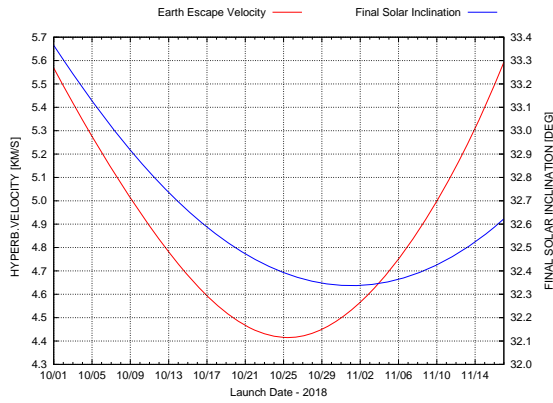


Figure 4-15 2018 October launch window: variation of launch infinite velocity

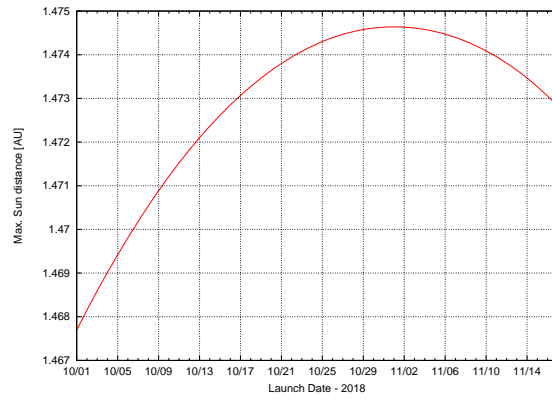


Figure 4-16 2018 October launch window: variation of maximum Sun distance

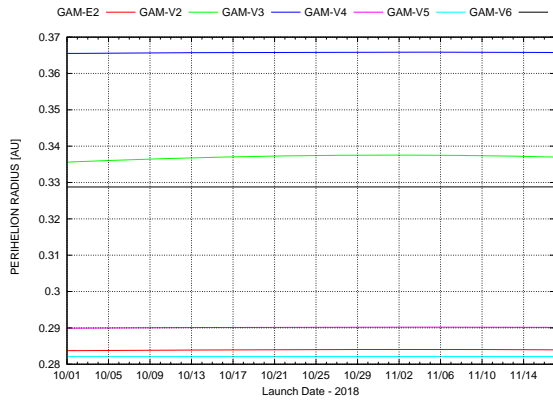


Figure 4-17 2018 October launch window: variation of perihelion radius and GAM fly-by altitude

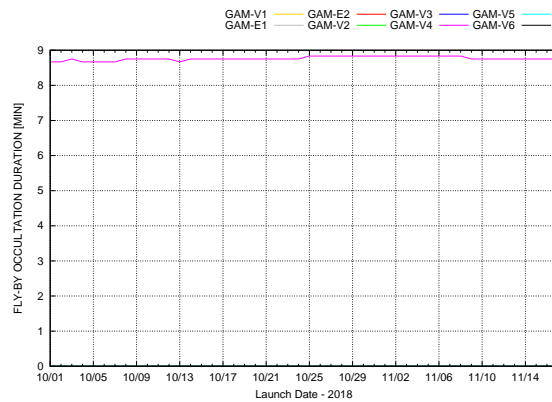
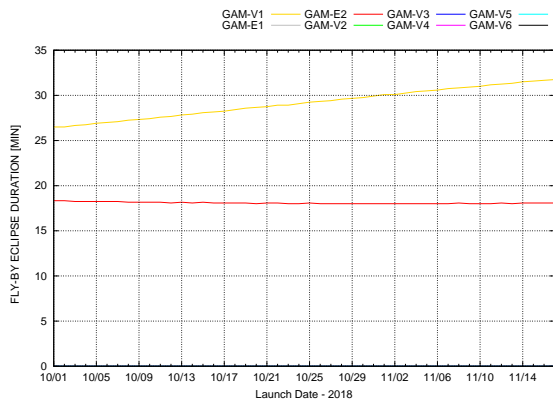
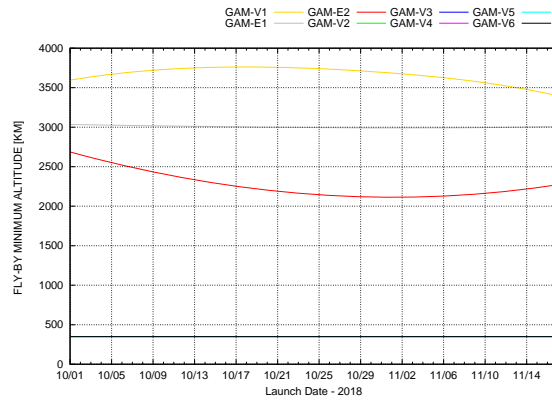


Figure 4-18 2018 October launch window: variation of GAM eclipses and occultations



The blinding of star trackers during the LEOP has been analysed as a function of the launch day. The analysis has been performed with the same assumptions as in Section 4.2 (page 130).

Figure 4-19 shows the evolution during LEOP of the angle from the star tracker bore sight to the Earth and Moon limb for the launch days between October 1st and November 17th. The star tracker will be initially blinded by Earth after separation for a period that grows with the launch day and can reach several hours at the end of the launch period. Blinding by the Moon is possible for launches earlier than September 29th and last hours. Blinding by the Moon is possible around two periods of the analysed launch window at about the middle and the end.

Figure 4-20 show the corresponding analysis assuming the alternative spacecraft attitude with the +Ysc axis pointing towards the celestial North. The star tracker will be initially blinded by Earth after separation up to 46 minutes. The Moon can produce blindings around the middle and the end of the launch period.

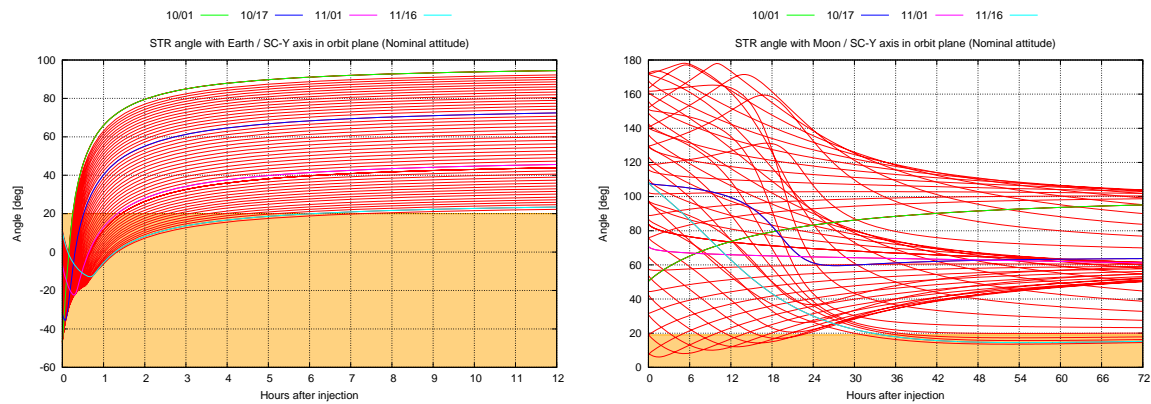


Figure 4-19 2018 October launch window: evolution of angles from Star Tracker bore sight to Earth and Moon limbs in the nominal attitude

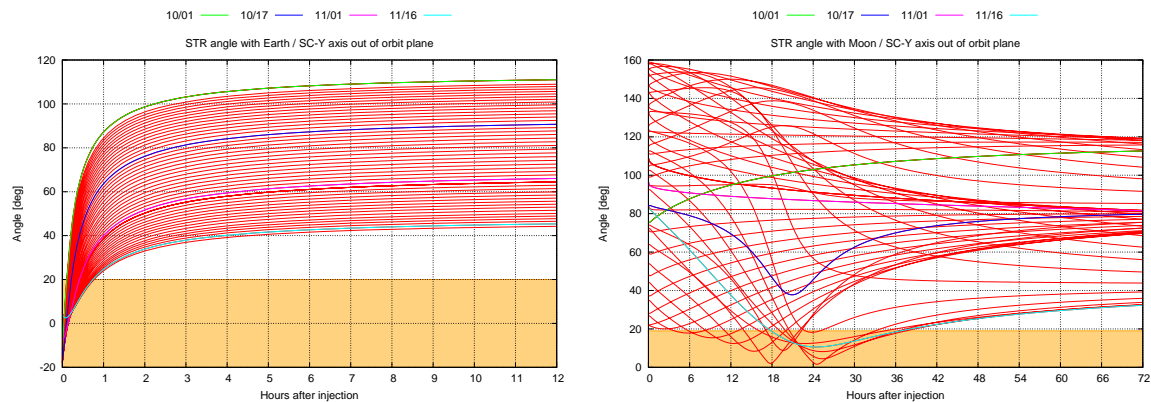


Figure 4-20 2018 October launch window: evolution of angles from Star Tracker bore sight to Earth and Moon limbs in the alternative attitude

Table 4-5 shows a summary of the star tracker blinding analysis as a function of the launch day. Separation always occurs under Earth blinding and it can last up to 7.3 hours in the nominal attitude and 46 minutes in the alternative attitude. Moon blinding can occur only at specific launch days and can have long durations even in the order of days.



	Nominal S/C attitude				Alternative S/C attitude			
	Earth	Moon	Moon	Moon	Earth	Moon	Moon	Moon
	Duration min	Start h	End h	Duration h	Duration min	Start h	End h	Duration h
10-01	15.3				6.4			
10-02	15.3				6.4			
10-03	16.5				7.0			
10-04	17.2				7.3			
10-05	17.9				7.6			
10-06	18.6				8.0			
10-07	19.4				8.3			
10-08	20.2				8.7			
10-09	21.2				9.1			
10-10	22.1				9.5			
10-11	23.1				9.9			
10-12	24.2				10.4			
10-13	25.4				10.9			
10-14	26.6				11.4			
10-15	27.9				11.9			
10-16	29.4				12.4			
10-17	31.2				13.1			
10-18	32.9				13.7	17.15	22.28	5.1
10-19	34.8				14.3	13.94	21.95	8.0
10-20	36.8				14.9	11.12	19.99	8.9
10-21	38.9	15.98	22.32	6.3	15.6	8.40	16.93	8.5
10-22	41.3	11.59	21.83	10.2	16.3	5.85	12.96	7.1
10-23	43.9	7.41	19.98	12.6	17.0	3.78	8.03	4.3
10-24	46.7	3.37	17.16	13.8	17.8			
10-25	49.7	0.00	13.57	13.6	18.6			
10-26	53.0	0.00	9.35	9.3	19.4			
10-27	56.6	0.00	4.68	4.7	20.2			
10-28	60.6	0.00	0.02	0.0	21.1			
10-29	64.8				22.0			
10-30	69.5				23.0			
10-31	74.5				23.9			
11-01	80.0				24.9			
11-02	86.1				25.9			
11-03	92.8				27.0			
11-04	100.2				28.0			
11-05	108.4				29.2			
11-06	117.5				30.3			
11-07	127.8				31.5			
11-08	139.4				32.7			
11-09	152.5				34.0			
11-10	167.2				35.3			
11-11	184.4				36.9			
11-12	210.4				38.6	22.85	24.98	2.1
11-13	237.3				39.9	20.56	33.04	12.5
11-14	269.3	38.88	72.00	33.1	41.4	19.98	36.46	16.5
11-15	310.1	36.28	72.00	35.7	42.9	19.13	37.53	18.4
11-16	363.2	34.05	72.00	37.9	44.6	17.85	36.75	18.9
11-17	435.9	31.24	72.00	40.8	46.3	16.14	34.43	18.3

Table 4-5 2018 October launch window: Star tracker blinding events during LEOP

4.4.1 LAUNCH TARGETS

Table 4-6 shows the launch targets in terms of the escape velocity, DLA and RLA (in ICRF/EME2000) for the 48-day period, October 1st to November 17th, in which launching with an Atlas V 411 is feasible. In addition to the launch targets the separation time estimated by ESOC is provided. The computation of the separation time requires several assumptions of the departure hyperbola (perigee altitude, longitude of the ascending node and true anomaly at separation). These assumptions might be revisited once more data about the actual ascent trajectories is available from the launcher authority.



The launch targets are based on trajectory computations with a full dynamics model that includes the relevant third body and solar radiation pressure perturbations as in [23]. These high fidelity trajectories require small deterministic manoeuvres for the adjustment of some of the GAMs that are individually up to 4 m/s and require overall from 7 to 9 m/s for the entire trajectory. Such small manoeuvres are covered within the navigation Delta-V allocation.

Date 2018 mm-dd	Separation UTC	V_{∞} (km/s)	DLA ¹ ICRF (deg)	RLA ICRF (deg)	Final i_s (deg)
10-01	09:37:40	5.561	-7.30	-47.37	33.36
10-02	09:32:24	5.495	-7.15	-47.42	33.31
10-03	09:26:57	5.415	-7.06	-47.63	33.24
10-04	09:21:35	5.345	-6.96	-47.80	33.18
10-05	09:16:08	5.276	-6.87	-48.01	33.13
10-06	09:10:41	5.210	-6.79	-48.24	33.07
10-07	09:05:07	5.144	-6.71	-48.50	33.02
10-08	08:59:35	5.081	-6.65	-48.79	32.97
10-09	08:53:53	5.019	-6.59	-49.12	32.92
10-10	08:48:11	4.958	-6.55	-49.49	32.87
10-11	08:42:24	4.900	-6.51	-49.88	32.82
10-12	08:36:34	4.844	-6.49	-50.32	32.78
10-13	08:30:37	4.790	-6.47	-50.79	32.73
10-14	08:24:27	4.739	-6.45	-51.31	32.69
10-15	08:18:05	4.691	-6.41	-51.85	32.66
10-16	08:10:39	4.645	-6.29	-52.50	32.62
10-17	08:03:54	4.598	-6.38	-53.38	32.59
10-18	07:58:42	4.560	-6.57	-54.06	32.55
10-19	07:52:51	4.526	-6.68	-54.75	32.52
10-20	07:46:41	4.496	-6.78	-55.50	32.50
10-21	07:40:18	4.470	-6.87	-56.29	32.47
10-22	07:33:56	4.449	-6.98	-57.11	32.45
10-23	07:27:34	4.433	-7.10	-57.95	32.43
10-24	07:21:10	4.422	-7.23	-58.82	32.41
10-25	07:14:48	4.417	-7.37	-59.70	32.39
10-26	07:08:28	4.416	-7.52	-60.59	32.38
10-27	07:02:13	4.421	-7.68	-61.48	32.36
10-28	06:55:58	4.432	-7.84	-62.37	32.35
10-29	06:49:55	4.448	-8.02	-63.25	32.35
10-30	06:43:52	4.469	-8.19	-64.11	32.34
10-31	06:37:57	4.496	-8.37	-64.96	32.34
11-01	06:32:09	4.527	-8.55	-65.78	32.34
11-02	06:26:25	4.562	-8.73	-66.58	32.34
11-03	06:20:50	4.602	-8.91	-67.35	32.34
11-04	06:15:19	4.646	-9.09	-68.10	32.34
11-05	06:09:56	4.694	-9.27	-68.82	32.35
11-06	06:04:37	4.746	-9.44	-69.50	32.36
11-07	05:59:22	4.802	-9.61	-70.17	32.37
11-08	05:54:16	4.862	-9.78	-70.80	32.39
11-09	05:49:08	4.926	-9.93	-71.40	32.40
11-10	05:43:51	4.994	-10.04	-71.96	32.42
11-11	05:37:22	5.065	-10.03	-72.58	32.44
11-12	05:32:24	5.137	-10.29	-73.36	32.47
11-13	05:28:43	5.219	-10.56	-73.84	32.49
11-14	05:24:26	5.304	-10.74	-74.29	32.52
11-15	05:20:00	5.395	-10.90	-74.74	32.55
11-16	05:15:37	5.489	-11.05	-75.16	32.58
11-17	05:11:13	5.588	-11.19	-75.56	32.62

Table 4-6 2018 October launch window: Launch targets

¹ DLA and RLA are given in ICRF/EME2000 of date reference frame



4.5 2019 February Launch Window

The following analysis shows the variation of the main orbital parameters for the launch period around February 2019. The results are based on computations with the linked conics model. Part of the results is common to the 2020 launch window and is presented in the next sub-section.

The trajectory computation for each launch day includes the first 1-year Earth-Earth resonant arc and the Earth GAM that exactly matches the rest of the trajectory as if launching occurred in 2020. In order to distinguish between the Earth GAMs, in the following text of this section GAM-E1 designates the Earth GAM in 2020 and before GAM-V1, and GAM-E2 designates the Earth GAM in November 2021 required during the cruise phase.

There is freedom in the selection of the 1-year resonant parking orbit. This freedom has been removed by assuming a fixed DLA in order to simplify the definition of the launch targets. The value of the DLA is a free parameter that can be adjusted in order to provide a continuous launch window. The analysis has found a fixed DLA of +15 deg to be adequate for a launch window on Atlas V 411. This value might be refined in the future.

Two launch options exist for the 1-year Earth-Earth “parking orbit”: inwards and outwards from Earth. The two options differ in the lift-off time by about 12 hours and lead to different evolution of the Sun distance and geometry of GAM-E1. Both options are feasible as long as the altitude at GAM-E1 remains above the 350 km constraint without the need of a Delta-V manoeuvre. The inwards and outwards options have to be combined in order to provide a sufficiently long launch period. This was also the case for the old CReMA 3.1 July 2017 trajectory. In this case the launch window starts with outwards solutions and the transition from outwards to inwards occurs between February 15th and 16th.

The following figures show trajectory parameters for the 2019 February launch windows from launch until GAM-E1. The aphelion of the 1-year Earth-Earth “parking orbit” can be as high as 1.192 AU. This value determines the maximum Sun distance of the entire trajectory, because after GAM-E1 the spacecraft will remain closer to the Sun. In addition, the longest eclipse of up to 25 minutes occurs in the inwards option at GAM-E1, while no eclipse will be encountered in the outwards option.

Trajectory parameters after GAM-E1 are common with the 2020 launch and presented in Section 4.6.

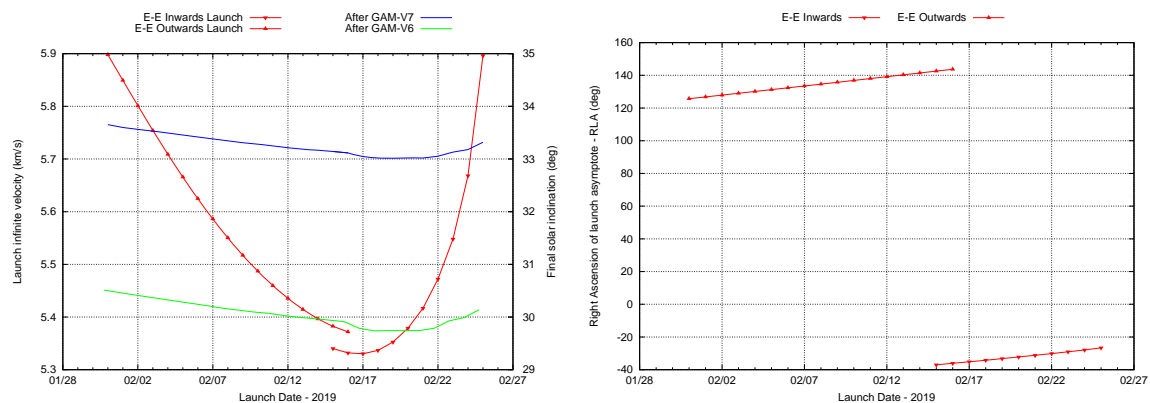


Figure 4-21 2019 February launch window: launch targets and solar inclination

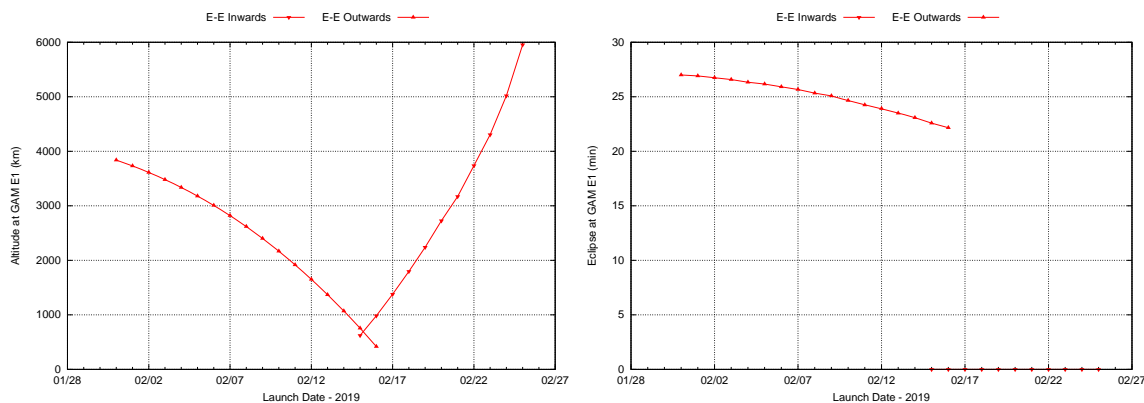


Figure 4-22 2019 February launch window: Altitude and eclipse duration at GAM-E1

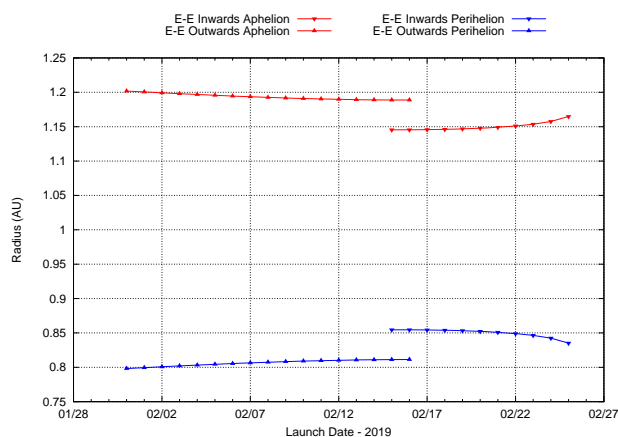


Figure 4-23 2019 February launch window: perihelion and aphelion radius of 1-year heliocentric parking orbit



The blinding of star trackers during LEOP has been analysed as a function of the launch day and for the 2 solutions, inwards and outwards. The analysis has been performed with the same assumptions as in Section 4.2 (page 130).

Figure 4-24 shows the evolution during LEOP of the angle from the star tracker bore sight to the Earth and Moon limb for the launch days between February 5th and 16th with the outwards solution. The star tracker will be initially blinded by Earth after separation for a short period of a few minutes. The Moon will not blind the star tracker.

Figure 4-25 shows the corresponding analysis assuming the alternative spacecraft attitude with the +Y_{sc} axis pointing towards the celestial North. The star tracker is not blinded.

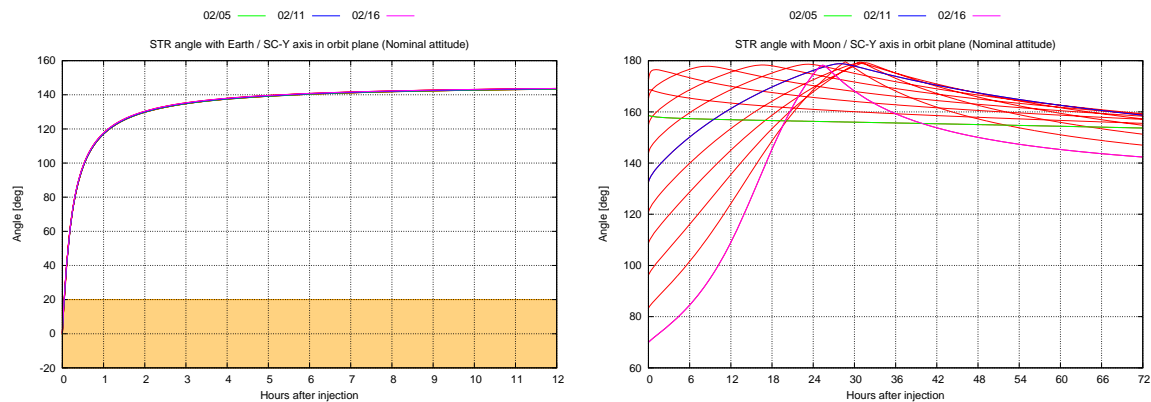


Figure 4-24 2019 February launch window - Outwards: evolution of angles from Star Tracker bore sight to Earth and Moon limbs in the nominal attitude

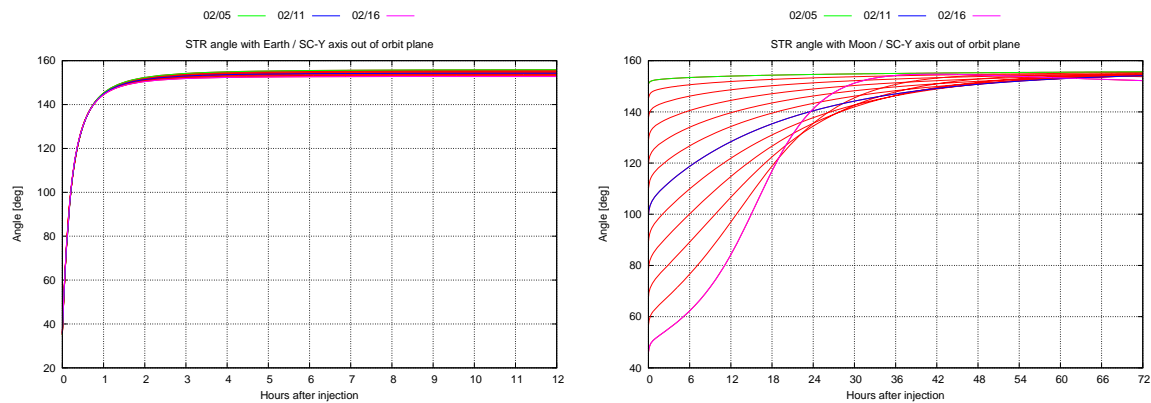


Figure 4-25 2019 February launch window - Outwards: evolution of angles from Star Tracker bore sight to Earth and Moon limbs in the alternative attitude

Figure 4-26 shows the evolution during LEOP of the angle from the star tracker bore sight to the Earth and Moon limb for the launch days between February 15th and 24th with the inwards solution. The star tracker will not be blinded by Earth, but for some launch days the Moon will be blinding the star tracker from separation for a period from 20 to 33 hours.



Figure 4-27 shows the corresponding analysis assuming the alternative spacecraft attitude with the +Y_{sc} axis pointing towards the celestial North. This geometry leads to very long blindings with both, Earth and Moon.

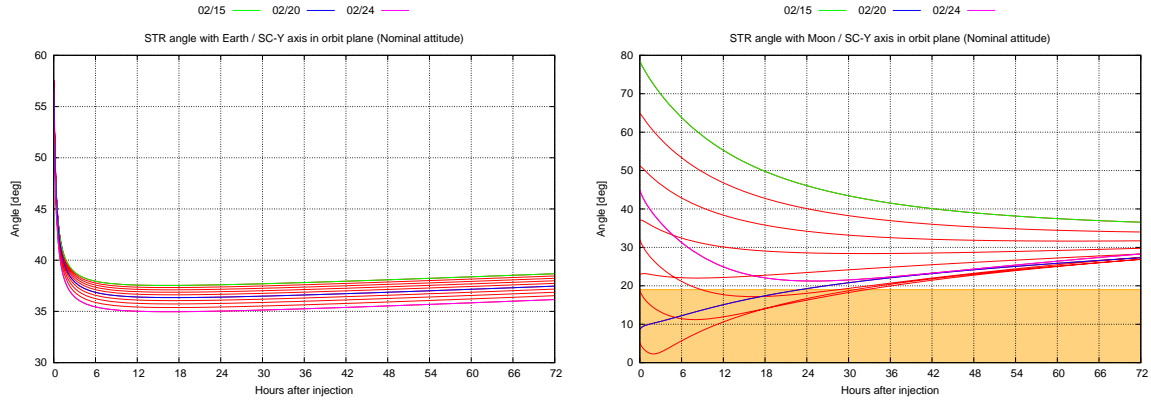


Figure 4-26 2019 February launch window - inwards: evolution of angles from Star Tracker bore sight to Earth and Moon limbs in the nominal attitude

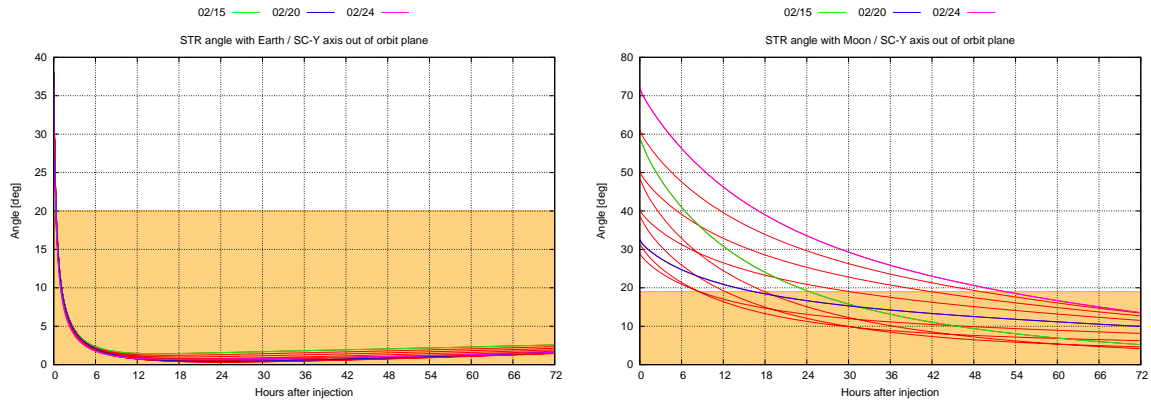


Figure 4-27 2019 February launch window - inwards: evolution of angles from Star Tracker bore sight to Earth and Moon limbs in the alternative attitude

Table 4-7 shows a summary of the star tracker blinding events as a function of the launch day.



		Nominal S/C attitude				Alternative S/C attitude			
		Earth Duration min	Moon Start h	Moon End h	Moon Duration h	Earth Duration min	Moon Start h	Moon End h	Moon Duration h
02-05	Outwards	2.9				0			
02-06	Outwards	2.9				0			
02-07	Outwards	2.8				0			
02-08	Outwards	2.8				0			
02-09	Outwards	2.8				0			
02-10	Outwards	2.8				0			
02-11	Outwards	2.8				0			
02-12	Outwards	2.8				0			
02-13	Outwards	2.7				0			
02-14	Outwards	2.7				0			
02-15	Outwards	2.7				0			
02-16	Outwards	2.6				0			
02-15	Inwards	0				>4300	24.40	72	47.6
02-16	Inwards	0				>4300	17.92	72	54.1
02-17	Inwards	0				>4300	12.30	72	59.7
02-18	Inwards	0				>4300	8.47	72	63.5
02-19	Inwards	0				>4300	8.58	72	63.4
02-20	Inwards	0	0	23.04	23.0	>4300	16.40	72	55.6
02-21	Inwards	0	0	30.93	30.9	>4300	30.20	72	41.8
02-22	Inwards	0	0	32.53	32.5	>4300	41.88	72	30.1
02-23	Inwards	0	8.85	28.53	19.7	>4300	49.12	72	22.9
02-24	Inwards	0				>4300	52.55	72	19.4

Table 4-7 2019 February launch window: Star tracker blinding events during LEOP

4.5.1 LAUNCH TARGETS

Table 4-10 shows the launch targets in terms of the escape velocity, DLA and RLA (in ICRF/EME2000) and ESOC estimation for separation time for the 2019 February launch window considering the 2 launch options, inwards and outwards. These targets are based on the linked conics model and will be subject to further refinement in the future. The identified launch period extends 18 days from February 6th to 23rd (extra days out of this period given for information in grey).

Date	Outwards				Inwards				Final i _s (deg)
	Sep. (UTC)	V _∞ (km/s)	DLA ¹ ICRF (deg)	RLA ICRF (deg)	Sep. (UTC)	V _∞ (km/s)	DLA ICRF (deg)	RLA ICRF (deg)	
2019-02-05	10:21:34	5.666	15	131.24					30.29
2019-02-06	10:22:07	5.625	15	132.36					30.25
2019-02-07	10:22:41	5.586	15	133.48					30.21
2019-02-08	10:23:16	5.550	15	134.61					30.16
2019-02-09	10:23:52	5.517	15	135.75					30.13
2019-02-10	10:24:29	5.487	15	136.88					30.09
2019-02-11	10:25:06	5.459	15	138.02					30.07
2019-02-12	10:25:43	5.435	15	139.16					30.03
2019-02-13	10:26:20	5.414	15	140.29					29.99
2019-02-14	10:26:57	5.396	15	141.43					29.97
2019-02-15	10:27:32	5.382	15	142.56	22:25:35	5.340	15	322.98	29.94
2019-02-16	10:28:07	5.372	15	143.69	22:25:19	5.332	15	323.90	29.91
2019-02-17					22:25:07	5.330	15	324.83	29.79
2019-02-18					22:24:59	5.337	15	325.79	29.74
2019-02-19					22:24:56	5.352	15	326.76	29.74
2019-02-20					22:24:59	5.379	15	327.76	29.74
2019-02-21					22:25:09	5.417	15	328.79	29.74
2019-02-22					22:25:26	5.472	15	329.85	29.79
2019-02-23					22:25:51	5.548	15	330.94	29.93
2019-02-24					22:26:30	5.668	15	332.09	29.99

Table 4-8 2019 February launch window: Launch targets

¹ DLA and RLA are given in ICRF/EME2000 of date reference frame



4.6 2020 February Launch Window

The following analysis shows the variation of the main orbital parameters for the launch period around February 2020. The results are based on computations with the linked conics model.

Figure 4-28 shows the evolution of infinite velocity, solar inclination at end of mission (after GAM-V7) and DLA. The analysed period covers a few days more than what is feasible to achieve with the Atlas V 411 launcher performance, from February 6th to 24th. The DLA for this trajectory is positive and between about 22 and 29 degrees. A solar inclination at mission end of at least 33 deg can be achieved for any launch day.

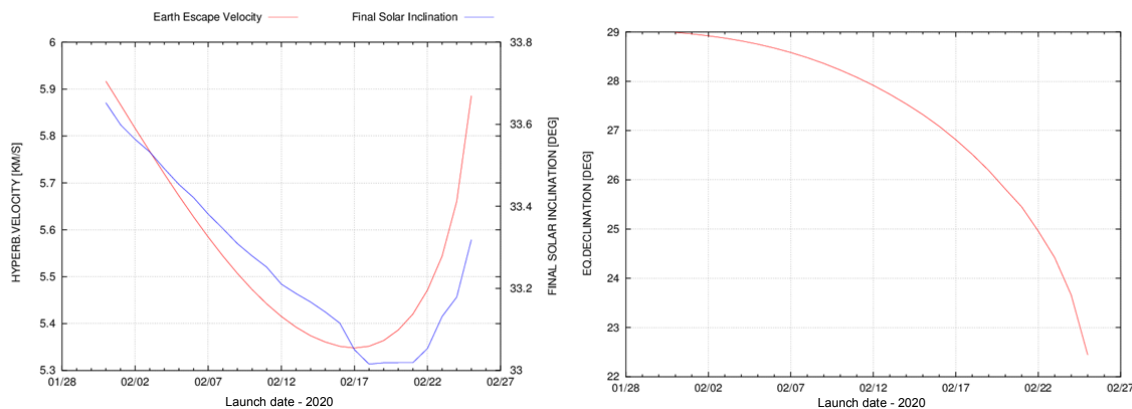


Figure 4-28 2020 February launch window: launch targets and solar inclination

The following figures show other relevant characteristics of the trajectories. Since the trajectory will be the same after February 2020 independently of the launch taking place in 2020 or in 2019, the plots are applicable to both launch opportunities. GAM-E1 in these plots refers to the Earth GAM in November 2021 in between of GAM-V2 and GAM-V3 (that would be GAM-E2 if launched in 2019). The entire range presented corresponds to January 31st-February 25th.

It can be seen that the perihelion radius, fly-by minimum altitudes and eclipse duration during the fly-bys are rather constant across the launch period. The only exception seems to be the minimum altitude at GAM-V3 that presents a smooth variation. A possible concern with respect to the spacecraft design comes from the variation of the longest safe mode blackout period (Figure 4-31). The previous February 7th reference trajectory (about launch window open) already presents a safe mode blackout of 63.2 days, which is marginal with respect to the spacecraft constraint. The worst case across the launch window occurs on February 18th with a period of 70.6 days.

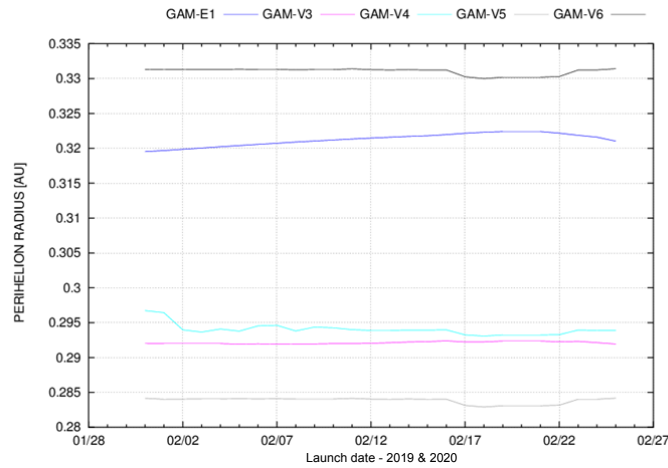


Figure 4-29 2019/2020 February launch window: Perihelion of science orbits

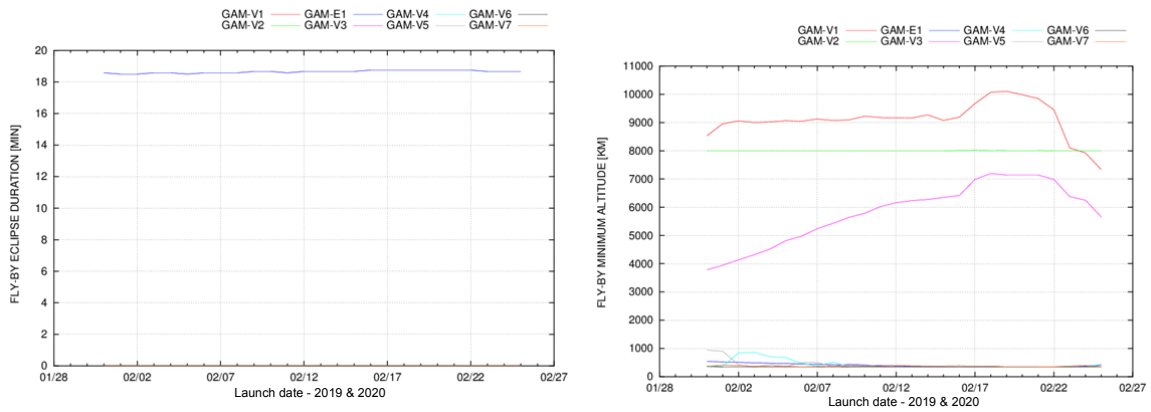


Figure 4-30 2019/2020 February launch window: GAM eclipse duration and minimum altitude

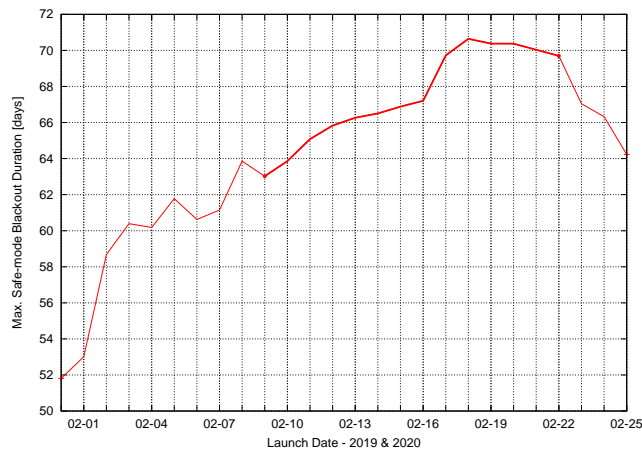


Figure 4-31 2019/2020 February launch window: longest safe mode blackout



The blinding of star trackers during the LEOP has been analysed as a function of the launch day. The analysis has been performed with the same assumptions as in Section 4.2 (page 130).

Figure 4-32 shows the evolution during LEOP of the angle from the star tracker bore sight to the Earth and Moon limb for the launch days between February 2nd and 24th. The star tracker will be initially blinded by Earth after separation for a period that grows with the launch day and can reach about 1.5 hours. Blinding by the Moon is possible for launches earlier than February 13th and it lasts from about 2 hours to almost half a day.

Figure 4-33 show the corresponding analysis assuming the alternative spacecraft attitude with the +Ysc axis pointing towards the celestial North. The star tracker will be initially blinded by Earth after separation up to about 30 minutes. The Moon can produce blindings only for the first 2 days considered in the analysis, February 5th and 6th.

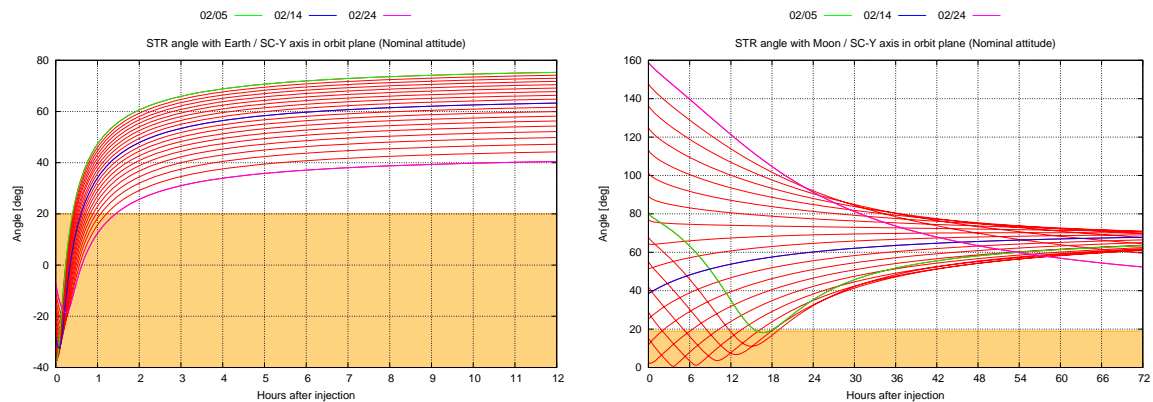


Figure 4-32 2020 February launch window: evolution of angles from Star Tracker bore sight to Earth and Moon limbs in the nominal attitude

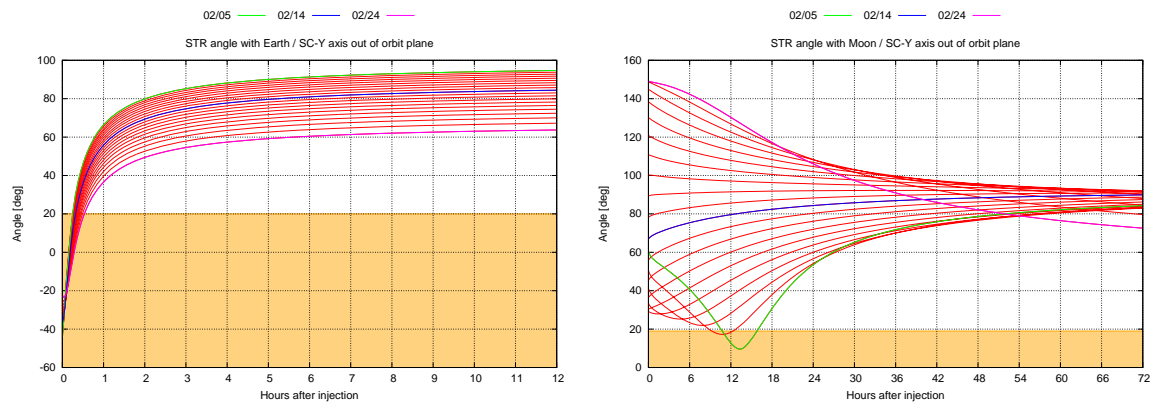


Figure 4-33 2020 February launch window: evolution of angles from Star Tracker bore sight to Earth and Moon limbs in the alternative attitude

Table 4-9 shows a summary of the star tracker blinding analysis as a function of the launch day. The alternative attitude reduces the Earth blindings and eliminates the Moon blinding of most of the days, except for the 5th and 6th of February.



	Nominal S/C attitude				Alternative S/C attitude			
	Earth Duration min	Moon Start h	Moon End h	Moon Duration h	Earth Duration min	Moon Start h	Moon End h	Moon Duration h
02-05	24.2	15.76	17.68	1.9	15.1	10.72	15.82	5.1
02-06	25.3	11.90	18.77	6.9	15.4	9.22	12.33	3.1
02-07	26.3	8.63	17.92	9.3	15.8			
02-08	27.5	5.31	16.00	10.7	16.2			
02-09	28.7	2.03	13.27	11.2	16.6			
02-10	30.0	0	9.89	9.9	17.1			
02-11	31.4	0	6.05	6.1	17.6			
02-12	32.9	0	1.99	2.0	18.1			
02-13	34.6				18.7			
02-14	36.4				19.4			
02-15	38.4				20.0			
02-16	40.7				20.8			
02-17	43.2				21.6			
02-18	46.1				22.5			
02-19	49.4				23.5			
02-20	53.4				24.6			
02-21	58.2				25.9			
02-22	64.4				27.5			
02-23	72.7				29.4			
02-24	85.9				32.1			

Table 4-9 2020 February launch window: Star tracker blinding events during LEOP

4.6.1 LAUNCH TARGETS

Table 4-10 shows the launch targets in terms of the escape velocity, DLA and RLA (in ICRF/EME2000) and ESOC estimated separation time for the 2020 February launch window. These targets are based on a refined trajectory computation with MANTRA including a full dynamics model with all relevant perturbations. A total of 9 m/s for the entire trajectory is needed for deterministic Delta-V manoeuvres. The launch period compatible with the Atlas V 411 performance extends for 19 days from February 6th to 24th.

Date	Sep. (UTC)	V _∞ (km/s)	DLA ¹ ICRF (deg)	RLA ICRF (deg)	Final i _s (deg)
2020-02-05	01:35:31	5.642	28.66	56.90	33.45
2020-02-06	01:41:22	5.604	28.58	56.84	33.42
2020-02-07	01:44:04	5.568	28.50	56.71	33.38
2020-02-08	01:45:46	5.533	28.40	56.53	33.35
2020-02-09	01:46:52	5.500	28.29	56.28	33.31
2020-02-10	01:47:33	5.470	28.17	55.98	33.28
2020-02-11	01:47:54	5.443	28.03	55.61	33.25
2020-02-12	01:47:57	5.420	27.88	55.17	33.21
2020-02-13	01:47:39	5.399	27.72	54.67	33.19
2020-02-14	01:47:05	5.383	27.54	54.10	33.17
2020-02-15	01:46:13	5.370	27.35	53.45	33.14
2020-02-16	01:45:05	5.361	27.13	52.72	33.12
2020-02-17	01:43:39	5.357	26.90	51.88	33.05
2020-02-18	01:41:56	5.358	26.65	50.93	33.02
2020-02-19	01:39:56	5.366	26.36	49.85	33.02
2020-02-20	01:37:39	5.381	26.04	48.59	33.02
2020-02-21	01:34:59	5.407	25.66	47.11	33.02
2020-02-22	01:31:57	5.448	25.22	45.33	33.05
2020-02-23	01:28:25	5.512	24.66	43.09	33.13
2020-02-24	01:24:03	5.620	23.88	39.98	33.18

Table 4-10 2020 February launch window: Launch targets

¹ DLA and RLA are given in ICRF/EME2000 of date reference frame



4.7 Summary

The variation of the trajectory parameters across the launch window periods presented in the previous sections has been analysed obtaining lower and upper limits for all variables relevant for the spacecraft design or the Solar Orbiter science mission. Table 4-11 provides all these relevant parameters for all the 5 launch opportunities currently regarded for Solar Orbiter and for both launch vehicles. The table considers the variations of the trajectory parameters with the launch day and provides the boundary minimum or maximum value as specified.

For each opportunity a period has been considered in which launch is compatible with Atlas V 411 and all spacecraft constraints are respected. For 2018 Option E the first launch date is September 22nd to avoid a too long safe mode blackout. For 2018 Option D a first launch date on October 8th is regarded.

The limit design value for each parameter is provided in the seventh column and the launch window for which the limit value is achieved is indicated with bold font. Additionally the rows of the most important parameters have been highlighted either with red background, for spacecraft design parameters, or green background, for parameters giving a figure of merit of science performance.

In order to ease tracing back the trajectory parameters with the corresponding requirements in the SSRD the eighth column provides the number of the applicable requirement. In addition the last column provides the limit value of the previous version of this document (CReMA 3.1). This allows comparison with the past requirements.

The only requirements that are exceeded with respect to the previous value are:

- The maximum infinite velocity: by making use of the full Atlas V 411 launch capability assumed for an 1800-kg Solar Orbiter spacecraft has increased slightly up to 5.625 km/s.
- DLA minimum value increases from -42.6 deg to -17.4 deg. Currently all the target DLA should be possible by using the standard parking orbit for Atlas V 411 launch with an inclination of 28.7 deg as the required DLA values are less than this in absolute value.
- Longest MGA safe-mode blackout period (MR-0305) has increased to 71 days as required by the 2019 & 2020 February backups.
- Mission duration: both the Cruise+NMP (SPR-0200) and the total mission duration (SPR-0205) have to be increased slightly to cope with the longer trajectories: Option E, Option D and 2019/2020 backups.

It is worth pointing out that the launch periods are dependent of the maximum capability assumed for Atlas V 411 launch of a 1800-kg spacecraft (section 4.1) of 5.64 km/s. Shall this value change due to more detailed data available from ULA or by a change of the spacecraft launch mass, this might lead to a redefinition of the limits of the launch periods.



	2018 E	2018 D	2018 Oct	2019 Feb	2020 Feb	Limit	SSRD-	Limit in 3.1
Launcher	Atlas V 411							
	Launch							
Feasible Period Open	2018-09-22	2018-10-08	2018-10-01	2019-02-06	2020-02-06		LIR-0020	
Feasible Period Close	2018-10-20	2018-11-07	2018-11-17	2019-02-23	2020-02-24		MR-0245	
Feasible Launch Days	29	31	48	18	19			
Min Launch V-Infinite (km/s)	5.169	3.994	4.416	5.330	5.357	3.986		3.373
Max Launch V-Infinite (km/s)	5.515	5.598	5.588	5.625	5.620	5.625		5.445
Min Launch DLA (deg)	-12.2	-17.3	-11.19	15	23.9	-17.4		-42.6
Max Launch DLA (deg)	-0.8	-15.2	-6.29	15	28.6	28.6		26.1
	Trajectory Limits							
Max Aphelion (AU)	1.149	1.449	1.475	1.195	1.017	1.475	MR-0290	1.478
Max Earth Range (AU)	2.007	2.001	2.016	1.992	1.992	2.016	MR-0295	2.017
Min Range Rate (km/s)	-58.7	-57.6	-59.5	-58.5	-58.5	-59.5	MR-0350	-60.6
Max Range Rate (km/s)	59.2	60.1	61.9	60.0	60.0	61.9	MR-0350	62.2
Max HGA Solar Conj. (days)	36.6	24.5	28.8	25.9	25.9	36.6	MR-0300	44
Max MGA Solar Conj. (days)	64.1	48.7	53.9	70.6	70.6	70.6	MR-0305	61
Max Cruise Duration (years)	2.30	3.10	3.20	2.80	1.80	3.20		3.40
Max C+NMP Duration (years)	6.20	8.20	7.00	7.90	6.90	8.20	SPR-0200	7.78
Max Total Duration (years)	10.50	10.70	9.50	10.34	10.60	10.7	SPR-0205	10.24
	Properties for science mission							
Max time to 1st <0.3AU (years)	3.51	4.02	3.51	3.68	2.68	4.02		4.67
Max time to max latitude (years)	9.59	9.67	8.46	9.35	9.58	9.67		9.20
Max Angular Rate (deg/d)	7.86	7.73	8.14	7.68	7.68	8.14		8.31
Min Time spent <0.3AU (days)	69	56.1	61.9	75.7	75.7	56.1		46.5
Max Time spent <0.3AU (days)	70.8	60.9	62.4	78.5	78.5	78.5		101.6
Shortest pass <0.3AU (days)	4.2	1.0	6.7	5.0	5.0	1		5.5
Longest pass <0.3AU (days)	9.5	6.7	9.1	8.9	8.9	9.5		9.5
Min Time spent <0.4AU (days)	489.1	403.9	321.1	406.3	461.4	321.1		292.8
Max Time spent < 0.4AU (days)	490.6	404.4	321.3	407.4	462.5	490.6		421.4
Shortest pass <0.4AU (days)	15.8	23.6	16.4	22.8	18.4	15.8		15.2
Longest pass <0.4AU (days)	28.2	26.9	27.1	27.1	27.1	28.2		28.4
NMP Min Aphelion (AU)	0.824	0.894	0.904	0.820	0.820	0.820	MR-0340	0.862
NMP Max Aphelion (AU)	1.009	1.023	1.111	1.017	1.017	1.111	MR-0340	1.126
NMP Min Perihelion (AU)	0.280	0.290	0.284	0.283	0.283	0.280	MR-0340	0.281
NMP Max Perihelion (AU)	0.350	0.308	0.366	0.322	0.322	0.366	MR-0340	0.372
NMP Min Solar INC (deg)	4.74	4.16	3.70	4.27	4.27	3.70	MR-0340	3.70
NMP Max Solar INC (deg)	22.52	21	22.27	24.43	24.43	24.43	MR-0340	25.69
EMP Min Aphelion (AU)	0.723	0.765	0.775	0.773	0.731	0.723		0.735
EMP Max Aphelion (AU)	0.778	0.813	0.822	0.820	0.820	0.822		0.824
EMP Min Perihelion (AU)	0.296	0.291	0.282	0.284	0.284	0.282		0.280
EMP Max Perihelion (AU)	0.381	0.339	0.329	0.331	0.373	0.381		0.334
Final Min Solar INC (deg)	32.41	31.96	32.34	29.74	33.02	29.74		27.33
Final Max Solar INC (deg)	33.93	32.4	33.37	30.25	33.38	33.93		36.36
	Earth and Venus GAMs							
Min EGAM Vinf (km/s)	9.470	11.177	11.698	5.348	10.584	5.348		5.024
Max EGAM Vinf (km/s)	9.721	11.273	12.074	10.705	10.705	12.074		12.167
Min EGAM altitude (km)	350	3945	2113	350	350	350	MR-0275	300
Max EGAM altitude (km)	398	4679	3033	4306	439	4679		6633
Min VGAM Vinf (km/s)	9.731	8.416	9.15	11.473	11.473	8.416		5.208
Max VGAM Vinf (km/s)	17.771	19.178	20.214	18.560	18.560	20.214		20.452
Min VGAM altitude (km)	350	350	350	350	350	350	MR-0280	300
Max VGAM altitude (km)	9000	7375	3762	10105	10105	10105		21111
Min Earth Range at VGAM (AU)	0.335	0.391	0.625	0.396	0.396	0.335		0.310
Max Earth Range at VGAM (AU)	1.632	1.669	1.685	1.667	1.667	1.685		1.687
Min Sun-SC-Earth VGAM (deg)	21.4	17.7	14.6	18.0	18.0	14.6		14.3
Min Sun-Earth-SC VGAM (deg)	15.5	12.5	10.4	12.7	12.7	10.4		10.2
Max Eclipse duration (min)	26.8	30.8	31.8	25.9	18.8	31.8	MR-0285	37.1
Occultation black-out (min)	11.2	4.8	8.8	17.3	17.3	17.3	MR-0310	35.3

Table 4-11 Summary of launch windows parameters



5 NAVIGATION ANALYSIS

A dedicated analysis of the navigation of the entire mission has been performed for the 2018 Option E trajectory scenario. Due to the consistency of the trajectory design for Solar Orbiter, these results are also applicable to other launch opportunities. The results obtained for this trajectory are fully in line with previous navigation analyses of the 2017 January (previous CReMA Issue 3 Rev 1) and 2017 July launch scenarios [27].

New in this CReMA issue is the analysis performed in Section 5.3.3 that investigates the alternate use of both DDOR baselines such as to improve the navigation while relying only on one DDOR baseline at each GAM.

5.1 Assumptions

Reference Trajectory

The navigation analysis requires a reference trajectory including all the relevant orbit perturbations (gravity effects of third bodies: Earth, Moon, Venus, other planets; solar radiation pressure) and the precise computation of the GAMs in a full dynamics model. Such a trajectory has been computed with the operational software MANTRA and has been extensively detailed in section 3.1.

For the resonant arcs of the trajectory a small deterministic Delta-V adjustment is required such that the same planet, Earth or Venus, is encountered again at the desired position. These Delta-Vs are typically small (less than 3 m/s each) requiring about 10-15 m/s over the entire mission, so that the trajectory can still be considered ballistic. The Delta-V for these residual manoeuvres is considered included by the allocation for navigation of the Delta-V budget.

Ideally the spacecraft should fly-by as close as possible to Venus such as to obtain the maximum velocity change and effect on the heliocentric trajectory from the GAM. However, low fly-by altitudes also imply higher risk of a failed navigation that can eventually lead to impact with the planet and loss of the mission. The Solar Orbiter spacecraft is designed for a minimum altitude of 300 km during a GAM. The navigation has to ensure that the actual fly-by altitude is higher including all uncertainties and dispersion of the spacecraft trajectory. For this reason a fly-by target altitude of 350 km is used at trajectory design level, which gives a comfortable 50-km margin to accommodate the navigation error.

Navigation with the current DDOR technique leads to pericentre dispersions of the 10-km level, thus smaller than the margin between the target altitude and the atmosphere and therefore safe to navigate. On the other hand, lower altitude targets would report insignificant improvements of the trajectory science merits like final solar inclination and duration of the close approaches to the Sun.

Measurements and Operations Approach

Solar Orbiter navigation will be based on the use of radiometric measurements taken from ESA's Deep Space antennas in order to perform the orbit determination (OD). Trajectory correction manoeuvres (TCM) are computed on ground and commanded for execution by the spacecraft so that the actual trajectory does not diverge from the reference one.

This navigation analysis has considered the operational constraints that are typical for interplanetary missions. In particular, the type and frequency of the measurements and the timeline of TCMs have been made compatible with the Solar Orbiter preliminary operational concept for the GAMs [5]. The aim of the TCM plan is to minimise the number of required TCMs while ensuring a safe navigation. In addition it is pursued that all the TCMs are to be executed in the proximity of a GAM, thus avoiding executing TCMs during the remote sensing windows in which the spacecraft is devoted to the science.



Range and Doppler measurements from the baseline ground station in Malargüe are assumed to be collected together with the telemetry downlink. The frequency for range measurements is 1 every 4 h; while the continuous Doppler signal is assumed to be reduced to 1 measurement every 30 min. In order to reduce the operational workload during the routine cruise and science phases the orbit will be determined at a weekly basis using the tracking data of 1 day pass.

The operations for a GAM will extend typically from 1 month before to 1 week after the GAM. In preparation for the GAM the frequency of contacts with the spacecraft is increased gradually until reaching 24-h support near the closest approach. The frequency of measurements is also increased accordingly. In addition DDOR measurements from the ESA baselines, Cebreros-New Norcia and Cebreros-Malargüe, will be taken in order to improve the accuracy of the orbit determination. Each baseline is assumed to produce 1 DDOR measurement per day. The frequency of DDOR measurements is also increased close to the GAM up to 4 measurements per week.

The GAM operations timeline with TCMs and measurements frequencies is given in Table 5-1.

The above assumes an inbound Venus GAM, that is, the spacecraft is approaching Venus after the aphelion pass with decreasing Sun distances. The same timeline can also be applied to the Earth GAMs for which there is no conflict of the manoeuvres with the science operations, since the remote sensing observations are expected to start after the Earth GAM(s). In the case of an Earth GAM, however, the benefit of using DDOR measurements is reduced and depending on the characteristics of the trajectory it can be recommended to reduce the frequency and number of baselines used, or even not to use any DDOR measurement at all, in order to reduce operations costs. A dedicated analysis of this issue has been carried out and documented in [28]. For the 2018 Option E trajectory, the recommendation is not to use DDOR for the single Earth GAM.

In the case that the Venus GAM is outbound, the spacecraft will come from the perihelion towards Venus. The TCM at GAM-30 days would then lie close to the perihelion. This presents two major disadvantages: 1- the spacecraft will be required to implement a TCM very close to the Sun, for which the spacecraft design might not be compatible (currently a Type-2 manoeuvre is possible only for Sun distances >0.6 AU TBC) and 2- the TCM will interfere with the science operations. Both issues are mitigated by advancing the TCM to about the last aphelion before the Venus GAM. The operations timeline proposed for an outbound Venus GAM looks as presented in Table 5-2.

Table 5-2 includes a free parameter, N =number of days from aphelion to the first TCM to target the next GAM. This parameter can be adjusted together with the trajectory optimization such as to combine the deterministic Delta-V adjustments needed in the resonant arcs between two GAMs of the same planet with the stochastic correction for the navigation. For some trajectories, as 2017 July from CReMA Issue 3.1, it has been observed that lowest deterministic Delta-V is achieved for manoeuvres at the aphelion, thus with the value of N equals 0. For the baseline trajectory regarded in this document, an optimal location of the manoeuvres was found to be slightly past the aphelion for N taking a value of about 25-35 days.



Time (relative)	Activity	Measurements frequency	
		Range&Doppler	DDOR (per baseline)
< GAM-45 days	Routine	1 pass per week	No
GAM-45 days	Start OD campaign		
		4 passes per week	1 per week
GAM-30 days	TCM		
		4 passes per week	1 per week
GAM-14 days	TCM		
		7 passes per week	2 per week
GAM-7 days	TCM		
		7 passes per week	4 per week
GAM-3 days	TCM		
		7 passes per week	4 per week
GAM			
		7 passes per week	4 per week
GAM+7 days	TCM		
> GAM+7days	Routine	1 pass per week	No

Table 5-1 Timeline for GAM operations – inbound Venus GAM or Earth GAM

Time (relative)	Activity	Measurements frequency	
		Range&Doppler	DDOR (per baseline)
< Last Aphelion + N-14 days	Routine	1 pass per week	No
Last Aphelion + N-14 days	Start OD campaign		
		4 passes per week	1 per week
Last Aphelion + N days	TCM		
	Routine including perihelion science pass	1 pass per week	No
GAM-21 days	Start OD campaign		
		4 passes per week	1 per week
GAM-14 days	TCM		
		7 passes per week	2 per week
GAM-7 days	TCM		
		7 passes per week	4 per week
GAM-3 days	TCM		
		7 passes per week	4 per week
GAM			
		7 passes per week	4 per week
GAM+7 days	TCM		
> GAM+7days	Routine	1 pass per week	No

Table 5-2 Timeline for GAM operations – outbound Venus GAM

Orbit Determination Model

The results of the navigation analysis are based on covariance analysis. The orbit determination process is simulated with a square root information filter (SRIF) incorporating the two-way ranging and Doppler data and the DDOR measurements. For each TCM the orbit determination covariance matrices are updated via Monte Carlo simulation assuming a linear guidance law and modelling the manoeuvre execution errors.

The assumptions for the orbit determination and navigation models are summarized in the following table:



Observations & Measurements	1- σ 2-way range random error	4 m
	1- σ 2-way range consider bias	20 m
	1- σ 2-way Doppler random error	0.075 mm/s
	1- σ 2-way Doppler consider bias	None
	1- σ DDOR random error	5 cm
	1- σ ESA DS ground station coordinates consider bias	For Range&Doppler: 50 cm For Δ DOR: 5 cm
	Minimum elevation for GS visibility	10 deg
	Data cut-off before each TCM	1 day
	Solar conjunctions data blackout	SES angle < 3 deg
Dynamics & Navigation Uncertainties	1- σ 3-axis NGA correlated noise Autocorrelation time	1e-11 km/s ² 1 day
	1- σ Solar radiation pressure bias	5 % ~ 5e-4 m ² /kg
	1- σ Venus Ephemeris position error bias	0.5 km
Manoeuvre Execution Errors	1- σ Delta-V modulus proportional error	For nominal Delta-V > 0.6 m/s: 0.5%
	1- σ Delta-V modulus absolute error	For nominal Delta-V < 0.6 m/s: 3 mm/s
	1- σ Delta-V direction error (semi-cone angle)	0.25 deg

Table 5-3 Assumptions for the orbit determination and navigation models

The provided assumptions are conservative, in particular for the Doppler random error. The 20 m bias in the 2-way range measurements takes into account ranging systems calibration errors and delays due to the Earth troposphere. The DDOR random error assumes that the Solar Orbiter transponder generates DDOR tones and that the accuracy of ESA Δ DOR ground stations will improve to NASA level by 2016. Errors in ground station location take into account errors in the rotational parameters of the Earth.

Non-gravitational accelerations are included to account for unmodeled accelerations, such as gas leaks or the residual effect of wheel-offloadings. The magnitude of the NGA errors is representative of disturbances created by wheel-offloadings (the part of the wheel-offloading parasitic Delta-V that cannot be predicted): assuming one wheel-off-loading per day with a residual ΔV of 1.0 mm/s, which is considered conservative. In addition solar radiation pressure has also a noise component of 1% (1- σ) that is considered included in the NGA errors.

The maximum solar radiation pressure acceleration when the spacecraft is near the minimum perihelion distance of 0.28 AU is estimated about 5e-10 km/s² considering a surface of 7.3 m² for the solar shield normal to the Sun direction and 13.7 m² for the solar arrays with an incidence angle to the Sun of 80 deg. The solar radiation pressure drops by one order of magnitude for Sun distances of 1 AU and beyond. A 5% bias has been included in the orbit determination model to take into account uncertainties of the cross-section or reflectivity coefficient and also the incidence angle of the Sun on the solar array, which is controlled during the mission to protect the solar arrays from the high radiation input at low Sun distances.

This updated navigation analysis includes as well the effect of uncertainties in the ephemeris of Venus. Such uncertainties are included in the navigation process as consider parameter or bias with a 1- σ value of 0.5 km that is consistent with the Orbit Determination experience of ESA missions.

The model for the execution errors of the correction manoeuvres has been also updated. The new model takes into account that the magnitude error for small manoeuvres reaches a limit level and does not behave as proportional to the nominal Delta-V magnitude any longer. The Delta-V threshold assumed for Solar Orbiter is 0.6 m/s: above this magnitude the modulus error is assumed proportional at 0.5% (1- σ) and below it the modulus error is fixed to 3 mm/s (1- σ) independently of the nominal Delta-V size. This model is therefore more pessimistic than only the proportional error assumed in previous Solar Orbiter navigation analyses. Differences in the results are however small.



5.2 Launcher Injection Correction and Initial OD

The first TCM after launch is dedicated to correct the launcher injection errors. The magnitude of this manoeuvre depends on the size of the injection errors and the time when the correction is executed.

The ΔV allocation for this correction is derived from the requirements imposed to the launcher injection errors in the LIRD [18], which are given in Table 5-4. These requirements are compatible with a ΔV of 25 m/s (at 3- σ level).

	Baseline Scenario Atlas V
3- σ error in V_{inf} (m/s)	12.5
3- σ error in RLA (deg)	0.1
3- σ error in DLA (deg)	0.1

Table 5-4 Requirements on launch vehicle injection errors from LIRD [18]

Injection error covariance matrices have been provided by ULA in the frame of the feasibility studies carried out in 2013 [26, 31]. The provided data covers the 2018 October trajectory and the 2018 Option E. This input data has been used to perform an analysis of the early orbit determination and the Delta-V required for the LIC. The required LIC Delta-V is well below the 25 m/s allocation.

For the orbit determination during the LEOP it is assumed that range and Doppler measurements from the ESA Deep Space stations are used. Figure 5-1 shows the evolution of the knowledge and dispersion errors during the first days of the mission for the 2018 Option E trajectory (very similar results are obtained for the other trajectories). One day of measurements is enough to reach a stationary level of the orbit estimation of about 5 km in position and 5 cm/s in velocity (both 3- σ values).

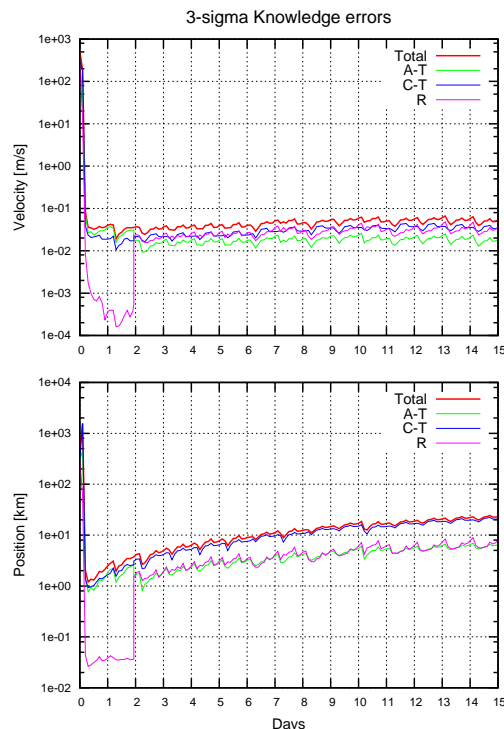


Figure 5-1 Evolution of knowledge and dispersion errors after launch (2018 Option E)



5.3 *Trajectory Navigation of all GAMs*

For the analysis of the navigation of the entire trajectory the timeline of correction manoeuvres is provided in Table 5-5. The table also provides some geometric characteristics: distances to the Sun - Rs, Earth - Re and Venus Rv; Equatorial right ascension α and declination δ of the Earth-satellite line; and the communication angles: Sun-Spacecraft-Earth (SSE) and Sun-Earth-Spacecraft (SES).

For the analysis the LIC (=TCM1) was assumed 5 days after launch. An additional correction TCM2 executed 15 days later has been considered to clean-up the execution errors of the LIC. Then the operations approach of Table 5-2 (for outbound Venus GAMs) is repeated for each of the 8 Venus GAMs: 4 pre-swingby corrections at last aphelion + N days, then at GAM - 14, -7 and -3 days, respectively, and one post-swingby correction at GAM + 7 days. The first pre-GAM TCM ranges from 89 to 165 days, depending on the period and geometry of the spacecraft heliocentric orbit and by how far from the aphelion an optimal deterministic Delta-V is obtained. Only TCM28 does not follow this rule, because a solar superior conjunction occurs close to the last aphelion before GAM-V5. To avoid any conflict of navigation operations with the solar conjunction, it has been decided to shift TCM28 to the previous aphelion so that this manoeuvre takes place 285 days before GAM-V5. The advance of the TCM does not imply any significant penalty in terms of Delta-V or navigation accuracy.

For the Earth GAM the operations timeline corresponds to Table 5-1 with the first pre-GAM TCM at GAM - 30 days. For this trajectory the accuracy of Range+Doppler only for the navigation of the Earth GAM is enough to guarantee a precise GAM navigation. The penalty for not using DDOR measurements is only an error in the pericentre radius just 1-3 km larger and an increase of up to 3 m/s in the post-GAM clean-up TCM. With such small penalties, it is justified not to use any DDOR measurement at the Earth GAM. This has been assumed in the baseline navigation scenario.

From Table 5-5 it is seen that GAM operations are away of the solar conjunctions as has been aimed at the trajectory and navigation design. The minimum SSE and SES angles at a TCM time are above 10 deg and occur at TCM23, which is the first pre-GAM TCM for GAM-V4 and thus not critical since other TCMs are planned in the approach to Venus.

Of relevance for the implementation of the manoeuvres is the distance to the Sun. The Solar Orbiter spacecraft design is based on a Sun pointing attitude. At distances far away from the Sun it is allowed to temporarily slew the spacecraft such as to implement a Delta-V manoeuvre with the optimal attitude (Type-1 manoeuvre). However, for lower Sun distances it is critical for the survival of the spacecraft to maintain the Sun pointing attitude even for the implementation of Delta-V manoeuvres. In this case the spacecraft must perform a Type-2 manoeuvre by rotating around the Sun-spacecraft line and making use of a lateral thruster to provide omni-directional Delta-V coverage, but with a significant efficiency loss. Currently the limiting distance between both types of manoeuvres is 0.95 AU.

With the TCM timeline of Table 5-5 the LIC manoeuvres and all TCMs around GAM-E1 navigation occur above 0.95 AU and will be Type-1 burns. All the TCMs for the Venus GAMs will occur below 0.94 AU and therefore implemented as Type-2 burns. TCM24 14 days before GAM-V4 is the closest to the Sun at roughly 0.58 AU.

It must be pointed out that this navigation analysis considers only the magnitude of the optimal Delta-V manoeuvres to correct the spacecraft trajectory and has not taken into account any efficiency loss due to the manoeuvre type. It is the responsibility of the industry contractor to guarantee a sufficient propellant allocation for the navigation of all GAMs when taking into account the actual efficiencies due to the manoeuvre type.



Event	TCM #	Time	Target	Rs (AU)	Re (AU)	Rv (AU)	α (deg)	δ (deg)	SSE (deg)	SES (deg)
LIC	TCM1	L + 5 d	V1	1.007	0.015	0.335	-51.2	-8.8	63.2	116.0
LIC	TCM2	L + 20 d	V1	1.011	0.060	0.290	-49.8	-8.7	73.9	102.8
V1	TCM3	V1 - 112 d	V1	0.877	0.174	0.531	-51.0	-9.6	123.6	47.9
V1	TCM4	V1 - 14 d	V1	0.652	1.138	0.083	-31.8	-14.0	60.6	34.8
V1	TCM5	V1 - 7 d	V1	0.689	1.221	0.040	-24.7	-11.4	54.8	34.3
V1	TCM6	V1 - 3 d	V1	0.711	1.264	0.017	-20.8	-9.9	52.1	34.2
V1	TCM7	V1 + 7 d	V2	0.766	1.352	0.040	-11.4	-6.4	47.1	34.1
V2	TCM8	V2 - 165 d	V2	0.926	1.538	0.440	35.1	11.6	39.6	35.6
V2	TCM9	V2 - 14 d	V2	0.646	1.505	0.084	-125.7	-19.6	29.2	18.5
V2	TCM10	V2 - 7 d	V2	0.687	1.505	0.040	-115.3	-21.9	31.9	21.5
V2	TCM11	V2 - 3 d	V2	0.711	1.508	0.017	-109.4	-23.0	33.0	23.0
V2	TCM12	V2 + 7 d	V3	0.764	1.516	0.040	-95.2	-25.0	34.6	26.0
V3	TCM13	V3 - 162 d	V3	0.914	1.596	0.448	-28.6	-17.1	34.1	31.4
V3	TCM14	V3 - 14 d	V3	0.651	0.370	0.083	73.1	25.8	167.6	7.9
V3	TCM15	V3 - 7 d	V3	0.690	0.357	0.040	67.7	21.6	150.8	19.4
V3	TCM16	V3 - 3 d	V3	0.712	0.358	0.017	65.4	19.3	141.6	25.8
V3	TCM17	V3 + 7 d	E1	0.761	0.389	0.040	62.4	12.7	120.9	40.0
E1	TCM18	E1 - 30 d	E1	1.080	0.170	1.473	118.2	-14.4	52.6	119.6
E1	TCM19	E1 - 14 d	E1	1.035	0.079	1.539	120.2	-16.4	48.2	128.4
E1	TCM20	E1 - 7 d	E1	1.010	0.039	1.554	120.6	-16.9	46.1	132.2
E1	TCM21	E1 - 3 d	E1	0.995	0.017	1.559	120.8	-17.0	44.9	134.4
E1	TCM22	E1 + 7 d	V4	0.961	0.039	1.574	-17.7	-1.4	122.9	55.1
V4	TCM23	V4 - 111 d	V4	0.939	1.917	1.348	124.5	19.9	11.5	10.7
V4	TCM24	V4 - 14 d	V4	0.582	0.626	0.145	-99.4	-25.5	110.1	33.5
V4	TCM25	V4 - 7 d	V4	0.658	0.539	0.067	-86.1	-26.3	111.0	38.4
V4	TCM26	V4 - 3 d	V4	0.699	0.500	0.026	-77.9	-26.3	109.8	41.7
V4	TCM27	V4 + 7 d	V5	0.775	0.454	0.067	-58.6	-26.0	103.7	49.8
V5	TCM28	V5 - 265 d	V5	0.818	0.226	1.395	-33.5	-44.1	131.6	38.5
V5	TCM29	V5 - 14 d	V5	0.584	0.507	0.148	149.7	13.0	134.1	24.7
V5	TCM30	V5 - 7 d	V5	0.660	0.505	0.071	145.4	12.4	118.5	35.3
V5	TCM31	V5 - 3 d	V5	0.698	0.507	0.030	144.0	11.7	111.8	40.3
V5	TCM32	V5 + 7 d	V6	0.765	0.510	0.071	144.3	7.2	101.4	48.6
V6	TCM33	V6 - 89 d	V6	0.724	1.290	1.409	146.8	4.6	50.8	34.0
V6	TCM34	V6 - 14 d	V6	0.606	0.868	0.144	-65.3	-19.2	81.8	37.5
V6	TCM35	V6 - 7 d	V6	0.671	0.839	0.071	-52.6	-18.8	80.5	42.2
V6	TCM36	V6 - 3 d	V6	0.703	0.831	0.030	-45.7	-18.4	79.3	44.6
V6	TCM37	V6 + 7 d	V7	0.752	0.826	0.070	-30.9	-17.9	76.9	48.1
V7	TCM38	V7 - 97 d	V7	0.689	0.494	1.331	-145.4	-45.8	111.7	40.6
V7	TCM39	V7 - 14 d	V7	0.638	1.556	0.141	-5.8	-0.1	21.5	13.6
V7	TCM40	V7 - 7 d	V7	0.686	1.592	0.071	2.9	1.9	22.4	15.2
V7	TCM41	V7 - 3 d	V7	0.709	1.609	0.030	7.6	2.9	22.7	16.0
V7	TCM42	V7 + 7 d	V8	0.733	1.626	0.070	18.4	4.9	23.3	16.9
V8	TCM43	V8 - 96 d	V8	0.628	0.907	1.313	161.3	-7.6	78.8	38.2
V8	TCM44	V8 - 14 d	V8	0.671	1.151	0.139	-39.2	-11.9	58.4	35.5
V8	TCM45	V8 - 7 d	V8	0.703	1.154	0.070	-29.7	-11.1	58.1	37.4
V8	TCM46	V8 - 3 d	V8	0.716	1.156	0.030	-24.6	-10.7	57.8	38.1
V8	TCM47	V8 + 7 d	V9	0.718	1.142	0.070	-13.3	-10.2	58.8	38.6

Table 5-5 Navigation analysis: times and geometry properties of TCMs



The navigation analysis has been performed for 4 measurements scenarios:

- No DDOR: OD considers only Range and Doppler measurements.
- DDOR only from Cebreros-New Norcia
- DDOR only from Cebreros-Malargüe: regarded as nominal reference case for navigation.
- DDOR from both baselines Cebreros-New Norcia & Cebreros-Malargüe.

It is clear that the No DDOR scenario provides a bound pessimist case, but it is useful to show the benefit of using DDOR. If both DDOR baselines are available, measurements from both baselines will be taken in order to reach the best OD accuracy and navigation performance. The analysis of the cases with only one baseline permits to identify the effect of each baseline separately.

Reference Navigation Case: DDOR only from Cebreros – Malargüe baseline

The DDOR with Cebreros-Malargüe only is the reference for the navigation analysis. Table 5-6 summarizes the statistics of the estimated Delta-V required per TCM. The first column specifies to which GAM each TCM is related to. The fourth column gives the target of the TCM, always at the B-plane target of the next GAM. The fifth column identifies the Type-1 & Type-2 manoeuvres according to a limiting Sun distance of 0.95 AU.

The Delta-V information provided in the table refers to the deterministic Delta-V, if any, always to be combined with the first pre-GAM TCM; the mean, standard deviation, 95-th percentile and 99-th percentile of the Delta-V distribution as determined by the Monte Carlo guidance algorithm. The last two columns show the accumulated Delta-V per GAM of the 95-th and 99-th percentiles.

The results show that the navigation of each GAM requires distinct Delta-V values, basically in dependence of the Earth-Venus geometry. On one side GAM-V1 requires about 5 m/s to be accurately navigated, while on the other side GAM-V7 requires up to 29 m/s (at 99% level). This difference is related to the accuracy of the OD before the GAM and the orientation of the error ellipse in the B-plane. Typically, B-plane errors in the cross-track direction (perpendicular to radial) are more costly to correct at the post-GAM TCM. The Earth GAM can also easily be navigated with 6.5 m/s (at 99%).

The following conclusions can be drawn:

- In general the largest Delta-V required for navigating each GAM corresponds to the post-swingby TCM at GAM+7 days to correct the errors amplified by the swing-by. This TCM can reach sizes up to almost 30 m/s.
- The pre-GAM TCMs are typically small and below 3 m/s. Of the pre-GAM TCMs only the 1st and 2nd (at GAM - 14 days) can reach sizes of the order of 1 m/s. All TCMs at GAM - 7 and -3 days are typically below 0.3 m/s (at 99% level).
- The Delta-V required for the entire trajectory is 109 m/s, which divided by the 9 GAMs in the trajectory corresponds to 12.1 m/s per GAM (99% values).
- The largest Delta-V required for a single correction occurs for TCM42 at the post-flyby manoeuvre of GAM-V7 with up to 27.3 m/s. Since this TCM has to be implemented in Type-II mode, it will be affected by the propellant management device (PMD) constraints. In the real operations such a large manoeuvre will have to be split in a number of burns. It is advisable to improve the robustness of these operations by following TCM42 implementation with an OD campaign and an additional clean-up TCM some days later. Numerical analysis has shown an improvement of the next GAM navigation by allowing a fast correction of execution errors or underperformances of TCM42 with no Delta-V penalty.



Event	TCM #	Time	Target	Type	Delta-V (m/s)						
					Deter.	Mean	1-σ	95%	99%	Sum 95%	Sum 99%
V1	TCM3	V1 - 112 d	V1	2		0.03	0.02	0.06	0.07		
V1	TCM4	V1 - 14 d	V1	2		0.22	0.15	0.51	0.67		
V1	TCM5	V1 - 7 d	V1	2		0.06	0.04	0.13	0.17		
V1	TCM6	V1 - 3 d	V1	2		0.10	0.07	0.23	0.31		
V1	TCM7	V1 + 7 d	V2	2		1.26	0.95	3.10	4.09	4.04	5.31
V2	TCM8	V2 - 165 d	V2	2	0.07	0.07	0.01	0.09	0.10		
V2	TCM9	V2 - 14 d	V2	2		0.38	0.26	0.89	1.16		
V2	TCM10	V2 - 7 d	V2	2		0.04	0.03	0.09	0.12		
V2	TCM11	V2 - 3 d	V2	2		0.08	0.05	0.18	0.24		
V2	TCM12	V2 + 7 d	V3	2		1.87	1.42	4.62	6.04	5.86	7.66
V3	TCM13	V3 - 162 d	V3	2	2.57	2.57	0.02	2.60	2.61		
V3	TCM14	V3 - 14 d	V3	2		0.51	0.36	1.21	1.59		
V3	TCM15	V3 - 7 d	V3	2		0.03	0.02	0.06	0.07		
V3	TCM16	V3 - 3 d	V3	2		0.04	0.03	0.10	0.13		
V3	TCM17	V3 + 7 d	E1	2		1.85	1.16	4.11	5.38	8.07	9.77
E1	TCM18	E1 - 30 d	E1	1		0.28	0.19	0.65	0.86		
E1	TCM19	E1 - 14 d	E1	1		0.03	0.02	0.06	0.08		
E1	TCM20	E1 - 7 d	E1	1		0.02	0.01	0.05	0.06		
E1	TCM21	E1 - 3 d	E1	1		0.03	0.01	0.05	0.07		
E1	TCM22	E1 + 7 d	V4	1		2.17	1.13	4.28	5.42	5.09	6.48
V4	TCM23	V4 - 111 d	V4	2	0.33	0.34	0.04	0.41	0.44		
V4	TCM24	V4 - 14 d	V4	2		0.23	0.15	0.52	0.68		
V4	TCM25	V4 - 7 d	V4	2		0.05	0.03	0.11	0.15		
V4	TCM26	V4 - 3 d	V4	2		0.06	0.04	0.15	0.19		
V4	TCM27	V4 + 7 d	V5	2		1.54	1.16	3.79	4.98	4.97	6.43
V5	TCM28	V5 - 265 d	V5	2	1.92	1.93	0.02	1.97	1.99		
V5	TCM29	V5 - 14 d	V5	2		0.57	0.40	1.36	1.79		
V5	TCM30	V5 - 7 d	V5	2		0.04	0.03	0.09	0.12		
V5	TCM31	V5 - 3 d	V5	2		0.06	0.04	0.15	0.19		
V5	TCM32	V5 + 7 d	V6	2		1.06	0.80	2.60	3.44	6.17	7.53
V6	TCM33	V6 - 89 d	V6	2	0.66	0.68	0.03	0.73	0.76		
V6	TCM34	V6 - 14 d	V6	2		0.16	0.10	0.36	0.47		
V6	TCM35	V6 - 7 d	V6	2		0.04	0.02	0.08	0.11		
V6	TCM36	V6 - 3 d	V6	2		0.06	0.04	0.14	0.18		
V6	TCM37	V6 + 7 d	V7	2		4.30	3.24	10.54	13.89	11.85	15.41
V7	TCM38	V7 - 97 d	V7	2	0.11	0.19	0.09	0.38	0.49		
V7	TCM39	V7 - 14 d	V7	2		0.18	0.12	0.41	0.54		
V7	TCM40	V7 - 7 d	V7	2		0.05	0.04	0.13	0.16		
V7	TCM41	V7 - 3 d	V7	2		0.11	0.07	0.25	0.33		
V7	TCM42	V7 + 7 d	V8	2		8.48	6.39	20.79	27.29	21.96	28.81
V8	TCM43	V8 - 96 d	V8	2	0.53	0.65	0.15	0.97	1.18		
V8	TCM44	V8 - 14 d	V8	2		0.19	0.12	0.43	0.56		
V8	TCM45	V8 - 7 d	V8	2		0.04	0.03	0.09	0.12		
V8	TCM46	V8 - 3 d	V8	2		0.07	0.05	0.17	0.22		
V8	TCM47	V8 + 7 d	V9	2		6.04	4.55	14.81	19.45	16.47	21.54
Sum of all TCM – LIC					6.2					84.5	108.9
Required Delta-V per GAM					0.7					9.4	12.1

Table 5-6 Navigation analysis: TCM Delta-V statistics (DDOR Cebreros-Malargüe only)



Table 5-7 shows the achieved B-plane delivery errors after the implementation of each of the TCMs. The errors are represented by the dimensions of the error ellipse projected on the B-plane, SMA – semimajor axis and SMI – semiminor axis, the angle θ measured between the semimajor axis of the ellipse and the radial direction, and the linearized time of flight (LTF), which gives the error perpendicular to the B-plane, i.e. along the incoming infinite velocity vector. In addition the table also includes the error of the pericentre altitude at the swing-by pass. All the values in the table are 3- σ .

The B-plane delivery accuracy achieved at the Earth GAM is in the order of 9 km SMA even in the absence of DDOR measurements on the approach to the Earth. The pericentre radius error is 5 km after the last targeting manoeuvre TCM21 at GAM-E1 - 3 days. Right before this manoeuvre and after TCM20 at GAM - 7 days the delivery errors are about twice as large, with a pericentre radius error of 9.4 km. These results confirm the proposed approach of not using DDOR measurements for the Earth GAM.

The delivery accuracy at the Venus GAMs is such that after the last pre-GAM TCM at GAM – 3 days the pericentre radius error ranges between 5 and 27 km. Thus there is in any case a comfortable margin between the 350 km target and the 300 km spacecraft design limit. The delivery accuracy after the TCM at GAM – 7 days ranges from 9 to 35 km and after the TCM at GAM – 14 days from 14 to 49 km, being the worst case always at GAM-V5 for which a nominal target altitude of 350 km is required. Consequently, it is ensured in all cases that after the implementation of the TCM at GAM – 14 days the spacecraft is in a ballistic trajectory that in nominal conditions is compatible with the 300 km design limit. This could be not true in the case of an anomalous situation that introduces a parasitic Delta-V perturbation such as an ultimate safe-mode or a contingency due to stuck-on thruster.



Event	TCM #	Time	Target	3- σ Errors Pericentre (km)	3- σ B-plane Delivery Errors			
					SMA (km)	SMI (km)	θ (deg)	LTF (s)
LIC	TCM1	L + 5 d	V1	2109.2	3732.6	315.2	-124.5	0.276
LIC	TCM2	L + 20 d	V1	315.4	480.5	68.4	-130.9	0.270
V1	TCM3	V1 - 112 d	V1	158.5	231.1	31.1	-133.3	0.270
V1	TCM4	V1 - 14 d	V1	16.4	68.3	16.5	-89.8	0.285
V1	TCM5	V1 - 7 d	V1	14.7	51.5	13.3	-82.3	0.285
V1	TCM6	V1 - 3 d	V1	12.4	43.3	7.6	-76.55	0.285
V1	TCM7	V1 + 7 d	V2	40.9	1464.8	9.50	-91.6	0.417
V2	TCM8	V2 - 165 d	V2	68.6	539.0	68.5	-91.3	0.417
V2	TCM9	V2 - 14 d	V2	15.2	53.3	15.2	-87.6	0.417
V2	TCM10	V2 - 7 d	V2	14.0	47.3	13.8	-86.1	0.417
V2	TCM11	V2 - 3 d	V2	9.6	42.9	8.9	-84.8	0.417
V2	TCM12	V2 + 7 d	V3	1504.9	2089.4	13.6	-42.4	0.264
V3	TCM13	V3 - 162 d	V3	1221.9	1589.8	141.1	-38.2	0.264
V3	TCM14	V3 - 14 d	V3	13.8	38.2	13.5	-96.8	0.324
V3	TCM15	V3 - 7 d	V3	9.2	29.6	7.3	-102.2	0.324
V3	TCM16	V3 - 3 d	V3	5.1	23.9	2.7	-101.0	0.324
V3	TCM17	V3 + 7 d	E1	1608.8	1984.5	101.0	-28.6	0.051
E1	TCM18	E1 - 30 d	E1	41.4	91.7	41.3	-102.6	0.090
E1	TCM19	E1 - 14 d	E1	17.6	35.3	16.4	-107.9	0.090
E1	TCM20	E1 - 7 d	E1	9.4	18.0	8.9	-109.5	0.090
E1	TCM21	E1 - 3 d	E1	4.8	9.0	4.5	68.9	0.090
E1	TCM22	E1 + 7 d	V4	823.4	1504.7	457.3	-119.0	0.012
V4	TCM23	V4 - 111 d	V4	262.3	490.8	87.5	-121.2	0.012
V4	TCM24	V4 - 14 d	V4	19.6	20.7	12.8	-158.0	0.015
V4	TCM25	V4 - 7 d	V4	9.9	11.4	4.3	-31.2	0.015
V4	TCM26	V4 - 3 d	V4	6.8	8.4	1.3	-36.0	0.015
V4	TCM27	V4 + 7 d	V5	1474.2	3153.7	10.7	-118.2	0.066
V5	TCM28	V5 - 265 d	V5	400.7	1024.8	99.6	-112.6	0.066
V5	TCM29	V5 - 14 d	V5	49.2	52.9	13.5	-159.3	0.072
V5	TCM30	V5 - 7 d	V5	35.3	38.0	7.9	-159.2	0.072
V5	TCM31	V5 - 3 d	V5	26.7	28.8	3.8	-159.3	0.072
V5	TCM32	V5 + 7 d	V6	172.5	1795.1	8.2	-95.6	0.483
V6	TCM33	V6 - 89 d	V6	75.9	327.0	64.3	-82.5	0.480
V6	TCM34	V6 - 14 d	V6	24.5	36.2	15.0	-126.6	0.483
V6	TCM35	V6 - 7 d	V6	15.6	29.1	11.6	-113.4	0.480
V6	TCM36	V6 - 3 d	V6	7.1	22.5	6.5	-98.3	0.480
V6	TCM37	V6 + 7 d	V7	2395.2	4692.2	30.3	-121.0	0.414
V7	TCM38	V7 - 97 d	V7	131.6	320.0	30.8	-113.9	0.411
V7	TCM39	V7 - 14 d	V7	27.5	78.4	13.5	-108.3	0.411
V7	TCM40	V7 - 7 d	V7	21.3	68.2	10.5	-106.1	0.411
V7	TCM41	V7 - 3 d	V7	17.4	60.4	6.7	-105.7	0.411
V7	TCM42	V7 + 7 d	V8	3916.1	11212.3	59.9	-69.4	0.582
V8	TCM43	V8 - 96 d	V8	210.0	415.3	52.0	-60.1	0.576
V8	TCM44	V8 - 14 d	V8	25.6	62.7	13.3	-111.3	0.576
V8	TCM45	V8 - 7 d	V8	12.8	46.9	9.9	-100.6	0.576
V8	TCM46	V8 - 3 d	V8	7.0	40.5	5.6	-96.2	0.576
V8	TCM47	V8 + 7 d	V9	388.1	6986.1	42.3	93.2	0.621

Table 5-7 Navigation analysis: B-plane delivery errors (DDOR Cebreros-Malargüe only)



B-Plane Error Ellipses

The following figures show a collection of plots of the 3- σ B-plane error ellipses achieved after the last TCM before each GAM considering all 4 DDOR measurements scenarios. The X-direction in the plots is defined by the intersection of the B-plane with the Mean Earth Equator of J2000.0. A line from the centre of the planet to the target in the B-plane has been drawn representing the radial direction. In order to visualize the error in the pericentre altitude, curves of equal pericentre radial error at fixed steps have been mapped into the B-plane and included in the plot. The radial error between two of these lines is given on the plot.

For each DDOR measurement case, 2 ellipses are provided corresponding to the regarded values of NGA. The thicker line shows the 1.E-11 km/s² NGA level, while the thinner line shows the 2.E-11 km/s² NGA level. Generally, due to the larger dynamical noise, the second ellipses are larger and contain the first ones.

The B-plane delivery ellipses for GAM-V1 perfectly illustrate the effect of DDOR measurements. From each DDOR baseline the measurements provide very accurate information in a specific direction of the plane of the sky. This reduces the error ellipsoid in this direction such that when mapped onto the B-plane it is seen as an improvement of the error ellipse in one direction with respect to the no DDOR case. In the other direction the errors remain approximately the same.

The two ESA DDOR baselines are located in almost perpendicular directions on the Earth. Therefore each baseline improves the OD accuracy in a different direction. When including both DDOR baselines the benefit in both directions is combined resulting in a smaller error ellipse that is confined approximately by the two ellipses of the single DDOR cases.

From the figure it is seen that the pericentre altitude 3- σ error is large when using only Range and Doppler measurements. DDOR measurements from Cebreros-Malargüe improve the accuracy mostly in the radial direction. When both DDOR baselines are considered the pericentre error is reduced to about 9 km.

Similar trends are observed for the rest of Venus GAMs.

Figure 5-2 shows the B-plane delivery ellipses for GAM-E1 comparing the 4 DDOR scenarios. In this case it is seen that the Range & Doppler measurements are good enough to provide good navigation accuracy in the order of a few km. Only a reduced improvement can be achieved by adding DDOR measurements.

Figure 5-3 shows a case with very elongated B-plane delivery ellipses for GAM-V4. DDOR from Cebreros-Malargüe is in this case very effective in reducing the radial component of the error.

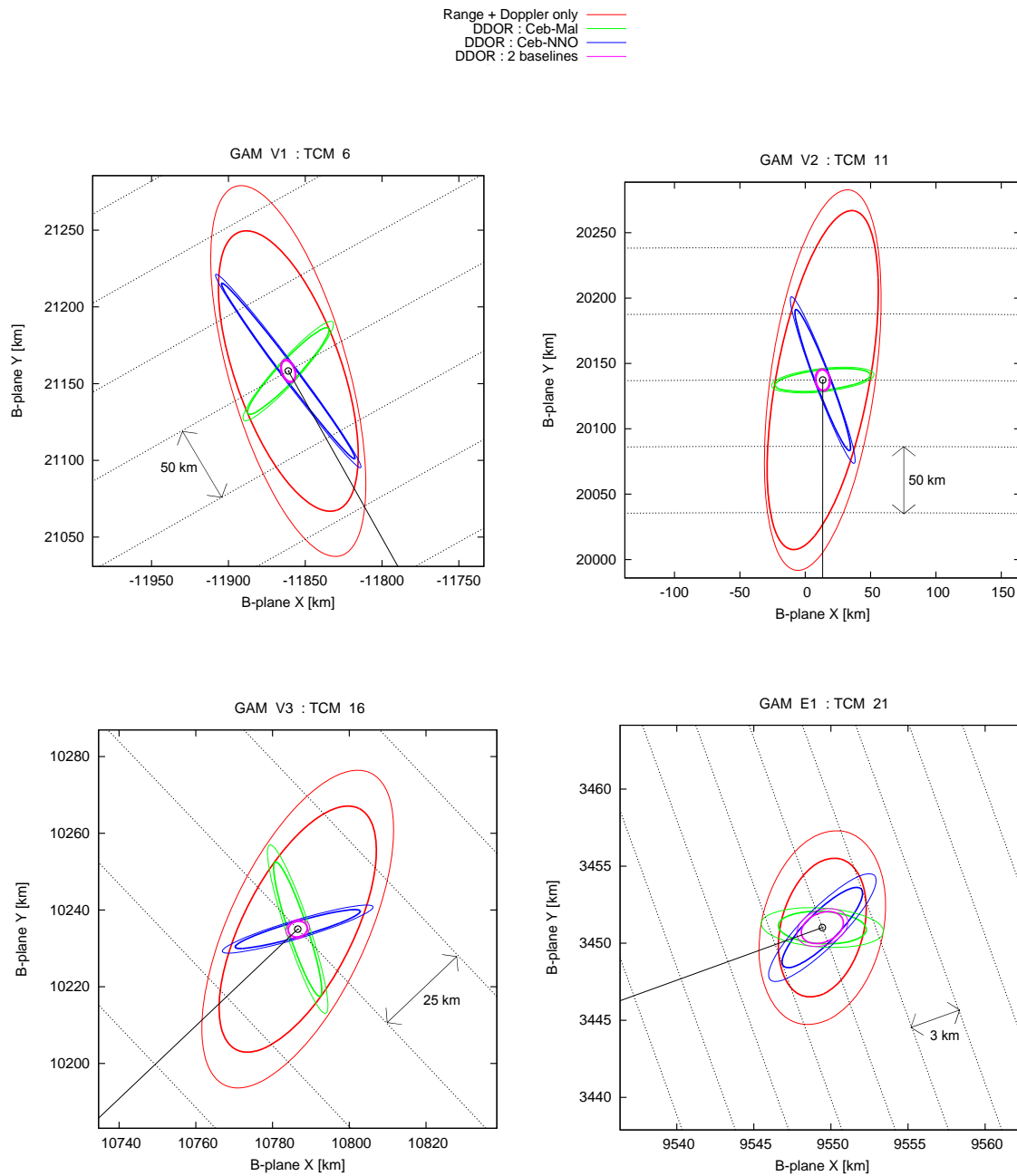


Figure 5-2 B-plane 3- σ delivery ellipses for GAM-V1 to GAM-E1



Range + Doppler only
 DDOR : Ceb-Mal
 DDOR : Ceb-NNO
 DDOR : 2 baselines

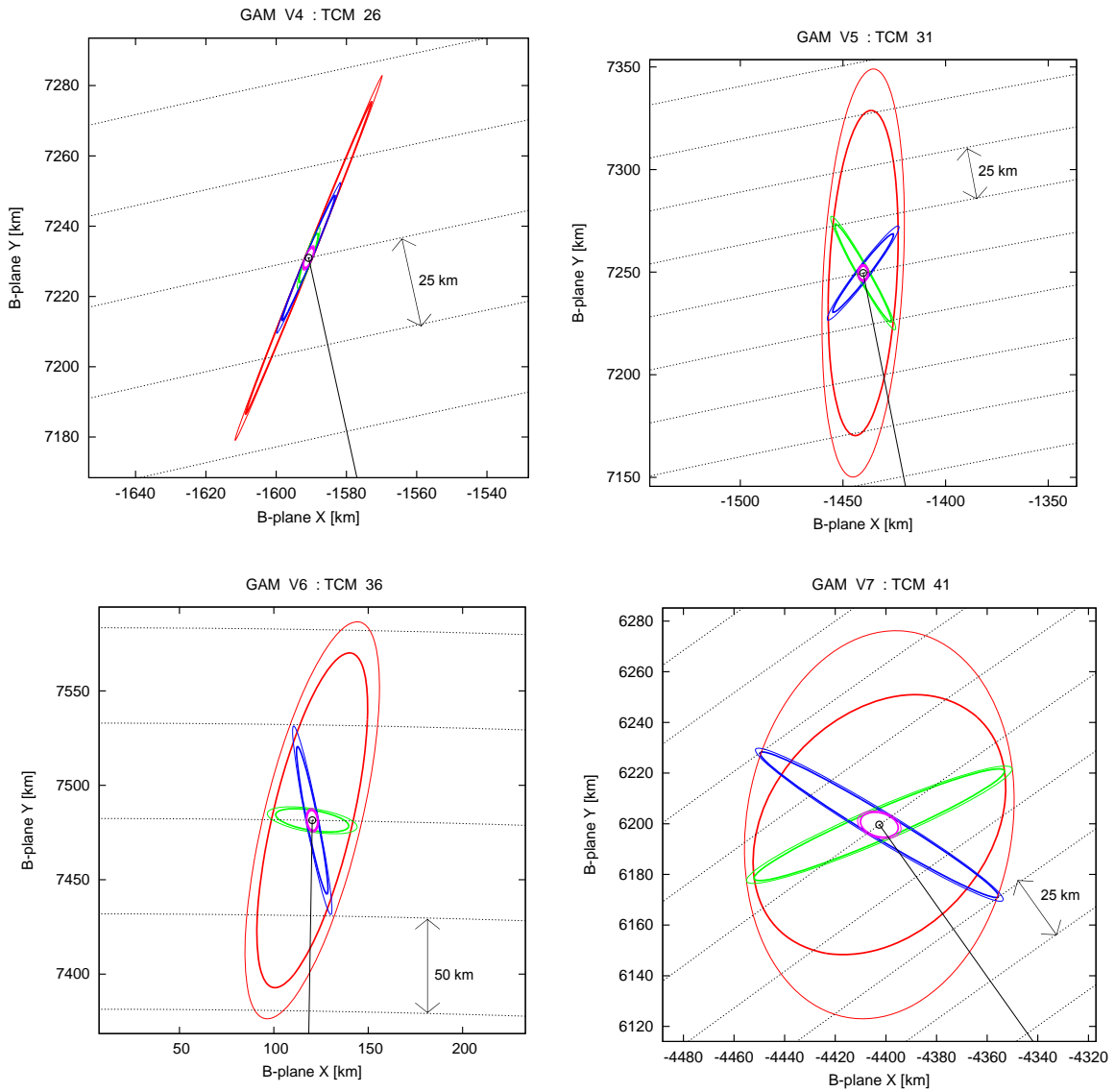


Figure 5-3 B-plane 3- σ delivery ellipses for GAM-V4 to GAM-V7

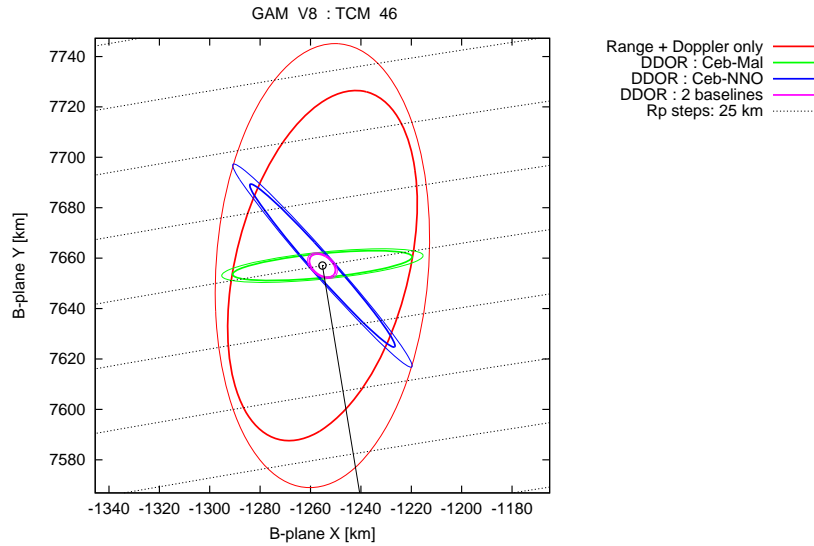
Figure 5-4 B-plane 3- σ delivery ellipses for GAM-V8

Table 5-8 summarizes the Delta-V required for the 4 different measurements scenarios. The table includes the accumulated Delta-V of the 95-th and 99-th percentiles of the TCMs related to the navigation of each GAM. The benefit of DDOR measurements to save Delta-V is clear. Without DDOR the Delta-V required per GAM lies at almost 23 m/s (at 99%, for 9 GAMs). This would exceed the current Delta-V budget planned allocation of 15 m/s per GAM. Thus, the use of the DDOR technique is critical for the mission not only to ensure safe Venus swing-bys as mentioned above, but also to maintain a low ΔV allocation.

GAM	Sum of the Delta-V (m/s)							
	NO DDOR		DDOR only Ceb-NNOR		DDOR only Ceb-Malargüe		DDOR Both: Ceb-NNor & Ceb-Mal	
	Sum 95%	Sum 99%	Sum 95%	Sum 99%	Sum 95%	Sum 99%	Sum 95%	Sum 99%
V1	6.77	8.82	3.61	4.73	4.04	5.31	1.41	1.84
V2	6.98	9.17	4.27	5.58	5.86	7.66	2.18	2.83
V3	15.93	19.60	9.73	11.95	8.07	9.77	5.31	6.07
E1	9.36	12.09	5.87	7.32	5.09	6.48	4.71	6.06
V4	24.54	32.20	10.70	13.94	4.97	6.43	3.09	3.95
V5	27.61	35.90	15.72	19.99	6.17	7.53	5.97	7.25
V6	16.60	21.72	7.94	10.27	11.85	15.41	3.25	4.08
V7	30.00	39.49	5.46	7.20	21.96	28.81	3.64	4.77
V8	20.53	27.04	18.03	23.52	16.47	21.54	4.27	5.46
Total	158.31	206.03	81.31	104.51	84.47	108.94	33.83	42.30
Total per GAM	17.59	22.89	9.03	11.61	9.39	12.10	3.76	4.70

Table 5-8 Navigation analysis: accumulated Delta-V statistics

In this respect both scenarios with DDOR from only one baseline yield very similar results, with Cebreros-Malargüe requiring just slightly higher Delta-V per GAM. By using DDOR from both baselines the required Delta-V goes down to about 5 m/s per GAM, halving the Delta-V required when only one DDOR baseline is used. All the previous values are at 99% level and assume navigation performed under the nominal conditions.



Table 5-9 provides a summary of the B-plane delivery errors for the 4 measurements scenarios. The values given in the table correspond to the mapping onto the B-plane of the dispersions after the implementation of the last manoeuvre 3-days before each GAM.

3- σ B-plane Delivery Errors & Pericentre Errors					
		NO DDOR	DDOR only Ceb-NNOR	DDOR only Ceb-Mal	DDOR Both: Ceb-NNor & Ceb-Mal
V1	SMA (km)	93.76	71.81	43.26	8.19
	SMI (km)	40.09	5.96	7.64	5.52
	θ (deg)	-192.2	-171.9	-76.5	-194.6
	LTF (s)	0.303	0.297	0.285	0.285
	Peri. (km)	91.09	70.31	12.45	7.95
V2	SMA (km)	131.77	58.60	42.87	8.94
	SMI (km)	41.46	7.64	8.94	6.95
	θ (deg)	-12.9	-155.8	-84.8	-173.2
	LTF (s)	1.734	1.548	0.417	0.294
	Peri. (km)	126.98	52.82	9.56	8.78
V3	SMA (km)	39.11	17.92	23.91	3.43
	SMI (km)	18.08	4.18	2.66	2.66
	θ (deg)	40.9	-21.2	-101.0	-90.8
	LTF (s)	2.370	1.173	0.324	0.270
	Peri. (km)	30.99	16.31	5.07	2.53
E1	SMA (km)	9.58	9.09	8.98	8.93
	SMI (km)	5.06	4.66	4.51	4.48
	θ (deg)	62.1	67.3	68.9	69.3
	LTF (s)	0.204	0.102	0.090	0.054
	Peri. (km)	4.83	4.83	4.83	4.83
V4	SMA (km)	52.16	20.99	8.41	4.20
	SMI (km)	1.34	1.25	1.30	1.27
	θ (deg)	-38.3	-39.6	-36.0	-39.1
	LTF (s)	0.030	0.018	0.015	0.015
	Peri. (km)	40.51	16.04	6.76	3.32
V5	SMA (km)	79.01	26.22	28.82	4.44
	SMI (km)	19.71	3.78	3.84	3.47
	θ (deg)	-16.7	-54.1	-159.3	-18.9
	LTF (s)	0.330	0.135	0.072	0.051
	Peri. (km)	75.08	15.50	26.72	4.30
V6	SMA (km)	90.62	39.72	22.49	6.67
	SMI (km)	24.62	4.12	6.48	3.92
	θ (deg)	-14.5	-165.9	-98.3	-171.6
	LTF (s)	1.242	0.258	0.480	0.099
	Peri. (km)	87.05	38.15	7.11	6.55
V7	SMA (km)	64.85	54.05	60.36	8.93
	SMI (km)	43.29	6.44	6.73	5.75
	θ (deg)	-85.0	-159.7	-105.7	-136.5
	LTF (s)	1.710	0.552	0.411	0.135
	Peri. (km)	43.05	50.23	17.42	7.52
V8	SMA (km)	71.42	43.88	40.53	7.30
	SMI (km)	37.87	5.04	5.64	4.66
	θ (deg)	-33.0	-146.7	-96.2	-129.4
	LTF (s)	1.965	1.002	0.576	0.195
	Peri. (km)	62.73	36.42	7.00	5.81

Table 5-9 Navigation analysis: B-plane delivery errors

Since the majority of the navigation Delta-V has to be performed at the clean-up manoeuvres 7 days after each GAM, it is interesting to observe the probability distributions of the Delta-V Sun aspect angle. This aspect angle has a direct impact on the propellant required for the manoeuvre as it drives the manoeuvre efficiency for Type-2 burns.

Figure 5-5 shows these distributions based on Monte Carlo analysis with 100000 shots for all the Venus GAMs. The Sun aspect angle for the clean-up TCMs is not close to an isotropic distribution. Instead 2 directions are typically very dominant as seen by the peaks in the probability density. These directions typically lie between 60-80 deg and 100-120 deg, which correspond to direction for which the Solar Orbiter thrusters configuration provides a reduced efficiency.

Currently the effective Delta-V and propellant allocations calculated by industry are based on isotropic Delta-V distributions. The impact of the real distributions on those allocations needs to be assessed.

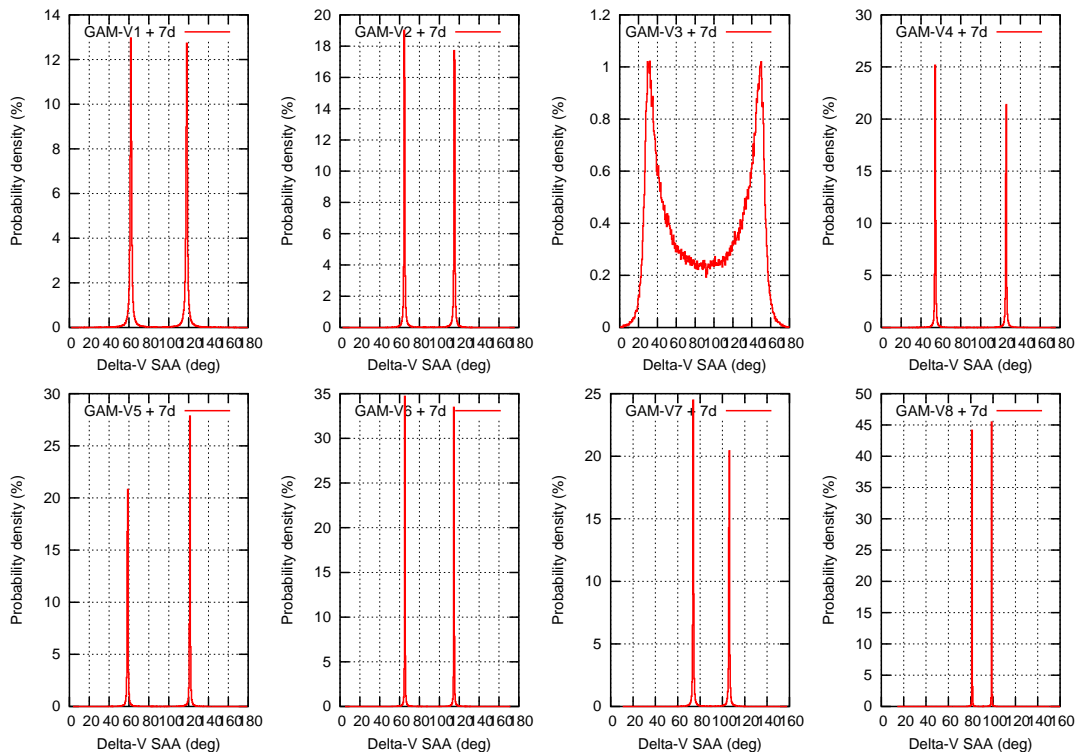


Figure 5-5 Delta-V Sun aspect angle distributions for post-GAM clean-up TCMs



5.3.1 IMPACT OF INCREASED DYNAMIC NOISE

A parameter that is determinant for the accuracy and propellant requirements of the navigation is the level of dynamic noise. As stated above non-gravitational accelerations have been modelled as exponentially correlated random noise in order to include the effect of dynamic perturbations mainly due to the residual Delta-V of wheel-offloadings. The magnitude of the NGA errors of 10^{-11} km/s² is representative of a residual ΔV of 1.0 mm/s, which is in line with the operational experience of previous ESA interplanetary missions with force-free RCS, i.e. Rosetta.

A first assessment of the sensitivity of the navigation results to the dynamic noise has been carried out. For the three DDOR scenarios, the entire analysis has been repeated for a NGA $1-\sigma$ value of $2 \cdot 10^{-11}$ km/s². This could be considered a more conservative value to account for the lower mass of the Solar Orbiter S/C compared to Rosetta and to account for the fact that average Solar Orbiter WOL's at closer Sun distances will have a bigger size in terms of angular momentum compared to Rosetta.

Table 5-10 shows the Delta-V results of this analysis in the same way as Table 5-8. When considering the increased value of the NGA the resulting Delta-V required for the navigation of Solar Orbiter experiences an increase of about 25% for the 1 DDOR baseline cases and about 40% for the 2 DDOR baselines case. The Delta-V per GAM with only 1 DDOR baseline is just below the 15 m/s allocated in the Delta-V budget, while for 2 DDOR baselines about 6.4 m/s per GAM are required (all 99% values).

Therefore, the dynamic noise introduced by the residuals of the wheel-offloadings is driving the Delta-V required for an adequate navigation of Solar Orbiter. At this stage of the mission design it is considered adequate to base the navigation analysis on the baseline NGA value of 10^{-11} km/s² in line with previous ESA missions. The Solar Orbiter spacecraft shall be designed such as to minimize the residual Delta-V effect of wheel off-loadings. If the spacecraft is eventually incompatible with this level of NGA, the entire navigation analysis shall be revisited.

Sum of the Delta-V (m/s)						
GAM	DDOR only Ceb-NNOR		DDOR only Ceb-Malargüe		DDOR Both: Ceb-NNor & Ceb-Mal	
	Sum 95%	Sum 99%	Sum 95%	Sum 99%	Sum 95%	Sum 99%
V1	4.43	5.82	4.97	6.54	2.00	2.62
V2	5.74	7.51	7.12	9.33	3.38	4.41
V3	11.57	14.33	9.95	12.21	6.38	7.42
E1	7.86	9.83	7.20	9.21	6.76	8.71
V4	13.48	17.65	6.62	8.57	4.10	5.27
V5	19.69	25.25	8.50	10.60	8.30	10.33
V6	10.45	13.60	15.11	19.73	4.12	5.24
V7	7.14	9.39	24.17	31.91	4.70	6.14
V8	23.20	30.46	19.30	25.23	5.50	7.13
Total	103.55	133.83	102.94	133.32	45.23	57.28
Total per GAM	11.51	14.87	11.44	14.81	5.03	6.36

Table 5-10 Navigation analysis: accumulated Delta-V statistics for increased NGA of $2 \cdot 10^{-11}$ km/s²



3-σ B-plane Delivery Errors & Pericentre Errors				
		DDOR only Ceb-NNOR	DDOR only Ceb-Mal	DDOR Both: Ceb-NNor & Ceb-Mal
V1	SMA (km)	80.73	50.12	9.91
	SMI (km)	7.38	9.14	6.72
	θ (deg)	-172.5	-75.4	-197.4
	LTF (s)	0.321	0.303	0.303
	Peri. (km)	79.15	15.36	9.55
V2	SMA (km)	71.48	47.57	10.71
	SMI (km)	8.99	10.77	8.55
	θ (deg)	-155.9	-84.8	-168.7
	LTF (s)	1.734	0.450	0.312
	Peri. (km)	64.47	11.36	10.47
V3	SMA (km)	22.26	30.87	4.43
	SMI (km)	5.32	3.40	3.41
	θ (deg)	-20.4	-101.0	-97.2
	LTF (s)	1.401	0.408	0.348
	Peri. (km)	20.37	6.55	3.27
E1	SMA (km)	12.68	12.59	12.54
	SMI (km)	6.71	6.56	6.52
	θ (deg)	69.7	-109.1	-108.8
	LTF (s)	0.132	0.120	0.078
	Peri. (km)	6.79	6.79	6.79
V4	SMA (km)	25.87	10.97	5.35
	SMI (km)	1.66	1.73	1.67
	θ (deg)	-39.7	-35.6	-39.1
	LTF (s)	0.027	0.024	0.021
	Peri. (km)	19.73	8.87	4.23
V5	SMA (km)	32.21	33.89	5.70
	SMI (km)	4.80	4.88	4.31
	θ (deg)	-53.5	-159.6	-18.3
	LTF (s)	0.171	0.102	0.078
	Peri. (km)	19.32	31.49	5.51
V6	SMA (km)	53.02	28.68	8.15
	SMI (km)	5.12	8.00	4.89
	θ (deg)	-165.9	-97.5	-172.1
	LTF (s)	0.324	0.567	0.135
	Peri. (km)	50.93	8.69	8.01
V7	SMA (km)	58.76	65.83	10.93
	SMI (km)	7.80	8.09	6.87
	θ (deg)	-160.1	-106.1	-136.4
	LTF (s)	0.726	0.489	0.177
	Peri. (km)	54.74	19.68	9.13
V8	SMA (km)	56.88	47.01	8.85
	SMI (km)	6.14	6.74	5.58
	θ (deg)	-147.1	-96.1	-127.9
	LTF (s)	1.170	0.672	0.255
	Peri. (km)	47.39	8.23	6.92

Table 5-11 Navigation analysis: B-plane delivery errors for increased NGA of $2 \cdot 10^{-11} \text{ km/s}^2$



5.3.2 DISPERSION OF THE SCIENCE ORBITS

Of interest for the science phase is the effect of the navigation errors in the orbit after the navigation of a GAM. Table 5-12 provides the errors in the perihelion radius and the solar inclination achieved after the post-swingby TCM at each GAM for the two levels of NGA disturbances considered in the navigation analysis.

For GAM-V3 it is more interesting to look at the aphelion radius since this is the arc in the trajectory with the maximum Sun-spacecraft distance (nominally 1.124 AU). The results show that the expected dispersion of the aphelion radius is below $3 \cdot 10^{-5}$ AU ($3\text{-}\sigma$).

For the rest of the GAMs the table provides the perihelion error. The lowest nominal perihelion radius close to the 0.28 AU constraint is encountered after GAM-V5. The maximum dispersion of the perihelion radius is 0.00063 AU ($3\text{-}\sigma$), for the pessimistic scenario of no DDOR and NGA of $2\text{E-}11$ km/s². In all cases with DDOR the perihelion dispersion is below 0.0002 AU ($3\text{-}\sigma$). As a minimum this margin will have to be added in the final trajectory computations such as to avoid that the spacecraft gets closer to the Sun than the 0.28 AU design limit. This is a very small trajectory adjustment that has no impact to the results of the previous chapters.

Regarding the solar inclination achieved by the science orbits, the expected dispersions are in any case lower than 0.1 deg ($3\text{-}\sigma$) with no DDOR and lower than 0.04 deg ($3\text{-}\sigma$) in the cases with DDOR. This small dispersion is not expected to produce any impact to the mission science.

GAM		3-σ Error	NO DDOR		DDOR only Ceb-NNOR		DDOR only Ceb-Mal		DDOR Both: Ceb-NNor & Ceb-Mal		
NGA = 1.E-11 km/s2											
V1	TCM7	Rper (10-3 AU) / is (deg)	0.02	0.011	0.02	0.010	0.02	0.003	0.01	0.002	
V2	TCM12	Rper (10-3 AU) / is (deg)	0.17	0.028	0.08	0.014	0.02	0.003	0.02	0.003	
V3	TCM17	Rapo (10-3 AU) / is (deg)	0.02	0.014	0.01	0.007	0.01	0.004	0.00	0.002	
E1	TCM22	Rper (10-3 AU) / is (deg)	0.02	0.002	0.02	0.001	0.02	0.001	0.02	0.001	
V4	TCM27	Rper (10-3 AU) / is (deg)	0.14	0.027	0.07	0.012	0.03	0.006	0.03	0.004	
V5	TCM32	Rper (10-3 AU) / is (deg)	0.48	0.074	0.13	0.014	0.16	0.032	0.06	0.008	
V6	TCM37	Rper (10-3 AU) / is (deg)	0.80	0.077	0.27	0.030	0.19	0.022	0.08	0.008	
V7	TCM42	Rper (10-3 AU) / is (deg)	0.41	0.049	0.21	0.027	0.12	0.029	0.05	0.007	
V8	TCM47	Rper (10-3 AU) / is (deg)	0.05	0.023	0.02	0.011	0.02	0.018	0.01	0.005	
NGA = 2.E-11 km/s ²											
V1	TCM7	Rper (10-3 AU) / is (deg)	0.02	0.014	0.02	0.011	0.02	0.003	0.02	0.002	
V2	TCM12	Rper (10-3 AU) / is (deg)	0.19	0.033	0.10	0.016	0.03	0.004	0.03	0.003	
V3	TCM17	Rapo (10-3 AU) / is (deg)	0.03	0.017	0.01	0.009	0.01	0.005	0.00	0.002	
E1	TCM22	Rper (10-3 AU) / is (deg)	0.03	0.003	0.03	0.002	0.03	0.001	0.02	0.001	
V4	TCM27	Rper (10-3 AU) / is (deg)	0.17	0.032	0.09	0.016	0.04	0.007	0.04	0.005	
V5	TCM32	Rper (10-3 AU) / is (deg)	0.63	0.096	0.17	0.019	0.20	0.038	0.08	0.011	
V6	TCM37	Rper (10-3 AU) / is (deg)	1.02	0.098	0.36	0.041	0.23	0.026	0.12	0.011	
V7	TCM42	Rper (10-3 AU) / is (deg)	0.53	0.060	0.25	0.033	0.14	0.032	0.07	0.009	
V8	TCM47	Rper (10-3 AU) / is (deg)	0.06	0.031	0.03	0.014	0.03	0.020	0.01	0.007	

Table 5-12 Navigation analysis: orbital errors achieved after each GAM



5.3.3 OPERATIONAL APPROACH TO REDUCE MEASUREMENTS

In the real operations it will be convenient to baseline the GAM navigation campaigns with the use of only one DDOR baseline in order to reduce ground station costs. In the previous sections the analysis provides results assuming that only one DDOR baseline is continuously used for all the GAMs throughout the mission. Because the effect of the DDOR measurements depends strongly on the Earth-Venus geometry a large variability of the delivery accuracy and required Delta-V is observed for the different GAMs. Also very different result can be obtained depending on the specific baseline used. For instance, GAM-V7 requires the largest Delta-V over 28 m/s (at 99%) when using only Cebreros-Malargüe DDOR, but using Cebreros-New Norcia it requires much less Delta-V (below 10 m/s).

A strategy is proposed here that relies on the use of only one DDOR baseline at each of the Venus GAMs (no DDOR is used for the Earth GAM) and alternates the use of Cebreros-Malargüe and Cebreros-New Norcia such that the best DDOR baseline in terms of the required Delta-V is used to navigate through the GAM. In the real operations a reduced number of DDOR measurements from the other DDOR baseline might be considered in order to increase the robustness of the navigation process. The number of such measurements will be much less, and the operational costs will be reduced, compared with the full use of both DDOR baselines as assumed in the previous sections.

This “mixed” 1-DDOR-baseline strategy makes use of Cebreros-Malargüe for GAM-V3, -V4, -V5 and -V8 and of Cebreros-New Norcia for GAM_V1, -V2, -V6 and -V7. The results of required Delta-V and navigation accuracy should be the same as presented in the previous section, except because there is a small dependency of each GAM with respect to the previous one. The entire navigation analysis using this strategy has been run for the 2 values of NGA levels, $1 \cdot 10^{-11} \text{ km/s}^2$ and $2 \cdot 10^{-11} \text{ km/s}^2$.

Table 5-13 provides the accumulated 99% Delta-V resulting from the analysis. The values compare well with the results of the previous sections as expected.

Sum of the Delta-V (m/s)					
	DDOR baseline	NGA $1 \cdot 10^{-11} \text{ km/s}^2$		NGA $2 \cdot 10^{-11} \text{ km/s}^2$	
GAM	Ceb+	Sum 95%	Sum 99%	Sum 95%	Sum 99%
V1	NNO	3.61	4.73	4.43	5.82
V2	NNO	4.27	5.58	5.74	7.51
V3	Mal	10.01	12.19	12.03	14.77
E1	-	6.11	7.65	8.14	10.15
V4	Mal	4.98	6.45	6.64	8.62
V5	Mal	6.17	7.52	8.51	10.60
V6	NNO	8.25	10.62	10.71	13.88
V7	NNO	5.92	7.77	7.59	9.97
V8	Mal	16.85	22.00	19.78	25.90
Total		66.2	84.5	83.6	107.2
Total per GAM		7.35	9.4	9.3	11.9

Table 5-13 Navigation analysis: accumulated Delta-V statistics for “Mixed” 1-DDOR-baseline strategy.

Figure 5-6 shows a comparison of the Delta-V required in each of the DDOR scenarios that have been analysed for the 2 levels of NGA. The “mixed” 1-DDOR-baseline strategy provides benefits compared to the single DDOR strategies, as it reduces the maximum Delta-V to be expected (now at GAM-V8) and the average Delta-V per GAM, that gets below 10 m/s and 12 m/s for the NGA of $1 \cdot 10^{-11} \text{ km/s}^2$ and $2 \cdot 10^{-11} \text{ km/s}^2$, respectively. Thus this strategy gives an adequate margin with respect to the current Delta-V allocation of 15 m/s per GAM without requiring the use of both DDOR baselines. The full use



of both DDOR baselines might be justified for GAM-V8, for which a significant Delta-V saving can be achieved.

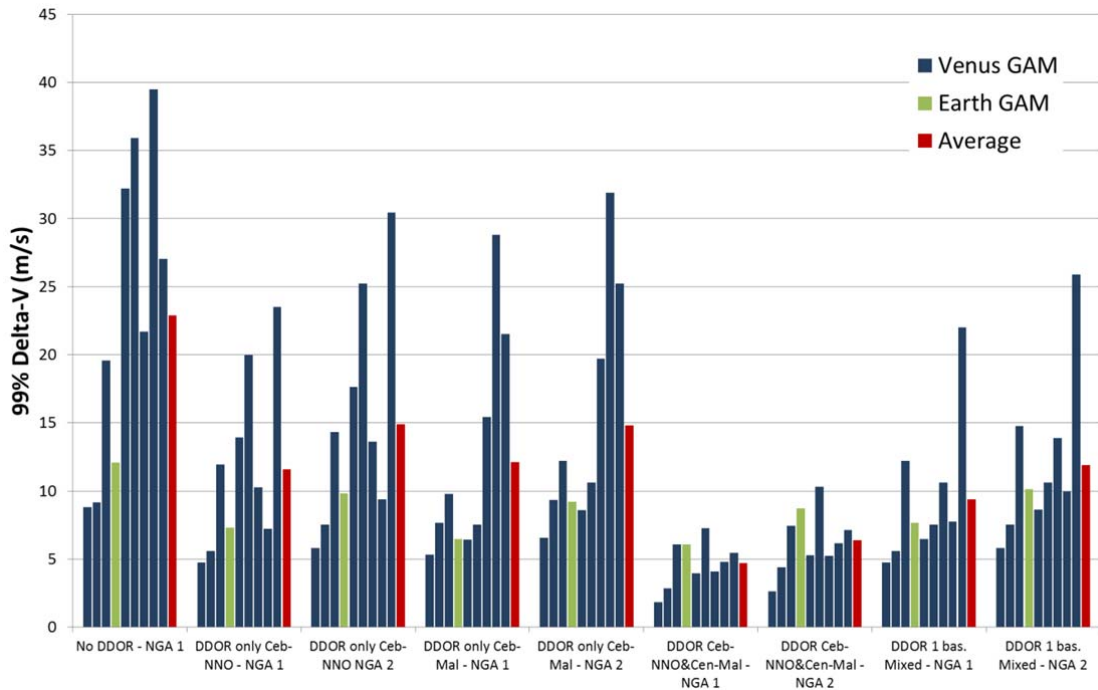


Figure 5-6 Comparison of Delta-V required for the regarded DDOR scenarios

In terms of the B-plane 3- σ delivery ellipses the results are the same as presented in previous sections (Figure 5-2 to Figure 5-4) by applying the corresponding DDOR baseline for each of the GAMs.

5.3.4 CONTINGENCY CASE – THRUSTER FAILURE

This section addresses the navigation of Venus or Earth GAM in the case that the spacecraft suffers a thruster failure. The analysis assumes several failure scenarios depending on the failure of spacecraft thrusters 1 to 8 (providing thrust mainly in the $\pm X_{sc}$ axes) and thruster 9 (providing thrust mainly in the $-Y_{sc}$ axes) and when the failure occurs.

The parasitic Delta-V magnitudes expected from thruster failure when performing a representative Delta-V manoeuvre of 0.3 m/s are summarised in the table.

Parasitic Delta-V 3- σ (mm/s)	Earth GAM	Venus GAM
Thrusters 1-8	75	66
Thruster 9	117	113

Table 5-14 Parasitic Delta-V for thruster failure

The considered failure & recovery scenarios are described by the following:

- Scenario A.1: Failure of thruster 1-8 during a WOL just before TCM at GAM -7 days followed by safe-mode. Not possible to recover the spacecraft fast enough to perform TCM at GAM -3 days. The clean-up TCM at GAM +7 days is performed.



- Scenario A.2: Failure of thruster 1-8 during a WOL just before TCM at GAM -7 days followed by safe-mode, spacecraft normal mode recovered in 48 hours. Tracking data during the safe mode is lost. TCMs at GAM -3 days and at GAM +7 days are both performed.
- Scenario A.3: TCM at GAM -7 days nominally implemented. Failure takes place during WOL just before TCM at GAM -3 days. Safe mode follows with no possibility to perform a TCM before the GAM. 48 hours of tracking data are lost. The clean-up TCM at GAM +7 days is performed.
- Scenario B.1: Failure of thruster 9 (stuck open) after implementation of TCM at GAM -7 days followed by safe mode. Not possible to recover the spacecraft fast enough to perform TCM at GAM -3 days. The clean-up TCM at GAM +7 days is performed.
- Scenario B.2: same failure as 3.0, but spacecraft is recovered to normal mode in 48 hours. Tracking data during the safe mode is lost. TCMs at GAM -3 days and at GAM +7 days are both performed.

Scenarios A.# refer to failure of thrusters 1-8. As a worst case this failure is assumed to occur during a WOL just before the manoeuvre and preventing its nominal execution. Scenarios B.# refer to failure of thruster 9, which can only occur during a Delta-V manoeuvre as thruster 9 is not used during WOLs. Completion of the Delta-V manoeuvre is assumed and the parasitic Delta-V is added on top of the manoeuvre execution error. In all the cases the parasitic Delta-V is assumed unknown in direction (isotropic).

The same navigation analysis process has been repeated now considering the above-mentioned failure scenarios. The results of the failure case are provided in terms of the additional Delta-V (of the accumulated 99%) required for the recovery and the delivery accuracy in the periapsis altitude error in Table 5-15. The cases of GAM-E1 and GAM-V5 are regarded, the latter one as it leads to the worst results among all Venus GAMs.

DDOR	CebMal only				CebNNO only				Both : CebMal + CebNNO			
NGA 1-σ	1·10 ⁻¹¹ km/s ²		2·10 ⁻¹¹ km/s ²		1·10 ⁻¹¹ km/s ²		2·10 ⁻¹¹ km/s ²		1·10 ⁻¹¹ km/s ²		2·10 ⁻¹¹ km/s ²	
	DV 99%	3-σ Hp	DV 99%	3-σ Hp	DV 99%	3-σ Hp	DV 99%	3-σ Hp	DV 99%	3-σ Hp	DV 99%	3-σ Hp
	[m/s]	[km]	[m/s]	[km]	[m/s]	[km]	[m/s]	[km]	[m/s]	[km]	[m/s]	[km]
GAM-E1												
A.1	+31.65	46.1	+37.98	53.5	+31.00	46.1	+37.50	53.6	+31.60	46.1	+38.29	53.5
A.2	+0.10	4.5	+0.60	6.6	+0.10	4.5	+0.47	6.6	+0.08	4.5	+0.61	6.6
A.3	+11.48	20.6	+12.72	23.6	+10.72	20.6	+12.21	23.6	+11.45	20.6	+12.87	23.6
B.1	+43.53	66.1	+42.75	67.0	+42.77	66.1	+42.18	67.0	+43.78	66.1	+42.91	67.0
B.2	+0.36	5.0	+0.66	6.9	+0.30	5.0	+0.59	6.9	+0.33	5.0	+0.77	6.9
GAM-V5												
A.1	+23.59	63.7	+26.15	75.8	+23.30	50.9	+29.70	62.5	+23.61	42.8	+26.19	48.7
A.2	+0.09	28.1	+0.26	35.0	+0.17	15.3	+1.93	20.3	+0.09	4.2	+0.20	5.9
A.3	+8.80	39.3	+8.96	46.5	+5.07	24.8	+6.93	30.8	+8.79	19.5	+9.00	22.5
B.1	+39.78	76.1	+38.90	80.0	+30.38	69.8	+29.38	72.0	+39.65	68.1	+38.44	68.9
B.2	+0.19	28.5	+0.30	35.2	+0.30	15.5	+1.95	20.5	+0.30	4.5	+0.33	6.1

Table 5-15 Navigation results in case of thruster failure at GAM-E1 and at GAM-V5



The results of the thruster failure contingency analysis show that additional up to +44 m/s might be required to navigate the GAM in the pessimistic A.1 and B.1 scenarios and the periapsis radius 3-s error might increase up to roughly 80 km. This is due to the fact that in these scenarios no correction manoeuvre is performed before the GAM. In the scenarios in which such a correction takes place, the additional Delta-V and altitude error are significantly smaller.

5.4 Summary

The following conclusions can be derived from the navigation analysis:

- The results demonstrate the feasibility of the navigation of the entire Solar Orbiter trajectory using the operations approach in which TCMs are only executed in the vicinity of the GAMs. Thus during the majority of each orbit the spacecraft will be devoted to its science mission.
- The navigation of the Solar Orbiter trajectory requires the use of DDOR measurements to guarantee the safety of the navigation of Venus GAMs at a nominal target altitude of 350 km and to reduce the stochastic Delta-V required for the navigation TCMs. In addition, DDOR measurements improve the robustness of the navigation and reduce the mission risk.
- The navigation of the Earth GAMs generally does not demand the use of DDOR measurements.
- The best overall results will be obtained by using both ESA DDOR baselines: Cebreros-New Norcia and Cebreros-Malargüe, but the mission design is compatible with the use of only 1 DDOR baseline. In particular, using only the best performing DDOR baseline at each GAM is a recommended approach as it allows reducing the operational cost with minor delivery accuracy or Delta-V impact.
- From the navigation point of view the most demanding case will be GAM-V7 at an Earth distance of 1.62 AU. This GAM leads to the largest B-plane errors and correction Delta-V. In order to improve the navigation of this GAM navigation, the use DDOR measurements from both ESA DDOR baselines is recommended.
- The results presented in this chapter in terms of delivery accuracy and required Delta-V consider the navigation performed under nominal operations in the absence of contingencies, for instance, a safe mode occurring short before a GAM. It is regarded necessary to maintain some margin in the Delta-V allocation to be able to cope with such contingencies in the real operations. The Delta-V allocation of 15 m/s per GAM of the previous CReMA provides a margin of about 25% of the Delta-V required in the worst of the DDOR scenarios (only Cebreros-Malargüe) and is considered in this respect adequate for the Solar Orbiter mission.
- The Delta-V required for the navigation of Solar Orbiter is driven by the level of dynamic noise introduced by the residuals of the spacecraft wheel off-loadings. The current results are provided for wheel off-loading residuals compatible with the operational experience of ESA interplanetary missions with force-free RCS: approx. 1 mm/s per day. Significant Delta-V penalties are expected if the Solar Orbiter spacecraft is not designed in compliance with this level of spacecraft dynamic noise. In particular, for wheel off-loading residuals of 2 mm/s per day the expected increase in Delta-V varies between 25% and 40%.



6 DELTA-V BUDGET

Table 6-1 gives the current status of the Delta-V budget for Solar Orbiter, which considers worst cases for all the items. The total Delta-V budget is maintained with respect to the previous version of this document (CReMA 3.1).

The item Launcher Injection Correction (LIC) has been verified as sufficient using actual covariance matrices of the injection errors as given by the launcher providers.

A correction manoeuvre due to a finite number of flight programs is not needed as the backup launch scenario with Ariane 5 ECA is no longer regarded. The same Delta-V previously allocated to this item is now allocated as a margin to recover from the contingency of thruster failure during the GAM navigation. Section 5.3.4 presents an analysis of this issue and provides an assessment of the required extra Delta-V needed for the recovery. 45 m/s allow recovery from the worst case thruster failure including a small margin.

The item for navigation Delta-V is maintained from previous versions of this document at 120 m/s. The maximum number of GAMs has been increased by 1 to a total of 9 for the 2018 Option E trajectory only, whereas all the other trajectories make use of 8 GAMs (or less) as considered in the previous CReMA. The results of the navigation analysis in Section 5.3 confirm that this allocation is sufficient for the 2018 Option E trajectory even with the use of 1-DDOR baseline per GAM.

This Delta-V budget considers only the pure trajectory change manoeuvres necessary for the mission. Any propellant budget based on it will have to include the effect of all the losses and inefficiencies in the implementation of the Delta-V, i.e. ramp-up losses, efficiency due to thrusters orientation and/or constraints due to the manoeuvre type.

Delta-V Budget Item	(m/s)
Launcher Injection Correction - LIC	25
Launcher Flight Programs	0
GAMs Navigation	120
Contingency (thruster failure)	45
Total	190

Table 6-1 Delta-V Budget



7 CONCLUSIONS

This report summarises the mission analysis results obtained for the Solar Orbiter mission. The Solar Orbiter mission is divided in three major phases:

1. Launch and transfer cruise phase for acquisition of the operational orbit
2. Nominal Science Phase, when scientific requirements for solar observation are satisfied
3. Extended Science Phase, when the inclination of the orbit is further raised

A sequence of Venus and Earth GAMs is necessary to reach Venus with a high relative velocity and optimal conditions for the science mission. During the science and extended mission phases, only GAMs with Venus are used by keeping the spacecraft orbit in resonance with Venus orbit period in order to achieve a solar inclination higher than 32 deg.

The mission design has successfully incorporated the mission constraints: minimum distance to the Sun of 0.28 AU to reuse as much as possible the technologies developed for the Bepi-Colombo mission; the periods of solar conjunction do not interfere with the critical GAM operations; and the duration of communications blackout in safe mode while in the vicinity of a solar conjunction is kept at levels acceptable for the spacecraft design.

The current mission design regards 3 launch opportunities in the 2018 October-November timeframe that are compatible with an Atlas V 411 launch from KSC, and in addition 2 backup launch opportunities to accommodate programmatic delays. Feasible launch periods have been identified as follows:

- Baseline launch:
 1. 2018 Option E: 29 days from 09-22 to 10-20.
 2. 2018 Option D: 31 days from 10-08 to 11-07 (earlier than 10-08 possible).
 3. 2018 October: 48 days from 10-01 to 11-17.
- Backup launch:
 1. 2019 February: 18 days from 02-06 to 02-23.
 2. 2020 February: 19 days from 02-06 to 02-24.

Only one of the baseline trajectories will be finally selected for Solar Orbiter, but the spacecraft design has to be compatible with all the presented options.

All the launch opportunities are based on ballistic trajectories providing long launch periods when large deterministic Delta-V manoeuvres are not required. Small deterministic manoeuvres in the order of 1-4 m/s can be required to produce small adjustments of the trajectory especially between two resonant GAMs with the same body. Overall this is typically less than 10 m/s for the entire trajectory and is considered included in the navigation allocation. The spacecraft will require manoeuvre capability to perform the correction of the launcher injection errors and guidance during the navigation of the GAMs. The overall Delta-V allocation of 190 m/s does not change from the previous version of this document.



7.1 *Requirements applicable to industry*

The specified values that follow are purely coming from the mission analysis calculations of the reference trajectory and do not include margins, qualification factors and safety factors. The rules in the current applicable SSRD [19] shall be considered and the contractor shall derive the required additional factors and specify them in their specifications.

The following provides justifications and explanations for those requirements in the SSRD that are either derived from the mission analysis results or related to the mission design. The formulation of the requirements is as in the current version of the SSRD Issue 3 Rev 5. Whenever there appears a conflict or contradiction between both documents, it is reminded that the applicable requirements are always given in the latest version of the SSRD.

SSRD-MR-0210

The spacecraft shall be able to perform nominal science operations down to at least 0.28AU of the Sun.

This is the minimum distance to guarantee reuse of the Bepi Colombo technology and imposed as a trajectory constraint in the CREMA during the cruise phase and science operational orbits.

SSRD-MR-0215

The spacecraft shall be able to perform nominal science operations in solar orbit with inclinations up to at least 36.5deg (w.r.t. solar equator).

The driving case for this requirement is the 2017 March trajectory of the previous CReMA 3.1 that reaches the largest final solar inclinations.

SSRD-MR-0255

The spacecraft shall be compatible with an overall launch duration from lift-off to separation of 3600s.

The value above has been set to cover Atlas V 411 launch with short coast phase as described in 4.1.

SSRD-MR-0125

The spacecraft shall be capable of providing a total velocity increment of 190m/s over its complete mission.

The overall Delta-V budget required for the mission is maintained from the previous CReMA. This Delta-V does not include allocations for thruster inefficiencies, attitude control or margins. It is responsibility of the contractor to determine the corresponding propellant budget considering the required Delta-V budget and all relevant inefficiency factors.

SSRD-MR-0135

The spacecraft shall be able to perform a launcher dispersion correction maneuver between zero and 20m/s in any celestial direction.

The required Delta-V for this manoeuvre based on the requirements imposed to the launcher providers in the LIRD is justified in section 5.2. The launcher dispersion correction is stochastic and can be in any direction.

Note: the SSRD needs to be updated to the new value of 25 m/s.

SSRD-MR-0260

The spacecraft shall be able to perform a launcher dispersion correction maneuver within 7 days after launch.



In order to limit the propellant required for the launcher dispersion correction, this must be implemented as soon as possible during the LEOP. The 7 days is an upper limit, but in the actual operations the manoeuvre will be performed much earlier, if possible.

SSRD-MR-0265

The spacecraft shall be able to perform Trajectory Correction Maneuvers in any direction at any time during the mission following the first launcher dispersion maneuver and up until decommissioning.

Trajectory correction manoeuvres are required in the vicinity of the GAMs during the entire mission. Section 5.3 and specifically Table 5-5 provides a detailed description of a nominal navigation timeline for a selected trajectory case. This can be taken as guideline too for the other trajectories. From the trajectory analysis in the CReMA and considering launch window variations, TCMs of the nominal navigation timeline are expected at Sun distances from 0.58 AU to 1.1 AU.

SSRD-MR-0270

The spacecraft shall be able to perform trajectory correction maneuvers between zero and up to 30m/s in any direction relative to the sun direction vector during GAM, at a rate of at least 1m/s per hour.

Navigation results show that the Delta-V for a single TCM can reach up to about 27.3 m/s for the post-correction after GAM V7 (Table 5-6). This value might be affected if the dynamic noise perturbing the spacecraft trajectory (non-gravitational accelerations) is larger than expected as shown in section 5.3.1. The requirement calls then for the feasibility to implement such large Delta-V stochastic manoeuvres (in any direction) and within periods of time that do not compromise the safety of the navigation operations.

SSRD-MR-0145

The Spacecraft shall provide an average 15 m/s velocity increment for each GAM (including preparation prior to GAM and correction after GAM), with isotropic probability of direction.

Direct consequence of the navigation analysis of section 5.3, the average Delta-V required for navigating a GAM is 15 m/s and since the required TCMs are stochastic they can be in any direction. As indicated in Figure 5-5 (page 172) the Delta-V for the post-GAM clean-up tends to be concentrated along two directions rather than being isotropically distributed in direction.

SSRD-MR-0275

The spacecraft shall be compatible with a minimum Earth fly-by altitude of 300km.

SSRD-MR-0280

The spacecraft shall be compatible with a minimum Venus fly-by altitude of 300km.

Both requirements above have been set at mission design level as the minimum values that allow maximising the science return while guaranteeing that the GAM can be safely navigated. Plots containing the delivery errors ellipses projected onto the B-plane and indicating the errors in the hyperbola pericentre altitude are provided in section 5.3 for all the GAMs. In order to account for the navigation dispersions the nominal trajectories are actually designed using a minimum fly-by altitude of 350 km.

SSRD-MR-0285

The spacecraft shall be able to operate nominally, with in-situ payload on, through eclipse durations of up to 45min during GAM.

The contractor shall consider in addition the variations of the eclipse duration across the launch window as presented in section 4 and summarised in Table 4-11. The worst case corresponds to the 2018 October trajectory for which currently a longest duration of 32 minutes is expected. This value has no added margin. The requirement covered the worst case of the previous CReMA, which lead to eclipses durations up to 37 min.



SSRD-MR-0290

The spacecraft shall be able to survive out to a distance of 1.47AU from the sun without degradation of the nominal mission.

Considering launch window variations as in Table 4-11 the current maximum distance to the Sun is expected 1.475 AU for the 2018 October trajectory.

SSRD-MR-0295

The spacecraft shall provide nominal mission operations at Earth ranges up to 2AU.

Considering launch window variations as in Table 4-11 the current maximum distance to the Earth is expected 2.02 AU for the 2018 October trajectory.

SSRD-MR-0300

The spacecraft shall be able to continue normal operations with a continuous superior solar conjunction of up to 50 days during cruise or science operations.

Solar conjunctions are here defined as when Sun-Earth-Spacecraft angle is below 3 deg preventing communications through the HGA. Considering launch window variations as in Table 4-11 the longest duration of a single HGA solar conjunction event is 37 days, corresponding to the worst case for launch on 2018 Option E. The requirement adds a margin to this.

SSRD-MR-0305

The spacecraft shall be able to survive loss of communication with Earth due to superior or inferior conjunction for a period of up to 66days.

This is derived from SES limit of 5 deg and SSE limit of 10 deg for the MGA communications black-out in Safe Mode. Considering launch window variations as in Table 4-11 the longest duration of a single MGA solar conjunction event is 64 days for the worst case of the 2018 trajectories (Option E) and 71 days for the 2019/2020 backups. The requirement is thus slightly exceeded.

SSRD-MR-0310

The spacecraft shall be compatible with occultation black-out of up to 35min during GAM.

Considering launch window variations as in Table 4-11 the longest duration of a GAM occultation blackout is 17.3 min, corresponding to the worst case for launch on the 2019/2020 February backups. The requirement covers the worst case of the previous CReMA 3.1.

SSRD-MR-0320

The spacecraft shall not create parasitic forces creating unpredicted dV at an average rate in excess of 5mm/s per day, and applies also in the case of a single failure and entry into Survival and Safe mode. This constraint applies from 30days prior to GAM fly-by until periapsis passage, and may be averaged over a 3day period.

This requirement stands for the limitation of the dynamic noise during the navigation of the GAMs. This is crucial to keep the current navigation Delta-V budget and to ensure the safety of the GAM operations (section 5.3.1).

SSRD-MR-0350

The spacecraft shall provide nominal function under spacecraft to ground station range dynamic conditions as follows:

Range Rate from: +65 km/s to -65 km/s

Range Acceleration from +35 m/s² to -15 m/s²



This requirement is derived from the range rate and Doppler rates presented in the trajectory descriptions in sections 3.1.1 and covers the maximum values seen for the current trajectories.

SSRD-MR-0340

The spacecraft shall be compatible with the following operational orbit parameter ranges:

Parameter	Min	Max	Unit
Aphelion	0.789	1.112	AU
Perihelion	0.280	0.37	AU
Heliolatitude	2.92	17.45	deg
Solar Inclination	5.91	31.47	deg

This requirement applies to the NMP. Considering launch window variations as in Table 4-11 (except for the heliolatitude at perihelion, which is based on the reference trajectories) the bounds for the orbit parameters result (indicated below each value is the driving trajectory case):

Parameter	Min	Max	Unit
Aphelion	0.820 2019/2020	1.111 October	AU
Perihelion	0.280 Option E	0.366 October	AU
Heliolatitude	1.35 October -0.67 Option D	8.49 Option E -11.26 October	deg
Solar Inclination	3.7 October	24.43 2019/2020	deg

SSRD-SPR-0200

The Spacecraft shall have a nominal lifetime of 2841 days in orbit.

The current maximum nominal lifetime considering launch window variations as in Table 4-11 corresponds to the 2018 Option D trajectory with 8.2 years (2995 days).

SSRD-SPR-0205

The Spacecraft shall be compatible with an extended lifetime of 3739 days.

The current maximum extended lifetime considering launch window variations as in Table 4-11 corresponds to the 2018 Option D trajectory with 10.7 years (3908 days).



8 TRAJECTORY FILES

Trajectory files for the each one of the launch opportunities described in this document are distributed so that analysis of the trajectories can be performed by science and industrial partners.

The format of the trajectory file is the Orbit Ephemeris Message (OEM) which is part of the CCSDS standard for Orbit Data Messages [6]. The Solar Orbiter OEM files specify the position and velocity vectors (X,Y,Z Cartesian components) of the spacecraft at multiple epochs for the entire mission duration. The reference frame used in the OEM files is the Mean Earth Equator of J2000 (EME2000) centred in the Sun. The OEM consists of a series of metadata blocks that describe continuous trajectory arcs. At the boundaries of the metadata block a discontinuity of the velocity occurs when the spacecraft implements a GAM (in the OEM simplified as an instantaneous velocity change) and also at several points where the trajectory optimization software introduces a spurious deep space manoeuvre that typically requires very low Delta-V.

The OEM requires the use of an interpolation technique to obtain the position and velocity at times different from the tabular epochs. The interpolation shall be done within one single metadata block. Interpolation of data between different blocks will produce wrong velocity results and shall be avoided.

Table 8-1 provides a summary of the OEM files related to this document. These OEM files are fully compatible with the launch scenarios described in this document and shall be used as reference in any trajectory analysis. It should be noted that the current OEM files have been produced such that the key dates of the launch and GAMs coincide with the trajectory description in this document.

With respect to the last major update of this document (Issue 3 Rev 1, 2011-10-06) the OEM file for 2018 October is exactly the same.

CReMA Launch Scenario	OEM Filename	OEM Start date	OEM End date
2018 Option E	2018_Option_E_CReMA_Issue4-0.oem	2018-09-30	2029-04-12
2018 Option D	2018_Option_D_CReMA_Issue4-0.oem	2018-11-07	2029-06-08
2018 October	2018_October_CReMA_Issue4-0.oem	2018-10-10	2028-03-24
2019 February Inwards	2019_February_In_CReMA_Issue4-0.oem	2019-02-14	2029-06-11
2019 February Outwards	2019_February_Out_CReMA_Issue4-0.oem	2019-02-14	2029-06-11
2020 February	2020_February_CReMA_Issue4-0.oem	2020-02-07	2030-09-02

Table 8-1 Description of OEM files accompanying this document



9 DISTRIBUTION LIST

ESOC:

OPS-GFA

A. Accomazzo	OPS-OP
I. Tanco	OPS-OPS
M. Lauer	OPS-GFS
G.Ravera	OPS-ONO

ESTEC:

Ph. Kletzkine	SRE-PS
S. Strandmoe	SRE-PSS
P. Olivier	SER-PSQ
S. Thuerey	SRE-PSA
D. Mueller	SRE-SM

ESAC:

L. Sánchez	SRE-ODS
------------	---------



10 APPENDIX A – DETAILED DATA OF REMOTE SENSING WINDOWS

This appendix provides tables detailing trajectory characteristics at each of the 10-days remote sensing windows encountered during the mission. The tables are divided by science orbit, thus one table corresponds to a period between two GAMs. The tables contain data for the start and end of each remote sensing window at -5 days and +5 days from the point of extreme solar latitude and the perihelion. At the moment there has been no consideration for windows overlapping. When an overlap occurs, this has been only highlighted.

10.1 2018 Option E Launch

	Date	From launch (y)	From GAM (d)	To GAM (d)	Sun (AU)	Earth (AU)	DEC (deg)	SSE (deg)	SES (deg)	Sol. lat. (deg)	wrot (deg/day)
GAM-E1	2021-01-01										
MINLAT-5d	2021-02-17	2.38	46.6	-280.0	0.695	0.296	-6.2	170.3	6.8	-5.05	1.469
MINLAT	2021-02-22	2.40	51.6	-275.0	0.644	0.346	-7.1	174.1	3.9	-5.10	1.714
MINLAT+5d	2021-02-27	2.41	56.6	-270.0	0.589	0.408	-8.0	166.9	7.8	-5.03	2.048
MINRP-5d	2021-03-21	2.47	78.6	-248.1	0.361	0.869	-7.4	99.8	20.9	-0.40	5.414
MINRP	2021-03-26	2.49	83.6	-243.1	0.346	1.015	-5.5	77.2	19.8	2.09	5.880
MINRP+5d	2021-03-31	2.50	88.6	-238.1	0.361	1.155	-3.0	55.9	17.4	4.06	5.433
MAXLAT-5d	2021-04-03	2.51	91.6	-235.1	0.382	1.232	-1.3	45.1	15.7	4.74	4.864
MAXLAT	2021-04-08	2.52	96.6	-230.1	0.430	1.343	1.6	31.3	12.9	5.10	3.845
MAXLAT+5d	2021-04-13	2.53	101.6	-225.1	0.486	1.438	4.3	21.8	10.4	4.88	3.005
MINLAT-5d	2021-09-08	2.94	249.9	-76.7	0.695	1.679	9.3	11.6	8.0	-5.05	1.471
MINLAT	2021-09-13	2.95	254.9	-71.7	0.644	1.633	6.9	10.1	6.4	-5.10	1.716
MINLAT+5d	2021-09-18	2.97	259.9	-66.7	0.588	1.585	4.3	7.7	4.5	-5.03	2.051
MINRP-5d	2021-10-10	3.03	281.7	-44.9	0.361	1.288	-10.3	31.7	10.9	-0.42	5.406
MINRP	2021-10-15	3.04	286.7	-39.9	0.346	1.180	-13.9	50.7	15.6	2.07	5.880
MINRP+5d	2021-10-20	3.06	291.7	-34.9	0.361	1.059	-17.1	70.0	19.9	4.05	5.440
MAXLAT-5d	2021-10-23	3.06	294.8	-31.8	0.382	0.984	-18.8	80.5	22.3	4.74	4.857
MAXLAT	2021-10-28	3.08	299.8	-26.8	0.430	0.868	-21.2	93.8	25.6	5.10	3.838
MAXLAT+5d	2021-11-02	3.09	304.8	-21.8	0.486	0.764	-23.2	102.7	28.6	4.88	3.000
GAM-V4	2021-11-23										

Table 10-1 2018 Launch Option E: remote sensing windows from GAM-E1 to GAM-V4



	Date	From launch (y)	From GAM (d)	To GAM (d)	Sun (AU)	Earth (AU)	DEC (deg)	SSE (deg)	SES (deg)	Sol. lat. (deg)	wrot (deg/day)
GAM-V4	2021-11-23										
MINLAT-5d	2022-02-26	3.41	94.2	-579.9	0.643	0.549	-2.4	112.1	37.0	-12.87	1.629
MINLAT	2022-03-03	3.42	99.2	-574.9	0.589	0.540	-2.2	122.8	29.9	-13.03	1.947
MINLAT+5d	2022-03-08	3.44	104.2	-569.9	0.529	0.538	-2.2	137.0	21.3	-12.80	2.405
MINRP-5d	2022-03-26	3.49	122.1	-552.0	0.315	0.755	-2.1	133.1	13.4	-1.56	6.442
MINRP	2022-03-31	3.50	127.1	-547.0	0.295	0.913	-0.7	98.3	17.0	6.29	7.432
MINRP+5d	2022-04-05	3.51	132.1	-542.0	0.316	1.079	1.4	67.3	16.9	11.80	6.703
MAXLAT-5d	2022-04-04	3.51	131.3	-542.8	0.310	1.054	1.1	71.5	17.1	11.25	6.918
MAXLAT	2022-04-09	3.52	136.3	-537.8	0.357	1.204	3.5	48.1	15.4	13.03	5.289
MAXLAT+5d	2022-04-14	3.54	141.3	-532.8	0.419	1.327	5.8	33.1	13.2	12.06	3.814
MINLAT-5d	2022-08-14	3.87	262.8	-411.3	0.643	1.642	13.4	9.4	5.9	-12.87	1.631
MINLAT	2022-08-19	3.88	267.8	-406.3	0.588	1.593	11.7	7.4	4.3	-13.03	1.950
MINLAT+5d	2022-08-24	3.90	272.8	-401.3	0.529	1.537	9.8	4.6	2.4	-12.80	2.410
MINRP-5d	2022-09-10	3.95	290.5	-383.5	0.316	1.231	1.0	39.4	11.5	-1.62	6.431
MINRP	2022-09-15	3.96	295.5	-378.5	0.295	1.087	-1.6	66.3	15.6	6.23	7.431
MINRP+5d	2022-09-20	3.97	300.5	-373.5	0.315	0.927	-3.7	94.8	18.2	11.77	6.715
MAXLAT-5d	2022-09-20	3.97	299.9	-374.2	0.310	0.949	-3.4	91.1	18.0	11.28	6.908
MAXLAT	2022-09-25	3.99	304.9	-369.2	0.358	0.796	-5.1	115.4	18.8	13.03	5.276
MAXLAT+5d	2022-09-30	4.00	309.9	-364.2	0.419	0.665	-6.4	133.7	17.6	12.05	3.805
MINLAT-5d	2023-01-29	4.33	431.3	-242.8	0.643	0.357	-29.8	159.1	13.4	-12.87	1.629
MINLAT	2023-02-03	4.35	436.3	-237.8	0.589	0.408	-26.8	162.7	10.2	-13.02	1.946
MINLAT+5d	2023-02-08	4.36	441.3	-232.8	0.529	0.473	-24.0	159.7	10.8	-12.80	2.404
MINRP-5d	2023-02-26	4.41	459.1	-215.0	0.315	0.885	-14.2	100.1	18.3	-1.58	6.437
MINRP	2023-03-03	4.42	464.1	-210.0	0.295	1.046	-11.2	71.1	16.4	6.27	7.430
MINRP+5d	2023-03-08	4.44	469.1	-205.0	0.316	1.196	-7.9	43.8	12.7	11.78	6.706
MAXLAT-5d	2023-03-07	4.43	468.3	-205.8	0.310	1.174	-8.4	47.6	13.3	11.23	6.920
MAXLAT	2023-03-12	4.45	473.3	-200.8	0.357	1.299	-5.2	26.7	9.3	13.02	5.293
MAXLAT+5d	2023-03-17	4.46	478.3	-195.8	0.419	1.398	-2.2	13.3	5.6	12.06	3.817
MINLAT-5d	2023-07-17	4.79	599.8	-74.3	0.643	1.645	17.6	9.3	5.9	-12.87	1.630
MINLAT	2023-07-22	4.81	604.8	-69.3	0.589	1.585	16.6	11.8	6.8	-13.02	1.947
MINLAT+5d	2023-07-27	4.82	609.8	-64.3	0.529	1.514	15.4	15.8	8.1	-12.80	2.406
MINRP-5d	2023-08-14	4.87	627.7	-46.4	0.315	1.121	9.9	62.3	16.0	-1.55	6.445
MINRP	2023-08-19	4.88	632.7	-41.4	0.295	0.956	8.8	92.4	16.9	6.30	7.432
MINRP+5d	2023-08-24	4.90	637.7	-36.4	0.316	0.794	8.9	125.6	14.7	11.80	6.700
MAXLAT-5d	2023-08-23	4.89	636.9	-37.2	0.310	0.818	8.8	120.6	15.3	11.25	6.915
MAXLAT	2023-08-28	4.91	641.9	-32.2	0.357	0.684	9.7	150.7	10.0	13.02	5.285
MAXLAT+5d	2023-09-02	4.92	646.9	-27.2	0.419	0.593	11.1	171.5	3.5	12.06	3.812
GAM-V5	2023-09-28										

Table 10-2 2018 Launch Option E: remote sensing windows from GAM-V4 to GAM-V5



	Date	From launch (y)	From GAM (d)	To GAM (d)	Sun (AU)	Earth (AU)	DEC (deg)	SSE (deg)	SES (deg)	Sol. lat. (deg)	wrot (deg/day)
GAM-V5	2023-09-28										
MINLAT-5d	2023-12-15	5.21	76.9	-372.5	0.580	0.670	-30.9	103.7	34.9	-20.91	2.026
MINLAT	2023-12-20	5.22	81.9	-367.5	0.523	0.731	-30.3	102.1	31.3	-21.29	2.504
MINLAT+5d	2023-12-25	5.23	86.9	-362.5	0.460	0.807	-29.1	98.0	27.6	-20.70	3.202
MINRP-5d	2024-01-07	5.27	100.1	-349.3	0.302	1.082	-23.4	63.1	15.9	-5.18	6.578
MINRP	2024-01-12	5.28	105.1	-344.3	0.280	1.191	-20.6	37.4	10.0	8.56	7.733
MINRP+5d	2024-01-17	5.30	110.1	-339.3	0.302	1.272	-17.8	15.2	4.6	18.82	7.258
MAXLAT-5d	2024-01-17	5.30	109.6	-339.8	0.298	1.265	-18.1	16.8	5.0	18.11	7.403
MAXLAT	2024-01-22	5.31	114.6	-334.8	0.348	1.319	-15.4	14.0	4.9	21.29	5.632
MAXLAT+5d	2024-01-27	5.32	119.6	-329.8	0.412	1.354	-12.9	22.2	9.1	19.64	3.943
MINLAT-5d	2024-05-13	5.62	226.7	-222.7	0.580	1.327	15.9	45.6	24.2	-20.91	2.025
MINLAT	2024-05-18	5.63	231.7	-217.7	0.523	1.249	16.8	51.7	23.9	-21.29	2.502
MINLAT+5d	2024-05-23	5.64	236.7	-212.7	0.461	1.155	17.8	60.6	23.4	-20.70	3.199
MINRP-5d	2024-06-05	5.68	249.9	-199.5	0.302	0.841	23.5	117.1	15.4	-5.22	6.573
MINRP	2024-06-10	5.69	254.9	-194.5	0.280	0.753	27.0	155.7	6.5	8.51	7.732
MINRP+5d	2024-06-15	5.71	259.9	-189.5	0.302	0.752	28.9	145.5	9.7	18.81	7.262
MAXLAT-5d	2024-06-14	5.71	259.4	-190.0	0.298	0.748	28.9	149.3	8.6	18.09	7.407
MAXLAT	2024-06-19	5.72	264.4	-185.0	0.348	0.812	28.6	116.4	17.9	21.29	5.638
MAXLAT+5d	2024-06-24	5.73	269.4	-180.0	0.412	0.903	27.6	93.8	23.9	19.65	3.947
MINLAT-5d	2024-10-09	6.03	376.5	-72.9	0.580	1.272	-3.1	49.6	26.2	-20.91	2.023
MINLAT	2024-10-14	6.04	381.5	-67.9	0.523	1.274	-5.6	47.4	22.7	-21.29	2.501
MINLAT+5d	2024-10-19	6.05	386.5	-62.9	0.461	1.281	-8.0	43.2	18.5	-20.70	3.197
MINRP-5d	2024-11-02	6.09	399.7	-49.7	0.302	1.289	-13.7	9.7	2.9	-5.26	6.568
MINRP	2024-11-07	6.10	404.7	-44.7	0.280	1.255	-15.3	17.3	4.8	8.47	7.730
MINRP+5d	2024-11-12	6.12	409.7	-39.7	0.302	1.187	-16.6	43.4	12.1	18.79	7.266
MAXLAT-5d	2024-11-11	6.12	409.2	-40.2	0.298	1.196	-16.5	40.9	11.4	18.07	7.411
MAXLAT	2024-11-16	6.13	414.2	-35.2	0.348	1.113	-17.5	60.5	17.8	21.29	5.644
MAXLAT+5d	2024-11-21	6.14	419.2	-30.2	0.412	1.033	-18.2	72.1	23.4	19.66	3.951
GAM-V6	2024-12-21										
MINLAT-5d	2025-02-26	6.41	66.7	-382.7	0.587	0.692	-14.2	101.1	35.6	-27.56	2.175
MINLAT	2025-03-03	6.42	71.7	-377.7	0.541	0.656	-13.6	111.6	30.5	-28.08	2.589
MINLAT+5d	2025-03-08	6.44	76.7	-372.7	0.491	0.623	-12.6	125.7	23.7	-27.35	3.104
MINRP-5d	2025-03-25	6.48	93.2	-356.2	0.339	0.711	-2.9	140.8	12.4	-4.32	5.149
MINRP	2025-03-30	6.50	98.2	-351.2	0.325	0.836	1.1	110.6	17.8	9.91	5.736
MINRP+5d	2025-04-04	6.51	103.2	-346.2	0.339	0.983	4.5	83.0	19.7	21.81	5.945
MAXLAT-5d	2025-04-06	6.52	105.7	-343.7	0.355	1.056	6.0	71.3	19.6	25.52	5.732
MAXLAT	2025-04-11	6.53	110.7	-338.7	0.399	1.188	8.4	53.2	18.6	28.08	4.762
MAXLAT+5d	2025-04-16	6.54	115.7	-333.7	0.449	1.301	10.3	40.7	17.0	26.49	3.641
MINLAT-5d	2025-07-26	6.82	216.6	-232.8	0.587	1.573	11.6	14.5	8.3	-27.57	2.179
MINLAT	2025-07-31	6.83	221.6	-227.8	0.540	1.528	10.6	14.7	7.7	-28.08	2.594
MINLAT+5d	2025-08-05	6.85	226.6	-222.8	0.490	1.476	9.5	16.0	7.7	-27.33	3.110
MINRP-5d	2025-08-21	6.89	243.0	-206.4	0.339	1.207	6.9	47.9	14.4	-4.37	5.146
MINRP	2025-08-26	6.91	248.0	-201.4	0.325	1.081	7.1	68.8	17.5	9.86	5.734
MINRP+5d	2025-08-31	6.92	253.0	-196.4	0.339	0.944	7.9	91.2	19.6	21.78	5.945
MAXLAT-5d	2025-09-03	6.93	255.5	-193.9	0.355	0.875	8.5	101.8	20.2	25.50	5.734
MAXLAT	2025-09-08	6.94	260.5	-188.9	0.398	0.749	9.8	119.7	20.1	28.08	4.766
MAXLAT+5d	2025-09-13	6.95	265.5	-183.9	0.449	0.641	11.0	133.9	18.8	26.50	3.645
MINLAT-5d	2025-12-23	7.23	366.4	-83.0	0.587	0.615	-42.1	109.9	34.1	-27.57	2.178
MINLAT	2025-12-28	7.24	371.4	-78.0	0.540	0.673	-39.3	107.8	31.5	-28.08	2.593
MINLAT+5d	2026-01-02	7.26	376.4	-73.0	0.490	0.743	-36.0	103.9	28.9	-27.34	3.108
MINRP-5d	2026-01-18	7.30	392.8	-56.6	0.339	1.058	-22.8	68.3	18.7	-4.21	5.154
MINRP	2026-01-23	7.32	397.8	-51.6	0.325	1.165	-18.7	49.4	14.5	10.03	5.740
MINRP+5d	2026-01-28	7.33	402.8	-46.6	0.339	1.258	-15.0	31.5	10.4	21.89	5.943
MAXLAT-5d	2026-01-31	7.34	405.4	-44.0	0.356	1.298	-13.3	24.4	8.6	25.56	5.727
MAXLAT	2026-02-05	7.35	410.4	-39.0	0.399	1.363	-10.3	16.2	6.5	28.08	4.752
MAXLAT+5d	2026-02-10	7.36	415.4	-34.0	0.450	1.414	-7.8	15.0	6.8	26.47	3.632
GAM-V7	2026-03-15										

Table 10-3 2018 Launch Option E: remote sensing windows from GAM-V5 to GAM-V7



	Date	From launch (y)	From GAM (d)	To GAM (d)	Sun (AU)	Earth (AU)	DEC (deg)	SSE (deg)	SES (deg)	Sol. lat. (deg)	wrot (deg/day)
GAM-V7	2026-03-15										
MINLAT-5d	2026-05-09	7.60	53.8	-620.3	0.495	1.272	11.9	47.9	21.4	-30.04	2.978
MINLAT	2026-05-14	7.62	58.8	-615.3	0.441	1.174	13.1	57.8	21.6	-31.14	3.850
MINLAT+5d	2026-05-19	7.63	63.8	-610.3	0.384	1.060	15.0	72.3	21.2	-29.27	4.868
MINRP-5d	2026-05-26	7.65	71.5	-602.6	0.313	0.863	20.2	109.9	16.9	-14.68	5.986
MINRP	2026-05-31	7.67	76.5	-597.6	0.295	0.761	25.7	143.6	10.0	3.06	6.294
MINRP+5d	2026-06-05	7.68	81.5	-592.6	0.312	0.729	30.7	151.4	8.5	19.92	6.347
MAXLAT-5d	2026-06-10	7.69	85.9	-588.2	0.349	0.761	32.7	128.3	15.7	28.45	5.807
MAXLAT	2026-06-15	7.71	90.9	-583.2	0.403	0.832	32.7	105.4	22.5	31.14	4.604
MAXLAT+5d	2026-06-20	7.72	95.9	-578.2	0.459	0.910	31.9	89.5	26.9	29.60	3.437
MINLAT-5d	2026-09-20	7.97	188.6	-485.5	0.496	1.291	-0.8	45.1	20.5	-30.02	2.972
MINLAT	2026-09-25	7.99	193.6	-480.5	0.441	1.304	-3.0	39.4	16.2	-31.13	3.843
MINLAT+5d	2026-09-30	8.00	198.6	-475.5	0.385	1.315	-5.1	30.3	11.2	-29.29	4.861
MINRP-5d	2026-10-08	8.02	206.4	-467.7	0.312	1.309	-7.4	6.4	2.0	-14.56	5.990
MINRP	2026-10-13	8.04	211.4	-462.7	0.295	1.271	-8.3	19.9	5.8	3.21	6.295
MINRP+5d	2026-10-18	8.05	216.4	-457.7	0.313	1.199	-8.8	43.6	12.5	20.03	6.345
MAXLAT-5d	2026-10-23	8.06	220.8	-453.3	0.350	1.121	-9.1	60.3	17.8	28.50	5.799
MAXLAT	2026-10-28	8.08	225.8	-448.3	0.403	1.031	-9.7	73.4	22.9	31.13	4.594
MAXLAT+5d	2026-11-02	8.09	230.8	-443.3	0.459	0.949	-10.4	81.7	27.3	29.58	3.428
MINLAT-5d	2027-02-02	8.34	323.4	-350.7	0.496	0.617	-31.4	124.2	24.6	-30.01	2.967
MINLAT	2027-02-07	8.36	328.4	-345.7	0.441	0.622	-30.4	135.4	18.3	-31.13	3.836
MINLAT+5d	2027-02-12	8.37	333.4	-340.7	0.385	0.653	-27.5	142.7	13.7	-29.32	4.853
MINRP-5d	2027-02-20	8.39	341.2	-332.9	0.313	0.784	-19.2	122.6	15.4	-14.67	5.987
MINRP	2027-02-25	8.41	346.2	-327.9	0.295	0.923	-13.0	94.3	17.3	3.07	6.294
MINRP+5d	2027-03-02	8.42	351.2	-322.9	0.312	1.073	-7.8	66.5	16.8	19.93	6.346
MAXLAT-5d	2027-03-06	8.43	355.5	-318.5	0.349	1.192	-4.0	47.8	15.1	28.45	5.806
MAXLAT	2027-03-11	8.44	360.5	-313.5	0.403	1.306	-0.7	33.1	12.8	31.13	4.603
MAXLAT+5d	2027-03-16	8.46	365.5	-308.5	0.459	1.399	1.9	23.3	10.5	29.60	3.436
MINLAT-5d	2027-06-17	8.71	458.2	-215.8	0.496	1.439	14.8	25.8	12.3	-30.02	2.973
MINLAT	2027-06-22	8.73	463.2	-210.8	0.441	1.357	15.0	33.0	13.7	-31.14	3.844
MINLAT+5d	2027-06-27	8.74	468.2	-205.8	0.385	1.259	15.5	43.8	15.2	-29.29	4.861
MINRP-5d	2027-07-05	8.76	476.0	-198.1	0.312	1.064	17.9	72.9	17.1	-14.55	5.990
MINRP	2027-07-10	8.77	481.0	-193.1	0.295	0.921	21.5	100.4	16.6	3.22	6.296
MINRP+5d	2027-07-15	8.79	486.0	-188.1	0.313	0.796	26.7	127.3	14.2	20.04	6.344
MAXLAT-5d	2027-07-19	8.80	490.4	-183.7	0.350	0.722	31.5	140.3	12.7	28.50	5.798
MAXLAT	2027-07-24	8.81	495.4	-178.7	0.403	0.682	35.4	137.3	15.6	31.13	4.593
MAXLAT+5d	2027-07-29	8.83	500.4	-173.7	0.460	0.674	36.9	126.1	21.4	29.57	3.427
MINLAT-5d	2027-10-30	9.08	593.0	-81.0	0.496	1.028	-15.1	72.0	28.3	-30.01	2.967
MINLAT	2027-11-04	9.09	598.0	-76.0	0.441	1.084	-16.8	66.2	24.0	-31.14	3.837
MINLAT+5d	2027-11-09	9.11	603.0	-71.0	0.385	1.146	-17.8	57.1	19.0	-29.32	4.854
MINRP-5d	2027-11-17	9.13	610.8	-63.3	0.313	1.238	-18.1	32.5	9.8	-14.66	5.987
MINRP	2027-11-22	9.14	615.8	-58.3	0.295	1.274	-17.6	12.5	3.7	3.09	6.295
MINRP+5d	2027-11-27	9.16	620.8	-53.3	0.312	1.278	-16.8	18.5	5.7	19.94	6.347
MAXLAT-5d	2027-12-01	9.17	625.2	-48.9	0.349	1.262	-16.1	32.8	11.1	28.46	5.805
MAXLAT	2027-12-06	9.18	630.2	-43.9	0.403	1.233	-15.4	44.2	16.6	31.14	4.602
MAXLAT+5d	2027-12-11	9.20	635.2	-38.9	0.459	1.205	-14.8	51.2	21.3	29.59	3.435
GAM-V8	2028-01-18										

Table 10-4 2018 Launch Option E: remote sensing windows from GAM-V7 to GAM-V8



	Date	From launch (y)	From GAM (d)	To GAM (d)	Sun (AU)	Earth (AU)	DEC (deg)	SSE (deg)	SES (deg)	Sol. lat. (deg)	wrot (deg/day)
GAM-V8	2028-01-18										
MINLAT-5d	2028-03-07	9.43	48.1	-401.5	0.520	0.828	-9.9	91.9	31.6	-31.79	2.991
MINLAT	2028-03-12	9.45	53.1	-396.5	0.482	0.758	-9.7	104.2	28.1	-32.85	3.562
MINLAT+5d	2028-03-17	9.46	58.1	-391.5	0.446	0.691	-8.9	120.7	22.6	-31.38	4.041
MINRP-5d	2028-03-28	9.49	68.8	-380.8	0.388	0.620	-3.3	163.5	6.3	-15.69	4.194
MINRP	2028-04-02	9.50	73.8	-375.8	0.380	0.658	1.1	147.4	11.8	-3.32	4.062
MINRP+5d	2028-04-07	9.52	78.8	-370.8	0.388	0.740	5.5	121.9	19.2	9.46	3.996
MAXLAT-5d	2028-04-22	9.56	93.9	-355.7	0.478	1.064	14.2	69.9	26.5	31.73	3.544
MAXLAT	2028-04-27	9.57	98.9	-350.7	0.515	1.158	15.9	60.2	26.4	32.85	3.118
MAXLAT+5d	2028-05-02	9.59	103.9	-345.7	0.552	1.240	17.3	52.9	25.9	32.02	2.665
MINLAT-5d	2028-08-04	9.84	197.9	-251.7	0.520	1.483	9.6	21.1	10.6	-31.78	2.988
MINLAT	2028-08-09	9.86	202.9	-246.7	0.482	1.459	8.1	18.8	8.8	-32.85	3.559
MINLAT+5d	2028-08-14	9.87	207.9	-241.7	0.446	1.428	6.6	17.7	7.7	-31.39	4.039
MINRP-5d	2028-08-24	9.90	218.6	-231.0	0.388	1.329	4.4	29.9	11.0	-15.74	4.194
MINRP	2028-08-29	9.92	223.6	-226.0	0.380	1.260	3.9	41.9	14.6	-3.38	4.063
MINRP+5d	2028-09-03	9.93	228.6	-221.0	0.388	1.179	3.9	55.1	18.4	9.40	3.996
MAXLAT-5d	2028-09-19	9.97	243.7	-205.9	0.477	0.910	4.7	87.0	28.3	31.72	3.546
MAXLAT	2028-09-24	9.98	248.7	-200.9	0.515	0.827	4.8	93.9	30.8	32.85	3.120
MAXLAT+5d	2028-09-29	10.00	253.7	-195.9	0.552	0.749	4.6	99.5	32.9	32.03	2.667
MINLAT-5d	2029-01-01	10.25	347.7	-101.9	0.520	0.599	-46.9	122.7	26.4	-31.77	2.985
MINLAT	2029-01-06	10.27	352.7	-96.9	0.483	0.660	-42.8	117.9	25.7	-32.85	3.556
MINLAT+5d	2029-01-11	10.28	357.7	-91.9	0.446	0.733	-38.1	110.7	25.1	-31.41	4.036
MINRP-5d	2029-01-21	10.31	368.5	-81.1	0.388	0.931	-26.9	86.1	23.1	-15.63	4.193
MINRP	2029-01-26	10.33	373.5	-76.1	0.380	1.034	-22.0	71.8	21.5	-3.25	4.063
MINRP+5d	2029-01-31	10.34	378.5	-71.1	0.388	1.136	-17.4	57.8	19.5	9.53	3.996
MAXLAT-5d	2029-02-15	10.38	393.5	-56.1	0.478	1.384	-6.9	28.0	13.1	31.75	3.543
MAXLAT	2029-02-20	10.39	398.5	-51.1	0.516	1.446	-4.3	22.3	11.4	32.85	3.116
MAXLAT+5d	2029-02-25	10.41	403.5	-46.1	0.553	1.500	-2.0	18.1	10.0	32.01	2.663
Mission End	2029-04-12										

Table 10-5 2018 Launch Option E: remote sensing windows from GAM-V8 to end of mission

10.2 2018 Option D Launch

	Date	From launch (y)	From GAM (d)	To GAM (d)	Sun (AU)	Earth (AU)	DEC (deg)	SSE (deg)	SES (deg)	Sol. lat. (deg)	wrot (deg/day)
GAM-E2	2021-11-24										
MINLAT-5d	2022-03-05	-102.96	101.1	-180.9	0.504	0.492	-1.5	168.8	5.7	-4.37	2.675
MINLAT	2022-03-10	-102.94	106.1	-175.9	0.438	0.560	-4.0	168.9	4.9	-4.53	3.555
MINLAT+5d	2022-03-15	-102.93	111.1	-170.9	0.375	0.660	-5.8	146.5	12.0	-4.23	4.849
MINRP-5d	2022-03-20	-102.92	115.7	-166.2	0.329	0.787	-6.4	120.6	16.5	-3.09	6.290
MINRP	2022-03-25	-102.90	120.7	-161.2	0.309	0.948	-5.7	89.9	18.0	-0.70	7.098
MINRP+5d	2022-03-30	-102.89	125.7	-156.2	0.329	1.110	-3.7	62.0	16.9	1.93	6.274
MAXLAT-5d	2022-04-09	-102.86	136.4	-145.6	0.451	1.380	2.2	27.3	11.9	4.38	3.354
MAXLAT	2022-04-14	-102.85	141.4	-140.6	0.517	1.475	4.9	19.6	10.0	4.53	2.545
MAXLAT+5d	2022-04-19	-102.83	146.4	-135.6	0.582	1.556	7.3	14.7	8.5	4.44	2.010
GAM-V2	2022-09-02										

Table 10-6 2018 Launch Option D: remote sensing windows from GAM-E1 to GAM-V2



	Date	From launch (y)	From GAM (d)	To GAM (d)	Sun (AU)	Earth (AU)	DEC (deg)	SSE (deg)	SES (deg)	Sol. lat. (deg)	wrot (deg/day)
GAM-V2	2022-09-02										
MINLAT-5d	2022-09-27	-102.39	24.8	-874.0	0.415	1.416	-2.2	4.4	1.8	-11.72	3.892
MINLAT	2022-10-02	-102.38	29.8	-869.0	0.350	1.342	-6.5	11.5	4.0	-12.73	5.507
MINLAT+5d	2022-10-07	-102.37	34.8	-864.0	0.303	1.243	-10.6	32.1	9.3	-10.84	7.269
MINRP-5d	2022-10-05	-102.37	33.4	-865.4	0.312	1.272	-9.5	25.7	7.8	-11.78	6.861
MINRP	2022-10-10	-102.36	38.4	-860.4	0.290	1.151	-13.3	52.1	13.3	-6.48	7.706
MINRP+5d	2022-10-15	-102.34	43.4	-855.4	0.312	1.007	-15.9	79.3	17.9	1.38	6.575
MAXLAT-5d	2022-11-03	-102.29	62.3	-836.5	0.552	0.572	-15.8	123.9	27.5	12.55	2.209
MAXLAT	2022-11-08	-102.28	67.3	-831.5	0.614	0.499	-14.1	125.5	30.3	12.73	1.790
MAXLAT+5d	2022-11-13	-102.26	72.3	-826.5	0.670	0.441	-11.9	124.5	33.9	12.60	1.500
MINLAT-5d	2023-03-26	-101.90	204.6	-694.2	0.414	0.588	0.2	168.5	4.7	-11.73	3.901
MINLAT	2023-03-31	-101.89	209.6	-689.2	0.350	0.666	-2.2	157.6	7.7	-12.73	5.520
MINLAT+5d	2023-04-05	-101.87	214.6	-684.2	0.302	0.795	-2.6	125.0	14.3	-10.81	7.277
MINRP-5d	2023-04-03	-101.88	213.1	-685.7	0.313	0.754	-2.8	134.9	12.8	-11.81	6.846
MINRP	2023-04-08	-101.86	218.1	-680.7	0.290	0.912	-1.5	99.3	16.6	-6.54	7.707
MINRP+5d	2023-04-13	-101.85	223.1	-675.7	0.312	1.081	1.5	67.3	16.7	1.32	6.589
MAXLAT-5d	2023-05-02	-101.80	242.0	-656.8	0.552	1.513	14.0	18.9	10.2	12.54	2.213
MAXLAT	2023-05-07	-101.79	247.0	-651.8	0.613	1.587	16.5	15.4	9.3	12.73	1.793
MAXLAT+5d	2023-05-12	-101.77	252.0	-646.8	0.670	1.651	18.6	13.1	8.7	12.61	1.502
MINLAT-5d	2023-09-21	-101.41	384.3	-514.5	0.415	1.418	-0.7	3.5	1.4	-11.71	3.888
MINLAT	2023-09-26	-101.40	389.3	-509.5	0.350	1.336	-4.8	15.3	5.3	-12.73	5.502
MINLAT+5d	2023-10-01	-101.38	394.3	-504.5	0.303	1.228	-8.9	36.5	10.4	-10.85	7.265
MINRP-5d	2023-09-30	-101.39	392.9	-505.9	0.313	1.260	-7.8	29.9	9.0	-11.79	6.856
MINRP	2023-10-05	-101.37	397.9	-500.9	0.290	1.129	-11.6	56.8	14.1	-6.50	7.706
MINRP+5d	2023-10-10	-101.36	402.9	-495.9	0.312	0.978	-14.1	84.7	18.1	1.36	6.579
MAXLAT-5d	2023-10-29	-101.31	421.8	-477.0	0.552	0.531	-13.6	133.0	24.0	12.55	2.211
MAXLAT	2023-11-03	-101.29	426.8	-472.0	0.614	0.456	-11.8	135.5	25.7	12.73	1.791
MAXLAT+5d	2023-11-08	-101.28	431.8	-467.0	0.670	0.395	-9.4	135.4	28.4	12.61	1.501
MINLAT-5d	2024-03-19	-100.92	564.0	-334.8	0.415	0.583	-3.7	171.9	3.4	-11.72	3.894
MINLAT	2024-03-24	-100.90	569.0	-329.8	0.350	0.678	-5.5	150.1	10.1	-12.73	5.509
MINLAT+5d	2024-03-29	-100.89	574.0	-324.8	0.303	0.818	-5.3	118.6	15.4	-10.83	7.269
MINRP-5d	2024-03-28	-100.89	572.7	-326.1	0.312	0.776	-5.5	127.6	14.4	-11.78	6.862
MINRP	2024-04-02	-100.88	577.7	-321.1	0.290	0.941	-3.8	93.1	16.9	-6.47	7.704
MINRP+5d	2024-04-07	-100.87	582.7	-316.1	0.313	1.109	-0.4	62.0	16.0	1.39	6.572
MAXLAT-5d	2024-04-26	-100.81	601.6	-297.2	0.552	1.528	12.7	15.4	8.4	12.55	2.208
MAXLAT	2024-05-01	-100.80	606.6	-292.2	0.614	1.600	15.3	12.0	7.3	12.73	1.790
MAXLAT+5d	2024-05-06	-100.79	611.6	-287.2	0.670	1.662	17.5	10.0	6.6	12.61	1.500
MINLAT-5d	2024-09-15	-100.42	743.8	-155.0	0.414	1.417	0.9	6.1	2.5	-11.73	3.899
MINLAT	2024-09-20	-100.41	748.8	-150.0	0.350	1.327	-3.2	19.4	6.7	-12.73	5.517
MINLAT+5d	2024-09-25	-100.40	753.8	-145.0	0.302	1.211	-7.2	41.2	11.4	-10.82	7.275
MINRP-5d	2024-09-23	-100.40	752.5	-146.3	0.312	1.245	-6.2	34.5	10.1	-11.77	6.869
MINRP	2024-09-28	-100.39	757.5	-141.3	0.290	1.105	-9.8	61.9	14.8	-6.44	7.704
MINRP+5d	2024-10-03	-100.37	762.5	-136.3	0.313	0.948	-12.2	90.5	18.2	1.43	6.566
MAXLAT-5d	2024-10-22	-100.32	781.3	-117.5	0.551	0.498	-10.7	142.8	19.6	12.55	2.214
MAXLAT	2024-10-27	-100.31	786.3	-112.5	0.613	0.424	-8.5	146.3	20.0	12.73	1.794
MAXLAT+5d	2024-11-01	-100.29	791.3	-107.5	0.670	0.362	-5.7	146.8	21.7	12.61	1.503
MINLAT-5d	2022-09-27	-102.39	24.8	-874.0	0.415	1.416	-2.2	4.4	1.8	-11.72	3.892
MINLAT	2022-10-02	-102.38	29.8	-869.0	0.350	1.342	-6.5	11.5	4.0	-12.73	5.507
MINLAT+5d	2022-10-07	-102.37	34.8	-864.0	0.303	1.243	-10.6	32.1	9.3	-10.84	7.269
MINRP-5d	2022-10-05	-102.37	33.4	-865.4	0.312	1.272	-9.5	25.7	7.8	-11.78	6.861
MINRP	2022-10-10	-102.36	38.4	-860.4	0.290	1.151	-13.3	52.1	13.3	-6.48	7.706
MINRP+5d	2022-10-15	-102.34	43.4	-855.4	0.312	1.007	-15.9	79.3	17.9	1.38	6.575
MAXLAT-5d	2022-11-03	-102.29	62.3	-836.5	0.552	0.572	-15.8	123.9	27.5	12.55	2.209
MAXLAT	2022-11-08	-102.28	67.3	-831.5	0.614	0.499	-14.1	125.5	30.3	12.73	1.790
MAXLAT+5d	2022-11-13	-102.26	72.3	-826.5	0.670	0.441	-11.9	124.5	33.9	12.60	1.500
GAM-V3	2025-02-16										

Table 10-7 2018 Launch Option D: remote sensing windows from GAM-V2 to GAM-V3

Date	From	From	To	Sun	Earth	DEC	SSE	SES	Sol.	wrot
------	------	------	----	-----	-------	-----	-----	-----	------	------



		launch (y)	GAM (d)	GAM (d)	(AU)	(AU)	(deg)	(deg)	(deg)	lat. (deg)	(deg/day)
GAM-V3	2025-02-16										
MINLAT-5d	2025-03-16	-99.93	27.3	-646.8	0.414	0.604	-11.7	154.9	10.2	-19.32	4.043
MINLAT	2025-03-21	-99.91	32.3	-641.8	0.355	0.713	-11.7	135.0	14.6	-21.03	5.632
MINLAT+5d	2025-03-26	-99.90	37.3	-636.8	0.312	0.856	-9.5	108.1	17.3	-18.09	7.031
MINRP-5d	2025-03-25	-99.90	36.1	-638.0	0.319	0.819	-10.2	115.0	16.9	-19.40	6.796
MINRP	2025-03-30	-99.89	41.1	-633.0	0.300	0.978	-6.5	85.1	17.4	-11.15	7.111
MINRP+5d	2025-04-04	-99.87	46.1	-628.0	0.320	1.134	-1.6	57.6	15.7	0.91	6.038
MAXLAT-5d	2025-04-24	-99.82	66.5	-607.6	0.558	1.537	15.8	14.3	7.9	20.72	2.260
MAXLAT	2025-04-29	-99.80	71.5	-602.6	0.615	1.600	18.7	12.2	7.4	21.03	1.873
MAXLAT+5d	2025-05-04	-99.79	76.5	-597.6	0.666	1.654	21.2	11.0	7.2	20.81	1.593
MINLAT-5d	2025-09-01	-99.46	195.9	-478.2	0.413	1.387	2.2	20.2	8.1	-19.35	4.054
MINLAT	2025-09-06	-99.45	200.9	-473.2	0.354	1.279	-1.6	34.6	11.5	-21.03	5.645
MINLAT+5d	2025-09-11	-99.44	205.9	-468.2	0.311	1.144	-5.0	56.5	15.0	-18.04	7.037
MINRP-5d	2025-09-09	-99.44	204.6	-469.5	0.320	1.181	-4.2	50.3	14.1	-19.44	6.787
MINRP	2025-09-14	-99.43	209.6	-464.5	0.300	1.028	-6.7	77.4	16.9	-11.23	7.115
MINRP+5d	2025-09-19	-99.41	214.6	-459.5	0.319	0.867	-7.1	106.3	17.8	0.82	6.048
MAXLAT-5d	2025-10-10	-99.36	235.0	-439.1	0.558	0.480	9.4	148.4	17.0	20.72	2.264
MAXLAT	2025-10-15	-99.34	240.0	-434.1	0.614	0.444	14.7	140.2	23.2	21.03	1.876
MAXLAT+5d	2025-10-20	-99.33	245.0	-429.1	0.665	0.421	19.5	131.6	30.0	20.82	1.595
MINLAT-5d	2026-02-16	-99.00	364.4	-309.7	0.414	0.711	-25.3	120.5	21.2	-19.33	4.044
MINLAT	2026-02-21	-98.99	369.4	-304.7	0.355	0.844	-23.1	103.5	20.4	-21.03	5.632
MINLAT+5d	2026-02-26	-98.98	374.4	-299.7	0.312	0.993	-19.5	80.5	18.1	-18.09	7.031
MINRP-5d	2026-02-25	-98.98	373.2	-300.9	0.319	0.957	-20.5	86.5	18.8	-19.40	6.797
MINRP	2026-03-02	-98.97	378.2	-295.9	0.300	1.107	-15.8	59.9	15.2	-11.14	7.111
MINRP+5d	2026-03-07	-98.95	383.2	-290.9	0.320	1.238	-10.4	34.8	10.6	0.92	6.038
MAXLAT-5d	2026-03-27	-98.90	403.6	-270.5	0.558	1.539	9.0	11.6	6.5	20.73	2.260
MAXLAT	2026-04-01	-98.88	408.6	-265.5	0.615	1.586	12.4	13.7	8.4	21.04	1.873
MAXLAT+5d	2026-04-06	-98.87	413.6	-260.5	0.666	1.629	15.4	15.0	9.9	20.82	1.593
MINLAT-5d	2026-08-04	-98.54	532.9	-141.2	0.413	1.302	9.2	39.0	14.9	-19.36	4.058
MINLAT	2026-08-09	-98.53	537.9	-136.2	0.354	1.173	6.3	55.3	16.7	-21.04	5.649
MINLAT+5d	2026-08-14	-98.51	542.9	-131.2	0.311	1.019	4.1	80.1	17.6	-18.02	7.039
MINRP-5d	2026-08-12	-98.52	541.7	-132.4	0.320	1.060	4.5	72.9	17.5	-19.43	6.790
MINRP	2026-08-17	-98.50	546.7	-127.4	0.300	0.896	3.6	104.3	16.7	-11.21	7.114
MINRP+5d	2026-08-22	-98.49	551.7	-122.4	0.319	0.747	5.7	139.4	11.8	0.85	6.045
MAXLAT-5d	2026-09-12	-98.43	572.1	-102.0	0.558	0.606	26.3	119.7	28.8	20.72	2.263
MAXLAT	2026-09-17	-98.42	577.1	-97.0	0.614	0.627	28.7	108.1	35.5	21.04	1.875
MAXLAT+5d	2026-09-22	-98.41	582.1	-92.0	0.665	0.650	30.1	99.5	40.8	20.82	1.594
GAM-V4	2026-12-22										

Table 10-8 2018 Launch Option D: remote sensing windows from GAM-V3 to GAM-V4



	Date	From launch (y)	From GAM (d)	To GAM (d)	Sun (AU)	Earth (AU)	DEC (deg)	SSE (deg)	SES (deg)	Sol. lat. (deg)	wrot (deg/day)
GAM-V4	2026-12-22										
MINLAT-5d	2027-01-22	-98.07	30.3	-419.1	0.419	0.895	-31.7	89.4	25.2	-25.38	4.005
MINLAT	2027-01-27	-98.06	35.3	-414.1	0.359	1.001	-30.0	77.0	20.8	-27.46	5.648
MINLAT+5d	2027-02-01	-98.04	40.3	-409.1	0.311	1.115	-26.5	57.8	15.5	-23.77	7.062
MINRP-5d	2027-02-01	-98.04	40.2	-409.2	0.312	1.115	-26.5	57.9	15.5	-23.81	7.058
MINRP	2027-02-06	-98.03	45.2	-404.2	0.292	1.219	-21.3	32.7	9.2	-11.18	6.977
MINRP+5d	2027-02-11	-98.02	50.2	-399.2	0.311	1.294	-15.1	8.3	2.6	5.22	5.960
MAXLAT-5d	2027-02-26	-97.98	65.0	-384.4	0.477	1.380	1.9	29.0	13.5	26.75	3.157
MAXLAT	2027-03-03	-97.96	70.0	-379.4	0.536	1.394	6.5	33.3	17.2	27.46	2.539
MAXLAT+5d	2027-03-08	-97.95	75.0	-374.4	0.589	1.409	10.6	35.7	20.3	26.99	2.082
MINLAT-5d	2027-06-21	-97.66	180.1	-269.3	0.418	1.056	14.5	73.1	23.2	-25.43	4.021
MINLAT	2027-06-26	-97.65	185.1	-264.3	0.358	0.938	13.2	92.1	20.6	-27.46	5.669
MINLAT+5d	2027-07-01	-97.63	190.1	-259.3	0.311	0.819	13.6	121.5	15.1	-23.67	7.071
MINRP-5d	2027-07-01	-97.63	190.0	-259.4	0.312	0.821	13.6	120.7	15.3	-23.84	7.055
MINRP	2027-07-06	-97.62	195.0	-254.4	0.292	0.739	17.0	158.6	6.0	-11.24	6.979
MINRP+5d	2027-07-11	-97.61	200.0	-249.4	0.311	0.739	22.8	147.9	9.4	5.16	5.964
MAXLAT-5d	2027-07-26	-97.57	214.8	-234.6	0.477	0.994	32.9	78.8	27.4	26.74	3.160
MAXLAT	2027-07-31	-97.55	219.8	-229.6	0.535	1.080	33.8	68.6	29.4	27.46	2.541
MAXLAT+5d	2027-08-05	-97.54	224.8	-224.6	0.589	1.153	34.1	61.5	30.7	27.00	2.083
MINLAT-5d	2027-11-18	-97.25	329.9	-119.5	0.418	1.290	-21.0	37.0	14.7	-25.41	4.017
MINLAT	2027-11-23	-97.24	334.9	-114.5	0.359	1.290	-24.2	28.0	9.8	-27.46	5.663
MINLAT+5d	2027-11-28	-97.22	339.9	-109.5	0.311	1.280	-26.1	17.1	5.3	-23.70	7.068
MINRP-5d	2027-11-28	-97.22	339.9	-109.5	0.311	1.280	-26.1	17.1	5.3	-23.74	7.064
MINRP	2027-12-03	-97.21	344.9	-104.5	0.292	1.247	-25.9	23.4	6.8	-11.04	6.970
MINRP+5d	2027-12-08	-97.20	349.9	-99.5	0.312	1.188	-23.6	43.5	12.6	5.34	5.950
MAXLAT-5d	2027-12-22	-97.16	364.6	-84.8	0.477	0.985	-11.2	75.8	28.0	26.74	3.162
MAXLAT	2027-12-27	-97.14	369.6	-79.8	0.535	0.933	-6.7	79.0	32.3	27.46	2.543
MAXLAT+5d	2028-01-01	-97.13	374.6	-74.8	0.589	0.891	-2.4	80.5	36.2	27.00	2.085
GAM-V5	2028-03-16										
MINLAT-5d	2028-04-20	-96.83	34.4	-415.0	0.462	0.655	-0.1	127.4	21.4	-30.71	3.622
MINLAT	2028-04-25	-96.82	39.4	-410.0	0.415	0.668	-1.4	135.3	16.8	-32.42	4.659
MINLAT+5d	2028-04-30	-96.80	44.4	-405.0	0.374	0.711	-0.5	134.2	15.4	-29.83	5.435
MINRP-5d	2028-05-03	-96.79	48.1	-401.3	0.352	0.765	1.6	124.8	16.6	-23.88	5.521
MINRP	2028-05-08	-96.78	53.1	-396.3	0.340	0.867	6.4	104.9	19.0	-10.78	5.124
MINRP+5d	2028-05-13	-96.77	58.1	-391.3	0.352	0.986	12.0	83.8	20.2	4.38	4.640
MAXLAT-5d	2028-05-31	-96.72	75.4	-374.0	0.497	1.343	27.5	40.0	18.3	31.55	3.185
MAXLAT	2028-06-05	-96.70	80.4	-369.0	0.543	1.418	30.1	34.0	17.4	32.42	2.713
MAXLAT+5d	2028-06-10	-96.69	85.4	-364.0	0.587	1.484	31.9	29.5	16.6	31.81	2.296
MINLAT-5d	2028-09-16	-96.42	184.2	-265.2	0.462	1.428	-6.4	19.6	8.9	-30.70	3.618
MINLAT	2028-09-21	-96.41	189.2	-260.2	0.415	1.349	-10.2	28.3	11.3	-32.42	4.655
MINLAT+5d	2028-09-26	-96.39	194.2	-255.2	0.374	1.255	-13.4	40.9	14.1	-29.85	5.433
MINRP-5d	2028-09-30	-96.38	197.9	-251.5	0.352	1.174	-15.1	52.8	16.2	-23.92	5.522
MINRP	2028-10-05	-96.37	202.9	-246.5	0.340	1.053	-16.0	71.8	18.8	-10.84	5.126
MINRP+5d	2028-10-10	-96.36	207.9	-241.5	0.352	0.929	-14.7	91.0	20.6	4.32	4.642
MAXLAT-5d	2028-10-28	-96.31	225.2	-224.2	0.497	0.625	1.6	124.2	24.5	31.57	3.180
MAXLAT	2028-11-02	-96.29	230.2	-219.2	0.544	0.580	7.0	123.9	27.0	32.42	2.708
MAXLAT+5d	2028-11-07	-96.28	235.2	-214.2	0.587	0.547	11.6	121.7	30.3	31.79	2.292
MINLAT-5d	2029-02-13	-96.01	334.0	-115.4	0.461	0.775	-33.5	103.1	27.1	-30.73	3.629
MINLAT	2029-02-18	-96.00	339.0	-110.4	0.414	0.882	-30.1	92.2	24.8	-32.42	4.667
MINLAT+5d	2029-02-23	-95.98	344.0	-105.4	0.373	0.997	-25.6	78.1	21.7	-29.78	5.438
MINRP-5d	2029-02-27	-95.97	347.6	-101.8	0.352	1.081	-21.6	65.8	18.9	-23.96	5.523
MINRP	2029-03-04	-95.96	352.6	-96.8	0.340	1.191	-15.4	47.1	14.5	-10.90	5.128
MINRP+5d	2029-03-09	-95.95	357.6	-91.8	0.352	1.283	-8.7	29.7	10.1	4.26	4.644
MAXLAT-5d	2029-03-26	-95.90	375.0	-74.4	0.497	1.458	11.2	18.0	8.9	31.56	3.182
MAXLAT	2029-03-31	-95.88	380.0	-69.4	0.544	1.487	15.5	21.1	11.3	32.42	2.709
MAXLAT+5d	2029-04-05	-95.87	385.0	-64.4	0.587	1.512	19.1	23.4	13.5	31.80	2.293
Mission end	2029-06-08										

Table 10-9 2018 Launch Option D: remote sensing windows from GAM-V4 to mission end



10.3 2019/2020 February Launch

Note: durations from launch are given with respect to 2020 launch; 2019 launch adds +1 year.

	Date	From launch (y)	From GAM (d)	To GAM (d)	Sun (AU)	Earth (AU)	DEC (deg)	SSE (deg)	SES (deg)	Sol. lat. (deg)	wrot (deg/day)
GAM-E1(E2)	2021-11-26	1.80									
MINLAT-5d	2022-03-05	2.07	98.4	-182.9	0.525	0.471	-1.5	169.2	5.7	-4.26	2.508
MINLAT	2022-03-10	2.09	103.4	-177.9	0.461	0.537	-3.8	169.2	5.0	-4.39	3.253
MINLAT+5d	2022-03-15	2.10	108.4	-172.9	0.399	0.630	-5.6	149.1	11.9	-4.15	4.330
MINRP-5d	2022-03-21	2.12	114.7	-166.6	0.339	0.794	-6.4	117.3	17.6	-2.74	5.997
MINRP	2022-03-26	2.13	119.7	-161.6	0.321	0.950	-5.5	88.9	18.8	-0.49	6.671
MINRP+5d	2022-03-31	2.14	124.7	-156.6	0.339	1.107	-3.5	62.8	17.6	1.91	5.994
MAXLAT-5d	2022-04-11	2.17	135.5	-145.8	0.454	1.375	2.4	28.8	12.6	4.25	3.351
MAXLAT	2022-04-16	2.19	140.5	-140.8	0.518	1.469	5.0	21.0	10.7	4.39	2.576
MAXLAT+5d	2022-04-21	2.20	145.5	-135.8	0.580	1.550	7.5	16.0	9.2	4.30	2.050
GAM-V3	2022-09-03	2.57									

Table 10-10 2019/2020 February Launch: remote sensing windows from GAM-E1 (GAM-E2 in 2019) to GAM-V3



	Date	From launch (y)	From GAM (d)	To GAM (d)	Sun (AU)	Earth (AU)	DEC (deg)	SSE (deg)	SES (deg)	Sol. lat. (deg)	wrot (deg/day)
GAM-V3	2022-09-03	2.57									
MINLAT-5d	2022-09-27	2.64	23.5	-875.3	0.436	1.436	-1.1	4.6	2.0	-8.10	3.500
MINLAT	2022-10-02	2.65	28.5	-870.3	0.369	1.367	-5.1	6.9	2.5	-8.66	4.886
MINLAT+5d	2022-10-07	2.66	33.5	-865.3	0.315	1.276	-9.3	25.3	7.7	-7.61	6.674
MINRP-5d	2022-10-07	2.66	33.7	-865.1	0.314	1.272	-9.4	26.1	7.9	-7.51	6.739
MINRP	2022-10-12	2.68	38.7	-860.1	0.292	1.149	-13.3	52.5	13.4	-3.43	7.673
MINRP+5d	2022-10-17	2.69	43.7	-855.1	0.314	1.004	-16.3	79.7	18.0	1.99	6.629
MAXLAT-5d	2022-11-01	2.73	58.8	-840.0	0.503	0.628	-19.6	122.3	25.3	8.48	2.638
MAXLAT	2022-11-06	2.75	63.8	-835.0	0.567	0.541	-19.5	126.8	27.3	8.66	2.070
MAXLAT+5d	2022-11-11	2.76	68.8	-830.0	0.628	0.469	-18.8	128.5	29.8	8.54	1.691
MINLAT-5d	2023-03-26	3.13	203.3	-695.5	0.436	0.568	3.5	166.7	5.8	-8.09	3.499
MINLAT	2023-03-31	3.14	208.3	-690.5	0.369	0.636	0.7	166.6	4.9	-8.66	4.884
MINLAT+5d	2023-04-05	3.16	213.3	-685.5	0.315	0.751	-0.8	135.2	12.8	-7.61	6.672
MINRP-5d	2023-04-05	3.16	213.5	-685.3	0.314	0.757	-0.8	133.9	13.1	-7.51	6.737
MINRP	2023-04-10	3.17	218.5	-680.3	0.292	0.917	-0.1	98.3	16.8	-3.44	7.673
MINRP+5d	2023-04-15	3.18	223.5	-675.3	0.314	1.086	2.4	66.5	16.7	1.99	6.631
MAXLAT-5d	2023-04-30	3.23	238.5	-660.3	0.502	1.455	11.5	22.1	10.8	8.48	2.639
MAXLAT	2023-05-05	3.24	243.5	-655.3	0.567	1.537	14.0	16.9	9.4	8.66	2.071
MAXLAT+5d	2023-05-10	3.25	248.5	-650.3	0.628	1.608	16.2	13.6	8.4	8.54	1.692
MINLAT-5d	2023-09-22	3.62	383.1	-515.7	0.435	1.439	0.4	0.9	0.4	-8.11	3.515
MINLAT	2023-09-27	3.63	388.1	-510.7	0.369	1.362	-3.5	11.1	4.1	-8.66	4.908
MINLAT+5d	2023-10-02	3.65	393.1	-505.7	0.315	1.262	-7.7	29.9	9.0	-7.57	6.696
MINRP-5d	2023-10-02	3.65	393.2	-505.6	0.314	1.259	-7.8	30.5	9.1	-7.52	6.735
MINRP	2023-10-07	3.66	398.2	-500.6	0.292	1.127	-11.6	57.3	14.2	-3.45	7.673
MINRP+5d	2023-10-12	3.68	403.2	-495.6	0.314	0.975	-14.6	85.1	18.2	1.98	6.634
MAXLAT-5d	2023-10-27	3.72	418.3	-480.5	0.502	0.590	-17.7	130.9	22.5	8.48	2.639
MAXLAT	2023-11-01	3.73	423.3	-475.5	0.567	0.500	-17.6	136.7	23.1	8.66	2.072
MAXLAT+5d	2023-11-06	3.74	428.3	-470.5	0.627	0.426	-16.9	139.7	24.1	8.54	1.692
MINLAT-5d	2024-03-19	4.11	562.8	-336.0	0.435	0.561	-0.5	176.7	1.5	-8.11	3.513
MINLAT	2024-03-24	4.13	567.8	-331.0	0.369	0.646	-2.8	157.7	8.1	-8.66	4.906
MINLAT+5d	2024-03-29	4.14	572.8	-326.0	0.315	0.775	-3.6	127.6	14.5	-7.58	6.694
MINRP-5d	2024-03-29	4.14	573.0	-325.8	0.314	0.778	-3.6	126.8	14.6	-7.52	6.733
MINRP	2024-04-03	4.15	578.0	-320.8	0.292	0.943	-2.4	92.6	17.0	-3.45	7.673
MINRP+5d	2024-04-08	4.17	583.0	-315.8	0.314	1.112	0.4	61.6	16.0	1.98	6.636
MAXLAT-5d	2024-04-24	4.21	598.1	-300.7	0.502	1.470	10.2	18.4	9.1	8.48	2.640
MAXLAT	2024-04-29	4.22	603.1	-295.7	0.567	1.550	12.8	13.4	7.5	8.66	2.072
MAXLAT+5d	2024-05-04	4.24	608.1	-290.7	0.627	1.619	15.1	10.2	6.4	8.54	1.693
MINLAT-5d	2024-09-15	4.61	742.6	-156.2	0.435	1.440	2.0	3.5	1.5	-8.11	3.512
MINLAT	2024-09-20	4.62	747.6	-151.2	0.369	1.355	-1.9	15.2	5.5	-8.66	4.904
MINLAT+5d	2024-09-25	4.63	752.6	-146.2	0.315	1.247	-6.0	34.3	10.2	-7.58	6.692
MINRP-5d	2024-09-25	4.63	752.7	-146.1	0.314	1.244	-6.1	34.8	10.3	-7.52	6.731
MINRP	2024-09-30	4.65	757.7	-141.1	0.292	1.104	-9.9	62.1	14.9	-3.46	7.673
MINRP+5d	2024-10-05	4.66	762.7	-136.1	0.313	0.946	-12.7	90.7	18.3	1.97	6.638
MAXLAT-5d	2024-10-20	4.70	777.8	-121.0	0.502	0.557	-15.2	140.2	18.8	8.48	2.641
MAXLAT	2024-10-25	4.72	782.8	-116.0	0.567	0.468	-14.8	147.7	17.7	8.66	2.073
MAXLAT+5d	2024-10-30	4.73	787.8	-111.0	0.627	0.393	-13.9	152.5	17.0	8.54	1.693
MINLAT-5d	2022-09-27	2.64	23.5	-875.3	0.436	1.436	-1.1	4.6	2.0	-8.10	3.500
MINLAT	2022-10-02	2.65	28.5	-870.3	0.369	1.367	-5.1	6.9	2.5	-8.66	4.886
MINLAT+5d	2022-10-07	2.66	33.5	-865.3	0.315	1.276	-9.3	25.3	7.7	-7.61	6.674
MINRP-5d	2022-10-07	2.66	33.7	-865.1	0.314	1.272	-9.4	26.1	7.9	-7.51	6.739
MINRP	2022-10-12	2.68	38.7	-860.1	0.292	1.149	-13.3	52.5	13.4	-3.43	7.673
MINRP+5d	2022-10-17	2.69	43.7	-855.1	0.314	1.004	-16.3	79.7	18.0	1.99	6.629
MAXLAT-5d	2022-11-01	2.73	58.8	-840.0	0.503	0.628	-19.6	122.3	25.3	8.48	2.638
MAXLAT	2022-11-06	2.75	63.8	-835.0	0.567	0.541	-19.5	126.8	27.3	8.66	2.070
MAXLAT+5d	2022-11-11	2.76	68.8	-830.0	0.628	0.469	-18.8	128.5	29.8	8.54	1.691
GAM-V4	2025-02-18	5.03									

Table 10-11 2019/2020 February Launch: remote sensing windows from GAM-V3 to GAM-V4

Date	From	From	To	Sun	Earth	DEC	SSE	SES	Sol.	wrot
------	------	------	----	-----	-------	-----	-----	-----	------	------



		launch (y)	GAM (d)	GAM (d)	(AU)	(AU)	(deg)	(deg)	(deg)	lat. (deg)	(deg/day)
GAM-V4	2025-02-18	5.03									
MINLAT-5d	2025-03-17	5.11	26.8	-647.3	0.414	0.598	-9.4	158.9	8.6	-15.88	3.951
MINLAT	2025-03-22	5.12	31.8	-642.3	0.352	0.709	-9.7	137.3	13.9	-17.22	5.536
MINLAT+5d	2025-03-27	5.13	36.8	-637.3	0.307	0.855	-8.0	109.0	16.9	-14.72	7.130
MINRP-5d	2025-03-26	5.13	35.7	-638.4	0.314	0.819	-8.5	115.9	16.5	-15.79	6.845
MINRP	2025-03-31	5.14	40.7	-633.4	0.294	0.984	-5.3	84.5	17.0	-8.63	7.427
MINRP+5d	2025-04-05	5.16	45.7	-628.4	0.314	1.144	-0.7	55.6	15.0	1.73	6.350
MAXLAT-5d	2025-04-23	5.21	64.1	-610.0	0.537	1.523	14.3	12.5	6.6	16.94	2.377
MAXLAT	2025-04-28	5.22	69.1	-605.0	0.596	1.589	17.2	9.9	5.8	17.22	1.934
MAXLAT+5d	2025-05-03	5.24	74.1	-600.0	0.650	1.646	19.7	8.6	5.5	17.03	1.623
MINLAT-5d	2025-09-02	5.57	195.3	-478.8	0.415	1.391	2.7	19.4	7.9	-15.86	3.939
MINLAT	2025-09-07	5.58	200.3	-473.8	0.353	1.282	-1.0	33.8	11.2	-17.22	5.520
MINLAT+5d	2025-09-12	5.60	205.3	-468.8	0.307	1.145	-4.5	56.1	14.7	-14.77	7.120
MINRP-5d	2025-09-11	5.59	204.2	-469.9	0.314	1.176	-3.8	50.7	14.0	-15.76	6.854
MINRP	2025-09-16	5.61	209.2	-464.9	0.294	1.017	-6.4	79.4	16.7	-8.57	7.424
MINRP+5d	2025-09-21	5.62	214.2	-459.9	0.315	0.852	-7.1	110.0	17.1	1.79	6.340
MAXLAT-5d	2025-10-09	5.67	232.7	-441.5	0.537	0.483	5.6	156.8	12.2	16.94	2.373
MAXLAT	2025-10-14	5.68	237.7	-436.5	0.596	0.442	10.5	147.2	18.9	17.22	1.932
MAXLAT+5d	2025-10-19	5.70	242.7	-431.5	0.650	0.416	15.0	137.1	26.4	17.03	1.621
MINLAT-5d	2026-02-17	6.03	363.8	-310.3	0.414	0.708	-23.3	121.1	21.0	-15.88	3.948
MINLAT	2026-02-22	6.04	368.8	-305.3	0.352	0.841	-21.4	104.3	20.2	-17.22	5.532
MINLAT+5d	2026-02-27	6.06	373.8	-300.3	0.307	0.991	-18.1	80.9	17.8	-14.73	7.127
MINRP-5d	2026-02-26	6.05	372.7	-301.4	0.315	0.957	-19.0	86.7	18.5	-15.80	6.841
MINRP	2026-03-03	6.07	377.7	-296.4	0.294	1.109	-14.7	59.2	14.7	-8.66	7.428
MINRP+5d	2026-03-08	6.08	382.7	-291.4	0.314	1.241	-9.6	32.9	9.9	1.71	6.354
MAXLAT-5d	2026-03-26	6.13	401.1	-273.0	0.537	1.521	7.4	10.4	5.6	16.94	2.378
MAXLAT	2026-03-31	6.15	406.1	-268.0	0.596	1.570	10.9	13.1	7.8	17.22	1.935
MAXLAT+5d	2026-04-05	6.16	411.1	-263.0	0.650	1.615	13.9	14.8	9.5	17.03	1.624
MINLAT-5d	2026-08-05	6.49	532.3	-141.8	0.415	1.305	9.9	38.7	14.8	-15.86	3.936
MINLAT	2026-08-10	6.50	537.3	-136.8	0.353	1.176	7.0	54.8	16.5	-17.22	5.515
MINLAT+5d	2026-08-15	6.52	542.3	-131.8	0.307	1.021	4.7	79.9	17.4	-14.78	7.117
MINRP-5d	2026-08-14	6.52	541.3	-132.8	0.314	1.055	5.1	73.8	17.3	-15.77	6.850
MINRP	2026-08-19	6.53	546.3	-127.8	0.294	0.888	4.1	106.6	16.1	-8.59	7.425
MINRP+5d	2026-08-24	6.54	551.3	-122.8	0.314	0.741	6.0	143.7	10.6	1.77	6.344
MAXLAT-5d	2026-09-11	6.59	569.7	-104.4	0.537	0.614	22.7	121.9	26.9	16.94	2.375
MAXLAT	2026-09-16	6.61	574.7	-99.4	0.596	0.636	25.1	109.3	34.0	17.22	1.933
MAXLAT+5d	2026-09-21	6.62	579.7	-94.4	0.650	0.660	26.4	100.1	39.6	17.03	1.622
GAM-V5	2026-12-24	6.88									

Table 10-12 2019/2020 February Launch: remote sensing windows from GAM-V4 to GAM-V5



	Date	From launch (y)	From GAM (d)	To GAM (d)	Sun (AU)	Earth (AU)	DEC (deg)	SSE (deg)	SES (deg)	Sol. lat. (deg)	wrot (deg/day)
GAM-V5	2026-12-24	6.88									
MINLAT-5d	2027-01-23	6.96	29.7	-419.7	0.414	0.898	-30.3	89.2	24.9	-22.55	3.980
MINLAT	2027-01-28	6.97	34.7	-414.7	0.352	1.005	-28.7	76.6	20.4	-24.43	5.674
MINLAT+5d	2027-02-02	6.99	39.7	-409.7	0.302	1.119	-25.4	56.6	14.8	-20.90	7.304
MINRP-5d	2027-02-02	6.99	39.4	-410.0	0.305	1.111	-25.7	58.2	15.3	-21.43	7.228
MINRP	2027-02-07	7.00	44.4	-405.0	0.284	1.216	-20.7	31.7	8.7	-9.78	7.437
MINRP+5d	2027-02-12	7.01	49.4	-400.0	0.305	1.290	-14.6	5.9	1.8	5.57	6.328
MAXLAT-5d	2027-02-25	7.05	63.1	-386.3	0.466	1.366	1.0	29.9	13.6	23.77	3.206
MAXLAT	2027-03-02	7.07	68.1	-381.3	0.527	1.381	5.7	34.3	17.4	24.43	2.533
MAXLAT+5d	2027-03-07	7.08	73.1	-376.3	0.583	1.396	9.8	36.8	20.6	24.00	2.057
MINLAT-5d	2027-06-22	7.37	179.5	-269.9	0.414	1.049	15.4	74.0	23.1	-22.55	3.979
MINLAT	2027-06-27	7.38	184.5	-264.9	0.352	0.931	14.2	93.7	20.2	-24.43	5.673
MINLAT+5d	2027-07-02	7.40	189.5	-259.9	0.302	0.814	14.6	124.7	14.2	-20.91	7.304
MINRP-5d	2027-07-02	7.40	189.2	-260.2	0.305	0.821	14.5	122.1	14.7	-21.43	7.227
MINRP	2027-07-07	7.41	194.2	-255.2	0.284	0.744	17.7	161.1	5.2	-9.79	7.437
MINRP+5d	2027-07-12	7.42	199.2	-250.2	0.305	0.755	22.9	143.7	10.2	5.56	6.329
MAXLAT-5d	2027-07-25	7.46	212.9	-236.5	0.466	1.007	31.3	77.8	26.6	23.77	3.206
MAXLAT	2027-07-30	7.48	217.9	-231.5	0.527	1.094	32.2	67.3	28.6	24.43	2.533
MAXLAT+5d	2027-08-04	7.49	222.9	-226.5	0.583	1.170	32.5	60.2	29.9	24.00	2.057
MINLAT-5d	2027-11-19	7.78	329.3	-120.1	0.414	1.293	-20.4	36.0	14.3	-22.55	3.978
MINLAT	2027-11-24	7.79	334.3	-115.1	0.352	1.290	-23.7	26.6	9.2	-24.43	5.672
MINLAT+5d	2027-11-29	7.81	339.3	-110.1	0.302	1.275	-25.7	15.1	4.6	-20.92	7.303
MINRP-5d	2027-11-28	7.81	339.0	-110.4	0.305	1.277	-25.6	15.6	4.8	-21.44	7.226
MINRP	2027-12-03	7.82	344.0	-105.4	0.284	1.239	-25.7	23.9	6.7	-9.80	7.438
MINRP+5d	2027-12-08	7.83	349.0	-100.4	0.305	1.171	-23.6	46.2	12.9	5.55	6.330
MAXLAT-5d	2027-12-22	7.87	362.7	-86.7	0.466	0.964	-12.6	78.6	27.7	23.77	3.207
MAXLAT	2027-12-27	7.89	367.7	-81.7	0.527	0.907	-8.2	82.0	32.0	24.43	2.533
MAXLAT+5d	2028-01-01	7.90	372.7	-76.7	0.583	0.863	-3.8	83.3	36.1	24.00	2.057
GAM-V6	2028-03-17	8.11									
MINLAT-5d	2028-04-20	8.20	33.6	-415.8	0.454	0.646	1.3	131.3	19.8	-28.56	3.648
MINLAT	2028-04-25	8.21	38.6	-410.8	0.405	0.664	0.0	139.2	15.2	-30.21	4.741
MINLAT+5d	2028-04-30	8.23	43.6	-405.8	0.362	0.716	0.7	135.5	14.6	-27.58	5.620
MINRP-5d	2028-05-03	8.24	46.6	-402.8	0.344	0.766	2.4	126.3	16.0	-22.98	5.778
MINRP	2028-05-08	8.25	51.6	-397.8	0.331	0.875	6.8	104.3	18.5	-10.43	5.462
MINRP+5d	2028-05-13	8.26	56.6	-392.8	0.345	1.001	12.1	81.7	19.7	4.36	4.915
MAXLAT-5d	2028-05-30	8.31	73.5	-375.9	0.494	1.358	26.8	37.8	17.4	29.42	3.134
MAXLAT	2028-06-04	8.32	78.5	-370.9	0.543	1.433	29.3	32.0	16.5	30.21	2.639
MAXLAT+5d	2028-06-09	8.34	83.5	-365.9	0.588	1.498	31.1	27.7	15.6	29.66	2.225
MINLAT-5d	2028-09-17	8.61	183.4	-266.0	0.454	1.423	-6.3	19.0	8.5	-28.55	3.647
MINLAT	2028-09-22	8.62	188.4	-261.0	0.405	1.340	-10.0	28.6	11.1	-30.21	4.739
MINLAT+5d	2028-09-27	8.64	193.4	-256.0	0.363	1.240	-13.3	42.3	14.1	-27.59	5.619
MINRP-5d	2028-09-30	8.65	196.4	-253.0	0.344	1.171	-14.7	52.8	15.9	-23.00	5.778
MINRP	2028-10-05	8.66	201.4	-248.0	0.331	1.044	-15.8	73.3	18.5	-10.46	5.463
MINRP+5d	2028-10-10	8.67	206.4	-243.0	0.344	0.912	-14.6	94.2	20.1	4.33	4.916
MAXLAT-5d	2028-10-27	8.72	223.3	-226.1	0.494	0.606	1.2	129.1	22.7	29.42	3.134
MAXLAT	2028-11-01	8.73	228.3	-221.1	0.542	0.561	6.6	128.2	25.4	30.21	2.639
MAXLAT+5d	2028-11-06	8.75	233.3	-216.1	0.588	0.529	11.3	125.1	29.0	29.66	2.225
MINLAT-5d	2029-02-14	9.02	333.2	-116.2	0.454	0.778	-32.0	103.4	26.6	-28.55	3.645
MINLAT	2029-02-19	9.04	338.2	-111.2	0.405	0.887	-28.8	92.1	24.2	-30.21	4.737
MINLAT+5d	2029-02-24	9.05	343.2	-106.2	0.363	1.006	-24.3	77.1	20.9	-27.60	5.618
MINRP-5d	2029-02-27	9.06	346.2	-103.2	0.344	1.077	-21.1	66.3	18.6	-23.02	5.778
MINRP	2029-03-04	9.07	351.2	-98.2	0.331	1.190	-15.0	46.4	14.0	-10.48	5.464
MINRP+5d	2029-03-09	9.08	356.2	-93.2	0.344	1.285	-8.4	27.7	9.3	4.31	4.917
MAXLAT-5d	2029-03-26	9.13	373.1	-76.3	0.494	1.457	10.8	17.6	8.6	29.42	3.135
MAXLAT	2029-03-31	9.14	378.1	-71.3	0.542	1.486	15.0	21.1	11.3	30.21	2.640
MAXLAT+5d	2029-04-05	9.16	383.1	-66.3	0.587	1.511	18.7	23.5	13.6	29.66	2.226
GAM-V7	2029-06-10	9.34									

Table 10-13 2019/2020 February Launch: remote sensing windows from GAM-V5 to GAM-V7



	Date	From launch (y)	From GAM (d)	To GAM (d)	Sun (AU)	Earth (AU)	DEC (deg)	SSE (deg)	SES (deg)	Sol. lat. (deg)	wrot (deg/day)
GAM-V7	2029-06-10	9.34									
MINLAT-5d	2029-07-19	9.45	39.1	-410.3	0.507	1.214	5.1	55.5	24.3	-32.19	3.139
MINLAT	2029-07-24	9.46	44.1	-405.3	0.468	1.118	2.7	65.3	24.7	-33.39	3.793
MINLAT+5d	2029-07-29	9.47	49.1	-400.3	0.430	1.009	1.0	78.5	24.5	-31.69	4.317
MINRP-5d	2029-08-07	9.50	58.0	-391.4	0.381	0.799	1.5	113.6	20.2	-18.16	4.403
MINRP	2029-08-12	9.51	63.0	-386.4	0.373	0.698	5.6	140.4	13.6	-5.46	4.197
MINRP+5d	2029-08-17	9.53	68.0	-381.4	0.381	0.636	12.7	168.1	4.5	7.96	4.056
MAXLAT-5d	2029-09-02	9.57	84.0	-365.4	0.483	0.739	31.0	109.4	26.9	32.31	3.466
MAXLAT	2029-09-07	9.58	89.0	-360.4	0.523	0.809	32.0	96.0	31.1	33.39	3.034
MAXLAT+5d	2029-09-12	9.60	94.0	-355.4	0.561	0.875	31.7	86.0	33.8	32.60	2.589
MINLAT-5d	2029-12-16	9.86	188.9	-260.5	0.507	1.245	-31.0	48.4	22.7	-32.19	3.138
MINLAT	2029-12-21	9.87	193.9	-255.5	0.468	1.272	-32.4	43.1	19.0	-33.39	3.792
MINLAT+5d	2029-12-26	9.88	198.9	-250.5	0.430	1.301	-32.4	35.6	14.7	-31.69	4.317
MINRP-5d	2030-01-04	9.91	207.8	-241.6	0.381	1.343	-28.7	16.7	6.4	-18.16	4.403
MINRP	2030-01-09	9.92	212.8	-236.6	0.373	1.350	-24.6	8.9	3.4	-5.47	4.197
MINRP+5d	2030-01-14	9.94	217.8	-231.6	0.381	1.342	-19.6	17.0	6.5	7.95	4.056
MAXLAT-5d	2030-01-30	9.98	233.8	-215.6	0.483	1.244	-2.6	47.6	21.2	32.31	3.467
MAXLAT	2030-02-04	9.99	238.8	-210.6	0.523	1.208	2.3	53.0	25.1	33.39	3.035
MAXLAT+5d	2030-02-09	10.01	243.8	-205.6	0.561	1.173	6.7	57.0	28.5	32.60	2.589
MINLAT-5d	2030-05-15	10.27	338.7	-110.7	0.507	0.747	5.7	105.8	28.9	-32.19	3.138
MINLAT	2030-05-20	10.28	343.7	-105.7	0.468	0.709	4.4	117.1	24.3	-33.39	3.792
MINLAT+5d	2030-05-25	10.29	348.7	-100.7	0.430	0.682	4.5	129.7	19.1	-31.69	4.317
MINRP-5d	2030-06-03	10.32	357.6	-91.8	0.381	0.702	9.9	136.7	15.0	-18.16	4.403
MINRP	2030-06-08	10.33	362.6	-86.8	0.373	0.766	15.3	122.2	18.1	-5.47	4.197
MINRP+5d	2030-06-13	10.35	367.6	-81.8	0.381	0.859	20.9	103.1	21.5	7.95	4.056
MAXLAT-5d	2030-06-29	10.39	383.6	-65.8	0.483	1.187	32.9	57.9	23.8	32.31	3.467
MAXLAT	2030-07-04	10.40	388.6	-60.8	0.523	1.274	34.4	49.7	23.1	33.39	3.035
MAXLAT+5d	2030-07-09	10.42	393.6	-55.8	0.561	1.350	35.1	43.2	22.2	32.60	2.589
Mission end	2030-09-02	10.57									

Table 10-14 2019/2020 February Launch: remote sensing windows from GAM-V7 to mission end